THE UNIVERSITY OF MANITOBA

COMPACTION AND STRENGTH CHARACTERISTICS OF SAND-CLAY BUFFER MATERIAL FORMED AT SWELLING PRESSURE - WATER CONTENT EQUILIBRIUM

by

ALAN WING-LON WAN

A THESIS

SUBMITTED TO THE FACULTY OF GRADUATE STUDIES

IN PARTIAL FULFILLMENT OF THE REQUIREMENTS FOR THE DEGREE OF

MASTER OF SCIENCE

DEPARTMENT OF CIVIL ENGINEERING

WINNIPEG, MANITOBA

AUGUST, 1987 

ISBN 0-315-37379-2

COMPACTION AND STRENGTH CHARACTERISTICS OF SAND-CLAY BUFFER MATERIAL FORMED AT SWELLING PRESSURE - WATER CONTENT EQUILIBRIUM

BY

ALAN WING-LON WAN

A thesis submitted to the Faculty of Graduate Studies of the University of Manitoba in partial fulfillment of the requirements of the degree of

MASTER OF SCIENCE

ABSTRACT

Compacted sand-clay buffer material has been selected as an engineered barrier in the Canadian program for long term disposal of nuclear waste. Laboratory test results are required for predicting short-term and long-term performance of the buffer under different conditions of stresses and strains. This study investigated a new procedure for preparing specimens for triaxial testing.

Triaxial tests up to confining pressures of 1.5 MPa have been performed at room temperature on mixtures consisting of 50% sand and 50% clay by mass. The mixtures were compacted at densities and water contents that were designed to be at swelling pressure - water content equilibrium under isotropic consolidation stresses. Consolidation tests and shear tests were used to determine the volume change, stress-strain, and strength characteristics of the buffer.

The results show that the swelling potential and the shear behaviour of the buffer are influenced by the soil fabric structure. This depends on the specimen preparation process and the testing techniques. The stress-strain behaviour of the material is slightly strain-softening in undrained shear; and both time- and stress level-dependent in drained shear. Average values of the normalized undrained shear moduli E_{50}/s_u and E_{50}/σ'_{cons} are 190 and 60 respectively. A strength envelope with c'= 0 kPa and Ø'= 13½° has been measured.

The conceptual model (Graham et al., 1986a) based on Critical State theory is shown to be generally valid, and has been modified to account for the effects of soil structure and testing technique.

ACKNOWLEDGEMENTS

The author would like to thank his adviser, Professor James Graham, for his technical input and constructive guidance during the research program and the preparation of this thesis.

The author also wishes to express his appreciation to Dr. M. N. Gray of Atomic Energy of Canada Limited (AECL) at Pinawa, and Professor M. G. Britton of the Department of Agricultural Engineering for reviewing this thesis.

Meaningful discussion with D. Dixon, and Dr. S.C.H. Cheung of AECL, and Dr. J. H. Atkinson of the City University at London, is gratefully acknowledged.

Financial support, in the form of research contract, from AECL contract No. WS-25K-31620, is also acknowledged.

Technical support from N. Piamsalee, B. Lingnau, C. Escobar, and K. J. George is greatly appreciated.

Thanks are also due to B. Sun, F. Saadat, Q.-Y. Zhang, S. Lau, J.-H. Yin, I. Trestrail, and G. Homenick.

Finally, the author is indebted to his family for their understanding and encouragement during the course of his graduate study.

TABLE OF CONTENTS

LIST OF SYMBOLS

A,B - Skempton's porewater pressure parameters

A_f - value of A at failure

C_c - ion concentration midway between two parallel clay particles

C_o - ion concentration in free water

CSL - Critical State Line

c' - effective coefficient of cohesion

E_{50} - undrained shear modulus at 50 percent of maximum deviator stress

e - void ratio

G - drained shear modulus

G_c - specific gravity of clay

G_{50} - undrained shear modulus = $E_{50}/3$

K - bulk modulus

m - porewater pressure parameter = $\Delta u / \Delta p$

NCL - Normal Consolidation Line

P - swelling pressure

p - total mean principal stress = $(\sigma_1 + 2\sigma_3)/3$

p_s - swelling pressure

p' - effective mean principal stress = $(\sigma_1' + 2\sigma_3')/3$

p_c' - effective preconsolidation pressure

p_f' - effective mean principal stress at failure

p_s' - effective swelling pressure

q - deviator stress = $(\sigma_1' - \sigma_3')$

q_f - deviator stress at failure

q_{max} - maximum deviator stress = q_f

q/p' - effective stress ratio

$(q/p')_f$ - effective stress ratio at failure

$(q/p')_{max}$ - maximum effective stress ratio

R - molar gas constant

S - specific surface area of clay

S_r - degree of saturation

SEL - Swelling Equilibrium Line

s_u - undrained shear strength = $q_{max}/2$

T - absolute temperature

u - porewater pressure

u_f - porewater pressure at failure

V - specific volume = (1 + e)

V - volume of specimen

V_c - clay specific volume = $G_c.\gamma_w/\gamma_c$

v - volume strain

w - water content

ϵ - shear strain = $2(\epsilon_1 - \epsilon_3)/3$

ϵ_1 - axial strain

ϵ_{1f} - axial strain at failure

ϵ_3 - radial strain

ϵ_v - volume strain

γ_c - effective clay dry density

γ_d - dry density of buffer

γ_w - density of water

γ_{bulk} - bulk density of buffer

σ_{cons} - total consolidation pressure

σ_{cons} - mean consolidation pressure

σ'_1, σ'_3 - major and minor effective principal stresses

σ'_v - effective vertical pressure

σ'_{cons} - effective consolidation pressure

σ'_1/σ'_3 - effective stress ratio

ϕ' - effective angle of shearing resistance

ν - Poisson's ratio

$\rho_{0.1}$ - strain rate parameter

ΔV - change in volume

Δp - change in mean principal stress

Δu - change in porewater pressure

Δq - change in deviator stress

$\Delta \sigma$ - change in total pressure

dv - incremental volume strain

dw - incremental work done

$d\epsilon$ - incremental shear strain

LIST OF TABLES

LIST OF FIGURES

CHAPTER 1

INTRODUCTION

1.1 BACKGROUND

With the oil crisis of the 1970's and the growing increase in energy consumption, nuclear power has become an economic choice of producing electricity. Olivier (1986) has stated that by the year 2000 fourteen out of twenty-four member countries of the Organization for Economic Cooperation Development (OECD) will have 11% to 80% of their electricity needs generated by nuclear power. Spent fuel from nuclear generation is strongly toxic and a considerable social hazard. As far as these countries are concerned, the development of national plans for radioactive waste fuel disposal is essential. Public pressures in many countries necessitate thorough, broadly-based, scientifically and socially acceptable fuel waste management programs.

1.2 DEVELOPMENT OF NUCLEAR WASTE MANAGEMENT PROGRAMS IN OECD COUNTRIES

The international program of nuclear waste management has been reviewed recently by Olivier (1986). The following paragraphs have been largely taken from his review.

In Belgium, the experimental program concentrates on the underground laboratory in stiff, plastic clay at Mol. Since the completion of the laboratory in 1984, research has been focused on

heat tests, corrosion tests and on the rheology of the disposal site.

France, where 60% of its electicity production is attributed to nuclear production, is currently looking at both low-level and high-level waste disposal plans. They are also working on a plan expected by the end of 1987 for the underground research laboratory.

The emphasis of the Dutch and West German programs is to investigate the potential of geological evaporite formations to receive all types of radioactive materials.

In Sweden, the KBS-3 program investigates the disposal of all types of waste, including spent fuel and high-level waste. Like the Canadian program, the Swedes are also looking at the possibility of disposal in crystalline bedrock. The Stripa Project involves full scale studies of embedment in former mine passages in granite, and forms an integral part of the Swedish program of international cooperation.

In Japan, the main focus is on low-level wastes. Extensive research has been carried out at a site in Northern Japan. Research is also conducted on high level waste disposal in granite. Japan is an active participant in the Swedish Stripa Project.

In Switzerland, the NAGRA program is responsible for planning the disposal of radioactive wastes, which includes both spent fuel and high-level waste from reprocessing, and also shorter-lived waste from reactor operations. Extensive research has been conducted in the Grimsel Underground Laboratory in a granitic formation in the Alps since its opening in 1984.

The main interest of the United Kingdom program is on securing the disposal of low-level and intermediate-level wastes. In 1985, the

United Kingdom Nirex Limited, a consortium of various electricity boards and government bodies, was set up to develop and operate disposal facilities for these kinds of waste. The Department of Energy is also researching ways of disposing of high-level waste, including both deep geological and sub-seabed disposal. The United Kingdom is actively involved in the Stripa Program and other international waste management programs (Ginniff, 1986).

In the United States, the Nuclear Waste Policy Act of 1982 provides a broad, flexible framework for achieving the capability to dispose of spent nuclear fuel and high-level waste. The U.S. program has been concentrating on the selection of its first repository. Recent U.S. involvement in the Canadian program result in further studies of disposal in crystalline rock formations.

1.3 CANADIAN NUCLEAR FUEL WASTE MANAGEMENT PROGRAM (CNFWMP)

1.3.1 BACKGROUND

The Canadian Nuclear Fuel Waste Management Program, established since 1978, is responsible for the safe management of radioactive fuel. This program was initiated by a Federal Government - Ontario Agreement, under which Atomic Energy of Canada Limited (AECL), a federal crown corporation, is responsible for coordinating and managing the research; and developing a program for the immobilisation of fuel wastes and their safe disposal.

1.3.2 CONCEPT

The Canadian program is based on the concept that the waste

can be isolated effectively and permanently by deep, underground disposal in stable geological formations (Bird and Cameron, 1982). The Canadian program has concentrated on disposal in stable hard rock formations, known as plutons in the Canadian Shield. Alternative host media such as salt beds, clays, till deposits or shales continue to be examined in a limited fashion (Bechai et al., 1986).

The basic concept being investigated is the emplacement of a chemically and mechanically stable waste form in a deep underground vault within a stable geological formation. The disposal vault will consist of a number of mined chambers some 500 to 1000 metres below the surface, together with the shafts leading to them and any other underground facilities. After disposal operations have been completed, the entire vault will be backfilled and sealed so as to return the site to a natural condition where no further maintenance or supervision will be necessary.

In the post-closure period the repository and surrounding rocks will be heated by the radioactive decay of the waste. The maximum temperature reached will depend on the amount of waste emplaced per unit area and is not expected to exceed 100°C at the surface of the waste package. The elevated temperature will last for several hundred years for immobilized fission product wastes, and a few tens of thousands of years in the case of high-level fuel waste disposal.

After closure, the only significant mechanism of radionuclides release which can be identified is due to ground water which may penetrate to the waste, dissolve the radionuclides, and carry them back to the surface. However, the rate at which this migration would

take place can be minimized by a number of protective barriers. In the Canadian proposal, these barriers include (Bird and Cameron, 1982):

(1) a corrosion-resistant container,

(2) compacted sand-clay buffer material surrounding the container,

(3) compacted backfill material in the vault and the shaft,

(4) the massive geological formation which must be free of joints

The concept will be explored in the Underground Research Laboratory (URL) currently being constructed at Lac du Bonnet, Manitoba. It is an experimental facility presently at a depth of about 240m in a large granitic pluton, and will shortly be deepened as part of the cooperative program with the United States. This will be the first such test facility built below the water table in previously undisturbed granitic rock. The URL will provide an appropriate environment for experiments to determine the thermal and mechanical response of the rock to excavation and thermal loading that would take place in the disposal vault; and for the testing of buffer and backfill performance.

1.3.3 VAULT SEALING PROGRAM

The vault sealing program is concerned with research and development of engineered barriers required to retard the migration of radionuclides from a nuclear fuel waste disposal vault to the biosphere. The development of the program has been described by Bird and Cameron (1982). Figure 1.1 shows the detailed structure of this program (Lopez,1985). The main features are :

(1) Buffer development

(2) Backfill development

(3) Grout, shaft and drift sealing development

(4) Borehole sealing development, and

(5) Underground Research Laboratory

1.3.4 BUFFER DEVELOPMENT

The development of suitable buffer material to place between the waste containers and the rock forms an integral part of the sealing program. Extensive research has been carried out in the Whiteshell Nuclear Research Establishment at Pinawa, in Ontario Hydro Research Division at Toronto, and in various universities and institutions.

It is appreciated that the buffer material will operate in a very severe environment in which the hydrostatic pressure will be as high as 10 MPa, and temperatures as high as 100°C will be encountered. It is therefore necessary to understand fully how the material will behave under such conditions. This understanding is needed for computer modelling studies that will examine the interaction of the waste containers with its environment (Selvadurai et al., 1985). This will contribute to decision-making regarding the acceptability of the proposed disposal system.

The Reference Buffer Material (RBM) is a mixture of 50 percent quartz sand and 50 percent bentonite by mass. Gray et al. (1984) and Dixon et al. (1985) showed that the presence of sand enhances the physical properties by decreasing the shrinkage potential; increasing the compacted density without any decrease in the swelling potential developed by the bentonite; and decreasing the hydraulic conductivity.

The properties of the buffer have been studied by various researchers. Quigley (1984) determined the mineralogical composition; Radhakrishna (1984) the thermal properties; Dixon and Gray (1985) the engineering properties; Dixon et al. (1985) the compaction properties; Gray et al. (1984, 1985) the swelling properties; Cheung et al. (1985) the hydraulic and ionic diffusion properties; Yong et al. (1985) the creep properties; Selvadurai et al. (1985) the canister - buffer - rockmass interaction; and Sun (1986) the stress-strain properties in triaxial tests. The first phase of the research at the University of Manitoba has been summarized by Graham et al. (1986a). Subsequent studies up to November, 1986 were reported by Graham et al. (1986b).

1.4 OBJECTIVES

While the physical and chemical properties of the buffer have received a lot of attention (see Section 1.3.4), the geotechnical properties (particularly the strength and deformation properties) have not been extensively studied.

Under an one-year research contract No. WS-24J-18735 between AECL, Pinawa and the University of Manitoba, Sun (1986) examined the stress - strain - time properties of the material up to a maximum confining pressure of 1.0 MPa in a room temperature environment. A summary of his investigation will be described in Chapter 3. It is appreciated that his study was confined to low stresses and low temperatures; and his findings are insufficient to characterize the actual buffer behaviour under the high stress and high temperature conditions in the disposal vault. His work however provides some

initial insights on the behaviour of the material, and identifies areas that need further research.

One of the problems that were encountered during Sun's investigation is the long duration required by the compacted buffer specimens to reach equilibrium in triaxial consolidation. Because of the time constraints, the majority of the specimens were sheared before they were fully equilibrated, and this caused difficulties in the data interpretation.

To minimize problems associated with the long consolidation time, this thesis study was focussed on the development of a specimen preparation technique that will lead to pressure - water content equilibrium of the buffer under isotropic consolidation stresses. Other specific objectives of this study are as follows:

(1) By triaxial testing, to verify and extend the swelling pressure - effective clay dry density relationship (Gray et al., 1985; Dixon et al., 1986; Graham et al., 1986a) described in Chapter 3.

(2) To investigate the applicability of the effective stress principle to the buffer.

(3) To determine the stress-strain and strength parameters (c', Ø', E, A_f, G).

(4) To increase the confining test pressure on the material to higher stress levels to obtain better simulation of the actual vault conditions.

(5) To enhance and modify the critical state conceptual model (Graham et al., 1986a) described in Chapter 2 so as to understand and predict the soil behaviour under different conditions.

Chapters 2 and 3 of this thesis will review the literature,

followed by basic properties of the buffer and specimen preparation in Chapter 4. Chapter 5 will outline the testing procedures. Test results will be summarized in Chapter 6. Discussion of the results and conclusions will be presented in Chapters 7 and 8 respectively.

CHAPTER 2

REVIEW: CLAY PROPERTIES AND CONCEPTUAL MODEL

2.1 INTRODUCTION

Due to their low hydraulic conductivity and resistance against mineralogical changes, clays are useful as sealing material in contructing barriers around hazardous waste (Lundgren and Soderblom, 1985). In the Canadian concept for nuclear waste containment, swelling smectitic clay, such as bentonite, has been selected to be used in forming buffer material. The Reference Buffer Material (RBM) is a 50:50 mixture of quartz sand and sodium bentonite. Dixon et al. (1985) showed that the clay has a dominant influence on the characteristics of the RBM. A study of clay properties through literature research is therefore an essential step in understanding the behaviour of the RBM.

The first part of this chapter will focus on the properties of clays in general, and the second part will discuss the theoretical background pertinent to the research.

2.2 PROPERTIES OF CLAYS

2.2.1 CLAY MINERALOGY

Clay minerals are colloidal size particles, usually resulting from chemical weathering of igneous or metamorphic rock (Grim, 1953). These particles are usually very small in size. Clay-size particles

are typically defined in geotechnical engineering as having an "equivalent sphere" of less than 2 microns ($2x10^{-6}m$). Most clay minerals are of "plate like" form and have a high specific surface, that is, a high surface area to mass ratio (Scott, 1963). As a result, the mineral properties are greatly influenced by the electrical charge forces between neighbouring clay particles (Lambe and Whitman, 1979).

The basic structural units of clay minerals consist of silica tetrahedra and alumina octahedra (Yong and Warkentin, 1975; Mitchell, 1976). These basic units combine to form sheet-like structures, and clay minerals are formed by the stacking of combinations of basic sheets with different types of bonding between the sheets. Silicon and aluminium may be partially replaced in these units by other elements with similar atomic size but different valency in the process known as "isomorphous substitution".

There are three basic types of clay minerals (Figure 2.1). Kaolinite has a repetitive structure based on successive packing of single sheets of silica tetrahedra combined with single sheets of alumina octahedra. There is very limited isomorphous substitution. The combined silica-alumina sheets are held together by strong hydrogen bonding between them.

The basic structure of illite is a sheet of alumina octahedra sandwiched between two sheets of silica tetrahedra. In the octahedra sheet, there is partial substitution of aluminum by magnesium and iron; and in the tetrahedra sheet, silicon is partially substituted by aluminum. The combined sheets are linked by weak ionic bonding by potassium ions.

Montmorillonite (smectite) has the same basic structure as illite with the basic unit consisted of one sheet of silica between two sheets of alumina. Substitution for aluminium and silicon within the lattice by other cations is extensive compared with illite. Bonding between successive layers is attributed to attractive van der Waals forces and to exchangeable cations that may be adsorbed onto the plate surfaces to balance charge deficiencies in the structure. These bonds are weak and easily separated by adsorption of water.

2.2.2 DOUBLE DIFFUSE LAYER

As a result of the basic structures outlined in the previous section, clay particles usually carry negative surface charges arising from the following conditions (Lambe and Whitman, 1979):

(1) Isomorphous substitution of aluminum and silicon by cations of lower valency.
(2) Imperfections within the crystal lattice, including broken bonds at the edges of the particles.
(3) Disassociation of hydroxyl ions.
(4) Adsorption of anions.
(5) Presence of amorphous organic matter.

Of these five possible causes, isomorphous substitution is the most important.

In addition to these charge deficiencies, clay particles have high affinity for water. When they are in aqueous solution, the positive cations in the solution will be attracted to the clay particles in order to balance the charge deficiency. However because of their thermal energy, the cations are not simply adsorbed onto the

surface of a particle, but form a dispersed layer adjacent to it. The term "double diffuse layer" describes the negatively charged particle surface and the associated dispersed layer of cations. The concentration of the cations reduces with distance away from the particle.

2.2.3 ADSORBED WATER

Water is a dipolar molecule (Yong and Warkentin, 1975), that is, it is electrically neutral, but the centre of the two hydrogen atoms does not coincide with the central oxygen atom. As a result, water is often held round clay particles by hydrogen bonding. This relatively strong bonding restricts easy movement of water molecules, and therefore the adsorbed water possesses characteristics which are different from those of the free water in interparticle spaces (Yong and Warkentin, 1975). For example, it has higher viscosity and density. Such properties, which are sensitive to temperature changes, can be expected to influence the consolidation and stress - strain behaviour of a clay.

2.2.4 SWELLING OF CLAYS

Swelling of clays in the presence of water is a manifestation of the repulsive forces acting between clay particles (Warkentin et al., 1957). The mechanism can be explained by the theories of double diffuse layer and osmotic pressure (Yong and Warkentin, 1975; Mitchell, 1976).

Due to the negatively charged nature of clay particles, the cations in a clay-water system are attracted to the particle surfaces,

and are not free to diffuse. As a result of this, the cation concentration in the vicinity of the clay particles is much higher than that in the free interstitial water. In addition, overlapping of clay particles or adsorbed water layers results in excess cation concentration between particles. The difference in ionic concentration gives rise to the development of an osmotic pressure that causes water to move from the zone of low concentration to the zone of high concentration. The swelling of the clay is attributed to this water movement, and the osmotic pressure that causes repulsion between clay particles is referred to as the swelling pressure p'_s.

Swelling pressure is often taken as the difference in osmotic pressure midway between parallel clay platelets relative to that in free water (Bolt, 1956; Sridharan et al., 1986); and can be determined using van't Hoff's equation (Yong and Warkentin, 1975),

$$P = RT(C_c - 2C_o),$$

where R = molar gas constant

T = temperature (K)

C_c = ion concentration midway between two parallel clay particles (mol/l)

C_o = ion concentration in the free water (mol/l)

The swelling pressure of a clay depends on the temperature, density, specific surface, and ionic concentration. It is also influenced by the soil fabric and the type of exchangeable cation.

2.2.5 EFFECTIVE STRESS CONCEPT

The concept of effective stress was proposed by Terzaghi in the early 1900's to describe the behaviour of saturated soils. It

forms the basis of modern soil mechanics. In its usual form, the concept states that when the area of contact between soil particles is small, the total stress at a point can be expressed as the tensor sum of the effective stress and the porewater stress. The implication of this statement is that particles transfer forces at "points" or "edges" of contact, and the void spaces are interconnected.

In the case of clays, the particles are small and often bounded by layers of adsorbed water; and therefore they are not in direct mineral-mineral contact. Long range particle interaction associated with repulsive forces due to electrical double diffuse layers, and attractive van der Waals forces, becomes a dominant factor in controlling the volume change behaviour and the strength of the soil (Graham et al., 1986a). It is postulated that, when in equilibrium with their environment, electro-chemical forces between the particles balance the difference between the external applied pressure and the free water pressure in the clay. Therefore, the effective stress can be considered to be equal to the electro-chemical repulsion pressure(Mitchell, 1976; Lambe and Whitman, 1979; Graham et al., 1986a).

2.3 THEORETICAL BACKGROUND

2.3.1 THEORY OF CRITICAL STATE CONCEPT

In conventional soil mechanics calculations, two approaches are used (Wroth and Houlsby, 1985):

(1) Limit analysis, which is concerned only with the equilibrium of

soil masses, deals with stress and strength, and takes no account of deformations.

(2) Deformation analysis deals only with displacements and consolidation properties, and pays no attention to the strength of the soil.

Current research strives to formulate a self-consistent soil model which will allow both deformation and collapse conditions to be dealt with together.

Based on the theories of elasticity and plasticity, Roscoe et al. (1958) introduced the Critical State concept. The basic theory suggests that, under the influence of a certain stress system, soils will continuously deform, and will eventually approach to a critical state, where no further change will take place in effective stress, shear stress, volume, or porewater pressure (Schofield and Wroth, 1961). The concept forms the basis of the so-called Cam-clay model, which was originally proposed to model the behaviour of normally and lightly over-consolidated clays. However, with suitable modification, Cam-clay is also useful in examining the behaviour of overconsolidated clays and sands (Houlsby et al., 1982).

Mathematical constitutive models have the merit that soil behaviour can be assessed quantitatively in a simple framework, which in turn can be used for analysis and design purposes. Cam-clay, in particular, has the advantages of coupling the volume changes and changes in shear stress; modelling strain hardening and softening behaviours of soils; linking together drained and undrained conditions; and accounting for the observed nonlinear behaviour by the specification of an appropriate yield function (Prevost and Hoeg,

1975).

2.3.2 DESCRIPTIVE PARAMETERS

In the past, the choice of test parameters had been dictated by the test type that was employed in the examination of soil behaviour. Very often, due to the simplification of the test and unrealistic assumptions, these parameters might not be representative of the real soil behaviour in the field. For example, the Mohr-Coulomb criterion was often applied to analyze laboratory data, with the consideration of the major and minor principal stresses only. The intermediate principal stress, which undoubtably has some influence on strength and other properties, was omitted. Also, due to lack of communication between laboratories, the same symbols were sometimes used to represent different soil parameters. This often led to confusion and made the interchange of ideas and understanding more difficult than necessary. This section will describe the choice of parameters used in the thesis, and aims at clarifying confusion that sometimes arises. It is based largely on the proposals suggested by Wood (1984), and outlined by Graham et al. (1986a).

In conventional triaxial tests, the specimens have a vertical axis of symmetry so that $\sigma_2 = \sigma_3$ and $\epsilon_2 = \epsilon_3$. As a result the following stress invariants are becoming increasingly used in geotechnical engineering:

Stress: Mean principal

effective stress: $p' = (\sigma_1' + 2\sigma_3')/3$

Deviator stress: $q = (\sigma_1 - \sigma_3)$

$= (\sigma_1' - \sigma_3')$

Strain: Volume strain: $v = \epsilon_1 + 2\epsilon_3$

Shear strain: $\epsilon = 2(\epsilon_1 - \epsilon_3)/3$

$= \epsilon_1 - v/3$

As conventionally assumed in soil mechanics, compressive stresses and strains are positive. These stress and strain variables are carefully chosen so that the incremental work done can be expressed as:

$$dw = p'dv + qd\epsilon$$

Soils are complex materials. In shear, they show dilative or compressive behaviour, associated with negative or positive volume change. Depending upon initial conditions, specimens may exist at different water contents, and their stress-strain characteristics may differ accordingly. This means that examining test results based on strain changes alone is insufficient to obtain a clear picture of the soil behaviour. It is often more useful to use a parameter such as voids ratio (e) - the volume of voids (including water) per unit volume of solids ; or as in Critical State Soil Mechanics (Atkinson and Bransby, 1979; Wroth and Houlsby, 1969), specific volume (V) - the volume of the soil specimen containing unit volume of soil grains.

In the buffer material, it has been shown by Dixon et al. (1985) that the clay dominates the behaviour up to quite large proportions of the sand in the mixture. The sand can be considered to act largely as an inert filler. In this case the complex sand-clay-water relationship can be simplified, and the behaviour of the mixture can be examined on the basis of γ_c, the dry density of the clay-water phase. Alternatively it is convenient to use the specific volume V_c of the clay-water phase, which is defined as the

volume of clay and water occupied by unit volume of clay solids.

In this thesis, the presentation of results will be given in terms of the parameters p', q, and V_c, which are used to uniquely define the "state" of a buffer specimen at any instant of a test.

2.3.3 CONCEPTUAL MODEL

Based on the Critical State concept, and using the test parameters described in Section 2.3.2, Graham et al. (1986a) proposed the conceptual model shown in Figure 2.2 for describing the behaviour of the buffer material. Implicit in the Figure is the q-axis perpendicular to the p',V_c section shown. The states of the material can be conveniently fixed in this three-dimensional space. Note that the stress axis is marked in terms of total stress or effective stress. When specimens are at equilibrium water content in relation to the applied stress level, the effective stress is considered to be the equilibrium osmotic pressure (Section 2.2.5).

In essence, the proposed model identifies two significantly important lines in the p', q, V_c-space. The line CDD' is the Swelling Equilibrium Line (SEL) reached by isotropically consolidated specimens (q=0) after complete water content equilibrium has been reached at any given pressure. The second line PQ is the Critical State Line(CSL) reached after large straining of the specimen has been reached. At this state there are no further changes in q, V or u with additional straining. However this condition cannot be reached definitively in triaxial tests, even in tests where up to 20% axial strain is applied. It is common to plot "end-of-test" or "large strain" values, corresponding to axial strains of 10% to 15%, but it is emphasized

that these specimens are often not classically at Critical States.

In Figure 2.2, test specimens can be envisaged as starting, just after compaction with zero confining stress, at A. Upon the application of consolidation pressure, specimens undergo elastic deformation with a slight reduction in volume, and reach an apparent equilibrium at B. Depending on the duration of consolidation, specimens will end up at points G, F, E, and C on the "time line". Specimens G and F, which lie on the left or "dry" side of the CSL, will reach a peak failure before moving towards critical states. This is similar to the dilative behaviour exhibited by dense sands and overconsolidated clays. On the other hand, specimens C and E lie on the right or "wet" side of PQ, and will show compressive behaviour. Specimens formed on the SEL, such as D, are in pressure - water content equilibrium, and will exhibit compressive characteristics in shear.

A detailed description of the conceptual model has been given by Sun (1986) and by Graham et al. (1986a).

CHAPTER 3

REVIEW: CONSTITUTIVE BEHAVIOUR OF CLAYS AND SAND-CLAY MIXTURES

3.1 INTRODUCTION

The long term disposal of nuclear fuel waste in an underground vault in a stable geological formation has not yet been done in practice. Such a proposal poses a challenge to the engineering industry because there is no basis of experience upon which to proceed with confidence. This necessitates the development of new technology to provide a safe method for the disposal of the waste.

As outlined in Chapter 1, proposals are being studied for disposal in hard crystalline rocks, in evaporites, and in hard clays. The proposals usually utilize a multi-barrier system, which is used primarily to prevent leaching of radionuclides from the containers to the biosphere. A typical system, such as that adopted in the Canadian program, consists of a corrosion-resistant container, a clay-based buffer material, a backfill material, and the rock mass (Bird and Cameron, 1982). These engineered and natural barriers will be expected to function in a variable environment of pressure, groundwater and temperature. Interaction between them is not fully understood. Computer modelling techniques are therefore required to assess the effectiveness of the various barriers and to predict the long term performance of the system. The performance of these computer models must in turn be assessed and improved by comparing obervations from experimental full scale tests, for example at the

Underground Research Laboratory at Pinawa, Manitoba, or at the Stripa test facility in Sweden.

Each component of the Canadian multi-barrier system has received considerable attention in research projects initiated by Atomic Energy of Canada Limited. This thesis considers one of the barriers, the sand-clay buffer used to fill the space between the waste container and the rock. It is a man-made material, and its properties are not well understood. To reach a better understanding, considerable research has already been carried out on the buffer material (for example, Yong et al., 1985; Dixon et al., 1986; Graham et al., 1986a), but further work remains to be done. Results from the research will be used in the formulation of a constitutive model for the buffer material, which will fully describe the stress - strain - time - temperature relationships of the material. It will also include consideration of the swelling - volume change behaviour. Information provided by the model is needed for computer modelling of the container - buffer - rock interaction (Selvadurai et al., 1985).

The following sections describe work that has already been done in the laboratories of AECL, ISMES, and the University of Manitoba on the properties of clays pertinent to nuclear waste management.

3.2 BUFFER RESEARCH AT AECL

Research on clay at AECL has concentrated on the swelling pressures developed in the sand-clay buffer material. An

understanding of the swelling behaviour is essential because the swelling property of the material is required to ensure proper functioning of the buffer in the vault (Gray et al., 1985). In addition, knowledge of the magnitude of the swelling pressure of the buffer is needed in the mechanical design of the waste containers (Dixon et al., 1986).

Graham et al. (1986a) reported a series of laterally confined tests performed on specimens 32 mm in diameter and 30 mm high. These specimens were made of compacted sand-bentonite mixtures having different proportions of sands to clays. The purpose of the tests was to investigate the swelling and compressive characteristics of the buffer material. The tests were carried out using two different testing techniques, namely confined swelling and one-dimensional compression.

In confined swell tests, the specimens were formed with different densities and water contents, and tested at constant volume. The specimens were given free access to water and this allowed swelling pressures p'_s to develop in the mixtures that depended on the conditions of testing.

From these tests, the swelling pressure - density relationship shown in Figure 3.1 has been postulated. It has been developed from the findings made by Gray et al. (1985) who showed that the swelling pressures in the sand-bentonite mixtures are independent of the sand content, but depend on the specific volume (void ratio) of the clay phase. The relationship shown in Figure 3.1 was later used as the SEL in the Critical State model shown in Figure 2.2, and has formed the starting point for the research program that will be described

subsequently.

Specimens in the one-dimensional compression test were formed at their liquid limits, and then compressed one-dimensionally under increasing axial stress. Results from these tests are shown in Figure 3.2 in terms of the clay specific volume V_c, and the axial stress σ'_v in log-log space. The relationship is approximately linear. Also shown in the same figure is the relationship established in Figure 3.1. The trends of the two lines in general are similar, although the positions of the lines in the Figure are somewhat different. The disagreement is probably because Figure 3.1 used spherical (mean principal) stress, and Figure 3.2 used vertical stress (Dr. M.N. Gray, personal communication to Dr. J. Graham). Another probable explanation is that the mechanism of test, and therefore the straining experienced by the clay particles, was different in the two tests (Seed et al., 1962; Mitchell, 1976; and Sridharan et al., 1986). In the former, the mixtures were allowed to develop their swelling pressures at constant volume, while the latter involved compression of the specimens.

In another investigation aimed at establishing the pressures acting on the waste containers, Dixon et al. (1986) investigated the validity of the effective stress concept in the buffer material (The effective stress concept was outlined in chapter 2). Tests were performed in a stiff confined apparatus, in which compacted sand-bentonite specimens were given free access to water and allowed to develop their swelling pressures. After equilibrium had been reached, the porewater pressure in the specimens was increased to 10.0 MPa in increments. The total pressure, which is the sum of the

swelling (osmotic) pressure and the pore pressure, was measured. Results are shown in Figure 3.3. It is clear that the measured total pressure was always larger than the applied porewater pressure and increased linearly with it. For expansive clays such as the bentonite in the buffer material, the effective stress can be considered as the swelling pressure (Lambe and Whitman, 1979). The investigation therefore tended to confirm the applicability of the effective stress concept on the reference buffer material.

3.3 RESEARCH ON TEMPERATURE EFFECT ON CLAYS AT ISMES (Bergamo, Italy)

One of the principal reasons that clays are useful in waste disposal is their low hydraulic conductivity (Bird and Cameron, 1982). Nuclear waste containment introduces the unique difficulty that the waste is a heat source that causes temperature increase in the clay. Little is known about how this affects clay behaviour, but it may result in an increase in porewater pressure caused by thermal expansion of water and water-mineral interaction (Baldi et al., 1985). In principle, the high porewater pressure buildup may give rise to the following:

(1) the generation of a hydraulic gradient in the vicinity around the waste container.

(2) a reduction in effective stress in the soil.

Baldi et al. (1985) reported the results of a series of thermal mechanical tests carried out on overconsolidated, normally consolidated, and remoulded clay specimens. The clays used in the study were a kaolin, Pontida silty clay, and intact Boom clay. The

specimens underwent a cycle of loading, consisting of (1) incremental consolidation at room temperature; (2) heating under constant pressure; (3) loading and unloading at constant elevated temperature; (4) cooling at constant low pressure; and (5) isothermal reloading involving normal consolidation. From their investigation, they concluded that:

(1) the thermally induced volume strains were compressive.

(2) the magnitude of thermal strains were stress and temperature dependent.

(3) the normally consolidated specimens exhibited larger thermal strains than the overconsolidated ones.

(4) thermal strains were irreversible in the normally consolidated and remoulded specimens.

It should be noted that this is the only triaxial test program known to include the effects of temperature on the stress-strain properties of clay mixture. Temperature effects on swell pressures have been presented by Yong (1967). Model heater tests have been performed in the laboratories of Carlton University in Ottawa and Ontario Hydro in Toronto (Dr. J. Graham, personal communication). The clay materials tested in the ISMES investigation differ from the sand - clay mixture used in the Canadian program. Nevertheless it addressed the problem of temperature effect, and points out the direction of future research on the sand-clay material in the Canadian investigation.

3.4 BUFFER RESEARCH AT THE UNIVERSITY OF MANITOBA

3.4.1 INTRODUCTION

Research on the sand-clay buffer material was first initiated by a contract proposal submitted by Dr. J. Graham and Dr. D. H. Shields to Atomic Energy of Canada Limited in 1984. The objective of the research is to gain an understanding of the buffer material and to obtain its stress - strain - time characteristics, which are required for computer modelling.

The research program was funded by two contracts from AECL resulting in two consecutive phases of research. The 800-series of the first phase was funded by contract No. WS-24J-18735. The second phase consists of two separate testing programs, the 900-series and 950-series, funded by contract No. WS-25K-31620.

The 800- and 900-series are the same in principle, with the later series extending to higher test pressures. The specimens were prepared utilizing the same specimen preparation technique. They were all compacted to a nominal dry density of 1.50 Mg/m^3 and a water content of 28%. The 800-series began in 1984 and completed in 1985. The highest effective pressure reached in the 800-series was 1.0 MPa, at room temperature of 23°C. The subsequent 900-series is currently still in progress. In this series, the effects of higher pressures up to 10.0 MPa and temperatures up to 100°C will be examined. This has necessitated the development of special testing equipment and development of a data acquisition and reduction system.

The 950-series forms the basis of this thesis. Triaxial specimens were prepared using different techniques that will be

described in detail in subsequent chapters. At this stage it is sufficient to note that the highest test pressure was 1.5 MPa at 23°C.

3.4.2 PREVIOUS WORK: 800-SERIES

3.4.2.1 PROGRAM

The findings of this series have been documented by Sun(1986) and by Graham et al. (1986a). A series of triaxial tests was performed on compacted sand-clay specimens measuring 50mm in diameter and 100mm high. Specimens were formed from a 50:50 sand-clay mixture, compacted to a nominal dry density of 1.50 Mg/m^3, and a water content of 28%.

Three types of tests were carried out.

(1) Isotropic consolidation tests with incremental cell pressures examined the pressure - volume - time relationship and to evaluate the psuedo-elastic bulk modulus of the material.

(2) Strain controlled triaxial compression tests were performed with porewater pressure measurement to determine the strength envelope.

(3) Load controlled drained tests were run with constant mean effective pressure, and incremental shear stresses were applied in succession. This gave estimates for the shear modulus.

3.4.2.2 RESULTS

The results are shown in Figure 3.4, plotted in the form of stress paths projected on the p', q stress plane. The specimens were initially consolidated isotropically along the p' axis (q=0). Two consolidation procedures were adopted. One was called the "short duration" test, in which the final pressure was applied in one

increment and the specimen was allowed to consolidate for about 10 days. In the other method, confining pressures were added in a series of 5 increments, each of which was held constant for about 10 days. The period of consolidation was therefore about 50 days. This was referred to as "long duration" testing.

A total of eight undrained strain-controlled triaxial tests were performed with porewater pressure measurement. Typical stress - strain curves are shown in Figure 3.5. Failure defined here as maximum shear stress typically occurred at axial strains in the range 4% to 8%. Porewater pressures in most of the tests increased initially, but then decreased as failure was approached. The shearing resistance decreased by a small amount after failure, indicating a slightly strain softening behaviour.

Five load-controlled drained shear tests were also carried out. Figure 3.6 shows axial strain and axial stress variations with time in a typical test. In general, little deformation was observed during early increments of shear stress. However the specimen accelerated towards rupture at the highest shear stress and showed large axial strains at failure. The shear stress - shear strain relationship obtained from the same test is given in Figure 3.7. The shear modulus of the buffer material was taken for simplicity as the secant modulus at $q_{max}/2$ and has a magnitude of (slope of q vs ϵ)/3 (Sun, 1986). Figure 3.8 summarizes the drained test results, and suggests that the shear moduli normalized by the consolidation pressure do not depend on the stress level of testing.

Figure 3.9 shows a typical plot of volume strain vs. time in a "long duration" consolidation test during increments of consolidation

pressure p'. The specimen initially showed a compressive response followed by swelling. From Figure 3.10, it can be seen that the pressure - volume - time behaviour of the buffer is nonlinear and complex. For the purpose of comparison, the results were described by the slope K of a straight line approximating the p', v relationship during the last two loading increments, as shown in Figure 3.11. It is evident in this case that the moduli are pressure-dependent, increasing with confining pressure.

3.4.2.3 CONCLUSIONS

The results from the investigation indicate that the buffer material has a complex, nonlinear stress - strain - time behaviour, featuring slightly strain softening characteristics. For the "fully softened" specimens, which had undergone a long period of consolidation, the Coulomb-Mohr strength parameters are c'= 0 kPa and Ø'= 16°. Specimens from "short duration" tests indicate a strength envelope of c'= 48 kPa and Ø'= 13°. Results obtained from this preliminary research enabled an initial understanding of the buffer. However because of limitations of the laboratory facilities at the time, the tests were run under conditions that were far from the actual environment in which the buffer material will eventually operate. For example, tests were performed at 23°C, with the maximum pressure restricted to 1.0 MPa, as opposed to the conditions of 100°C and 10.0 MPa that are anticipated in the vault. Nevertheless, problem areas were highlighted and preparation made for further research.

3.4.3 CURRENT RESEARCH: 900-SERIES AND 950-SERIES

Results from the early stages of this phase of testing up to November 1986 have been reported by Graham et al. (1986b).

3.4.3.1 900-SERIES

The purpose of this series has been to extend the scope of investigation to higher testing pressure levels and temperatures. The tests used the same specimen preparation technique as the earlier 800-series at the time of writing. Specimens are currently being tested at effective pressures up to 3.0 MPa at 23°C. The next stages of the study will increase the testing pressures to 10.0 MPa, and temperatures to 100°C. This will enable a better simulation of actual conditions existing in the underground vault. However the work forms the doctoral program of a fellow graduate student and will be reported in detail in his thesis. No further results of his work will be given here.

3.4.3.2 950-SERIES

One of the serious questions that were raised from the study in the 800-series regarded the pressure - water content equilibrium condition of the specimens prior to shear. Because of the initial conditions of pressure, void ratio and drainage in the tests and the low hydraulic conductivity of the buffer, the specimens required very long consolidation times of the order of several weeks to achieve what was taken as pressure - water content equilibrium. Due to time limitations, the majority of the tests were performed on specimens which had not reached the stage of full equilibrium. Graham et al.

(1986b) reported that the specimen had reached on average a low volume straining rate less than 0.1 %/day. Earlier work by M.N. Gray (personal communication) suggested that very long consolidation times are required to reach complete equilibrium.

The majority of specimens in the 800-series at the University of Manitoba swelled under the application of their consolidation pressure. "Equilibrium" in the tests was therefore taken as the end of swelling, but it should be recognized that full equilibrium had not been reached. Because the swelling was typically incomplete in the 800-series tests, the specimens had not swelled totally along the "time line" BC in Figure 2.2, and had not reached the Swelling Equilibrium Line (SEL). That is, they existed at a state such as E or F depending on the duration of the consolidation phase and the measured rate of volume change. Specimens consolidated for long periods (E) tended to be compressive when sheared. Specimens with shorter consolidations (F) tended to be dilative, and suggested behaviour similar to overconsolidation.

The main objective of the study in the 950-series which formed the work described in this thesis was therefore to investigate a proposal for minimising the duration of the initial consolidation phase of the specimens. This would enable more tests to be done on fully equilibrated specimens in a given timeperiod. To achieve this goal, an alternative preparation technique had to be explored for preparing specimens that would be close to water content equilibrium at the pressure to be used during consolidation. They could therefore reasonably be expected to exhibit only small volume changes, and therefore to be less influenced by factors such as drainage times and

low permeability. A detailed description of the method of specimen preparation will be given in Chapter 4.

The second objective in the study was to investigate the validity of the swelling pressure - density relationship proposed by Dixon et al. (1986) from their one-dimensional confined swell tests at stresses up to 3.0 MPa. Since the strain conditions in the two types of test were different, a new relationship would be developed using data obtained from triaxial tests on the buffer at effective testing pressures up to 1.5 MPa. The results will be described in detail in following chapters.

CHAPTER 4

BASIC PROPERTIES AND SPECIMEN PREPARATION

4.1 INTRODUCTION

This chapter reviews the basic properties of the Reference Buffer Material (RBM) and its components as they refer to the compaction of the test specimens. The techniques and procedures for preparing the specimens used in this study are also described.

4.2 PROPERTIES OF BUFFER

4.2.1 SOIL CLASSIFICATION

4.2.1.1 SODIUM BENTONITE

The clay used in forming the RBM is a sodium bentonite, sold commercially as "Avonseal", produced by Avonlea Mineral Industries at Regina. The natural material came from the Bearpaw Formation of Upper Cretaceous Age in South Saskatchewan. The clay is a whitish grey powdered clay obtained by controlled drying (less than 120°C) and grinding processes on the natural soil (Quigley, 1984; Dixon and Gray, 1985). It has a liquid limit of 250% and a plasticity index of 200%. The water content of the commercially available material is about 6% to 8%. The bentonite contains predominantly of sodium montmorillonite (79%) (Quigley, 1984), which causes the swelling behaviour of the RBM. Other minerals include illite, quartz, feldpar, gypsum and carbonate.

The material was selected by AECL as a potential constitutent of the RBM because of its abundance (Dixon and Wookcock, 1986) and its favourable compaction and swelling properties (Dixon et al., 1985).

4.2.1.2 SILICA SAND

The sand component of the RBM is a well-graded mixture of subrounded fine to medium crushed silica sand. Figure 4.1 shows the particle size distribution of the sand mixture. The particle size distribution was selected using the Talbot-Richart formula (Dixon and Woodcock, 1986) to facilitate obtaining high density in the buffer. High density is desirable in nuclear waste containment because it reduces the hydraulic conductivity and increases the sorptivity of radionuclides of the RBM (Gray et al., 1984). However this has to be balanced against the high swelling pressures produced by the dense buffer on fuel waste containers.

4.2.2 COMPACTION PROPERTIES

The compaction properties of sand-clay mixtures including the RBM have been studied by Dixon et al. (1985). Figure 4.2 shows the dry density-water content relationships developed for the mixtures as a result of their investigation.

They observed that optimum water content and corresponding maximum dry density could not be achieved in the 50:50 sand-clay buffer mixtures. This is because smectitic clays such as bentonite have a high affinity for water, and develop layers of adsorbed water on the particle surface on wetting. These adsorbed water layers have

higher viscosity than the normal interstitial water (Yong and Warkentin, 1975), and they are expected to influence on the shearing resistance of the buffer. At low water contents in the studies by Dixon et al. (1985), the compaction effort was not sufficient to overcome the high shearing resistance of the adsorbed water layers round the clay particles. The inability to measure maximum dry density in the buffer, however, has an important practical implication that readily attainable dry densities are relatively insensitive to the water content provided some critical water content is not exceeded. This has the advantage that during "insitu" compaction, stringent control of water content should not be required (Dixon et al., 1985).

Their test results also indicated that the average saturation of the specimens was only about 97%. Fully-saturated specimens could not be achieved. Similar degrees of saturation were observed in the specimens tested in the 800-series and 950-series at The University of Manitoba (Sun, 1986; Graham et al., 1986b). The incomplete saturation was in part due to the viscous nature of the adsorbed water layers round the clay particles, which requires a higher input of compactive energy to achieve full saturation. Also because of the confining nature of the compaction apparatus, air bubbles that were trapped during specimen preparation could not be driven out easily. They were therefore forced to dissolve into pore water during the application of the compaction pressure. Upon the removal of the pressure, some of the dissolved air was released from solution, causing incomplete saturation of specimens. Unloading also permits elastic expansion of the compacted soil fabric.

4.2.3 SWELLING PROPERTIES RELATED TO DESIGN OF TEST PROGRAM

The mechanism of swelling in clays has been described in Chapter 2. The swell phenomenon is particularly evident in smectitic clays because of the weak bonding between the sheets forming the clay particles and other factors such as temperature and cation exchange.

Gray et al. (1985) reported results from a series of one-dimensional confined swell tests on specimens of sand-clay mixtures compacted at different proportions. They concluded that the swelling pressure developed in the buffer material was controlled by the effective clay density and was independent of the sand content. They postulated the swelling pressure - effective clay dry density relationship shown in Figure 4.3a. An updated version of the relationship was later given by Dixon et al. (1986) and has been shown in Figure 3.1. This updated relationship covers the pressure range from 0.7 to 3.0 MPa in Figure 4.3a, and has been enhanced by additional data from one-dimensional compression tests. The pressure - density relationship in Figure 3.1 formed the basis of the research described in this thesis.

Gray et al. (1985) concluded from the data in Fig. 4.3a that, up to a threshold effective clay dry density of about 1.70 Mg/m^3, swelling pressures developed in the buffer are isotropic, and can be predicted on theoretical grounds using the equation,

$$p_s = \frac{80.3}{\left[\frac{10^4}{S}\left(\frac{1}{\gamma_c} - 0.364\right)\right]^2}$$

Comparison of their experimental data and the theoretical solution is shown in Figure 4.3b.

However at clay densities above the threshold value, the measured swelling pressures exceed those predicted from the above equation. This is because at high stresses, one-dimensional compaction in a mould results in the formation of dispersed (oriented) structures rather than flocculent (randomly oriented) structures in the clay mixture. That is, clay particles are forced to orientate themselves to a direction perpendicular to the axis of compaction. This induced anisotropy in the clay fabric causes the swelling pressure along the axis of compaction to exceed the pressures orthogonal to it.

For buffers compacted round the fuel waste containers under highly saline groundwater conditions, Dixon et al.(1986) showed that the swelling pressure should not be more than 1.5 MPa. The result is slightly modified from the corresponding value of 2.5 MPa given by Gray et al.(1985). From Figure 3.1, this pressure corresponds to a dry density of about 1.20 Mg/m^3, significantly less than the threshold value of 1.70 Mg/m^3 in Figure 4.3a. In field installations, the RBM can therefore be expected to exert an isotropic swelling pressure which is equal in all three orthogonal directions.

It should be noted that the effect of temperature on swelling pressure in the RBM has not yet been studied. This problem will shortly be examined in the laboratories of the University of Manitoba. However, research on the influence of temperature on compacted clays and clay mixtures has been reported. Yong (1967) investigated the swelling of a compacted montmorillonitic clay at elevated

temperatures; and Sheriff et al. (1982) researched the temperature effect on the swelling of sand-clay mixtures consisting of Wyoming montmorillonite and Ottawa sand. Results from both of these studies indicate that the swelling pressure increases with temperature. However recent work in Switzerland and Sweden suggest that this may not always be true (M.N. Gray, personal communication).

4.2.4 INFLUENCE OF CREEP PROPERTIES ON TESTING PROCEDURES

The creep properties of the RBM have been studied by Yong et al. (1985). Tests were conducted on a small-scale physical model simulating the rock - buffer - container system, under various combinations of overburden pressure and hydrostatic conditon. The effect of temperature, however, was not included in the investigation. A finite element analytical model was also employed. Results from the experimental and theoretical studies were then compared, and the creep behaviour of the full scale system was predicted with the analytical model.

Results from the model tests indicated that the amount of deformation of the RBM upon loading was primarily governed by the primary creep mechanism, which terminated typically after ten days. Secondary creep was negligible. It was also found that the effect of overburden pressure and water intake greatly affected the creep properties of the RBM. Low overburden pressure resulted in nonuniform deformation of the RBM at the top and bottom of the container, causing separation between the material and the container top. However it was anticipated that this problem would be avoided by the swelling properties of the RBM. The tests also indicated that the water intake

of the RBM caused substantial deformation of the material.

As pointed out by Sun (1986), a knowledge of the creep characteristics of the RBM is essential as they influence certain aspects of the buffer research, such as the duration of the load increments used in load-controlled drained tests. The load increment ratios used in the program were relatively small and much of the observed deformation behaviour resulted from creep movements of the interparticle structure of the clay.

4.3 SPECIMEN PREPARATION

4.3.1 INTRODUCTION

The test specimens used in this study were specifically prepared cylindrical specimens made of compacted sand-clay mixtures. The preparation procedures adopted in the study followed closely to those in the previous 800-series by Sun (1986). However some modifications were undertaken in order to facilitate the compaction process and to produce better quality, more consistent test specimens. In addition to these points that refined the techniques of specimen preparation, there was also a major and fundamental change whereby the specimens were compacted at a variety of densities and water contents, rather than at the fixed values used in the earlier work.

4.3.2 PREPARATION TECHNIQUE

In the 800-series, the buffer specimens were compacted in a cylindrical mould to a nominal dry density of 1.50 Mg/m^3 at 28% water

content (Sun, 1986; Graham et al., 1986a). In the conceptual model shown in Figure 2.2, this initial condition is depicted by point A. Initially the specimen at A will have pore suctions (negative porewater pressures) and hence positive (compressive) effective stresses that contribute its strength and rigidity under zero confining pressure. The specimen was allowed to consolidate under an all-round confining pressure. Depending on the magnitude of the consolidation pressure, the specimens would either swell or compress at constant applied pressure, and gradually move towards the Swelling Equilibrium Line (SEL). Graham et al. (1986a) argued that this represents an equilibrium condition where the effective stresses and osmotic pressures were equal. Due to the compactness of the buffer mixture and the high affinity of bentonite for water, the permeability of these specimens was very low, and complete pressure - water content equilibrium in these specimens could not be easily achieved in a short period of time. Volume straining rates of about 0.1 %/day were observed, even after test times approaching 10 to 30 days. The majority of the specimens tested in that series were therefore not fully equilibrated. To minimize disadvantages associated with long consolidation times and incomplete equilibrium of specimens prepared in this way, a new preparation technique was therefore developed for the specimens in the 950-series, and formed the basis of this thesis.

In formulating the conceptual model in Chapter 2, Graham et al. (1986a) took the swelling pressure - effective clay dry density relationship (Dixon et al., 1986) shown in Figure 3.1 to be the SEL. They assumed it to be equivalent to the NCL for non-swelling soils. As a corollary, when specimens are in equilibrium, the swelling pressure

(taken as the difference between the external applied pressure and the free porewater pressure) can be treated as the apparent preconsolidation pressure of the material (Sun, 1986). Hence, specimens which lie on the SEL, are in pressure - water content equilibrium. They should have no further tendency towards volume expansion or compression under the applied pressure.

Following this idea, the SEL shown in Figure 3.1 was therefore utilized in the development of the specimen preparation technique. Test specimens were formed at various water contents and dry densities that would place them on the SEL at the pressures at which they would be tested. However it should be noted that the SEL was originally determined from one-dimensional compression tests at pressures higher than 0.7 MPa. There was some concern regarding its capability of predicting pressure - water content equilibrium of specimens tested under traxial conditions in the pressure range 0.1 MPa to 1.5 MPa.

This concern led to the development of a new SEL derived from the end - of - consolidation data collected from specifically triaxial tests in the 800-series and the early tests from the 950-series. This new swelling pressure - effective clay dry density relationship is shown in Figure 4.4. To facilitate the calculation of water content at a given swelling pressure, the swelling pressure - water content relationship shown in Figure 4.5 was developed from Figure 4.4. Test specimens were then formed according to Figure 4.5. Figure 4.5 was in turn refined by the end-of-consolidation data obtained from subsequent tests in the 950-series to enhance its ability to predict equilibrium water content / density for the desired consolidation pressure. The volume change behaviour of the specimens prepared from this new

technique will be discussed in detail in Chapters 6 and 7.

4.3.3 COMPACTION OF SPECIMENS

The mixing procedure adopted in this study was similiar to that used in the 800-series. All test specimens (both quality control and triaxial) were cylindrical, measuring 50 mm in diameter and 100 mm in height. Deaired distilled water was used throughout the testing program. Prior to mixing, the silica sand and the sodium bentonite were ovendried for 24 hours at 110°C (ASTM, 1986). After cooling to room temperature, the weights of distilled water and silica sand were added to a large mixing bowl and mixed together. The required quantity of bentonite was then added slowly in several increments to the sand-water mixture, and stirred carefully until all the sand grains are bounded by clay particles. The mixture was then stored in an airtight plastic container and cured in a moisture room at 6°c for a period of 3 days. Before final compaction, the mixture was placed in a deairing chamber for a period of 5 minutes. This reduced the amount of air dissolved in porewater during mixing. (A balance had to be drawn between the advantage of removing air from the porefluid and the disadvantage of boiling off water vapour). The mixture was then compressed in 5 layers into a rigid cylindrical mould. (For quality control specimens, they were compacted into 5 to 8 layers to examine the influence of the number of layers).

In this study, a slightly modified compaction procedure from that used by Sun (1986) was adopted. Initially, the first thirteen quality control specimens were formed following the method used in the 800-series. However in this study, a wide range of water contents

from 18% to 40% were to be used, and some problems were encountered with mixtures having high water content. Because of the higher mobility of these mixtures, soil was observed to be intruded during compaction into the small gap between the compaction piston and the inner wall of the mould. The problem was twofold. First, this would result in non-uniform specimens as the intruded soil involved was predominantly bentonite. Second, the soil in the gap caused some friction between the mould and the piston, and this reduced the compactive force acting on the soil mixtures inside. The friction also caused difficulty in removing the piston from the mould, which led to concerns about specimen disturbance. There was also concern that the intruded soil formed a seal that permitted the generation of suctions and tensile stresses in the specimen as the piston was removed.

In the modified method, after the required quantity of soil mixture for one layer was placed in the mould, an O-ring seal was positioned between the mixture and the piston. The mixture was then compressed statically by the required amount. The ring was then removed and the top surface of the compacted material was lightly scraped to ensure good bonding between adjoining layers. The same procedure repeated for the following layers. Finally the specimen was extruded from the mould, and trimmed to size. Its bulk density and water content were determined. The setting up procedures for triaxial testing will be described in Chapter 5.

CHAPTER 5

TESTING PROGRAM AND TEST PROCEDURES

5.1 INTRODUCTION

The major component of this study consisted of triaxial testing on compacted sand-clay buffer specimens. Both undrained and drained triaxial tests were performed in order to obtain the stress - strain - time parameters and strength parameters of the buffer material. These parameters will be used at a later stage in the formulation of a constitutive relationship that describes the stress - strain - time - temperature behavior of the buffer. The relationship is needed in computer modelling studies of the buffer interaction with the rock mass and waste container in the disposal vault (Graham et al., 1986a). This chapter summarizes the triaxial testing program that has been accomplished and the test procedures used in the investigation.

5.2 TESTING PROGRAM

The program was essentially divided into three types of tests performed in triaxial load cells: consolidation tests, undrained shear tests, and drained shear tests. A total of twelve specimens was tested in this study. Table 5.1 summarizes the initial conditions of the test specimens. All specimens were initially subjected to consolidation stresses for periods from 10 days to 100 days, after

which they were sheared under either undrained or drained conditions. On the completion of shear, the bulk densities and water contents of the specimens were determined.

5.2.1 CONSOLIDATION

The primary purpose of the consolidation tests was to investigate the volume change behaviour of the specimens of the buffer material. The specimens were prepared according to the technique outlined in Chapter 4 so that they were notionally at pressure - water content equilibrium, and therefore should exhibit little volume change during the consolidation phase.

In this study, the effective consolidation pressure ranged from 0.1 MPa to 1.5 MPa. Two types of consolidation technique were used: single-stage and multi-stage consolidation. In single-stage consolidation, specimens T951 to T960 were consolidated directly to the desired effective pressures in one stage (for specimens T954 to T960, a nominal back pressure of 200 kPa was used during the tests and the total applied cell pressure was raised accordingly). These tests were carried out to examine whether the general consolidation behaviour of the buffer as presented for example in Figure 3.1 was applicable to specimens.

In the two specimens that used multi-stage consolidation, specimen T961 was consolidated in three stages, and specimen T962 in two stages. In the first stage, they were initially consolidated at their desired effective confining pressures and the corresponding water contents from Figure 4.5. A back pressure of 200 kPa was used. In the second stage, both the total confining pressures and the back

pressures on the specimens were increased by the same amount, thereby keeping the effective pressures constant. This step was used to investigate the applicability of the effective stress principle on the buffer. If the specimens were in fact fully consolidated under the pressures in the preceding stage, then no further volume straining should result. The third stage of consolidation on specimen T961 aimed at confirming the swelling pressure - water content relationship shown in Figure 4.5. In this case, the effective pressure on the specimen was increased by increasing the total confining pressure, but keeping the back pressure constant. The resulting volume changes were monitored. At the end of consolidation, the final water content of the specimen under its new effective pressure was measured. If the relationship represented the swelling pressure - water content equilibrium of the buffer, then the measured water content should compare well with the predicted value from Figure 4.5.

5.2.2 UNDRAINED SHEAR

Undrained tests with porewater pressure measurements were conducted on nine specimens (T951 to T957, T961 and T962). The tests were carried out to provide information on the strength, the stress-strain, and the porewater pressure generation characteristics on the buffer material. Important parameters obtained from the tests are the strength parameters (c' and Ø'), undrained shear moduli (E_{50} and G_{50}), and porewater pressure parameters at failure (A_f).

A major factor that affects the strength of the soil and the porewater pressure measurements in undrained testing is the choice of strain rate (Bishop and Henkel, 1962; Graham et al., 1983a). In the

previous 800-series study, a strain rate of 1.2 %/hour was used, and this rate conformed with those used in the early research on Winnipeg clay at the University of Manitoba (Noonan, 1980; Lew, 1981). Because of the low hydraulic conductivity of the compacted buffer specimens, some anxiety was raised regarding the time for full porewater pressure equalization in these specimens. For this reason, a much slower strain rate of the order of 0.12 %/hour was desired. However, without the aid of a data acquisition system (which was not available during the course of this research) this rate was not possible in the laboratory because of the long test times that would be needed. On the basis of practicality, a strain rate of 0.6 %/hour was used in seven of the nine undrained tests (T952 to T957, T962). This lengthened the test times significantly, and involved continuous monitoring of the specimens for periods of up to two days.

Some leakage problem was encountered with the first specimen (T951) that was tested. It was therefore sheared at the faster rate of 1.2 %/hour corresponding with the speed in the previous series. For specimen T961, the effect of strain rate variation on the undrained strength was examined. The specimen was sheared at three different rates of 3.0 %/hour, 0.6 %/hour, and 0.12 %/hour. In addition, a relaxation test (Graham et al., 1983a) was performed during the course of the shearing.

5.2.3 DRAINED SHEAR

Specimens T958 to T960 were subjected to load-controlled drained shear tests. Each of the specimens was designed to have a series of constant-sized increments of shear stress q at a constant

mean principal stress p' before it failed on the previously established strength envelope (Graham et al., 1986b) shown in Figure 5.1. Eight increments were used for T958; and six increments for T959 and T960. Each increment lasted for a period of five days, at which stage the shear strain creep rate was considered to be acceptably small (Yong et al., 1985; Sun, 1986). The stress paths for these drained tests are shown in Figure 5.2.

5.3 TEST PROCEDURES

Test procedures adopted in this study followed closely to those developed in the laboratories of University of Manitoba (see for example, Noonan, 1980) in previous years. Some modifications were however undertaken, and they are highlighted in the following sections.

5.3.1 SETTING UP

The setting up of specimens in a triaxial cell is an important process because improper installation of either the specimens, the drainage control systems, or the instrumentation affects the conclusions that can be drawn from the tests. In this study, special care was taken to ensure proper functioning of the triaxial apparatus. Prior to the commencement of each test, the triaxial cell and all drainage connections were checked for leakage. Steps were also taken to optimize the building-in process and therefore hopefully to minimise the disturbance of the specimens.

Some changes in the building-in procedures were made in this

study from those used by Sun (1986). First, only bottom-end drainage, as opposed to both top and bottom drainage in the 800-series, was used. This eliminated continuing leakage problems with the top drainage connections experienced in the parallel 900-series program during the early stages of this research. Second, side filter drains placed in the form of a spiral arrangement, instead of longitudinal vertical filter strips, were used on the specimens. This minimised both lateral and vertical restraints imposed on the specimens by the drains (Gens, 1982, reported by Head, 1986).

Prior to building-in, a thin layer of silicone grease was applied to the sides of the top cap and the pedestal on the cell base. The bottom drainage was flushed with deaired water to eliminate entrapped air, and a saturated deaired filter stone was placed on the pedestal. The compacted specimen with saturated filter paper discs attached to both ends was carefully slid on to the filter stone; the top cap slid on the top end of the specimen; and filter paper strips placed around the specimen. A latex membrane was then placed on the specimen, and sealed to the pedestal with two O-rings. Air trapped between the specimen and membrane was removed by stroking upwards with light finger pressure. A thin layer of silicone oil was then applied to the outside of the first membrane, followed by the application of a second membrane, which was sealed on the pedestal and top cap with a total of four O-rings. The cell top was then fitted onto the cell base, and the cell filled with deaired water. A 2 cm thick layer of engine oil was applied through the cell top to reduce cell water leakage, and to reduce piston friction during shear.

5.3.2 CONSOLIDATION TESTS

All twelve specimens were consolidated isotropically at effective pressures that ranged from 0.1 to 1.5 MPa. With the exception of the first three specimens (T951 to T953), all tests were carried out under a back pressure of 200 kPa or higher. The use of back pressure during the tests was another improvement of the test procedure used in the 800-series. The change was undertaken because the back pressure improved the saturation of the specimens and facilitated the volume change measurement.

The cell pressure was applied through deaired water in the triaxial cell, pressurised by compressed nitrogen gas through an external water reservoir. For specimens T954 to T960, the cell pressure and the back pressure in the speceimens were increased simultaneously in 4 increments of 50 kPa. The volume change of the specimens was recorded at convenient time intervals. Both the cell pressure and porewater pressure were monitored by electrical pressure transducers housed in rigid brass blocks attached to the cell base. They were re-zeroed to atmospheric pressure daily at mid-height of the specimen.

Because of the nature of the tests described in Section 5.2.1, a special consolidation procedure involving the use of higher back pressures was applied to specimens T961 and T962. For specimen T961 the consolidation test consisted of three stages. In the first stage, a total cell pressure of 700 kPa and a back pressure of 200 kPa were employed, resulting in an effective pressure of 500 kPa acting on the specimen. In the second stage, both the cell pressure and back pressure were raised by 300 kPa to 1000 kPa and 500 kPa respectively,

keeping the effective pressure constant at 500 kPa. The third stage involved increasing the total pressure to 1400 kPa, but keeping the back pressure constant at 500 kPa. The effective pressure in the specimen was therefore 900 kPa.

Specimen T962 was consolidated in two stages: first, under a total confining pressure of 500 kPa and a back pressure of 200 kPa; and then 700 kPa total pressure and 400 kPa back pressure. The effective pressure was kept at 300 kPa throughout the test, which lasted for 100 days.

5.3.3 UNDRAINED TESTS

Nine specimens (T951 to T957, T961, T962) were subjected to strain-controlled undrained shearing after consolidation. Prior to undrained shear, the saturation of the specimen was checked by performing a B-test. This was accomplished by shutting off the bottom drainage to the specimen; increasing the total cell pressure by an increment of 50 kPa; and then measuring the resulting porewater pressure response in the specimen. The saturation was then calculated from the equation $B = \Delta u / \Delta \sigma$. A B-value of 98% or more is considered acceptable for research purposes. Table 5.2 summarises the acceptable saturation levels of the specimens before undrained shear. Back pressuring has clearly produced better saturation and B-values than those achieved by Sun (1986).

Following the B-test, the triaxial cell was then carefully transferred to a Wykeham Farrance 10 kN compression frame. All the electrical and pressure connections were maintained in place during this transfer. The desired strain rate was then set, and the

compression machine was switched on to begin shearing.

During the test, readings of axial deformation, proving ring deflection, porewater pressure and cell pressure were taken at intervals of 5 to 10 minutes in the first 1 to 2 hours, and then at intervals of 30 to 60 minutes thereafter until the peak proving ring load had been reached. After that, readings were taken at a longer interval of 2 to 6 hours. The tests were typically terminated at axial strains of 12% to 15%.

The effect of changes in strain rate on the undrained shear resistance of the buffer was studied using specimen T961. This was accomplished by a "step changing" procedure and a relaxation test. The "step changing" procedure involved changing the rate of feed of the compression machine during the test. Three different rates of 3.0 %/hour, 0.6 %/hour and 0.12 %/hour were used in the test. The relaxation test was performed at about 10% axial strain, by switching off the compression manchine, allowing the specimen to continue straining at a decreasing rate as a result of the stored energy in the proving ring. Changes with time in axial deformation, proving ring deflection, porewater pressure and cell pressure were recorded. The test was continued overnight. On the following morning, the compression machine was switched on again, and the shearing resumed. The test was finally terminated in the usual fashion at about 13% axial strain.

5.3.4 DRAINED TESTS

Three specimens (T958-T960) were subjected to load controlled drained shearing after consolidation. As mentioned previously,

failure of each specimen was brought about by applying a series of constant-sized increments of deviator stress q at a constant mean principal stress p'. The failure stress was designed on the basis of the anticipated rupture envelope (Figure 5.1) determined from the results of the 900-series and the undrained data obtained from the earlier phase of the 950-series. Figure 5.2 presents the proposed stress paths used in the tests.

Each increment of shear stress was applied by increasing the axial stress on the specimen and then (after 30 to 60 minutes) decreasing the confining pressure correspondingly to produce the desired conditions of q and p'. Axial stresses were induced on the specimen by putting weights on a hanger which rested freely on the piston. After the application of the stresses, axial dial gauge and buret readings were taken at convenient time intervals. The increments of shear stress were typically kept on the specimens for periods of five days.

5.4 WATER CONTENT CONTROL

At the end of the shearing, the specimen was quickly built out of the triaxial cell. The bulk density and the final water content were determined. These two parameters are utilized in the calculation of the specific volume V_c of the specimen at various stages of the triaxial test, namely at the end of consolidation, at peak shear, and at the end of shear. The specific volume is needed in the formulation of the conceptual model for the buffer.

Taking into account the volume change during consolidation and drained shearing, the initial water content of the specimen can be calculated from the measured final water content. Likewise, the final water content can be determined from the measured initial water content. The measured and calculated water contents are then compared. The difference between the measured and calculated values reflects the changes in water content of the specimen resulted from the building-in procedures and the testing techniques. This gives an indication of the water content control in the specimen.

Table 5.3 summarizes the measured and calculated water contents of the twelve specimens. The first three specimens (T951 to T953) show large differences in excess of 3%. This is because the specimens were consolidated without back pressures and required constant flushing of water between the membrane and the specimen to eliminate trapped air. The particularly large difference of about 7% from specimen T951 was associated with leakage problems. The remaining nine specimens (T954 to T962) were consolidated under a back pressure of 200 kPa or higher, and therefore no flushing was needed during the consolidation. They show smaller differences of less than 1%.

Good water content control of the specimens is essential. It has been mentioned earlier that the conceptual model is formulated using values of V_c. Significant disagreement between the measured and calculated water contents will lead to uncertainties in the determination of V_c, and this will ultimately affect the accuracy of the model.

5.5 SUMMARY OF TESTING PROGRAM

The following schedule summarizes the testing program in the 950-series investigation:

T951: Compacted to 1.32 Mg/m^3 at 37.6%; consolidated to 0.4 MPa effective confining pressure with 0.2 MPa back pressure; sheared undrained at a strain rate of 1.2 %/hour.

T952: Compacted to 1.48 Mg/m^3 at 28.1%; consolidated to 1.0 MPa effective confining pressure with 0.25 MPa back pressure; sheared undrained at a strain rate of 0.6 %/hour.

T953: Compacted to 1.43 Mg/m^3 at 30.5%; consolidated to 0.8 MPa effective confining pressure with 0.25 MPa back pressure; sheared undrained at a strain rate of 0.6 %/hour.

T954: Compacted to 1.36 Mg/m^3 at 35.5%; consolidated to 0.2 MPa effective confining pressure with 0.2 MPa back pressure; sheared undrained at a strain rate of 0.6 %/hour.

T955: Compacted to 1.50 Mg/m^3 at 28.4%; consolidated to 0.6 MPa effective confining pressure with 0.2 MPa back pressure; sheared undrained at a strain rate of 0.6 %/hour.

T956: Compacted to 1.28 Mg/m^3 at 39.5%; consolidated to 0.1 MPa effective confining pressure with 0.2 MPa back pressure; sheared undrained at a strain rate of 0.6 %/hour.

T957: Compacted to 1.63 Mg/m^3 at 23.2%; consolidated to 1.5 MPa effective confining pressure with 0.2 MPa back pressure; sheared undrained at a strain rate of 0.6 %/hour.

T958: Compacted to 1.35 Mg/m^3 at 35.9%; consolidated to 0.2 MPa

effective confining pressure with 0.2 MPa back pressure; sheared in 8 increments of deviator stress in drained load-controlled shearing to examine shear modulus behaviour G.

T959: Compacted to 1.56 Mg/m^3 at 25.9%; consolidated to 1.0 MPa effective confining pressure with 0.2 MPa back pressure; sheared in 6 constant-sized increments of deviator stress in drained load-controlled shearing to examine shear modulus behaviour G.

T960: Compacted to 1.48 Mg/m^3 at 29.4%; consolidated to 0.6 MPa effective confining pressure with 0.2 MPa back pressure; sheared in 6 constant-sized increments of deviator stress in drained load-controlled shearing to examine shear modulus behaviour G.

T961: Compacted to 1.44 Mg/m^3 at 31.0%; consolidated in three stages:- (1) to 0.5 MPa effective confining pressure with σ= 0.7 MPa and u= 0.2 MPa, (2) to 0.5 MPa effective confining pressure with σ= 1.0 MPa and u= 0.5 MPa, (3) to 0.9 MPa effective confining pressure with σ= 1.4 MPa and u= 0.5 MPa; sheared undrained at three different strain rates of 3.0 %/hour, 0.6 %/hour and 0.12 %/hour; and relaxation test performed to study strain rate effect on undrained strength.

T962: Compacted to 1.38 Mg/m^3 at 33.8%; consolidated to 0.3 MPa effective confining pressure in two stages: first using 0.5 MPa total pressure with 0.2 MPa back pressure, then 0.7 MPa total pressure with 0.4 MPa back pressure; sheared undrained at a strain rate of 0.6 %/hour.

CHAPTER 6

RESULTS

6.1 INTRODUCTION

This chapter presents in two sections, the results obtained from this phase of the overall investigation. The first section presents findings from the quality control tests described in Chapter 4. The second section describes results from the triaxial testing program outlined in Chapter 5. Discussion and interpretation of results will be given in Chapter 7.

6.2 QUALITY CONTROL TESTS

Before the commencement of the triaxial testing program, fifteen quality control tests were conducted. The purpose of the tests was twofold. First, they ensured the repeatability and consistency of test specimens that were formed using the specimen preparation technique outlined in Chapter 5. Second, it was hoped to improve the saturation of the test specimens, during the quality control test program, by careful attention to density and water content relationships during development of the new compaction method.

The sand-clay mixtures for the quality control specimens were prepared using the same techniques and procedures outlined in Chapter 4 that were to be used for the triaxial specimens. However slightly modified procedures were adopted for the compaction process. Instead

of using 5 layers as in the case of the triaxial specimens, the quality control specimens were compacted in 5 to 8 layers. This step was taken to investigate the effect of the number of layers on the saturation of the specimens. After compaction, the specimens were carefully extruded from the mould, and their weights and dimensions were measured. They were then cut into a convenient number of transverse slices ranging from 4 to 8. Each slice was further divided into half. The water content of each half-slice was obtained, and the water content profiles across the specimens determined. The results from the tests are shown in Table 6.1.

Results from Table 6.1 indicate that the average difference between the "targetted" and "measured" water contents was -0.4% ± 0.6%. The corresponding difference in dry density was 0.00 ± 0.03 Mg/m^3. Figure 6.1 shows the water content profile in a typical specimen. The water content variation across the specimen is very small, typically less than 0.2%.

As pointed out earlier, it was intended to study how the saturation of the specimens would improve if more than 5 layers were used during compaction. It is hypothesized that, during compaction, air trapped between thinner layers of the soil mixture can be driven out more easily than those between thicker layers, thereby resulting in a lower air content in the specimen. As the saturation is inversely related to the air content, it could be argued that specimens formed with thinner layers should have a higher degree of saturation. Following this idea, for a given volume of the specimen, the thickness of each layer decreases with increasing number of layers, and hence specimens that are compacted in a larger number of

thinner layers should have a higher degree of saturation.

It is apparent from the results shown in Table 6.1 that in fact there was no improvement in the saturation with increasing number of layers. They instead indicate that slightly lower saturation would result if more than 5 layers were used, and the hypothesis suggested in the previous paragraph is invalid. This is probably due to an increase in compaction time, causing the soil mixture to lose moisture during the specimen forming process. Consequently, the soil became stiffer and less compactible, resulting in lower saturation.

The results in Table 6.1 also indicate that the saturation of the specimen generally increased with the water content of the mixture. This is because moisture was readily available in the mixtures having higher water content. The mixtures were less stiff, and were more easily compacted. They were however much more difficult to mix during the specimen preparation. This is due to the high affinity of the bentonite for water, which causes the clay particles to coalesce to form large-sized clay peds. These "macroscopic" ped structures have important implications in the understanding of the shear behaviour of the buffer, and this will be discussed in Chapter 7.

6.3 TRIAXIAL TESTS

In this investigation, a total of twelve compacted sand-clay buffer specimens was tested under triaxial conditions. The specimens were initially consolidated under isotropic conditions. On the completion of the consolidation phase, nine specimens (T951 to T957,

T961 and T962) were sheared in undrained triaxial compression and the remaining three specimens (T958 to T960) were sheared in drained compression at constant mean pressure. The experimental procedures of these tests were described in Chapter 5.

Figures 6.2 to 6.7, and Table 6.2 summarize the results from the consolidation tests. Results from the undrained shear tests are given in Figures 6.8 to 6.29, and Tables 6.3 to 6.5. Figures 6.30 to 6.38, and Table 6.6 present the drained test results.

6.3.1 CONSOLIDATION

Chapter 4 showed that in order to reduce the long consolidation times needed by previous specimens, the new specimens in this project were formed with a specimen preparation technique which utilized the swelling pressure - density relationship such as that shown in Figure 3.1. In principle, specimens formed with this technique should be at pressure - water content equilibrium, and therefore should exhibit small volume strains during consolidation. To validate this relationship for the purpose of specimen preparation, specimens were subjected to isotropic consolidation tests at pressures ranging from 0.1 MPa and 1.5 MPa.

Figures 6.2 to 6.6 showed the results from the consolidation phase of the tests plotted in terms of volume strains vs. elapsed time. The volume strains were taken as the volume of water expelled (or absorbed) divided by the whole volume of the specimen, expressed in percentage. That is, the strains are related to the total specimen, and not simply to the clay phase. Table 6.2 summarises the volume strains measured from the specimens, and the duration of the

tests. The measured volume strains ranged from -2.8% (swelling) to +9.7% (compressing) in the first specimen that was tested. Consolidation times in the single-stage consolidation tests (specimens T951 to T960) varied from 10 days to 19 days. In the multi-stage consolidation tests (specimens T961 and T962), longer durations up to 100 days were adopted. Most specimens in this program stopped expelling water after 2 to 4 days. In no case was the rate expulsion greater than 0.1 %/day, a criterion suggested by Graham et al., (1986b).

6.3.1.1 SINGLE-STAGE TESTS

Figures 6.2 to 6.4 summarise the results from the single-stage consolidation tests. It can be seen that specimens T951 to T953 exhibited quite large volume strains in excess of 3%. This is because their initial densities and water contents were designed by extrapolating the pressure-density relationship shown in Figure 3.1 to a lower stress level down to 0.4 MPa. This led to an overestimation of the water contents of the specimens at the corresponding consolidation pressures, and consequently larger volume strains. For specimen T951, the large volume change measurement was in part due to a leakage of cell water into the specimen through the pedestal on the cell base. Subsequent specimens (T954 to T962) were formed with a new pressure - density relationship developed from the "end-of-consolidation" data obtained from the 800-series and early phase of the 950-series (Figures 4.4 and 4.5). This relationship was constantly updated with consolidation data to improve its ability to predict the volume change behaviour of the buffer material. With the

exception of specimens T956 and T960, all of these later specimens showed small volume strains of less 1%. The swelling strain of about 3% exhibited by specimen T956 was due to the underestimation of water content of the specimen resulting from the extrapolation of the relationship to the lowest stress level tested in this series.

6.3.1.2 MULTI-STAGE TESTS

Results from the multi-stage consolidation tests are shown in Figures 6.5 and 6.6. During the first stage of consolidation, both specimens T961 and T962 showed small volume strains of less than 1%. After the specimens had reached equilibrium, the second stage of consolidation commenced. This involved increasing both the cell pressure and back pressure simultaneously by the same amount, but keeping the effective pressure on the specimens constant. According to the effective stress principle, if there is no change in the effective stress, then the specimens should experience no volume strains. However some volume changes were in fact recorded from the specimens, namely a swelling strain of about 0.8% in specimen T961 and a compressive strain of about 0.1% in specimen T962. These strains have been corrected for expansion in the drainage leads, as a result of the increased back pressure. The opposite behaviour of the two specimens and the apparent deviation from the principle are surprising and are not yet fully understood. This will be addressed in further tests that are currently in progress in the laboratories at the University of Manitoba. Factors such as incomplete saturation of the specimens and the soil fabric structures may have attributed to these deviations from the expected behaviour, and these will be discussed in

Chapter 7.

In the third stage of consolidation, the total confining pressure on specimen T961 was raised from 1.0 MPa to 1.4 MPa, while maintaining the back pressure constant at 0.5 MPa. This resulted in an increase in effective pressure causing a large volume strain of about 3% in the specimen (Figure 6.5). This required a lengthy period of consolidation (17 days) before the specimen could be moved into triaxial shear testing. It may be recalled from Section 5.2.1 that the purpose of this third stage of consolidation was to confirm the validity of the swelling pressure - water content relationship shown in Figure 4.5. Results are given in Figure 6.7. The Figure replots the relationship from Figure 4.5; and shows the positions of specimen T961 at the end of the second and third stages of consolidation by an open diamond and a cross respectively. The Figure shows that the equilibrium conditions of the specimen at the end of the two stages are different from those predicted by the relationship. It is also clear that the specimen followed one of the three paths suggested in the Figure, rather than the relationship in Figure 4.5. The disagreement between the actual and predicted behaviours is however small (the difference in water content is not more than 0.5%; the precision in fact, with which water contents can be measured). It should be noted that the relationship (Figure 4.5) was derived from the 800- and 950- series "end-of-consolidation" data, which show rather considerable scatter. The line shown in Figures 4.5 and 6.7 is therefore a simplification of a zone of "end-of-consolidation" data points from specimens tested under different triaxial conditions. Some of these specimens were however not in complete equilibrium

before shearing, and this contributed to the scatter in the data. This therefore affected the position of the relationship and its ability to make accurate swelling pressure - water content prediction.

6.3.2 UNDRAINED SHEAR

After consolidation, nine specimens (T951 to T957, T961 and T962) were sheared undrained in a strain-controlled compression load frame. These tests enabled the determination of the stress-strain and strength characteristics of the buffer material.

6.3.2.1 STRESS-STRAIN AND POREWATER PRESSURE CHARACTERISTICS

The normalized shear stress vs. axial strain curves shown in Figures 6.8 to 6.16 are consistent, and indicate a slightly strain-softening behaviour of the buffer material. The stress-strain curve for the specimen T961 (Figure 6.15) appears to be stepped and broken because the specimen was used to investigate the strain rate effect using "step changing" and "relaxation" procedures. Results from the tests will be given in a later section. The axial strains to failure, ϵ_{1f}, lie in a small range from 3.5% to 6.6% with the majority lying in the relative narrow range of 5% to 6% (Tables 6.3 and 6.4). This compared to the more scattered values of 3.8% to 11.5% reported by Sun (1986).

The elastic deformation characteristics of the buffer material were approximated by taking a secant modulus E_{50} from the beginning of shearing to 50 percent of the maximum deviator stress from the stress-strain curves (Graham, 1974). Figures 6.17 and 6.18, and Table 6.5 summarize the undrained shear moduli from the tests. Values of

E_{50} have been normalized by the undrained shear strength s_u and the effective consolidation pressure σ'_{cons} to give relative stiffnesses. The E_{50}/s_u values vary between 103 and 263, with an average of 190±60. The E_{50}/σ'_{cons} values range from 21 to 100, with an average of 60±29. Undrained shear moduli G_{50} have been calculated from the E_{50} values using the formula $G_{50} = E_{50}/3$, and normalized by the effective consolidation pressure. The average value of G_{50}/σ'_{cons} is 20±10.

Figures 6.8 to 6.16 also show the variation of porewater pressure with axial strain. Figures 6.19 to 6.27 give the relationships between porewater pressure changes Δu and total mean pressure changes Δp.

Values of the porewater pressure parameters at failure A_f ($= \Delta u_f/\Delta q_f$) and u_f/σ'_{cons} are summarized in Tables 6.3 and 6.4. The values of A_f and u_f/σ'_{cons} range from 0.12 to 0.98 and 0.14 to 0.35 respectively. Based on the porewater pressure generation characteristics shown in Figures 6.8 to 6.16 and Figures 6.19 to 6.27, two distinct types of failure can be noted. For specimens T951 to T953 and T961, which showed compressive behaviour in shear, the porewater pressure in the specimens continued to increase after reaching failure (Figures 6.8 to 6.10, Figure 6.15, Figures 6.19 to 6.21, and Figure 6.26). (The drop in porewater pressure in specimen T951 towards the end of the test, as seen in Figure 6.8, was due to the development of shear planes). In contrast, specimens T954 to T957 and T962, showed dilative behaviour in shear. In these specimens, the porewater pressure increased to a maximum at about 2% axial strain, and then dropped off abruptly towards the end of the tests as the critical state was approached (Figures 6.11 to 6.14, and Figure 6.16).

This is reflected very clearly by the shapes of the $\Delta u : \Delta p$ relationships in Figures 6.22 to 6.25 and Figure 6.27 which indicate typically dilative behaviour.

The effective stress ratio vs. axial strain curves are shown in Figures 6.8 to 6.16. The general shapes of these curves resemble those of the porewater pressure vs. axial strain relationships. The compression specimens (T951 to T953 and T961, Figures 6.8 to 6.10 and Figure 6.15) rise steeply at the beginning of the test, and then reach a constant value of q/p' (and therefore σ_1'/σ_3') at about 5% axial strain. Maximum q and maximum q/p' are reached at about the same axial strain. The dilative specimens (T954 to T957 and T961, Figures 6.11 to 6.14 and Figure 6.16) reach a peak value of $(q/p')_{max}$ at about 3% axial strain, whereas the peak value of q_f is reached at about 5% axial strain. This means that there is some uncertainty about whether "failure" should be defined by q_f or $(q/p')_{max}$. However the uncertainty is not large compared for example with tests on anisotropic consolidated clay specimens (Simons, 1960; Crooks and Graham, 1976; and Graham et al., 1983b). Failure is taken in the buffer specimens at the maximum value of the deviator stress, q_{max} or q_f.

Tables 6.3 and 6.4 summarize the effective stress ratios at failure (maximum deviator stress), $(q/p')_f$. The ratios for the compressive specimens (T951 to T953, and T961) lie in the range 0.44 to 0.60. For the dilative specimens (T954 to T957, and T962), the values are larger and lie in the range 0.60 and 0.93. There is a tendency for $(q/p')_f$ to decrease with increasing consolidation pressure.

6.3.2.2 EFFECTIVE STRESS PATHS

Figure 6.28 summarizes the effective stress paths from the tests, plotted in terms of the stress parameters, q and p'. Several observations can be made from the Figure.

First, the early parts of the stress paths are generally consistent, consisting of a relatively linear "elastic" section up to a large percentage of maximum shear stress. This is then followed by a non-linear post-failure section. Note that the nonlinearity of the "elastic" section of the stress paths for specimens T951 and T961 are respectively due to incomplete equalization of initial porewater pressure and change in strain rate during the test.

Second, inherent anisotropy of the specimens is reflected by the inclination of the stress paths with respect to the vertical. For an isotropic elastic material in an undrained test, an increase in the total stress in the specimen will cause the same increase in the porewater pressure, resulting in a "constant" mean effective stress. This is depicted by a vertical stress path in a q:p' diagram, and a linear relationship in a Δu vs. Δp plot with the slope m (= $\Delta u / \Delta p$) being 1.0 (Graham and Houlsby, 1983). Figure 6.28 shows that all the stress paths except for specimen T956, deviate to the left of the vertical ($m > 1.0$). Table 6.4 summarises the m-values measured from the Δu vs. Δp relationships shown in Figures 6.19 to 6.27. Except for specimens T951 and T956, the values lie in quite a narrow range from 1.89 to 2.23. This represents a strongly anisotropic nature of the test specimens, and reflects the influence of the compaction process on the structure of the buffer material. Specimen T951 experienced leakage problems and required unloading; and specimen T956 swelled

during consolidation. These factors could attribute to a more isotropic and randomly oriented structure in the specimens, and therefore lead to lower m-values of 1.43 and 1.25 for specimens T951 and T956 respectively. Further discussion of the relationship between m-values and consolidation strains will be given in Chapter 7.

Third, the two distinct types of failure mentioned in the previous section, can be readily distinguished from Figure 6.28. For specimens T951 to T953 and T961, which showed compressive behaviour in shear, the stress paths tend to the left after reaching failure, and gradually move towards states defined in Chapter 2 as "critical states". On the other hand, for the dilative specimens (T954 to T957 and T962), the stress paths move to the right with an increase in mean effective stress p' and some decrease in shear stress q after failure. This is caused partly by the development of decreasing porewater pressures and partly by strain softening. Both of these are common characteristics in dilative specimens.

6.3.2.3 STRAIN RATE EFFECT

The influence of strain rate on the undrained shear strength of the buffer material was studied by step-changing the speed of testing and by performing a relaxation test (Graham et al., 1983a) on specimen T961. This is the first such test on the buffer material. The resulting stress-strain curves have already been presented in Figure 6.15.

Results from the "step changing" procedure indicate that a tenfold change in strain rate would cause a change in undrained strength by about 7%.

Figure 6.29 shows a relationship of undrained shearing resistance s_u vs. log(strain rate) obtained from the relaxation test. The Figure shows that the undrained shearing resistance increases linearly with increasing log(strain rate). The change in shearing resistance can be described by the strain rate parameter, $\rho_{0.1}$ (Graham et al., 1983a). This parameter is defined as the percentage change in undrained strength related to the shearing resistance measured at 0.1 %/hour, produced by a tenfold change in strain rate. From the relaxation test, $\rho_{0.1}$ was determined to be about 5%.

6.3.3 DRAINED SHEAR

Three specimens (T958 to T960) were sheared with open drainage leads after consolidation. The purpose of these tests was to provide information on the drained shear behaviour of the buffer material. The loading schedules for these specimens were designed to apply six increments of shear stress before failure. Due to an error in determining the magnitude of its shear stress increments, specimen T958 required eight and one-half increments of shear stresses before reaching failure. However, about thirty minutes after the application of the last half-increment, the specimen ruptured abruptly, achieving 12% strains in less than two minutes. This half-increment was therefore discounted, and the failure of the specimen was taken as at the eighth increment. Failure in specimens T959 and T960 occurred at the sixth (last) increment after two hours and six hours respectively. Maximum axial and shear strains during this last increment of shear stresses are 12.8% in specimen T959 and 8.3 % in specimen T960. The theoretical stress paths for these tests are given in Figure 5.2.

Variations of strains and strain rates with time during the increments are shown in Figures 6.30 to 6.35. The Figures indicate that the axial strains and shear strains induced in the specimens during the early increments were small, typically less than 1%, but increased in magnitude with shear stress levels. The plots of log(strain rate) vs. log(time) also shown in Figures 6.30 to 6.35 indicate that, for the early increments, the log-log relationships are curvilinear, decreasing in strain rate with time. Failure of the specimens, associated with large strains occurring in a relatively short time period and with increasing strain rates, was induced by the application of the last increment of shear stresses. In the final (failure) increments, the strain rates initially decreased, but then began to increase as the specimens moved towards failure (Vaid and Campanella, 1977). There is no indication in these specimens that failure would have been initiated by holding the penultimate shear stress for longer periods.

Figures 6.31, 6.32, 6.34 and 6.35 suggest tentatively that specimens T959 and T960 both exhibited dilative behaviour in shear and perhaps, the development of localized shear bands (Vardoulakis, 1985). This is reflected by the downward concavity of the log(strain rate) vs. log(time) curves for the last shear stress increments, which indicates a decrease in strain rate resulting from the expansion of the specimens as they move towards failure.

Figures 6.36 to 6.38 plot normalized shear stress vs. accumulated shear strain relationships in '1-day', '2-day', and '3-day' strains. These figures allow the determination of the shear modulus (G) of the buffer materal, which is here taken as the tangent

to the slope of the relationship at $q_{max}/2$ divided by 3 (Graham et al., 1986a). As expected, the results indicate that the shear behaviour of the buffer material is nonlinear. The stiffness is both time and shear stress dependent, but appears to be relatively independent of the consolidation pressure. Table 6.6 summarises the shear moduli obtained from the tests and the results from the previous 800-series for the purpose of comparison. Average values of G/σ'_{cons} at '1-day', '2-day', and '3-day' strains are 14, 11, and 10 respectively. They are consistently higher than the corresponding values of 11, 8, and 7 reported by Sun (1986) (see also Chapter 7).

An interesting observation that can be made from these shear stress - shear strain plots (Figures 6.36 to 6.38) is the upward concavity in the initial section of the curves. This is probably due to the compacted structure of the specimens resulting from both the specimen preparation and the consolidation processes. As a result, the first increment of shear stresses was not sufficient to incur large shear strains in the specimens in the initial stage of the tests.

6.3.4 COULOMB-MOHR ENVELOPES

The effective stress paths obtained from both the undrained and drained test series respectively have been shown in Figure 6.28 and Figure 5.2. Figure 6.39 summarizes all the effective stress paths and the shear strength envelopes for the buffer material. Three strength envelopes have been identified and determined by drawing linear regression lines through the "end-of-test" and "peak failure" points of these stress paths. The measured friction angles are given

to the nearest half-degree. It is considered that they can be assessed to better than 1°, but not as well as 0.1°.

Using the end-of-test data from the compressive specimens (T951 to T953 and T961); and specimen T957 which was sheared to a large strain of about 21%, a compressive strength envelope with c'= 0 kPa, and Ø'= 13½° is obtained (5 data points; R^2= 0.97). This envelope is closely similar to the compressive envelope with c'= 0 kPa, and Ø'= 13° obtained for the 900-series (Graham et al., 1987). However, it indicates a slightly lower strength than the peak envelope from a limited number of "fully softened" specimens plus some end-of-test data that were reported by Sun (1986), who gave c'= 0 kPa, and Ø'= 16°.

Based on the peak failure points of the stress paths obtained for the undrained and drained specimens, two peak strength envelopes are suggested. For the **compressive** undrained specimens (T951 to T953 and T961), the strength parameters are c'= 0 kPa, and Ø'= 13½° (4 data points; R^2= 0.81). This envelope is the same as the end-of-test compressive envelope described earlier, but shows a lower strength than the compressive peak envelope with c'= 0 kPa, and Ø'= 16° reported by Graham et al. (1986b). For the **dilative** undrained specimens (T954 to T957 and T962) and the drained specimens (T958 to T960), a bilinear envelope is suggested. Up to an effective consolidation pressure of about 0.3 MPa, the strength parameters are c'= 0 kPa, and Ø'= 22° (4 data points; R^2= 0.98). From 0.3 MPa to 1.5 MPa, the envelope indicates c'= 40 kPa, and Ø'= 14½° (5 data points; R^2= 1.00). This envelope is different from those reported by Sun (1986) and Graham et al. (1986b). Sun (1986) concluded that for the

"overconsolidated" specimens tested in the effective pressure range of 0.1 MPa to 0.8 MPa, the strength parameters are c'= 48 kPa, and Ø'= 13°. Graham et al. (1986b) suggested that the strength values of the dilative peak envelope up to 1.5 MPa are c'= 24 kPa, and Ø'= 16°.

Although there may appear to be a relatively large number of strength parameters arising from various segments of the overall project, the variability in real, engineering terms is in fact rather small. Table 6.7 summarises all the undrained strength parameters for the buffer material obtained from the three phases of investigation at the University of Manitoba.

CHAPTER 7

DISCUSSION OF RESULTS

7.1 INTRODUCTION

The purpose of this research has been to investigate the geotechnical properties of the buffer material. It is appreciated that the buffer is a man-made material, and there is little existing knowledge of its engineering behaviour. An initial understanding of the behaviour was obtained by Sun (1986), who investigated the stress-strain-time characteristics of buffer material compacted at a density of 1.50 Mg/m^3 with a water content of 28%. To supplement and to extend his work, twelve triaxial tests were conducted on compacted sand-clay buffer specimens up to a pressure of 1.5 MPa. These specimens were prepared at densities and water contents that would lead to a pressure - water content equilibrium of the specimens after much shorter times during consolidation. This preparation technique would therefore enable more tests to be carried out in a shorter time period.

This chapter will discuss the results from the triaxial testing phase of the investigation that has been presented in Chapter 6. Because of the complex nature of the bentonite in the sand-clay mixture, which has undoubtedly influenced the volume change and shear behaviour of the buffer specimens, a hypothesis has been proposed based on the structure of the soil mixtures. This hypothesis will form a basis for explaining the behaviour of the buffer in the

consolidation and shearing phases of testing.

7.2 SOIL STRUCTURE CONSIDERATION

7.2.1 INTRODUCTION

The importance of soil structure in influencing the behaviour of compacted clay soils has long been recognised. Lambe (1958), and Seed and Chan (1959) demonstrated the effects of structure on shear behaviour. Mitchell et al. (1965) concluded that "structure is the most important single variable influencing the permeability of compacted clay". This in turn, affects the consolidation behaviour (Barden and Sides, 1970).

A common approach in explaining clay behaviour is by means of the physicochemical theories based on the interaction of single plates. However this approach is, to some extent, idealized, and does not adquately provide full explanation to some of the complex behaviour of clay soils. Barden (1972) reported Yong's (1971) suggestion that single plate theory is relevant only to dilute colloidal suspensions. Electron microscopy studies (Aylmore and Quirk, 1960; Barden, 1971; Barden, 1972) indicated that clay soils are made up of clay plates aggregated into domains, clusters, and peds, which behave as single particles (Terzaghi, 1956). Barden and Sides (1970) showed that these "macrostructures" play an important part in governing the engineering behaviour of clay soils. (The term "macrostructure" is being used here in a specific way that will be explained in Section 7.2.2.1. The usage decribes groups of particles that have combined together to form units larger than single

particles. It is not being used here in the sense of fissure systems and clay-silt doublets). Aylmore and Quirk (1959, 1960) pointed out the importance of domains of clay particles in influencing both the strength and the swelling potential of clays.

7.2.2 HYPOTHESIS

With the preceding brief discussion on soil structure in mind, it is possible to propose a soil structure hypothesis for the buffer material. It is appreciated that the hypothesis is rather speculative, formed only on the basis of visual examination of the buffer material and some electron micrographs of compacted specimens. However it can be used as a tool in the interpretation of test data on the buffer material at different stages of a triaxial test in a qualitatively way. The hypothesis will be divided into two parts. The first part will describe the soil fabric structure induced in the specimens as a result of the specimen preparation process. The second part will describe changes in the fabric structure due to the consolidation process and their implication on the subsequent shear behaviour of the buffer material.

7.2.2.1 SPECIMEN PREPARATION

The preparation process constitutes the initial mixing and curing of the sand-clay-water mixture; and compaction of the buffer specimens. The buffer material is obtained by mixing dry bentonite with a mixture of sand and water. In contact with moisture, some of the clay particles will adhere to the wetted sand grains, while the remainder will aggregate or flocculate together into groups of clay

particles. Aylmore and Quirk (1960) referred to these "submicroscopic" groups as domains. Due to interparticle forces acting on these small units (Bowles, 1979), domains group together to form "microscopic" clusters, which in turn group together to form "macroscopic" peds which are visible to the unaided eye (Yong and Warkentin, 1975). In this thesis, the assemblage of domains, clusters, and peds is referred to as soil fabric units for simplicity. Clay aggregates, which are easily visible, are simply collections of large numbers of peds. Figure 7.1 shows the diagrammetic representation of the structure of these soil fabric units, and the hierarchy of the fabric system.

The dimensions of the clay aggregates generally vary with the moulding water content, increasing in size with increasing water content. This is consistent with the observation made by Musa (1982), who tested remoulded clays. For the mixtures with low water content (about 20% in the present study), the maximum dimension of these aggregates is about 5 mm. Because of the low water content, the aggregates consist essentially of randomly oriented peds, clusters and domains. It is assumed here that the clay particles inside their fabric units will also possess a randomly oriented structure at low water content.

For high water content mixtures (about 40% in this study), the aggregates are larger in size, averaging about 25 mm in diameter. They consist of a larger number of clay fabric units, which stick together with smaller interpedal voids. Due to the higher water content of the soil, the clay fabric units and the clay particles in these units are expected to have a more oriented arrangement. It

should be emphasized that before compaction the larger pedal units will still be randomly oriented.

Because of the mixing technique, which involves sprinkling the clay on the wet sand mixture in several increments, some of the clay, especially those from the early increments, will be wetter. This will lead to a buffer mixture which will not be completely uniform in terms of water content. After mixing, the mixture has been cured in a moisture and temperature contolled environment for a period of three days in an attempt to achieve more uniform water content, and hence a more uniform fabric structure in the soil. However the overall structure of the soil is a function of the moulding water content (Barden and Sides, 1970). The curing process can therefore only lead to minor reorganization of the structure in the fabric units and not to a major change in the properties of the buffer.

The compaction phase of specimen preparation causes rearrange -ments of clay fabric units (Lambe, 1958; Yong and Warkentin, 1975). The degree of fabric (or particle) orientation has been shown depend on the type of compaction (Seed and Chan, 1959). Kneading compaction causes high localized shear strains, and therefore produces a higher degree of orientation in the particle structure. On the other hand, static compaction tends to cause a more uniform shear strain, and typically results in a less oriented structure.

During static compaction of the buffer material, the majority of the clay fabric units are assumed to orientate in a direction perpendicular to the compactive force, but the clay particles in these fabrics should attain their original structure. Also, due to their orientation prior to compaction, the smaller fabric units such as the

particles and domains will resist the compression forces by bending and storing distortional energy.

It should be noted that the compaction process itself does not cause complete "destructuration" of the structure of the fabric units (Barden, 1971; Musa, 1982). This is supported by the evidence of an electron microscopy study on compacted buffer specimens. Figures 7.2 and 7.3 respectively show electron micrographs of specimens with water contents of 40% and 20%. It can be seen that the fabric structures in both specimens are similar, consisting essentially of macropeds in a random arrangement. In spite of the high compressive stress of the order of 13.0 MPa applied to the soil during compaction, the macropeds retained their intregrity. This lack of orientation of the fabric units seen in the Figures is probably in part due to the release of the compression force at the end of compaction, causing some reorganization of the units. It should also be noted that the photographed structures are affected by the techniques used for preparing the specimens for electron microscopy (Baracos, 1977).

7.2.2.2 CONSOLIDATION AND SHEAR

The consolidation process is similar in one way to compaction: changes in soil fabric units are expected to occur in both processes. After close examination of data in Chapter 6, it is postulated that large volume strains (larger than 3%) duing consolidation will permit rearrangement of the fabric. Compressive strains during consolidation will increase the alignment of clay fabric units, and hence increase the anisotropy of the specimen. Dilative (expansive) strain will allows some rearrangement of the fabric units leading possibly to a

structure which is less oriented. This reduces the degree of anisotropy of the specimen. In the case of small compressive volume strains (less than 3%), there will be less disturbance of the soil structure, and the fabric structure induced during compaction will remain essentially intact.

The soil fabric structure produced by the compaction and consolidation procedures has a significiant influence on the shear behaviour of the buffer. Specimens which show large compressive strains during consolidation (and which have just been shown to have more oriented fabric structure) will show compressive type of failure in shear (Seed and Chan, 1959). In drained shear they will compress : in undrained shear they will produce increasing porewater pressures. In contrast, specimens which exhibit large dilative volume strains and specimens with smaller volume strains will show dilative shear behaviour because of the randomly arranged fabic structure.

7.3 VOLUME CHANGE BEHAVIOUR

7.3.1 GENERAL CONSOLIDATION BEHAVIOUR

Results from the consolidation tests have been shown in Figures 6.2 to 6.7 and Table 6.2. It was pointed out in Chapter 1 that one of the purposes of this investigation was to form specimens at pressure-water content equilibrium. To achieve this condition, the water contents of the test specimens were designed according to the swelling pressure-dry density relationships shown in Figures 3.1 and 4.4 (Figure 4.5).

The end-of-consolidation data from the tests in this research

program are summarized in a V_c:ln(p') plot in Figure 7.4. Specimens which exhibited large compressive volume strains (more than 3%) are shown by open squares having a "best-fit" line (DD), and specimens with small volume strains (less than 1%) by crosses and the "best-fit" line (CC). It should be noted that lines (CC) and (DD) are derived from the relatively small number of data points from this series shown in Figure 7.4. These two lines are therefore different from the swelling pressure - clay specific volume relationship shown in Figure 4.4, which were determined by regression through all the "end-of-consolidation" data points from the 800- and 950- series.

It is interesting to note that all three "large strain" specimens (T951 to T953) were formed with the Swelling Equilibrium Line (SEL) shown in Figure 3.1 proposed by Dixon et al. (1986); whereas the remaining nine "small strain" specimens were formed with the SEL in Figure 4.4, which was based on the "end of consolidation" data from the 800-series and 950-series.

During internal review of the data, some concern was raised regarding the possibility of leakage of cell water through the latex membranes which might affect the calculations of volume change behaviour of the specimens. For example, in the case of specimens T951 to T953, any leakage would have resulted in apparently large volume change measurement even though the specimens themselves did not change volume. For specimens T954 to T962, swelling strains might have been balanced by the leakage strains, resulting in an apparent pressure-water content equilibrium. However, results from latex membrane leakage tests shown in Figure 7.5 suggest that the maximum leakage rate is about 0.01 ml/day. This would produce incorrect

volume strains of about 0.005 %/day, which is at least two orders of magnitude lower than the measured volume strain of typically 1%. The leakage problem is therefore considered insignificant in influencing the measured volume change behaviour of the specimens.

From the results of the "large strain" specimens (T951 to T953), it must be therefore concluded that the SEL proposed by Dixon et al. (1986) overestimated the water content of the specimens for a given consolidation pressure. The inability of this relationship to predict the pressure - water content equilibrium is because it was derived from one-dimensional test data whereas the specimens in this study were straining three-dimensionally. It may be appreciated that the fabric structure of the specimens in the one-dimensional tests is therefore much more oriented as a result of the vertical compression. From the tests by Gray et al. (1985), this then results in a higher swelling pressure at the same specific volume (or effective clay density). Furthermore, the SEL (Dixon et al., 1986) covers the pressure range of 0.7 MPa and 3.0 MPa, and is weakly controlled at low stresses. Extrapolation of the relationship down to a pressure of 0.4 MPa would affect its ability to give good predictions.

Also shown in Figure 7.4 are SEL (BB) proposed by Graham et al. (1986a) for the conceptual model described in Chapter 2, and SEL (EE) based on all the "end-of-consolidation" data from the three series of tests so far completed at the University of Manitoba. Note that, as mentioned in Section 4.3.2, SEL (BB) is an extension of the relationship proposed by Dixon et al. (1986) shown in Figure 3.1, to the low pressure range. It can be seen that SEL (DD) from the "large strain" data is in good agreement with SEL (BB). However SEL (CC) and

SEL (EE) while rather similar, differ quite markedly from the other SEL's. From consideration of the effect of soil structure on swelling equilibrium of the buffer material (Section 7.3.2.3), the low gradient of (CC) and (EE) are probably due to the fabric structure of specimens tested in the low pressure range (up to 1.5 MPa). They may also be influenced by incomplete equalization of water content of compressive specimens tested in the high pressure range (up to 3.0 MPa). Both factors affect the swelling equilibrium of the buffer material and cause a counterclockwise rotational shift of the SEL's in the V_c:ln(p') space in Figure 7.4.

7.3.2 FABRIC STRUCTURE CONSIDERATION

7.3.2.1 EFFECT OF BACK PRESSURE ON FABRIC STRUCTURE

The use of back pressuring is a common technique in soil testing. The purpose of applying a back pressure is to saturate the soil specimen by dissolving air in the pore fluid (Bishop and Henkel, 1962) so that porewater pressures can be measured confidently.

In this series of tests, all the specimens were unsaturated at the end of compaction, having an average saturation of 95.5% (Table 5.1). To achieve full saturation, the majority of the specimens were consolidated under a nominal back pressure of 200 kPa through the whole consolidation process. For specimens T951 to T953, a back pressure of 200 kPa or 250 kPa was applied at the end of consolidation but before the undrained shearing.

The results in Chapter 6 showed that the three specimens (T951 to T953) which were consolidated without back pressuring exhibited

large volume strains and subsequent compressive shear behaviour; while the remaining nine specimens (T954 to T962) which were consolidated with back pressures showed relatively small strains. This raises questions on the effect of back pressuring on the buffer behaviour. At first sight, from the ideas on effective stress presented in Chapter 2, it is uncertain whether the applied back pressure can cause the suppression of volume strain. Volume change behaviour of the specimens is thought to be related to the accuracy of the water content prediction rather than to details of the testing technique. The effects of changes in back pressure (and the relevance of the effective stress principle) are examined further in Section 7.3.3. Nonetheless, back pressuring can be identified in playing an important role in affecting the soil structure.

As pointed out earlier in this section, all the specimens were initially unsaturated, and contained a small amount of air voids. The "nonsaturation" of the specimens can be expected to result in some fabric rearrangement during consolidation, especially in the vicinity of the voids, probably leading to a more oriented structure in the fabric units. For specimens T951 to T953, this process continued to function until a pressure - water content equilibrium was reached. The remaining nine specimens (T954 to T962) were consolidated under back pressure. The amount of air in these specimens would therefore be quickly reduced in volume according to Boyle's Law and Henry's Law (Lowe and Johnson, 1960). The number of air voids was therefore reduced (ideally to zero), minimizing further rearrangement of the fabric structure. This would then tend to preserve the "as compacted" randomly arranged soil structure of the specimens as indicated by the

electron micrographs.

7.3.2.2 EFFECT OF VOLUME STRAIN ON FABRIC STRUCTURE

The concept of changes in fabric structure as a result of large volume strains and its implication on the subsequent shear behaviour have been described in Section 7.2.2. This concept is well supported by the results of specimen T961, which was tested in a multi-stage consolidation test. During the first and second stages (point F in Figure 7.4), the specimen was consolidated under two different total pressures and back pressures, giving a constant effective pressure of 0.5 MPa. The volume strains during these two stages were small (about 1%, Table 6.2). It may therefore be assumed that there was no major structure disturbance during these stages, and the clay fabric units were essentially randomly oriented as at the end of compaction. The state of the specimen at the end of the second stage consolidation, as depicted by point F, lies on SEL (CC) in Figure 7.4. It will be shown in Section 7.4 that specimens with the end of consolidation represented by SEL (CC) showed dilative behaviour in shear. It therefore seems logical to assume that if the specimen had been sheared at that stage, it would have behaved in a dilative manner.

However a third consolidation stage was added before shearing. In this third stage, the effective pressure was raised to 0.9 MPa. This resulted a relatively large compressive volume strain of about 3%, and probably led to a more oriented fabric structure. The state of the specimen at the end of consolidation is shown by point G. This lies closer to the lines (BB) and (DD) which were identified in

Section 7.3.1 as coming from compressive specimens. Specimen T961 was finally sheared undrained and showed distinctly compressive behaviour in shear. This demonstrates the significant influence of volume strains during consolidation on the fabric structure, and their importance in influencing the shear behaviour of the buffer.

7.3.2.3 EFFECT OF FABRIC STRUCTURE ON SWELLING EQUILIBRIUM

The swelling pressure relationships derived from the "large strain" and "small strain" consolidation data have been described in Section 7.3.1. Figure 7.4 shows that "large strain" lines (BB and DD) are similar, probably because they were derived from tests on specimens which have similar type of fabric structure. On the other hand, SEL (CC) which was derived from the "small strain" data deviates quite sharply from the lines BB and DD.

As described in Chapter 2, the swelling pressure of clays can be predicted by van't Hoff's equation based on the parallel plate theory (Yong and Warkentin, 1975). For convenience, the equation will be rewritten as follows,

$$P = RT(C_c - 2C_o)$$

where R is the molar gas contant, T is the absolute temperature in Kelvin, C_c is the ion concentration (mol/l) at the half distance between two clay particles, and C_o is the ion concentration (mol/l) in the free water. Since R and C_o are constants, and at a given temperature T, the swelling pressure P depends on C_c. But C_c is related to the specific surface area S defined as the total particle surface area per unit mass (m^2/g), and decreases with decreasing S. Therefore P is also influenced by S.

It has been shown by electron micrographs (Figures 7.2 and 7.3) done at AECL that the buffer material consists of aggregations of clay particles, which behave rather like single particles. These aggregates will significantly reduce the specific surface area, resulting in a lower swelling pressure in the buffer specimen at the same average clay density and water content. Since the size of the aggregates increases with the moulding water content, the reduction in swelling pressure in the buffer from the "theoretical pressure" based on single particle theory will increase with water content.

Specimens T954 to T962, which were used to form SEL (CC), generally exhibited small volume strains, typically less than 1% during consolidation (Table 6.2). The fabric units in these specimens essentially retained the "as-compacted" structure of randomly arranged type. Since the specimens were formed at different moulding water contents, they should therefore have different fabric sizes. From Figure 7.4, it can be seen that at low V_c values (low water content and therefore smaller aggregates), both the reduction in swelling pressure and the deviation from the "large strain" lines is small. As V_c and the water content of the buffer material increase, the reduction in swelling pressure is more pronounced and the deviation is more obvious.

It should be noted that SEL (CC) only represents the equilibrium condition of a quasi-stable macro-fabric structure of the buffer material, and does not imply full equilibrium of the clay microstructure. The "stability" of the macro-structure is sensitive to changes in pressure. Any increase in external applied pressure will cause "instability" of the system and lead to changes in the

fabric units, thereby modifying the swelling properties of the buffer material. This point has been proven by the results from the multi-stage consolidation test on specimen T961 discussed in Section 7.3.2.2. (In Figure 7.4, point G does not lie on or close to SEL (CC) due to the modification of the fabric system in the specimen as a result of an increase in the effective confining pressure).

An interesting point that can be observed from Figure 7.4 is the tendency of SEL (CC) to merge with the "large strain" lines at a swelling pressure of about 1.5 MPa. This is because specimens tested at pressures above this threshold value will be formed with a relatively small range of low water contents, and the size of the aggregates in the buffer approaches to that of domains or single clay particles. The swelling pressure developed in these specimens will therefore be insensitive to the specimen preparation method.

7.3.3 EFFECTIVE STRESS PRINCIPLE

The applicability of the effective stress principle to the buffer material has been studied by performing multi-stage consolidation tests on specimens T961 and T962. During the first stages of consolidation, specimen T961 was consolidated with a total pressure of 700 kPa, a back pressure of 200 kPa, and an effective pressure of 500 kPa; and specimen T962 with a total pressure of 500 kPa, a back pressure of 200 kPa, and an effective pressure of 300 kPa. In the second stages, the total pressure and the back pressure on specimen T961 were both increased by 300 kPa, and those on specimen T962 by 200 kPa. In both specimens, the effective pressure defined as the difference between total pressure and applied back pressure in the

void space, was kept the same in the two stages. By the commonly accepted effective stress principle, no volume change should occur during the second stages of consolidation. Results from the tests have been shown in Figures 6.5 and 6.6.

The results indicate that both specimens showed some volume changes during the second stages of their consolidation. The two specimens behaved differently however, with T961 showing swelling strains of about 0.8%, while T962 showed compressive strains of about 0.1%. The apparent deviation from the effective stress principle and the inconsistent volume change behaviour of the specimens are not fully understood, but will be discussed qualitatively in following paragraphs.

It can be seen from Figure 6.6 that specimen T962 was not fully equilibrated at the end of the first stage of consolidation, and was still compressing at a rate of about 0.005 %/day. After some readjustment in the porewater pressure at the beginning of the second stage of consolidation, the specimen began to compress (at day 9) at a rate of about 0.002 %/day, which was of the same order of magnitude as that at the end of the first stage. This suggests that the apparent compression observed in the second stage was essentially the continuation of the creep mechanism experienced by the buffer towards the end of the first stage of consolidation.

Figure 6.5 indicates that specimen T961 had essentially reached equilibrium at the end of the first stage of consolidation with a swelling rate of only about 0.0008 %/day. This rate was two orders of magnitude lower than the rate of 0.03 %/day observed in the second stage. The preceding explanation for specimen T962 therefore

cannot be applied to specimen T961.

The rather large swelling strain of about 0.8% from specimen T961 was probably caused by the incomplete saturation of the specimen. It has been pointed out earlier in this section that a higher back pressure was used on this specimen. The higher pressure may have increased the solubility of air in the pore fluid by Henry's Law (Lowe and Johnson, 1960) and caused swelling. Another possible explanation for the swelling strain is the concept of water deficiency due to Lambe (1958). The concept states that any given soil particle under any given stress state requires a certain amount of water to develop its double diffuse layer fully, and the difference between the needed water and the existing water is deficient water that the particle will try to imbibe. Lambe (1958) has pointed out that because of the usual low water content of compacted clays, such soils are always in a state of water deficiency. Applying this argument to the compacted buffer material, the higher back pressure caused an increase in the solubility of air in the pore fluid, and the specimen started to imbibe water from the buret. As more water was drawn in by the specimen, the double diffuse layers of the clay particles became more fully developed. This would then increase the swelling potential of the buffer, and led to the expansion of the specimen.

The results shown in Figures 6.5 and 6.6 from tests T961 and T962 suggest that the two specimens deviated somewhat from the behaviour expected from the effective stress principle. The deviation is thought to be caused by factors such as the initially unsaturated nature of the specimens and the testing techniques that were used, rather than by any problems with the validity of the principle itself.

The deviations are small, as reflected by the relatively small volume strains (less than 1%), and should not significiantly affect the stress states of the specimens. Taking into account the usual variable nature of soil testing, we can therefore accept, with some small uncertainty, the applicability of the principle on the buffer material. The same conclusion has been drawn from confined swell tests by Dixon et al. (1986).

7.4 UNDRAINED SHEAR BEHAVIOUR

7.4.1 GENERAL DISCUSSION ON SHEAR BEHAVIOUR

Results from the undrained shear tests have been given in Figures 6.8 to 6.29 and Tables 6.3 to 6.5. It has been mentioned that four specimens (T951 to T953 and T961) tested in this series exhibited compressive behaviour, and the remaining five specimens (T954 to T957 and T962) showed a tendency to dilate in shear. It will be remembered that these specimens were prepared with the same specimen preparation technique, and all of them were "fully equilibrated" before the shearing commenced. The inconsistent shear behaviour of the buffer material was initially thought to be caused by the presence of sand particles, which interacted during shear. However the electron micrographs (Figures 7.2 and 7.3) have shown that the sand particles were distributed in the buffer material and too far apart to allow this interaction to take place. This is confirmed by the strength envelopes shown in Figure 6.39. The measured Ø-values correspond to the mineralogy of the clay phase, not the sand. The sand particles should not therefore contribute to the dilatancy of the specimens.

An explanation that can account for the different behaviours (compressive and dilative) that have been observed in shear is the different amount of volume strains exhibited by the specimens during consolidation, which affects the fabric structure of the specimens. As explained in Section 7.3.2.2, the large volume strains (more than 3%) from specimens T951 to T953 and T961 could attribute to a more oriented type of structure in the specimens. As a result of this, they were compressive in shear and produced increasing porewater pressure (Seed and Chan, 1959). On other hand, the small volume strains (less than 3%) from specimens T954 to T957 and T962 prevented significant fabric rearrangement, thereby maintaining the "as-compacted" randomly oriented structure of the specimens. As indicated by the electron micrographs, this "as-compacted" structure consists of randomly arranged closely packed clay peds. The deformation mechanism in these specimens therefore resembled to that of dense sands (Barden, 1972), which shows dilative behaviour and decreasing porewater pressures.

The size of the clay macrostructures in the "dilative" specimens plays an important role in affecting the degree of dilation of the specimens. It is postulated that because of the dense compacted nature, larger sized fabric units will increase the dilation of a buffer specimen. Since the size of these units increases with the moulding water content, which is in turn inversely related to the consolidation pressure by the swelling pressure - water content relationship shown in Figure 4.5, it is therefore expected that the degree of dilation will increase with the moulding water content but decrease with the consolidation pressure. This point is well

illustrated by Figure 7.6, which plots the drop in $\Delta u/\sigma_{cons}$ from peak (failure) to 12 % strain vs. the effective consolidation pressure and the moulding water content. The Figure shows that the drop in porewater pressure, which is an indication of dilation, decreases rather sharply with increasing consolidation pressure and decreasing water content. This is similar to the increase in ductility of sands that accompanies increasing confining pressures. The implication is that at high consolidation pressures and low water contents, the clay units are smaller, and their shearing resistance can be relatively easy to overcome. For low consolidation pressures and high water contents, these soil fabric structures are bigger, their interaction more significant, and therefore more energy is required to overcome their shearing resistance.

An interesting feature of the compressive / dilative nature of the buffer specimens has been observed. Care has been taken to measure the water contents across the length of the specimens immediately after the shearing was stopped. The results are summarized in Table 7.1. Except specimens for T957, T961 and T962, all the specimens showed different water content profiles depending on their mode of failure, whether compressive or dilative. The compressive specimens had higher water contents at the top. Profiles with a lower water content at the top were associated with the dilative specimens. For specimen T957 which was also dilative, there was no water content variation across the length. This uniform water content profile was due to an unavoidable 24 hour delay before the specimen was bulit out of the cell. There was also no apparent trend across specimens T961 and T962. They were tested in the multi-stage

consolidation tests, which involved in changing the cell pressures and back pressures during the course of the test. In any way, the apparent relationship between the water content profile and the corresponding behaviour exhibited by the specimens in undrained shear is not clear. This is perhaps due to the different relationships between elastic and plastic volume strains in the development of shear planes in the specimens (Dr. J.H. Atkinson, personal communication).

7.4.2 UNDRAINED SHEAR MODULUS

Values of the undrained shear modulus and the normalized modulus have been given in Table 6.5. The average normalized moduli from this series and the parallel 900-series are consistently lower that those from the 800-series reported by Sun (1986). Figure 6.17 indicates that the undrained shear modulus generally increases with the effective consolidation pressure. Figure 6.18 plots the normalized modulus with the effective consolidation pressure. The results show rather considerable scatter. However this is typical of results that are generally for modulus values from triaxial programs. The normalized undrained moduli appear to be largely independent of the undrained shear strength and the consolidation pressure, with some tendency to decrease with increasing pressure.

7.4.3 POREWATER PRESSURE GENERATION

The porewater pressure generation of the triaxial compression specimens is best characterized by the porewater pressure parameter at failure, A_f (Skempton, 1954). Values of A_f have been given in Table 6.3. Figure 7.7 summarizes the A_f values from all three series of

investigation in a plot of A_f vs. the effective consolidation pressure. The Figure appears to have a lot of scatter at first sight, but careful examination of the data reveals the existence of four behavioural trends.

Data from the 800-series are shown by open squares. There is some scatter in the data because of incomplete equilibrium of some of the specimens and the different test procedures that were used. The data suggests an increasing trend of A_f with the consolidation pressure. The 900-series data are shown by crosses. All the specimens tested in this series were compressive in nature in both consolidation and shear. The A_f values generally lie in a narrow range between 0.7 and 0.8. (The low A_f values of the two tests at 1.5 MPa labelled (A) are due to the presence of air in the specimens, which caused difficulty in the porewater pressure measurements. F. Saadat, personal communication).

Two types of failure have been observed from the 950-series specimens. The A_f values for the compressive specimens are shown by open diamonds, and those for the dilative ones by open triangles. As expected, the A_f values for the compressive specimens are higher than those for the dilative ones, ranging from 0.55 to 0.98, increasing with consolidation pressure. However for the dilative specimens, with the exception of specimen T956 tested at a very low pressure of 0.1 MPa, the A_f values lie in the narrow range between 0.40 and 0.45.

7.4.4 ANISOTROPY

The anisotropy of the specimens is best demonstrated by the relationships of normalized Δu vs. normalized Δp given in Figures

6.19 to 6.27. The values of m, which is the slope of the linear section of the relationship, have been summarized in Table 6.4. It can be observed that all the values are greater than 1.0, therefore indicating some anisotropy (Graham and Houlsby, 1983) induced in the specimens as a results of the one-dimensional compaction process during specimen preparation.

Figure 7.8 plots the m-values during shear from the three series (800, 900, 950) with the volume strains before shear during consolidation. The Figure shows that the anisotropy of the buffer material is strongly affected by the consolidation strains. Swelling strains lead to a more isotropic (more randomly oriented) nature of the material as indicated by the three data points in the left portion of the plot. On the other hand, compression strains will result in a more oriented (less randomly oriented) structure, and therefore a higher degree of anisotropy.

The compressive data suggests that the m-values are essentially insensitive to the compressive volume strain. The four data points labelled (A) that lie below the main group represent specimens which experienced leakage problems and required remedial measures such as unloading the specimens and fitting extra membranes to stop further leakage. It is believed that the unloading process by removing the total cell pressure could cause some fabic rearrangement of the soil structure leading to a less anisotropic nature of the buffer material.

Figure 7.9 plots the relationship of m and the consolidation pressure, including the data points in (A) in Figure 7.8. The m-values are essentially constant at pressures higher than 0.6 MPa. There is however some scatter in the lower pressure range up to 0.6

MPa. This is because some of the specimens tested in this range experienced swelling or unloading, and therefore had lower m-values.

7.4.5 STRAIN RATE EFFECT

Changes in strain rate during undrained shearing have a fairly pronounced effect on the measured shear strength of a soil. Graham et al. (1983a) reported that a tenfold change in strain rate in undrained shearing of undisturbed natural clays will result in 8% to 15% change in the undrained shearing strength. Li (1983) however reported smaller change of 5% to 8% in undrained shear strength for his remoulded clay, and other remoulded clays also show small changes (Bishop and Henkel, 1962).

Results for rate effects have been reported in Section 6.3.2.3. The change in shearing resistance is defined in Chapter 6 by the strain rate parameter, $\rho_{0.1}$. The values determined from the "step changing" procedure and the relaxation test are found to be 7% and 5% respectively. The values are relatively low, as compared to those for undisturbed natural clays (Graham et al., 1983a), but correspond well with those for remoulded clays (Li, 1983). The difference between the two $\rho_{0.1}$'s is because the tests were performed at different stages of the shearing. Graham et al. (1983a) showed that $\rho_{0.1}$ decreases with increasing strain, and in any case there is typically a wide variation in results obtained by these procedures. The relaxation test was performed at a later stage of the shearing at about 10% axial strain, and therefore a lower $\rho_{0.1}$ was measured.

The implication of the test results is that the undrained

shear strength of the buffer material is not significantly influenced by small variations in the strain rate, but will be affected by large changes over many orders of magnitude. The relatively fast strain rate of 0.6 %/hour adopted in this series seems to have small influence on the porewater pressure equalization of the buffer specimen, as indicated in Figure 6.15.

7.5 DRAINED SHEAR BEHAVIOUR

7.5.1 STRESS-STRAIN-TIME BEHAVIOUR

Results from the drained tests presented in Figures 6.30 to 6.35 show that in the early shear stress increments, the shear strains induced in the specimens were small, increasing with the stress level. The log(strain rate) vs. log(time) relationships are approximately linear, and indicate a decrease in strain rate with time during these early increments. The specimens finally failed in the last increment, with increasing strains and accelerating creep rates (Figures 6.30 to 6.35). Due to the low permeability of the buffer material, it is clear that full drainage did not occur during the final increments and some additional porewater pressure might build up in the specimens. However since the total mean principal stress p was held constant and the deviatior stress q was small, the generated porewater pressure Δu would also be small. The uncertainty in stress state was therefore also small, since q was unaffected by Δu and the effective mean stress p' was affected only by the uncertainty in Δu.

Shear moduli determined from the tests are given in Table 6.6.

The results indicate that the stiffness of the buffer decreases with both time and shear stress level. Note that the shear moduli for specimen T958 are consistently higher than those for specimens T959 and T960. This is due to the lower strain rates used on the specimens during the tests. Eight smaller-sized shear stress increments, as supposed to six increments as for specimens T959 and T960, was applied to specimen T958. This resulted in a slower shear rate, thereby increasing the stiffness of the specimen (Suklje, 1967).

7.5.2 COMPARISON WITH 800-SERIES

In general, the drained test results from this investigation are consistent with those obtained from the 800-series. The shear stress vs. shear strain relationships are similar (see for example, Figures 3.7 and 6.36). Shear moduli obtained from the two series have been shown in Table 6.6. The 950-series specimens appeared to have rather higher stiffnesses than the 800-series specimens tested at the same consolidation pressure. This is probably because of the slower strain rates used in the 950-series study. Differences in soil structure might also be a contributing factor to the higher stiffnesses. The 800-series specimens were consolidated for a long period of time (more than two weeks) and generally showed large volume strains (more than 3%). They therefore attained a softened structure. Specimens T958 to T960 reached consolidation equilibrium in less than two weeks and exhibited much smaller volume strains (less than 1%). So the specimens maintained their "as compacted" randomly arranged structure, and the specimens behaved in a much stiffer manner.

7.6 COULOMB-MOHR STRENGTH ENVELOPES

The various Coulomb-Mohr envelopes for the buffer material obtained from the three series of the buffer project at the University of Manitoba have been summarized in Table 6.7. The strength parameters suggested by these envelopes are consistently higher than the curved envelope of zero cohesion, and friction angles varying from 0° to 4° for sodium montmorillonite reported by Mesri and Olson (1970). However they are consistent with the friction angle of 12½° suggested by Sridharan and Narasimha Rao (1971). The low friction angles obtained by Mesri and Olson (1970) are probably attributed to the parallel clay structure of the test specimens, which were formed by one-dimensional consolidation of clay slurry.

The bilinear envelope in Figure 6.39 determined from the peak data of dilative specimens (T954 to T957 and T962) and drained sheared specimens (T958 to T960) may again be due to the soil structure in the specimens, which contained clay aggregates acting as single particles. Because of the presence of these macroped structures, the deformation mechanism of the buffer specimens was similar to that of sands (Barden, 1972). The friction angles of 22° at low pressures and 14½° at higher pressures suggested by this envelope are therefore an indication of the strength of these macrostructures. The higher friction angle in the low pressure range (up to about 300 kPa) is because the specimens tested in this range had initially higher moulding water content; aggregates were therefore bigger, and resulted in higher interaction between the fabric units, and hence a higher friction angle.

7.7 SYNTHESIS OF DATA AND THE CONCEPTUAL MODEL

One of the objectives given in Chapter 1 was to enhance and improve the conceptual model proposed by Graham et al. (1986a). The model, which has been described in Chapter 2, provides a framework for examining the volume change and shear behaviour of the buffer material. This section summarizes all the consolidation and shear data from this series of tests in a V_c:ln(p') plot, and compares the results with the conceptual model (Graham et al., 1986a).

A tentative model based on the test data up to November 1986 has been presented by Graham et al. (1986b) in a progess report to AECL, and is reproduced in Figure 7.10. Figure 7.11 shows the updated version of the model which includes all the test data from the twelve specimens tested in this series.

Consolidation data presented in terms of V_c vs. ln(p') have been discussed in Section 7.3 (Figure 7.4). Two SEL's are identified in Figure 7.11. SEL (DD) is based on the data from specimens which showed large compressive strains during consolidation, and SEL (CC) represents the consolidation equilibrium of those specimens that exhibited small volume strains. Note that ,as mentioned in Section 7.3.1, SEL (CC) in Figure 7.11 is the "best-fit" line determined from the 950-series "small strain" data, and it is therefore different from the SEL (CC) in Figure 7.10, which is based on all the data from the 800- and 950- series. Also note that SEL (CC) in Figure 7.10 is an early version of the relationship shown in Figure 4.4.

Figure 7.11 also includes line (BB) which is the SEL proposed by Graham et al. (1986a) for the conceptual model. SEL's (BB) and

(DD) are reasonably close, and have similar gradients, but SEL (CC) deviates rather markedly from these two lines. Specimens that lie on SEL (DD) were compressive in shear with increasing porewater pressure. Therefore, they were on the "wet" side of Critical States, and moved to the left towards the Critical State Line (CSL) as they approached failure. For the specimens that lie on SEL (CC), as a result of the larger-sized soil fabric units which affected the swelling equilibrium of the buffer, they ended up on the "dry" side of Critical States. In shear, they showed dilative behaviour with decreasing porewater pressure, and moved right to the CSL as failure was approached.

A tentative CSL for the buffer material has been interpreted from the "end of test" data, and is denoted by (QQ) in Figure 7.11. This CSL is the same as that reported by Graham et al. (1986b) shown in Figure 7.10. Since the majority of the specimens were sheared to an axial strain of up to about 15 % only, they were therefore not yet at their critical states. Porewater pressures and deviator stresses were still changing slowly with axial strains. Two criteria have to be satisfied in locating the position of CSL (QQ). First, it must be on the left side of, and parallel to, the SEL in the V_c:ln(p') space. Second, because the Critical State condition can be reached relatively easily in the compressive specimens, the line is closer to the compressive data points but further from the dilative ones.

The better-controlled CSL (QQ) in Figure 7.11 from the 950-series is an improvement of CSL (PP) which was based on only two "end-of-test" data points from the 800-series.

CHAPTER 8

CONCLUSIONS AND RECOMMENDATIONS

8.1 CONCLUSIONS

Based on the results obtained from this study, the following points are concluded.

1. A swelling pressure - effective clay dry density relationship (Figure 4.4) has been proposed on the basis of the "end-of-consolidation" data obtained from the 800-series and the present 950-series of triaxial tests. Specimens prepared according to this relationship generally exhibited small volume strains (less than 1%) during consolidation. For triaxial specimens, this should replace the one-dimensional swelling pressure - effective clay dry density relationship proposed by Gray et al. (1985) and Dixon et al. (1986) in Figure 3.1 for low pressures up to 1.0 MPa.

2. The differences between the various swelling pressure - effective clay dry density relationships (BB, CC, DD, and EE) examined in this study (Figure 7.4) were due to different soil fabric structures in the specimens. The fabric of the buffer is influenced by factors such as the specimen preparation technique, the use of back pressure, and the volume strains of specimens during consolidation.

3. Multi-stage consolidation test results indicated that the buffer deviated slightly from behaviour expected from the effective stress principle. The deviation was caused by factors such as incomplete saturation of specimens, rearrangement of clay fabric units and particles, creep strains, and expansion of the adsorbed water layers resulting in swell; but probably not due to the major difficulties with the inapplicability of the principle itself.

4. Specimens which exhibited large volume strains (larger than 3%) during consolidation were compressive in undrained shear, with increasing porewater pressures. Specimens which showed small volume strains (typically less than 1%) were dilative, with decreasing porewater pressures. The different shear behaviours exhibited by these specimens, all of which were "fully equilibrated", were due to differences in the soil fabric structure.

5. The "dilative" specimens exhibited increasing ductility with confining pressure in undrained shearing (Figure 7.6). This was due to the smaller-sized fabric units in specimens tested at higher pressures.

6. Anisotropy of the buffer resulted from the compaction process during specimen preparation. The anisotropy was largely independent of the consolidation pressure and the compressive consolidation strains. However swelling consolidation strains

and unloading during consolidation led to a less anisotropic nature of the buffer.

7. The stress-strain behaviour of the buffer was both time- and stress level- dependent.

8. Based on the "end-of-shear" data from the compressive specimens tested in undrained shearing, the strength envelope in the stress range up to 1.5 MPa was represented by the strength parameters of c'= 0 kPa, and Ø'= 13½°.

9. A bilinear strength envelope was suggested for the soil "macrostructures" in the buffer. For the low stress range up to 0.3 MPa, c'= 0 kPa, and Ø'= 22°. In the higher stress range between 0.3 MPa and 1.5 MPa, c'= 40 kPa, and Ø'= 14½°.

10. The conceptual model proposed by Graham et al. (1986a) has been updated and modified by incorporating the effects of soil structure and testing technique. This model will, in principle, enable engineers to make assess the time-dependent swelling pressure-volume change behaviour of buffer upon the influx of water into the disposal vault at the end of the emplacement; and the short-term and long-term stability of the buffer under static loading from the waste containers.

8.2 SUGGESTIONS FOR FURTHER RESEARCH

1. The buffer will operate in an environment with temperatures approaching 100°C, and porewater pressures up to 10 MPa. Tests which include these high temperatures and high pressures are necessary to be able to gain a complete understanding of the behaviour of the buffer under these conditions.

2. Electron microscopy testing should be performed on buffer specimens at various stages of a triaxial test (after compaction, end-of-consolidation, peak shear, and end-of-shear). This will hopefully lead to a better understanding of the influence of the soil fabric structure on the buffer behaviour.

3. More multi-stage consolidation tests, which involve changing the total pressures and the back pressures with the effective pressures kept constant, should be performed to confirm the applicability of the effective stress principle to the buffer.

4. Tests on specimens formed according to the swelling pressure - effective clay dry density relationship in a higher stress range (higher than 1.5 MPa) are recommended.

5. In the actual conditions in the disposal vault, the buffer will be compacted to a dry density of 1.67 Mg/m^3 with a water content of 17% to 19% (Dixon et al., 1986). Tests on specimens compacted to these conditions are recommended.

6. The conceptual model should be improved and extended to include the effects of high pressures and high temperatures. Particular attentions should be paid to considering the uncertainties in porewater pressure evaluation at the microfabric level.

REFERENCES

ASTM D-1557-78, 1986. "Standard Test Method for Determining the Moisture-density Relations of Soil". American Society for Testing and Materials, Philadelphia.

Atkinson, J.H., and Bransby, P.L., 1978. "The Mechanics of Soils". McGraw-Hill Book Company (U.K.) Ltd.

Aylmore, L., and Quirk, J.P., 1959. "Swelling of Clay-Water Systems". Nature, London, 183, pp. 1752-1753.

Aylmore, L., and Quirk, J.P., 1960. "Domain or Turbostratic Structure in Clays". Nature, London, 187, pp. 1046-1047.

Baldi, G., Borsetto, M., Huekel, T., Peano, A., and Tassoni, E., 1985. "Hard Clay as Host Medium: Thermo-mechanical Experiments and Model". Materials Research Society Symposium Proceedings, Vol. 50.

Baracos, A., 1977. "Compositional and Structural Anisotropy of Winnipeg Soils - a Study Based on Scanning Electron Microscopy and X-Ray Diffraction Analyses". Canadian Geotechnical Journal, Vol. 14, pp. 125-137.

Barden, L., 1971. "Examples of Clay Structure and its Influence on Engineering Behaviour". Proceedings of the Roscoe Memorial Symposium, Cambridge University, 29-31 March 1971, pp. 195-205.

Barden, L., 1972. "The Influence of Structure on Deformation and Failure in Clay Soil". Geotechnique, 22, pp. 159-163.

Barden, L., and Sides, G.R., 1970. "The Engineering Behaviour and Structure of Compacted Clay". ASCE Journal of the Soil Mechanics and Foundations Division, Vol. 96, SM4, pp. 1171-1200.

Bechai, M., Mansson, N.L., and Rao, P.K.M., 1986. "Disposal Concepts for Radioactive Wastes in Clay or Till Deposits". Proceedings of the Second International Conference on Radioactive Waste Management, Winnipeg, Canada.

Bird, G.W., and Cameron, D.J., 1982. "Vault Sealing Research for The Canadian Nuclear Fuel Waste Management Program". Atomic Energy of Canada Limited Technical Report TR-145.

Bishop, A.W., and Henkel, D.J., 1962. "The Measurement of Soil Properties in the Triaxial Test". Second Edition, Edward Arnold (Publishers) Ltd.

Bolt, G.H., 1956. "Physico-chemical Analysis of the

Compressibility of Pure Clays". Geotechnique, Vol.6, No. 2, pp. 86-93.

Bowles, J.E., 1979. "Physical and Geotechnical Properties of Soils ". McGraw-Hill Book Company, New York.

Cheung, S.C.H., Gray, M.N., and Dixon, D.A., 1985. "Hydraulic and Ionic Diffusion Properties of Bentonite-sand Buffer Materials". Proceedings of International Symposium on Coupled Processes Affecting The Performance of a Nuclear Waste Repository, Lawrence Berkeley Laboratories, California.

Crooks, J.H.A., and Graham, J., 1976. "Geotechnical Properties of the Belfast Estuarine Deposits". Geotechnique, Vol. 26, No. 2, pp. 293-315.

Dixon, D.A., and Gray, M.N., 1985. "The Engineering Properties of Buffer Material - Research at Whiteshell Nuclear Research Establishment". Proceeding of The Nineteenth Information Meeting of The Nuclear Waste Management Program, Atomic Energy of Canada Limited Technical Report TR-350, Vol. 3, pp. 513-530.

Dixon, D.A., and Woodcock, D.R., 1986. "Physical and Engineering Properties of Candidate Buffer Materials". Atomic Energy of Canada Limited Technical Report TR-352.

Dixon, D.A., Gray, M.N., and Thomas, A.W., 1985. "A Study of The Compaction Properties of Potential Clay-sand Buffer Mixtures for Use in Nuclear Fuel Waste Disposal". Engineering Geology, Vol. 21, pp. 247-255.

Dixon, D.A., Gray, M.N., Baumgartner. P., and Rigby G.L., 1986. "Pressures Acting on Waste Containers in Bentonite-Based Materials". Proceedings of the Second International Conference on Radioactive Waste Management, Winnipeg, Canada.

Gens, A., 1982. "Stress-Strain and Strength Characteristics of a Low Plasticity Clay". PhD Thesis, Imperial College of Science and Technology. University of London.

Ginniff, M.E., 1986. "Radioactive Waste Management in the United Kingdom". Proceedings of the Second International Conference on Radioactive Waste Management, Winnipeg, Canada.

Graham, J., 1974. "Laboratory Testing of Sensitive Clay from Lyndhurst, Ontario". Civil Engineering Research Report CE74-2, Royal Military College, Kingston, Ontario.

Graham, J., and Houlsby, G.T., 1983. "Anisotropic Elasticity in a Natural Plastic Clay". Geotechnique, Vol. 33, No. 2, pp. 165-180.

Graham, J., Crooks, J.H.A., and Bell, A.L., 1983a. "Time Effects on the Stress-strain Behaviour of Natural Soft Clays". Geotechnique, Vol. 33, No. 3, pp. 327-340.

Graham, J., Noonan, M., and Lew, K.V., 1983b. "Yield States and Stress - Strain Relationships in a Natural Plastic Clay". Canadian Geotechnical Journal, Vol. 20, pp. 502-516.

Graham, J., Gray, M.N., Sun, B.C.-C., and Dixon, D.A., 1986a. "Strength and Volume Change Characteristics of a Sand-Bentonite Buffer". Proceedings of the Second International Conference on Radioactive Waste Management, Winnipeg, Canada.

Graham, J., Saadat, F., and Wan A.W.-L., 1986b. "Geotechnical Properties of Sand-Clay Buffer Material". Unpublished Progress Report to AECL, November 1986.

Graham, J., Saadat, F.S., Gray, D.A., Dixon, D.A., and Zhang Q.-Y., 1987 "Strength and Volume Change Behaviour of a Sand-Bentonite Mixture". In Preparation.

Gray, M.N., Cheung, S.C.H., and Dixon, D.A., 1984. "The Influence of Sand Content on Swelling Pressures and Structure Developed in Statically Compacted Na-bentonite". Atomic Energy of Canada Limited Report AECL-7825.

Gray, M.N., Cheung, S.C.H., and Dixon, D.A., 1985. "Swelling Pressures of Compacted Bentonite/Sand Mixtures". Proceedings of The Nineteenth Information Meeting of The Nuclear Fuel Waste Management Program, Atomic Energy of Canada Limited Technical Report TR-350, Vol. 3, pp. 776-785.

Grim, R.E., 1953. "Clay Mineralogy". McGraw-Hill Book Company, Inc.

Head, K.H., 1986. "Manual of Soil Laboratory Testing, Volume 3: Effective Stress Tests". Pentech Press, London.

Houlsby, G.T., Wroth, C.P., and Wood, D.M., 1982. "Predictions of the Results of Laboratory Tests on a Clay using a Critical State Model". The International Workshop on Constitutive Relations for Soils, Grenoble, September 1982.

Lambe, T.W., 1958. "The Structure of Compacted Clay". ASCE Journal of Soil Mechanics and Foundations Division, Vol. 84, SM2, pp. 1-34.

Lambe, T.W. and Whitman R.V., 1979. "Soil Mechanics, SI Version". John Wiley & Sons, New York.

Lew, K.V., 1981. "Yielding Criteria and Limit-state in a Winnipeg Clay". M.Sc. Thesis, The University of Manitoba, Winnipeg,

Manitoba.

Li, E.C.C., 1983. "A Geotechnical Study of Remoulded Winnipeg Clay". M.Sc. Thesis, The University of Manitoba, Winnipeg, Manitoba.

Lopez, R.S., 1985. "Review of Vault Sealing Research". Proceedings of The Nineteenth Information Meeting of The Nuclear Waste Management Program, Atomic Energy of Canada Limited Technical Report TR-350, Vol. 3, pp. 499-506.

Low, J., and Johnson, T.C., 1960. "Use of Back Pressure to Increase Degree of Saturation of Triaxial Test Specimens". Research Conference on Shear Strength of Cohesive Soils, Boulder, Colorado, pp. 819-836.

Lundgren, T., and Soderblom, R., 1985. "Clay Barriers - A Not Fully Examined Possibility". Engineering Geology, Vol. 21, pp. 201-208.

Mesri, G., and Olson, R.E., 1970. "Shear Strength of Montmorillonite". Geotechnique, Vol. 20, No. 3, pp. 261-270.

Mitchell, J.K., 1976. "Fundamental of Soil Behaviour". John Wiley and Sons, Inc.

Mitchell, J.K., Hooper, D.R., and Campanella, R.G., 1965. "Permeability of Compacted Clay". ASCE Journal of Soil Mechanics and Foundations Division, Vol. 91, SM4, pp. 41-65.

Musa, A.M., 1982. "On the Yield of a Compacted Clayey Soil". M.Sc. Thesis, The University of Wales, University College, Cardiff.

Noonan, M.L., 1980. "Limit State Studies in Winnipeg Clays". M.Sc. Thesis, The University of Manitoba, Winnipeg, Manitoba.

Olivier, J.-P., 1986. "Radioactive Waste Management in OECD Countries National Programs and Joint Activities". Proceedings of the Second International Conference on Radioactive Waste Management, Winnipeg, Canada.

Prevost, J.-H., and Hoeg, K., 1975. "Effective Stress - Strain - Strength Model for Soils". ASCE Journal of the Geotechnical Engineering Division, Vol. 101, GT3, pp. 259-278.

Quigley, R.M., 1984. "Quantitative Mineralogy and Preliminary Porewater Chemistry of Candidate Buffer and Backfill Materials for a Nuclear Fuel Waste Disposal Vault". Atomic Energy of Canada Limited Report AECL-7827.

Radhakrishna, H.S., 1984. "Thermal Properties of Clay-based Buffer Materials for a Nuclear Fuel Waste Disposal Vault".

Atomic Energy of Canada Limited Report AECL-7805.

Roscoe, K.H., Schofield, A.N., and Wroth, C.P., 1958. "On Yielding of Soils". Geotechnique, Vol. 8, No. 1, pp. 22-53.

Schofield, A.N., and Wroth, C.P., 1968. "Critical State Soil Mechanics". McGraw-Hill Book Company (U.K.) Ltd.

Scott, R.F., 1963. "Principles of Soil Mechanics". Addison-Wesley Publishing Company, Inc.

Seed, H.B., and Chan, C.K., 1959. "Structure and Strength Characteristics". ASCE Journal of Soil Mechanics and Foundations Division, Vol. 85, SM5, pp. 87-128.

Seed, H.B., and Mitchell, J.K., and Chan, C.K., 1962. "Studies of Swell and Swell Pressure Characteristics of Compacted Clays". US Highway Research Board, Bulletin 313.

Selvadurai, A.P.S., Lopez, R.S., and Hartley, G.A., 1985. "Geomechanical Interaction in a Nuclear Waste Disposal Vault". Proceedings of the Eleventh International Conference on Soil Mechanics and Foundation Engineering, San Francisco, Vol. 3, pp. 1299-1305.

Sherif, M.A., Ishibashi, I., and Medhin, B.W., 1982. "Swell of Wyoming Montmorillonite and Sand Mixtures". ASCE Journal of the Geotechnical Engineering Division, Vol. 108, GT1, pp. 33-45.

Simons, N.E., 1960. "The Effect of Overconsolidation on the Shear Strength Characteristics of an Undisturbed Oslo Clay". Research Conference on Shear Strength of Cohesive Soils, Boulder, Colorado, pp. 747-763.

Skempton, A.W., 1954. "The Pore-pressure Coefficients A and B". Geotechnique, Vol. 4, pp. 143-147.

Sridharan, A., and Narasimha Rao, S., 1971. Discussion on "Shear Strength of Montmorillonite", Mesri and Olson, 1971. Geotechnique, Vol. 21, No. 2, pp. 180-181.

Sridharan, A., Rao, A., and Sivapullaiah, P.V., 1986. "Swelling Pressure of Clays". Geotechnical Testing Journal, Vol. 9, No. 1, pp. 24-33.

Suklje, L., 1967. "Common Factors Controlling the Consolidation and Failure of Soils". Proceedings of Geotechnical Conference, Olso, 1967, Vol. 1, pp. 153.

Sun, B.C.-C., 1986. "Stress-Strain Properties in Sand-Clay Buffer Materials". M.Sc. Thesis, The University of Manitoba, Winnipeg, Manitoba.

Terzaghi, K., 1956. Correspondence to "Physico-chemical Analysis of the Compressibility of Pure Clays", Bolt, 1956. Geotechnique, Vol. 6, pp. 191-192.

Vaid, Y.P., and Campanella, R.G., 1977. "Time Dependent Behaviour of Undisturbed Clay". ASCE Journal of the Geotechnical Engineering Division, Vol. 103, GT7, pp. 693-709.

Vardoulakis, I., 1985. "Stability and Bifurcation of Undrained Plane Rectilinear Deformations on Water-saturated Granular Soils". International Journal of Numerical Analysis Methods in Geomechanics, Vol. 9, No. 5, pp. 399-414.

Warkentin, B.P., Bolt, G.H., and Miller, R.D., 1957. "Swelling Pressure of Montmorillonite". Proceedings of Soil Science Society of America, Vol. 21, pp. 495-497.

Wood, D.M., 1984. "On Stress Parameters". Geotechnique, Vol. 34, No. 2, pp. 282-287.

Wroth, C.P., and Houlsby, G.T., 1985. "Soil Mechanics - Property Characterization and Analysis Procedures". State of the Art Report, Proceedings of The Eleventh International Conference on Soil Mechanics and Foundation Engineering, San Francisco, Vol. 1, pp. 1-54.

Yong, R.N., 1967. "The Swelling of a Montmorillonitic Clay at Elevated Temperatures". Proceedings of the Third Asian Regional Conference on Soil Mechanics and Foundation Engineering.

Yong, R.N., 1971. "Soil Technology and Stabilisation". General Report to Session 5, Proceedings of the Fourth Asian Regional Conference on Soil Mechanics and Foundation Engineering, Bangkok, Vol. 2.

Yong, R.N. and Warkentin B.P., 1975. "Soil Properties and Behaviour". Elsevier Scientific Publishing Company.

Yong, R.N., Boonsinsuk, P., and Yiotis, D., 1985. "Creep Behaviour of a Buffer Material for Nuclear Fuel Waste Vault". Canadian Geotechnical Journal, Vol. 22, No. 4, pp. 541-550.

TABLE 5.1 - INITIAL CONDITION OF TRIAXIAL SPECIMENS AT BEGINNING OF CONSOLIDATION

Specimen No.	Water Content (%)	Bulk Density (Mg/m^3)	Dry Density (Mg/m^3)	Eff. Clay Density (Mg/m^3)	V_c	Saturation (%)
T951	37.6	1.81	1.32	0.90	3.06	96.5
T952	28.1	1.90	1.48	1.08	2.55	92.5
T953	30.5	1.87	1.43	1.03	2.67	93.1
T954	35.5	1.84	1.36	0.93	2.96	97.0
T955	28.4	1.92	1.50	1.07	2.57	95.2
T956	39.5	1.79	1.28	0.87	3.16	96.6
T957	23.2	2.01	1.63	1.21	2.27	95.5
T958	35.9	1.83	1.35	0.93	2.97	96.4
T959	25.9	1.96	1.56	1.14	2.42	95.1
T960	29.4	1.91	1.48	1.05	2.62	95.7
T961	31.0	1.89	1.44	1.02	2.71	96.1
T962	33.8	1.85	1.38	0.96	2.86	95.8

TABLE 5.2 - SATURATION OF TRIAXIAL SPECIMENS AT END OF CONSOLIDATION

Specimen No.	B
T951	1.00
T952	0.99
T953	0.99
T954	0.99
T955	0.98
T956	0.99
T957	1.00
T961	0.99
T962	0.99
Average (950-series)	0.99
Average (800-series)	0.97

TABLE 5.3 - SUMMARY OF INITIAL AND FINAL WATER CONTENTS OF TRIAXIAL SPECIMENS

Specimen No.	Water Content (%)					
	Initial (Measured)	Initial (Calculated)	Difference[1]	Final (Measured)	Final (Calculated)	Difference[1]
T951	37.6	44.1	6.5	36.8	30.2	6.6
T952	28.1	31.2	3.1	28.6	25.6	3.0
T953	30.5	33.0	2.5	29.7	27.2	2.5
T954	35.5	37.2	1.7	36.7	35.0	1.7
T955	28.4	29.1	0.7	28.5	27.9	0.6
T956	39.5	39.4	0.1	41.6	41.7	0.1
T957	23.2	23.6	0.4	23.1	22.6	0.5
T958	35.9	36.1	0.2	36.9	36.7	0.2
T959	25.9	25.7	0.2	25.3	25.5	0.2
T960	29.4	30.4	1.0	28.8	27.8	1.0
T961	31.0	30.1	0.9	27.9	28.8	0.9
T962	33.8	34.2	0.4	33.6	33.2	0.4

1 Difference between measured and calculated values.

TABLE 6.1 - QUALITY CONTROL TEST RESULTS

Specimen No.	p'_s	TARGETTED Water Content	TARGETTED Dry Density	MEASURED Water Content		MEASURED Standard Deviation	MEASURED Dry Density	S_r	Layers[1]	Slices[2]
	(MPa)	(%)	(Mg/m^3)	(%), ± Range			(Mg/m^3)	(%)		
QC950-1	1.5	24.9	1.62	25.7	0.6	0.26	1.56	95.4	6	8
QC950-2	1.5	24.9	1.62	24.4	0.2	0.17	1.65	-	7	8
QC950-3	1.5	24.9	1.62	22.9	0.5	0.25	1.63	94.2	8	6
QC951-1	0.6	33.0	1.43	31.5	0.4	0.23	1.44	96.7	5	6
QC951-2	0.6	33.0	1.43	32.0	0.4	0.22	1.42	96.1	8	7
QC952-1	1.0	27.7	1.54	27.8	0.5	0.23	1.51	95.8	5	6
QC952-2	1.0	27.7	1.54	27.2	0.5	0.24	1.52	95.1	8	7
QC953-1	0.4	37.9	1.33	37.6	-	-	1.32	96.9	5	6
QC953-2	0.4	37.9	1.33	37.3	1.1	0.66	1.32	95.8	8	7
QC954-1	2.5	20.3	1.74	19.7	0.3	0.17	1.73	94.3	5	6
QC954-2	2.5	20.3	1.74	19.7	0.3	0.14	1.73	94.7	8	5
QC955-1	3.5	18.1	1.81	18.2	0.2	0.12	1.78	94.6	5	4
QC955-2	3.5	18.1	1.81	18.5	0.2	0.12	1.77	95.6	8	5
QC956-1	0.2	48.5	1.17	47.6	0.4	0.28	1.17	97.8	5	6
QC956-2	0.2	48.5	1.17	47.4	0.6	0.51	1.17	97.3	8	7

1 No. of layers used during compaction into mould.
2 No. of slices used for determining water content distribution in the specimen.

TABLE 6.2 - VOLUME STRAINS OF TRIAXIAL SPECIMENS DURING CONSOLIDATION

Specimen No.	Stage[1]	Consolidation Pressure (MPa)	Consolidation Duration (Days)	Volume Strain (%)
T951[2]	S	0.4	17	+ 9.7
T952	S	1.0	12	+ 3.7
T953	S	0.8	17	+ 4.7
T954	S	0.2	12	+ 0.7
T955	S	0.6	19	+ 0.9
T956	S	0.1	19	- 2.8
T957	S	1.5	14	+ 0.9
T958	S	0.2	13	- 0.5
T959	S	1.0	10	+ 0.4
T960	S	0.6	10	+ 1.8
T961	M	0.5/0.5/0.9	39	+ 1.2/- 0.8/+ 2.8
T962	M	0.3/0.3	100	+ 0.8/+ 0.1

1 S = Single-stage / M = Multi-stage
2 Continuing volume changes after 17 days suggested leakage in the volume change connection.

TABLE 6.3 - SUMMARY OF UNDRAINED SHEAR TEST RESULTS AT FAILURE

Specimen No.	σ'_{cons} (MPa)	ϵ_{1f} (%)	q_f (MPa)	p'_f (MPa)	$(q/p')_f$	u_f (MPa)	A_f
T951	0.4	3.5	0.17	0.36	0.48	0.10	0.57
T952	1.0	5.0	0.34	0.77	0.44	0.33	0.98
T953	0.8	6.1	0.33	0.62	0.53	0.28	0.86
T954	0.2	5.9	0.16	0.19	0.86	0.07	0.42
T955	0.6	5.7	0.37	0.55	0.68	0.16	0.44
T956	0.1	6.6	0.11	0.12	0.93	0.01	0.12
T957	1.5	5.0	0.84	1.40	0.60	0.41	0.49
T961	0.5/0.9	5.7	0.45	0.75	0.60	0.30	0.67
T962	0.3	4.3	0.23	0.27	0.86	0.10	0.45

TABLE 6.4 - SUMMARY OF NORMALIZED UNDRAINED SHEAR TEST RESULTS AT FAILURE

Specimen No.	σ'_{cons} (MPa)	ϵ_{1f} (%)	q_f/σ'_{cons}	$(q/p')_f$	u_f/σ'_{cons}	m
T951	0.4	3.5	0.44	0.48	0.25	1.43
T952	1.0	5.0	0.34	0.44	0.33	2.17
T953	0.8	6.1	0.41	0.53	0.35	2.23
T954	0.2	5.9	0.80	0.86	0.33	1.89
T955	0.6	5.7	0.63	0.68	0.27	2.14
T956	0.1	6.6	1.14	0.93	0.14	1.25
T957	1.5	5.0	0.56	0.60	0.27	2.13
T961	0.5/0.9	5.7	0.50	0.60	0.33	2.20
T962	0.3	4.3	0.77	0.86	0.34	1.92

TABLE 6.5 - SUMMARY OF VALUES OF UNDRAINED SHEAR MODULUS E_{50}

Specimen No.	σ'_{cons} (MPa)	s_u [1] (MPa)	E_{50} (MPa)	E_{50}/s_u	E_{50}/σ'_{cons}	G_{50}/σ'_{cons} [2]
T951	0.4	87	23	263	57	19
T952	1.0	169	23	137	23	8
T953	0.8	165	17	103	21	7
T954	0.2	80	20	244	98	33
T955	0.6	187	26	141	44	15
T956	0.1	57	8	146	83	28
T957	1.5	405	83	204	55	18
T961	0.5/0.9	224	50	221	55	18
T962	0.3	116	30	259	100	33
Average±Standard Deviation				190±60	60±29	20±10

1. $s_u = q_{max}/2$
2. $G_{50} = E_{50}/2(1 + \nu)$. In undrained tests $\nu = 0.5$, so $G_{50} = E_{50}/3$.

TABLE 6.6 - SUMMARY OF VALUES OF NORMALIZED DRAINED SHEAR MODULUS G/σ'_{cons}

Specimen No.	σ'_{cons} (MPa)	q_{max} (MPa)		Values of G/σ_{cons} at $q_{max}/2$ '1-day'	'2-day'	'3-day'
958	0.2	0.16		19	14	12
959	1.0	0.66		11	10	9
960	0.6	0.42		12	10	9
			Average	14	11	10
802	0.2	0.20		16	12	10
806	0.2	0.14		6	4	3
808	0.4	0.32		11	8	7
804	0.6	0.40		11	7	6
805	0.6	0.35		12	9	8
			Average	11	8	7

TABLE 6.7 SUMMARY OF COULOMB-MOHR STRENGTH PARAMETERS c' AND Ø'

Series	c' (kPa)	Ø' (°)	Range (MPa)	Source[1]	Reference
800	0	16	up to 1.0	E	Sun, 1986
800	48	13	0.1 to 0.8	E	Sun, 1986
All	0	16	up to 1.5	C;P	Graham et al., 1986b
All	24	16	up to 1.5	D;P	Graham et al., 1986b
900	0	13	up to 3.0	C;E	Graham et al., 1987
950	0	13½	up to 1.5	C;E	
950	0	13½	up to 1.5	C;P	
950	0	22	up to 0.3	D;P	
950	40	14½	0.3 to 1.5	D;P	

1 C = Compressive / D = Dilative
E = End-of-test / P = Peak

TABLE 7.1 - Water Content Gradients Related to Compressive / Dilative Shear Behaviour

Specimen No.	Water content (%) Top	Bottom	Vol. Strain During Consolidation[1]	Behaviour During Shear[1]
T951	38.4	35.0	C	C
T952	29.7	27.7	C	C
T953	30.0	29.4	C	C
T954	36.1	37.4	C	D
T955	28.0	29.2	C	D
T956	41.2	41.7	D	D
T957	23.0	23.0	C	D
T961	28.1	27.8	C	C
T962	33.7	33.7	C	D

1. C = Compressive; D = Dilative.

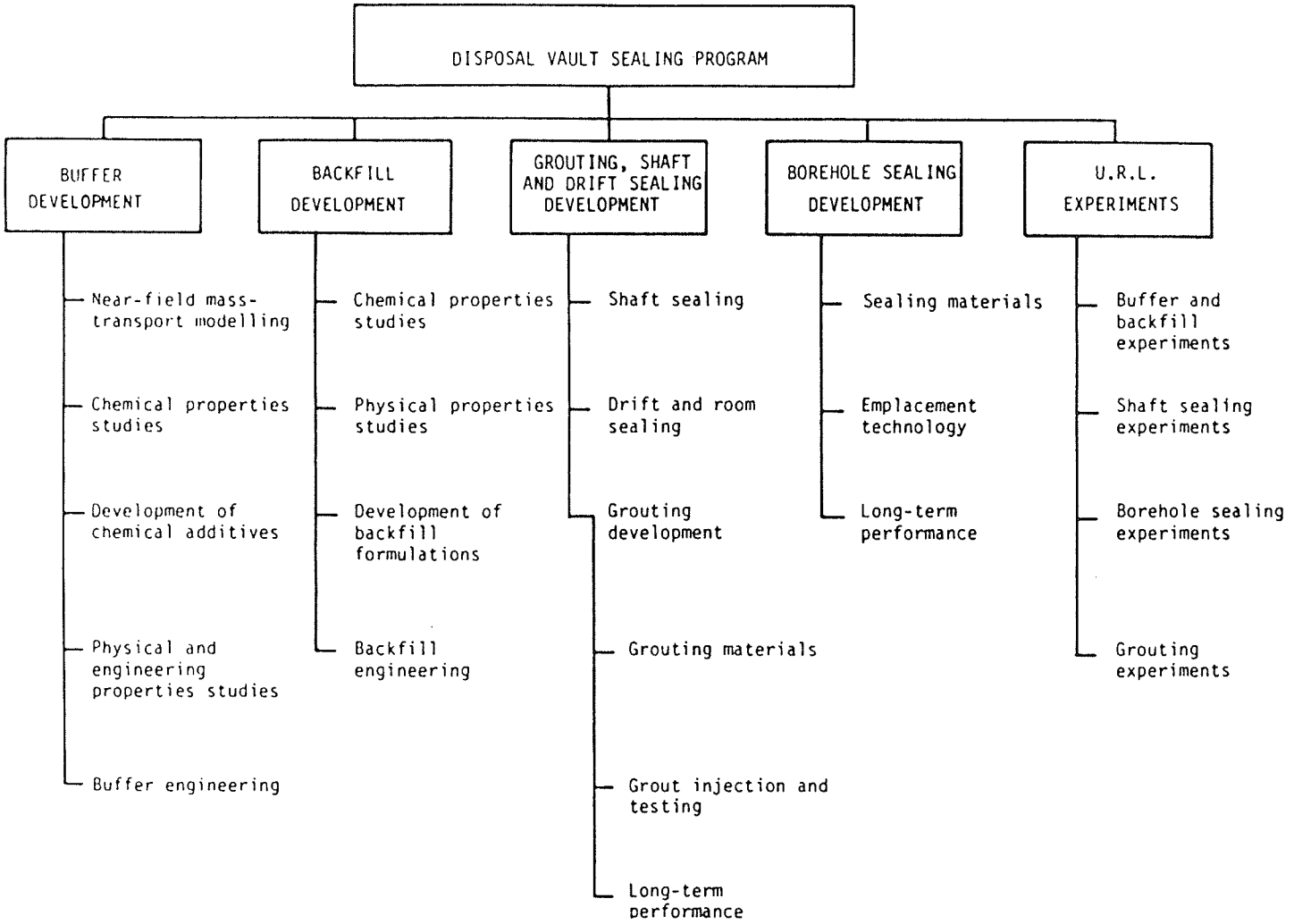

FIG. 1.1 - ORGANISATION CHART OF THE VAULT SEALING PROGRAM (AFTER BIRD AND CAMERON, 1982)

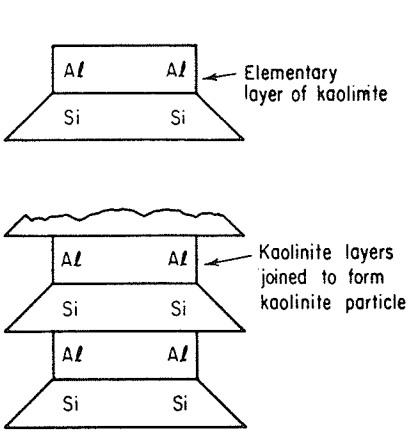

(A) KAOLINITE

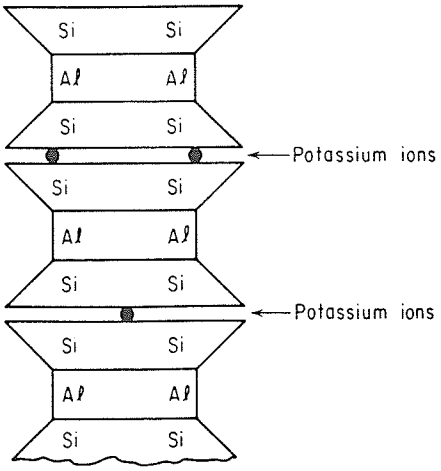

(B) ILLITE

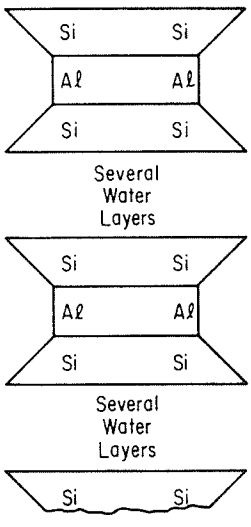

(C) MONTMORILLONITE

FIG. 2.1 - STRUCTURE OF (A) KAOLINITE (B) ILLITE (C) MONTMORILLONITE (AFTER YONG AND WARKENTIN, 1975)

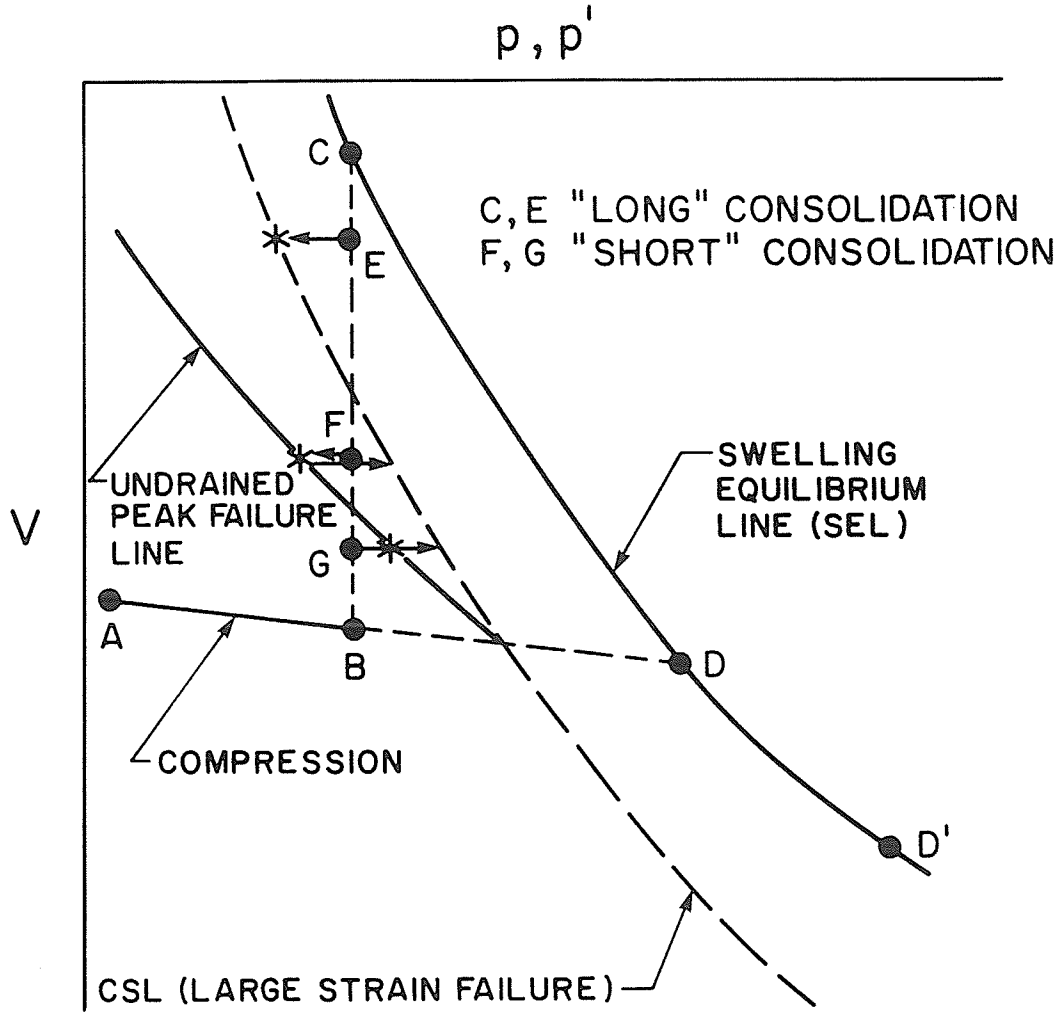

FIG. 2.2 - PROPOSED CONCEPTUAL MODEL FOR p',q,V-STATE BEHAVIOUR OF EXPANSIVE CLAY (AFTER GRAHAM ET AL., 1986a)

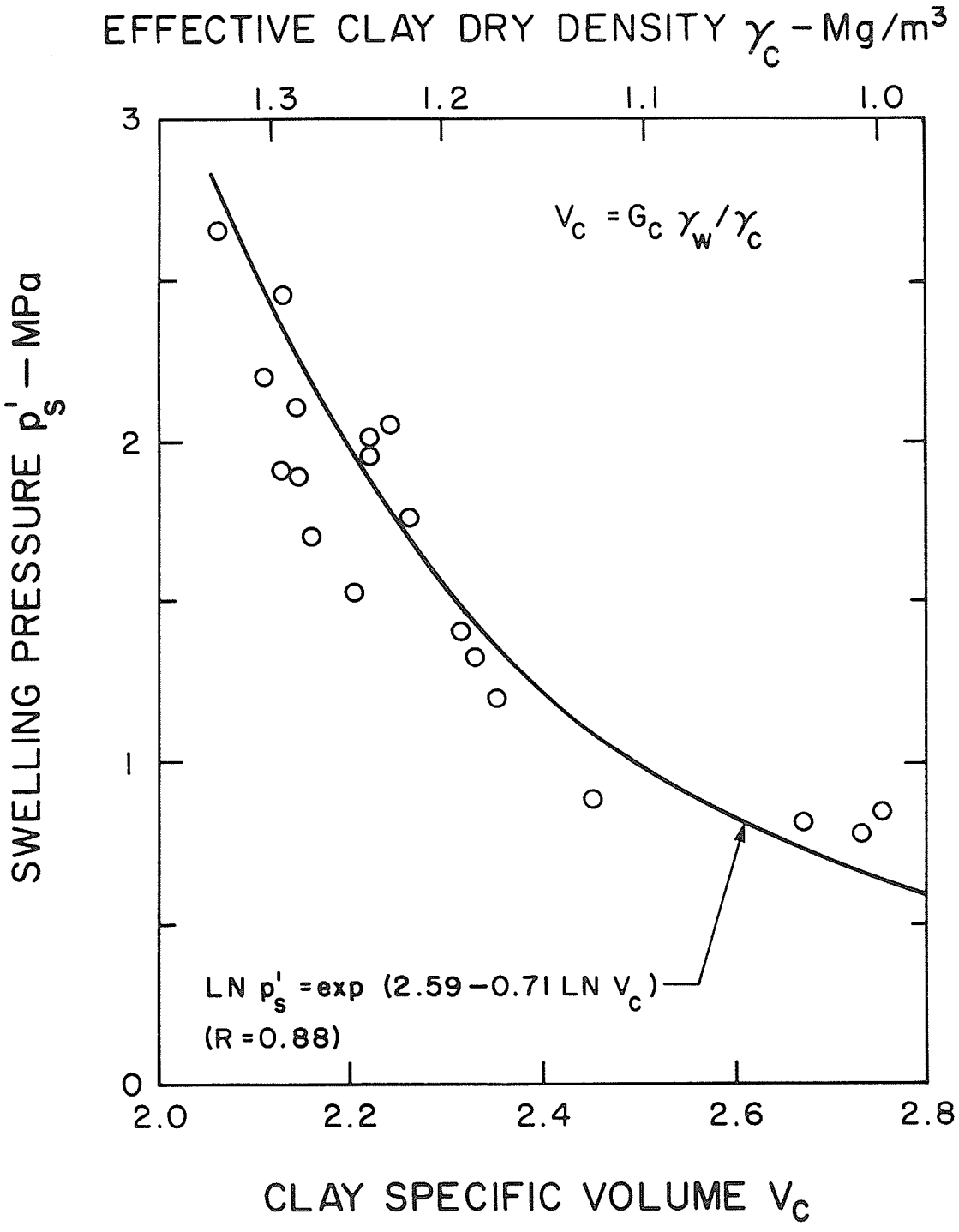

FIG. 3.1 - SWELLING PRESSURE VS. EFFECTIVE CLAY DRY DENSITY / CLAY SPECIFIC VOLUME (AFTER GRAHAM ET AL., 1986a)

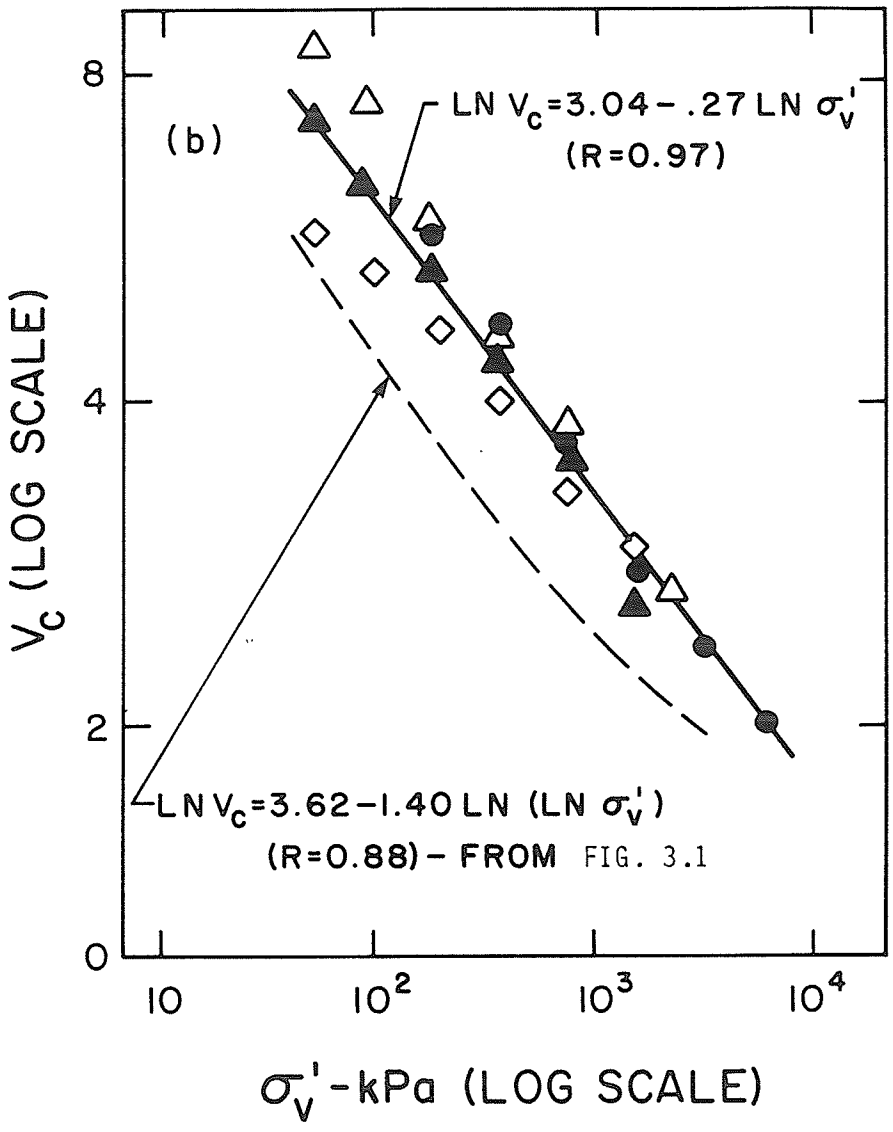

FIG. 3.2 - CLAY SPECIFIC VOLUME VS. VERTICAL PRESSURE IN 1-D COMPRESSION (AFTER GRAHAM ET AL., 1986a)

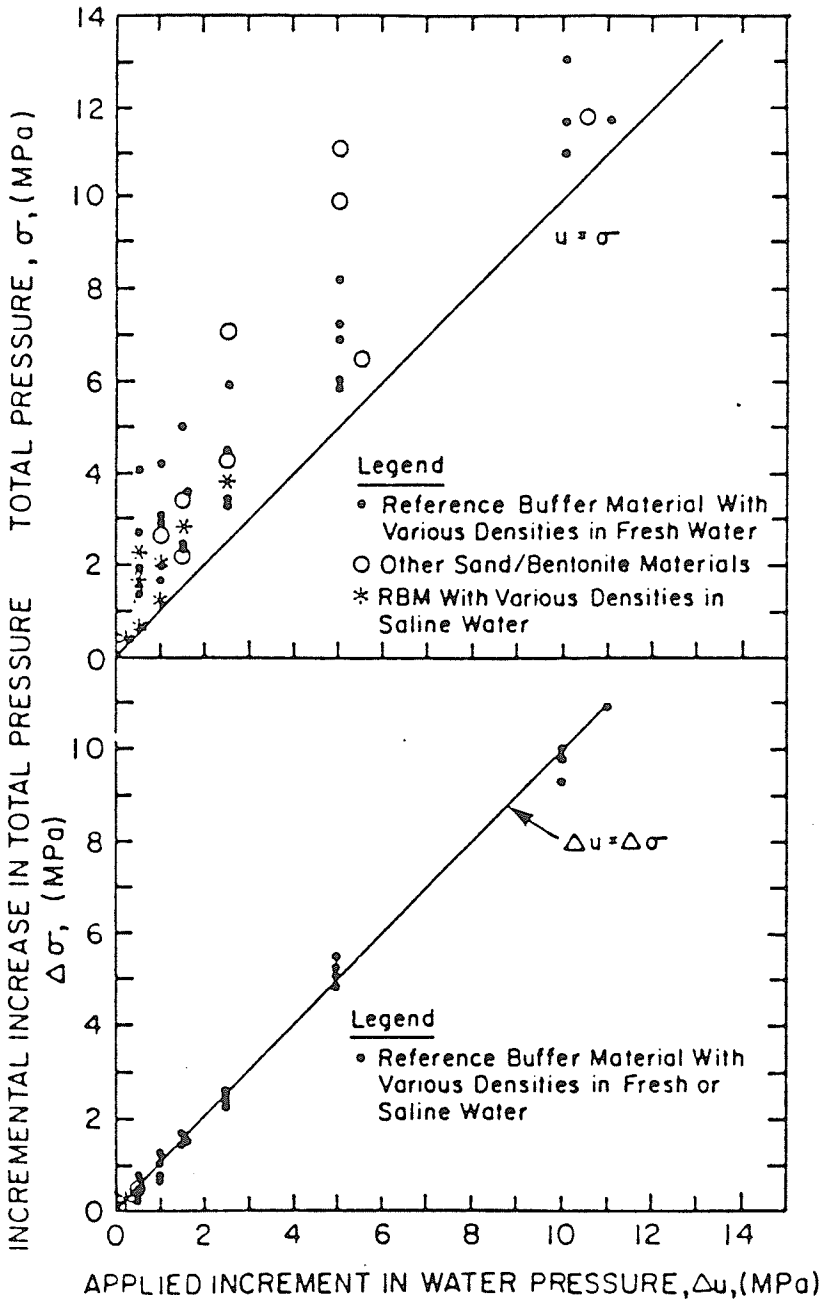

FIG. 3.3 - RELATIONSHIP BETWEEN APPLIED WATER PRESSURE AND (A) TOTAL PRESSURE (B) INCREASE IN TOTAL PRESSURE (AFTER DIXON ET AL.,1986)

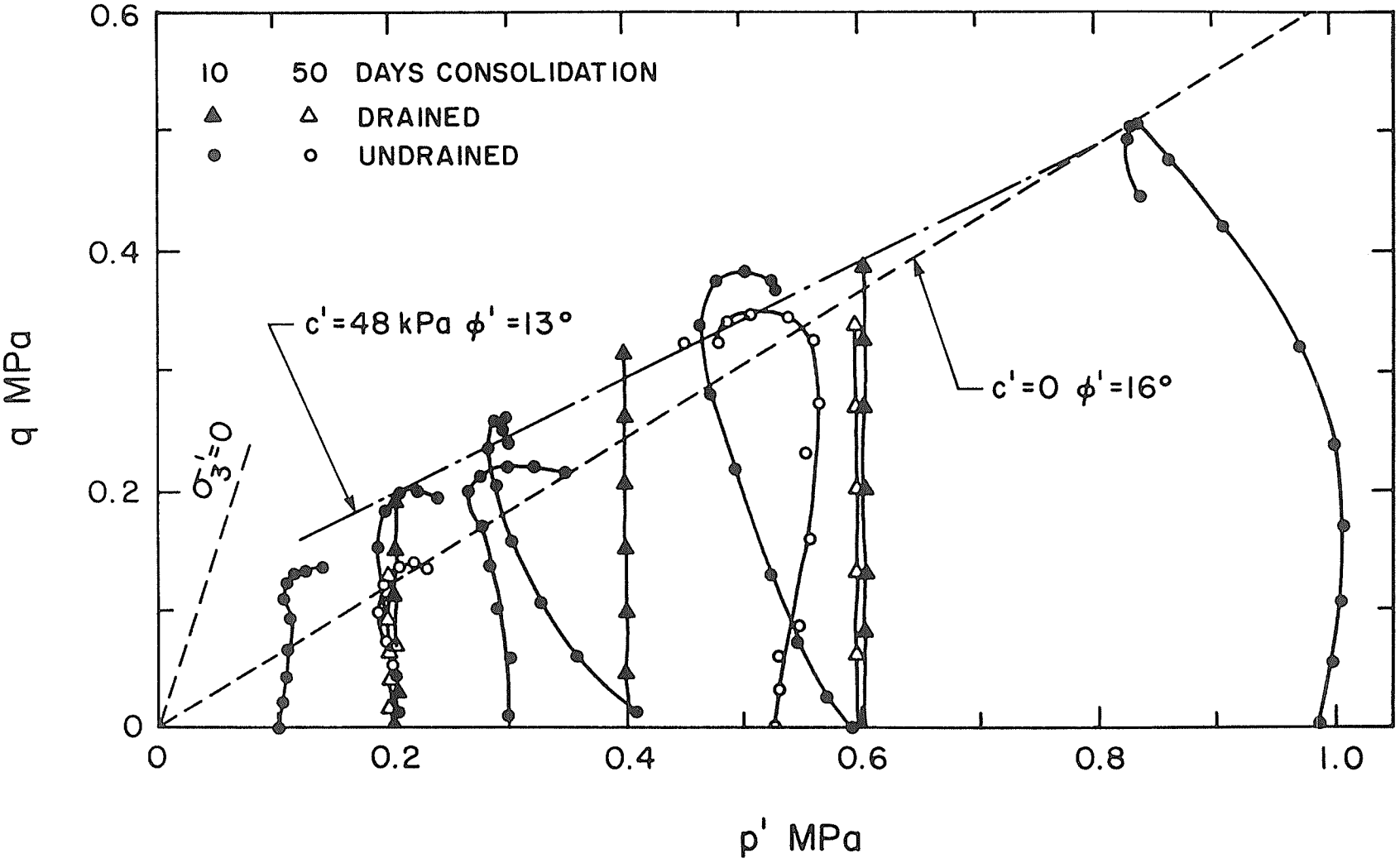

FIG. 3.4 - SHEAR STRENGTH ENVELOPE FROM 800-SERIES (AFTER SUN, 1986)

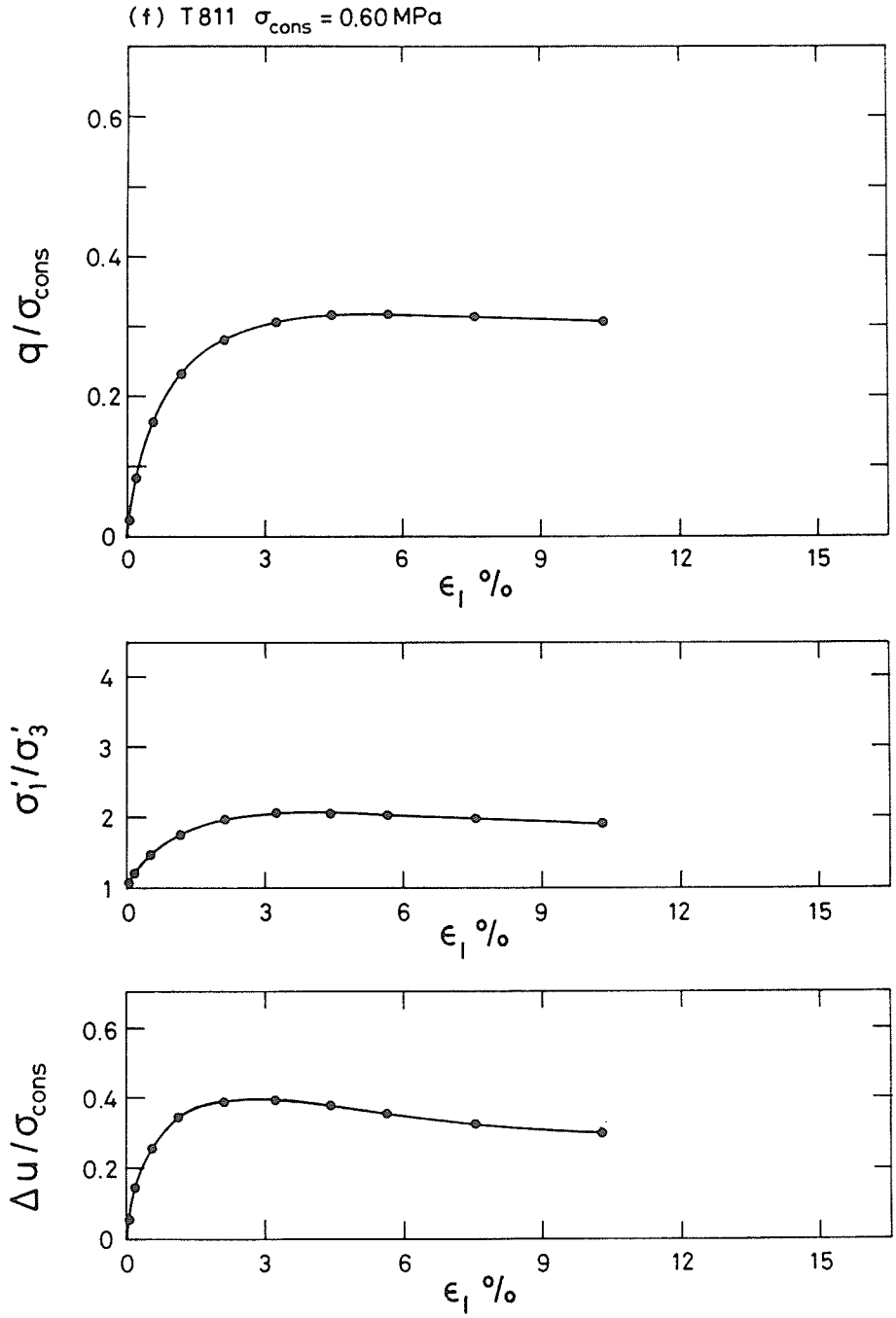

FIG. 3.5 - STRESS-STRAIN/POREWATER PRESSURE/STRESS RATIO CURVES IN UNDRAINED TRIAXIAL COMPRESSION (AFTER SUN, 1986)

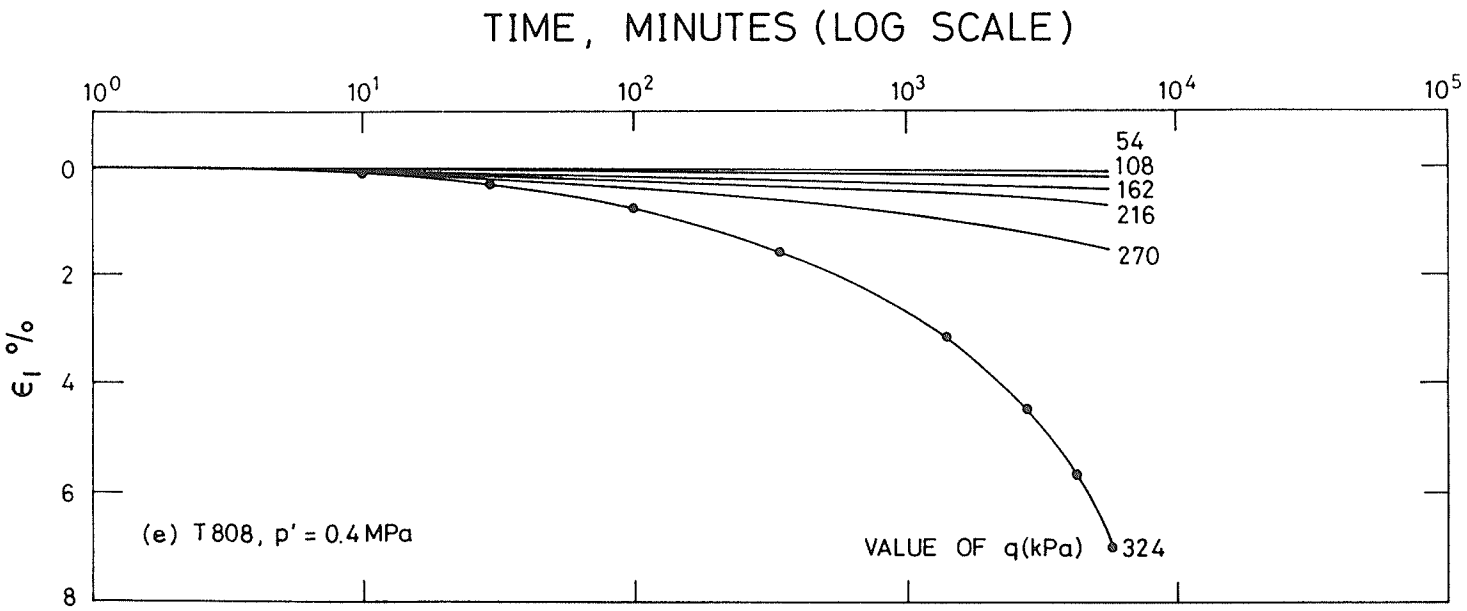

FIG. 3.6 - INCREMENTAL SHEAR LOADING AT CONSTANT MEAN PRESSURE
- AXIAL STRAIN VS. LOG<TIME> (AFTER SUN, 1986)

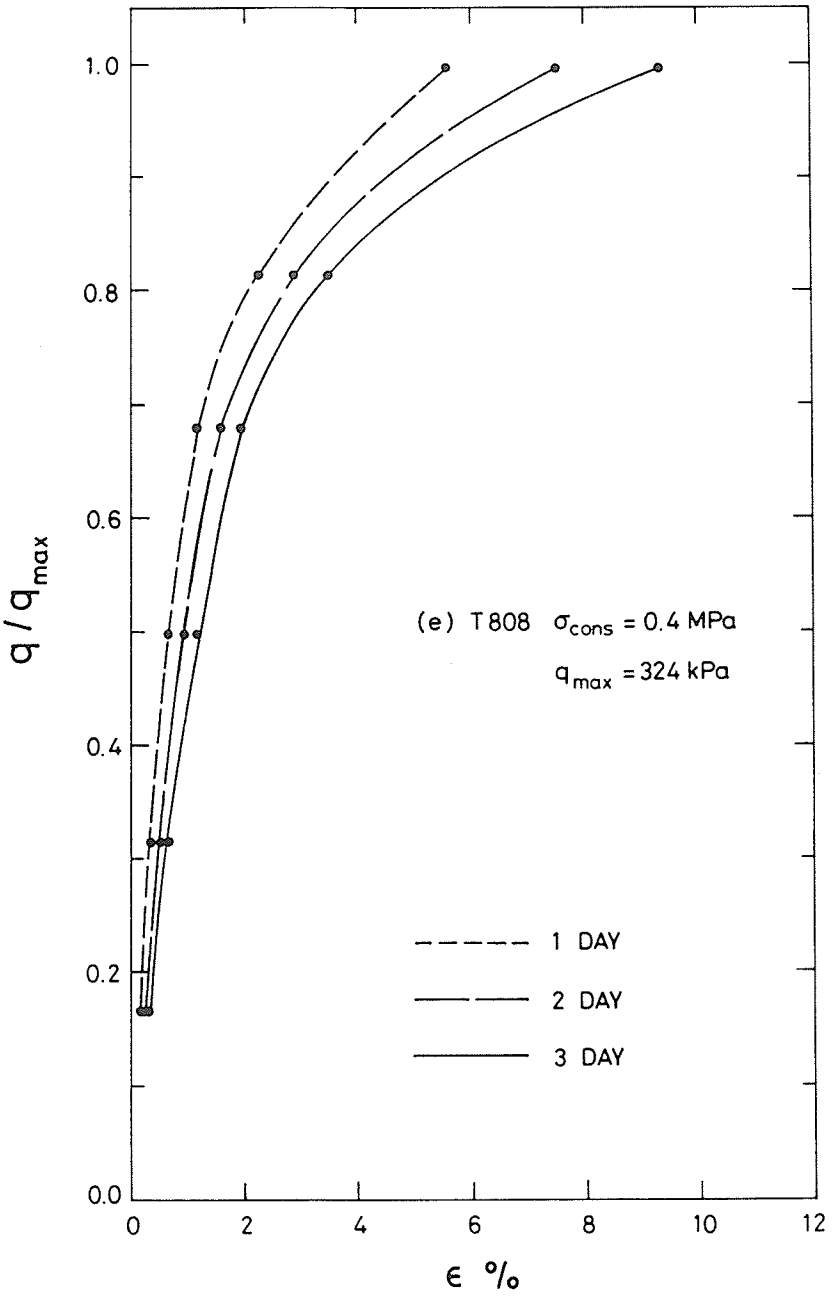

FIG. 3.7 - NORMALIZED SHEAR STRESS VS. ACCUMULATED SHEAR STRAIN (AFTER SUN, 1986)

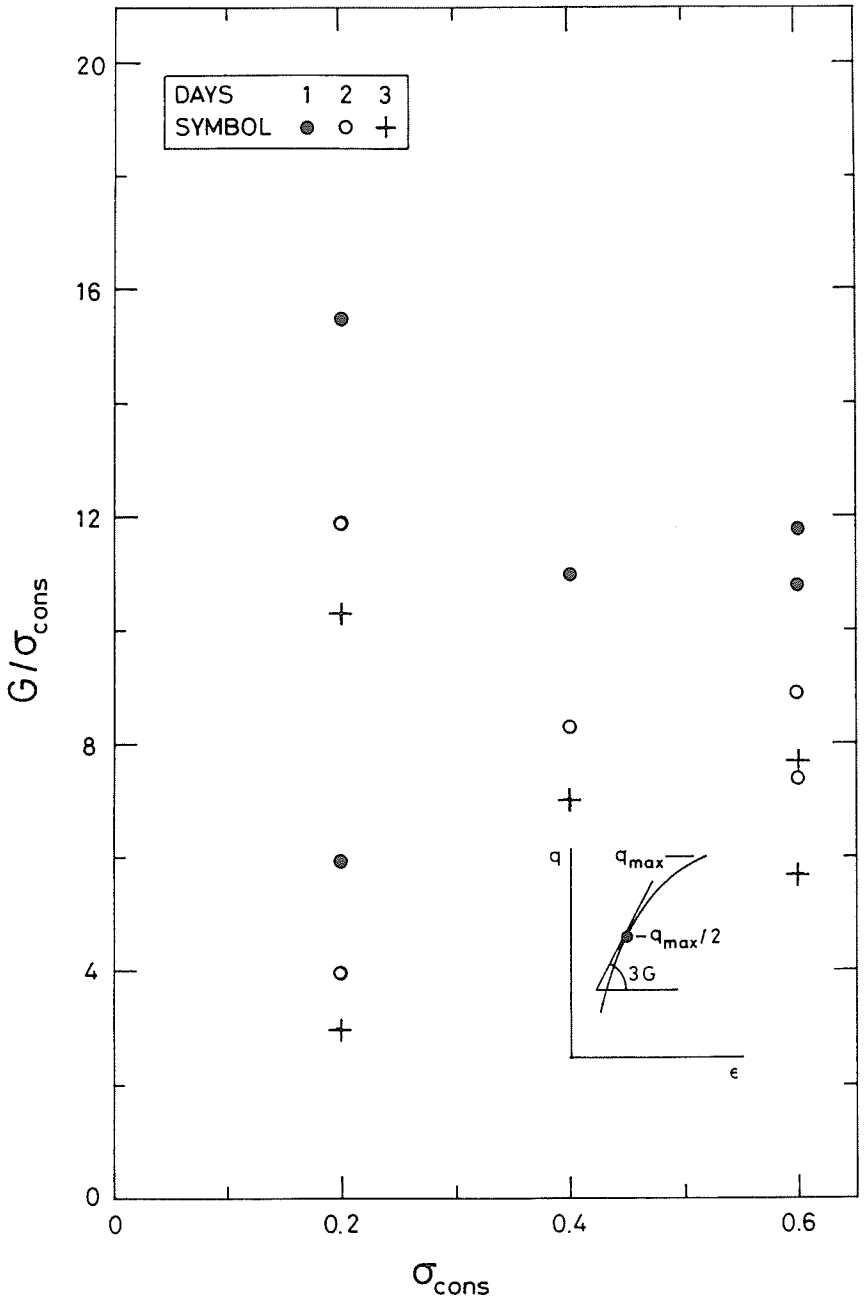

FIG. 3.8 - NORMALIZED QUASI-ELASTIC SHEAR MODULUS VS. CONSOLIDATION PRESSURE (AFTER SUN, 1986)

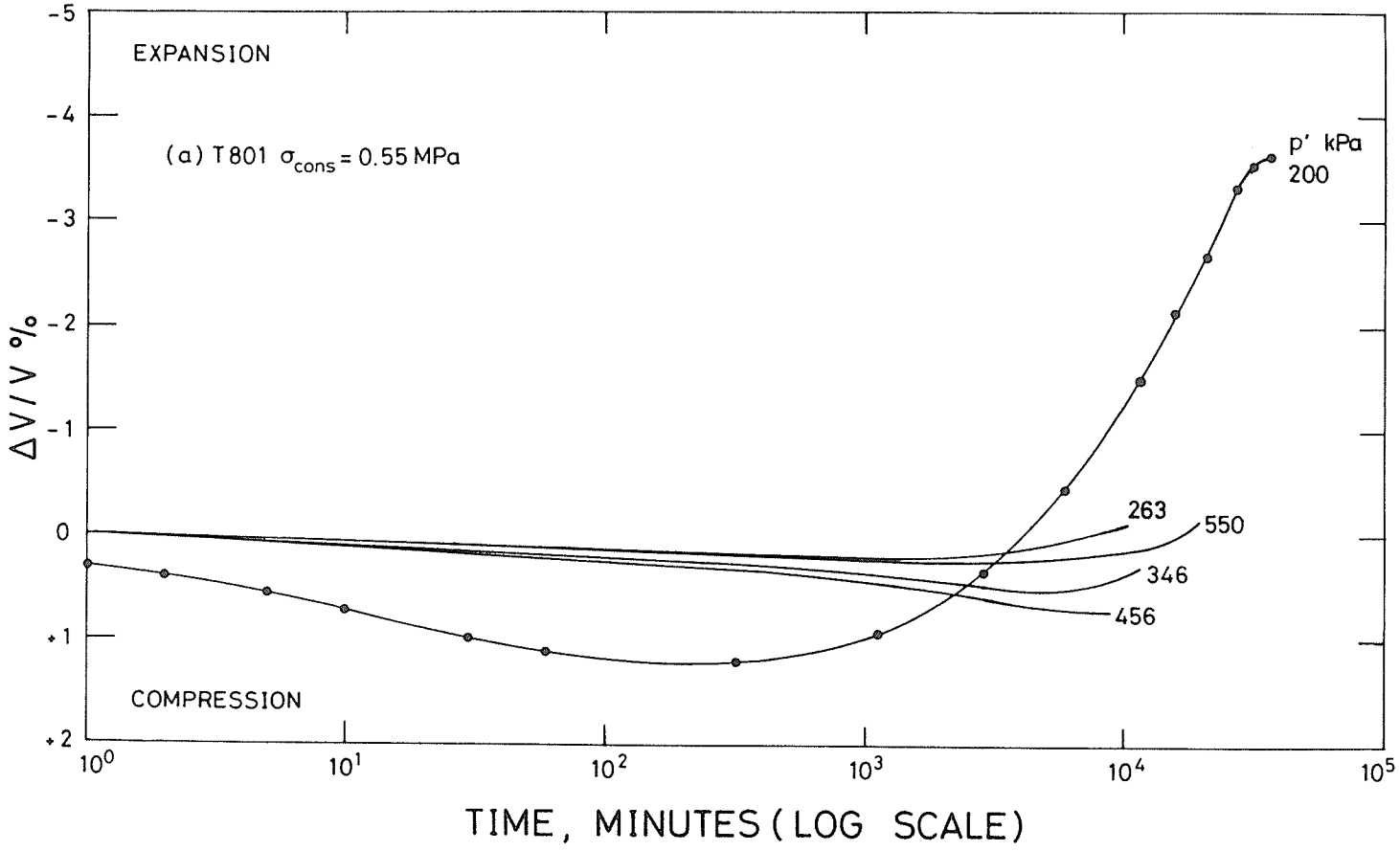

FIG. 3.9 - INCREMENTAL ISOTROPIC CONSOLIDATION : VOLUME STRAIN VS. LOG<TIME>
(AFTER SUN, 1986)

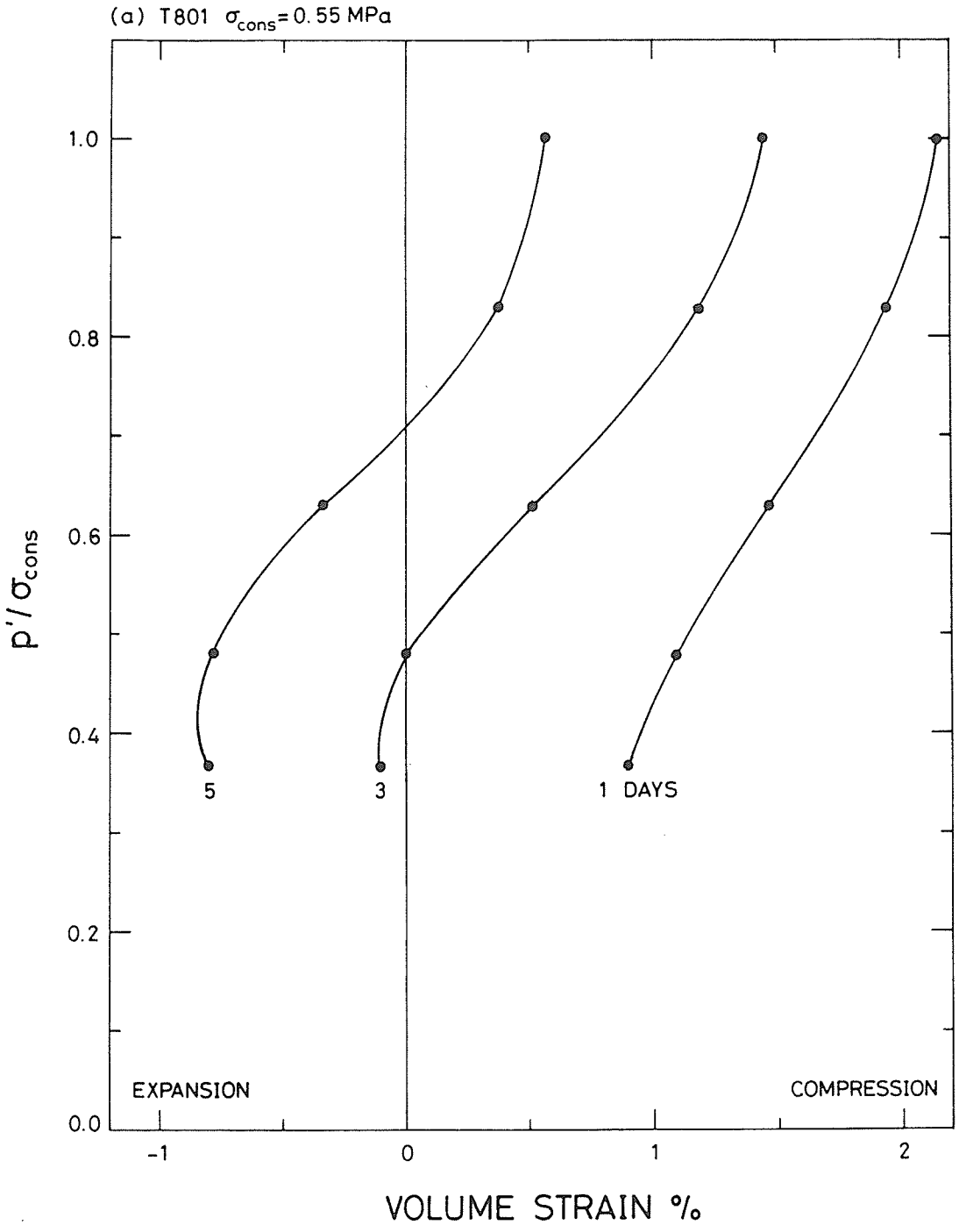

FIG. 3.10 - ISOTROPIC CONSOLIDATION MEAN PRESSURE VS. VOLUME STRAIN (AFTER SUN, 1986)

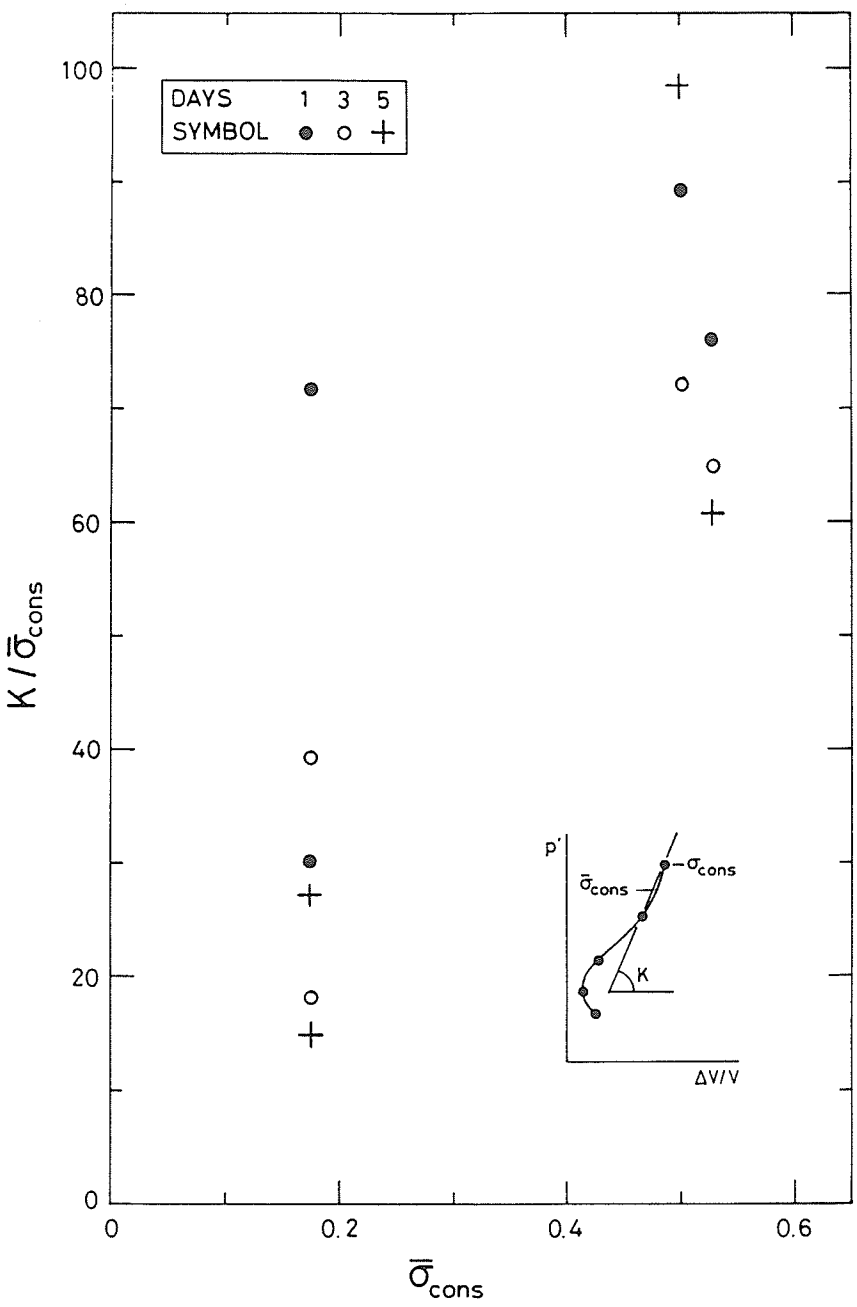

FIG. 3.11 - NORMALIZED QUASI-ELASTIC BULK MODULUS VS. MEAN CONSOLIDATION PRESSURE IN FINAL INCREMENT (AFTER SUN, 1986)

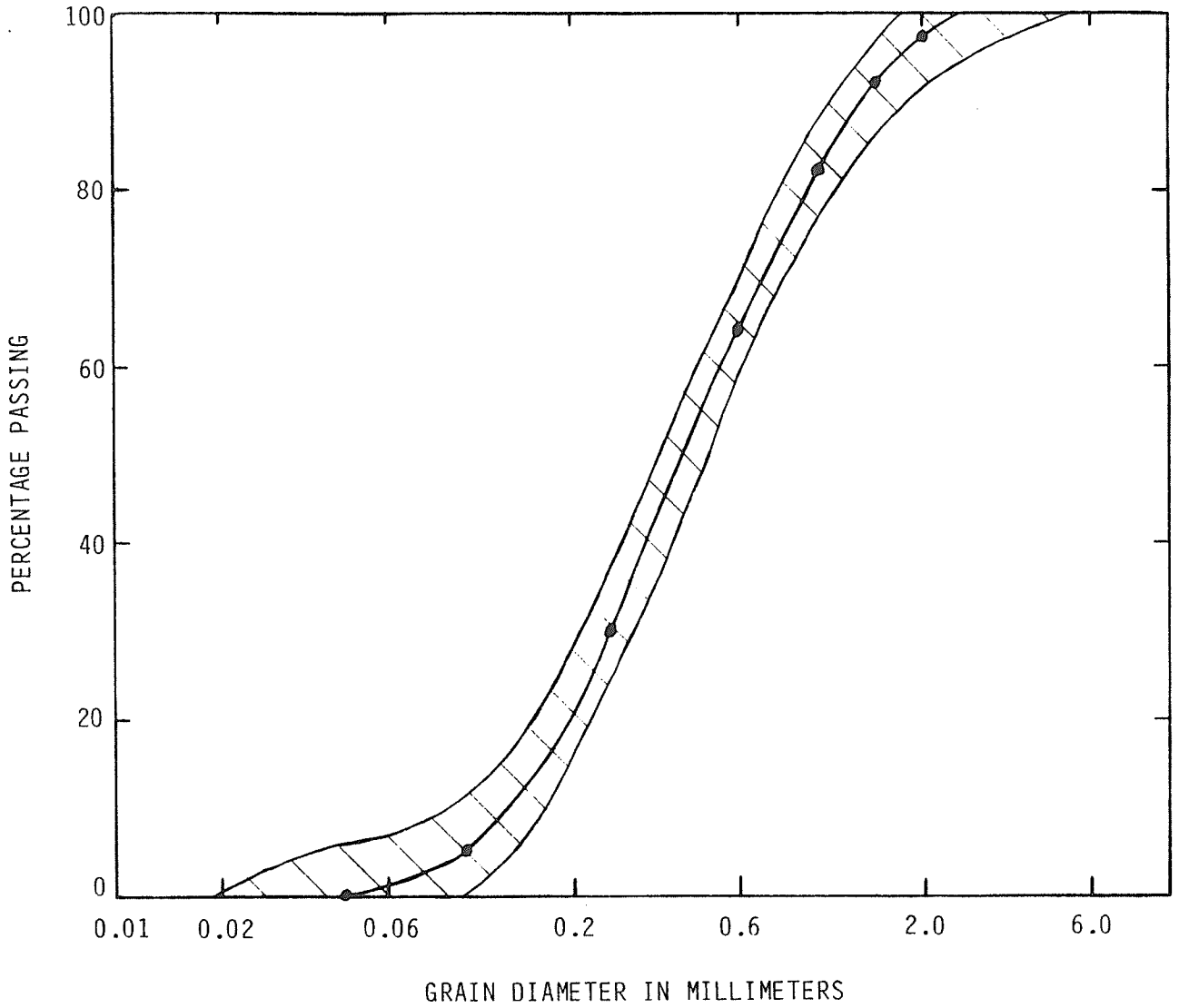

FIG. 4.1 - PARTICLE-SIZE DISTRIBUTION CURVE FOR SILICA SAND (AFTER DIXON AND WOODCOCK, 1986)

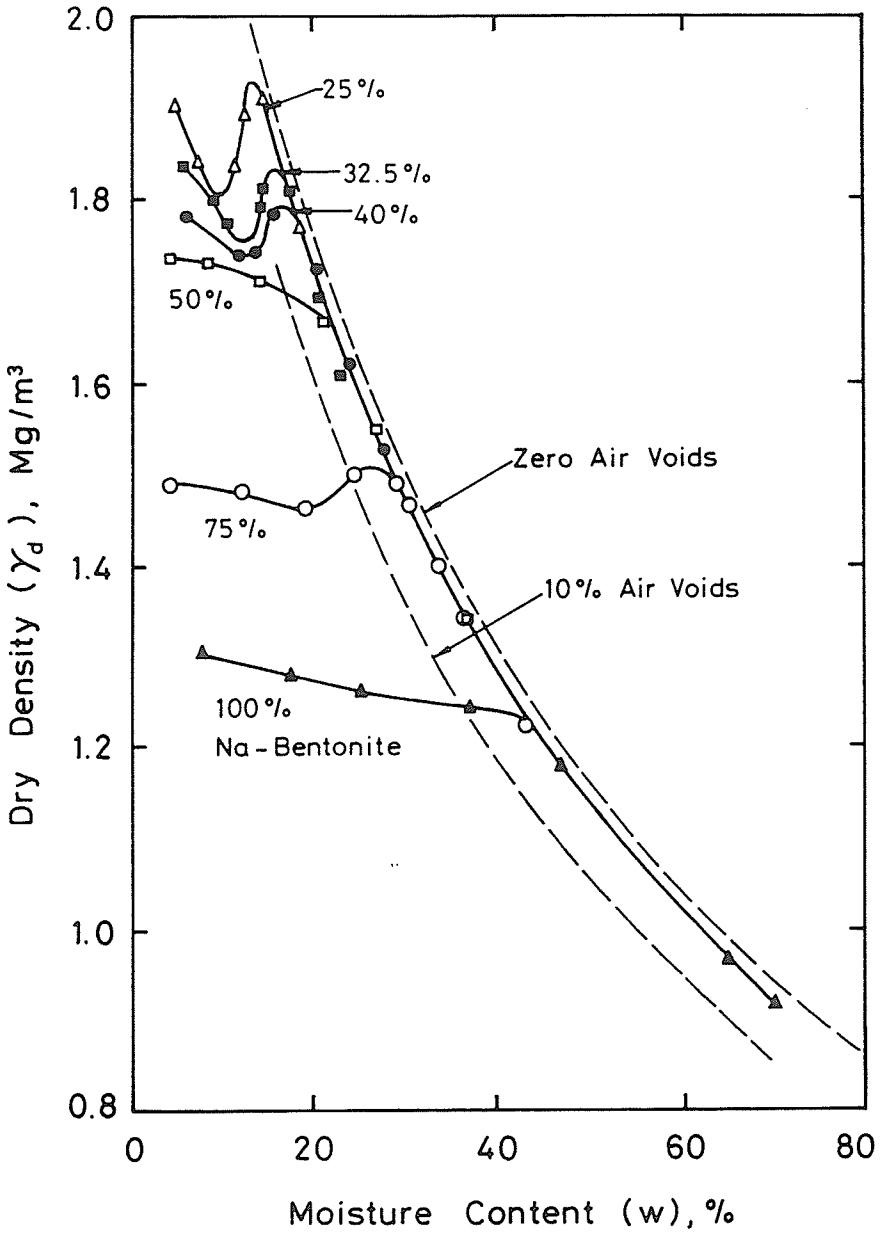

FIG. 4.2 - DRY DENSITY-WATER CONTENT RELATIONSHIP OF BUFFER MIXTURES (AFTER DIXON ET AL., 1985)

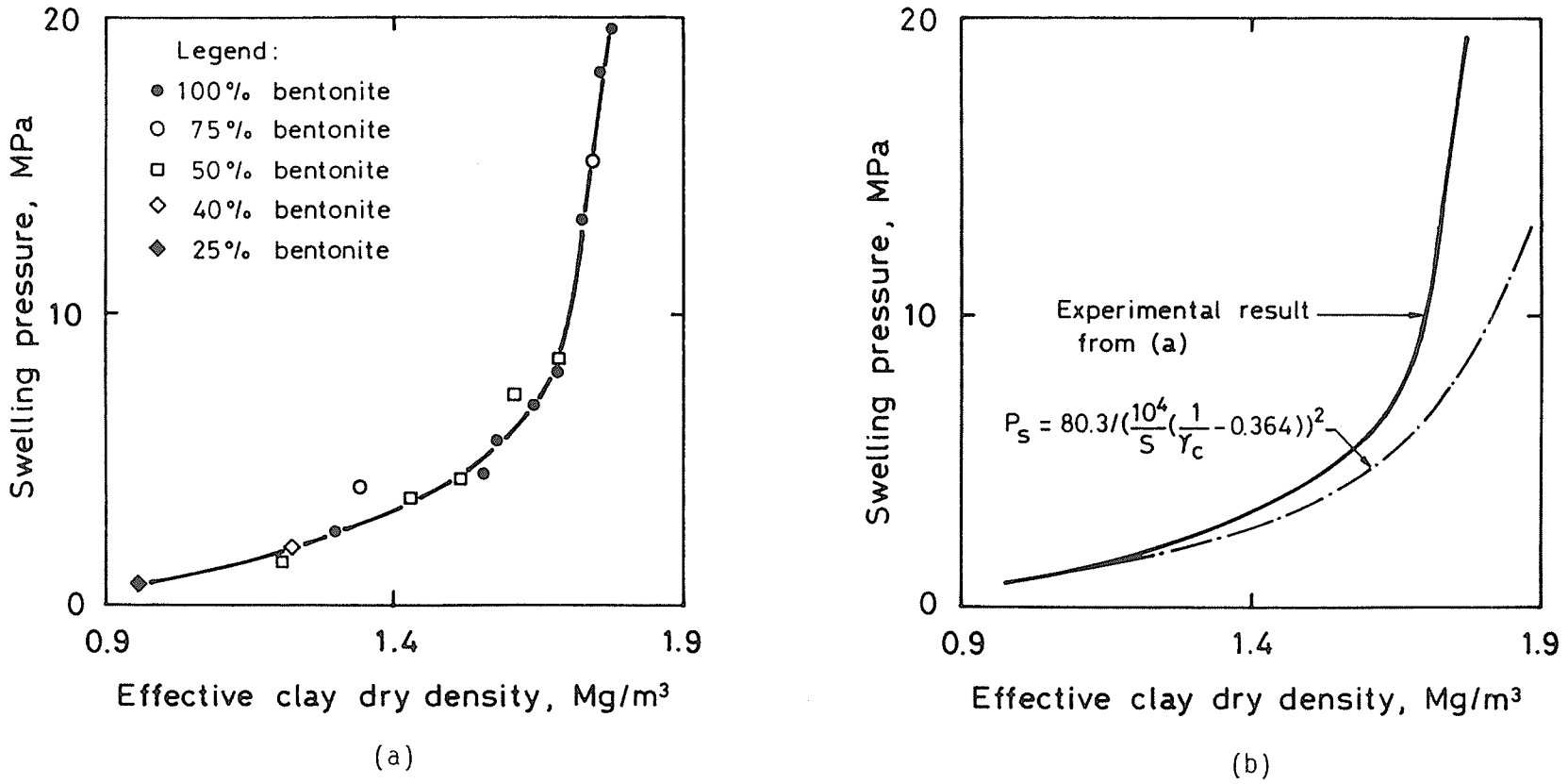

FIG. 4.3 - RELATIONSHIP BETWEEN SWELLING PRESSURE AND EFFECTIVE CLAY DRY DENSITY (AFTER GRAY ET AL., 1985)

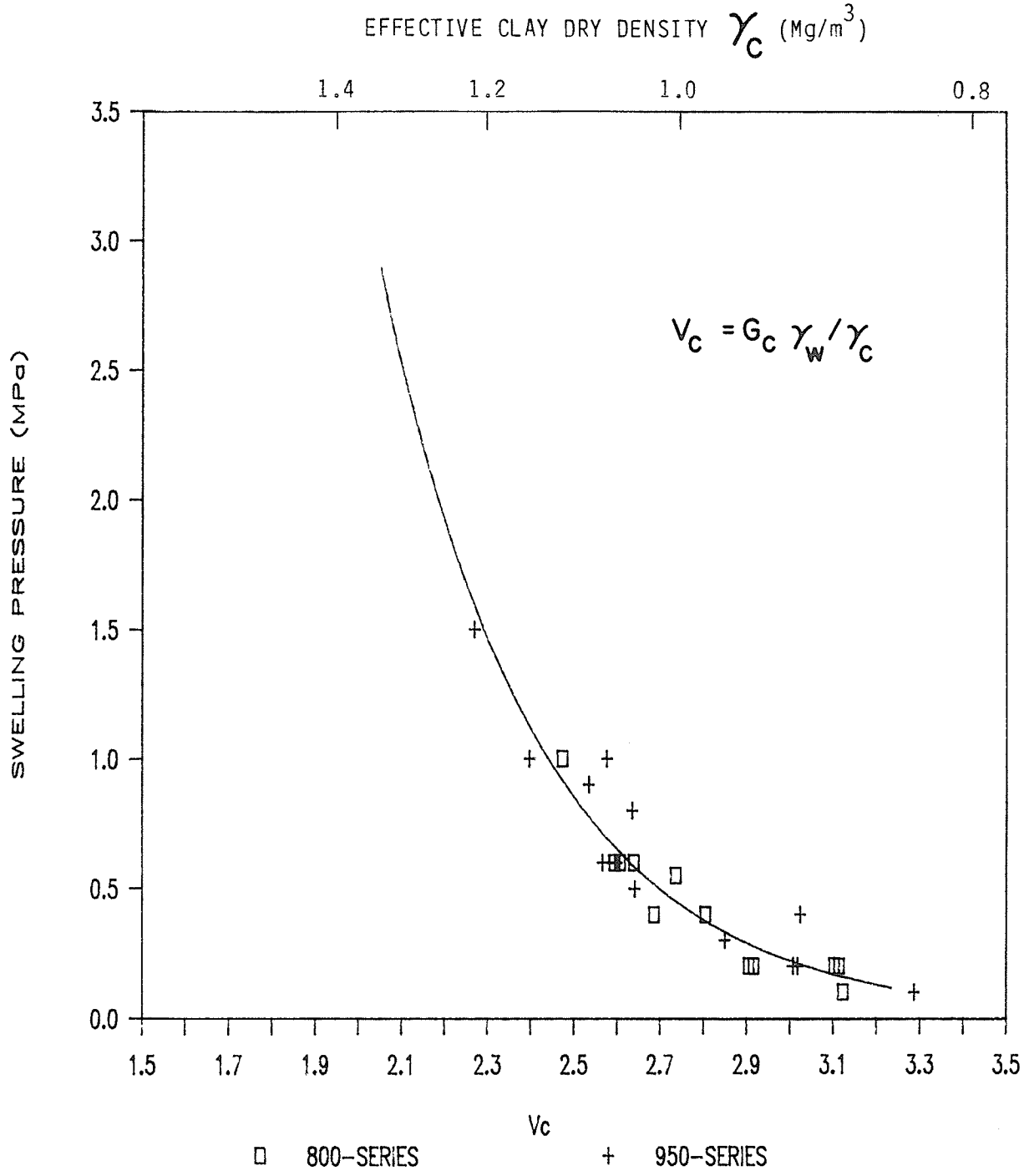

FIG. 4.4 - MODIFIED RELATIONSHIP BETWEEN SWELLING PRESSURE AND CLAY SPECIFIC VOLUME (EFFECTIVE CLAY DRY DENSITY) FROM TRIAXIAL TESTS (800-SERIES AND 950-SERIES)

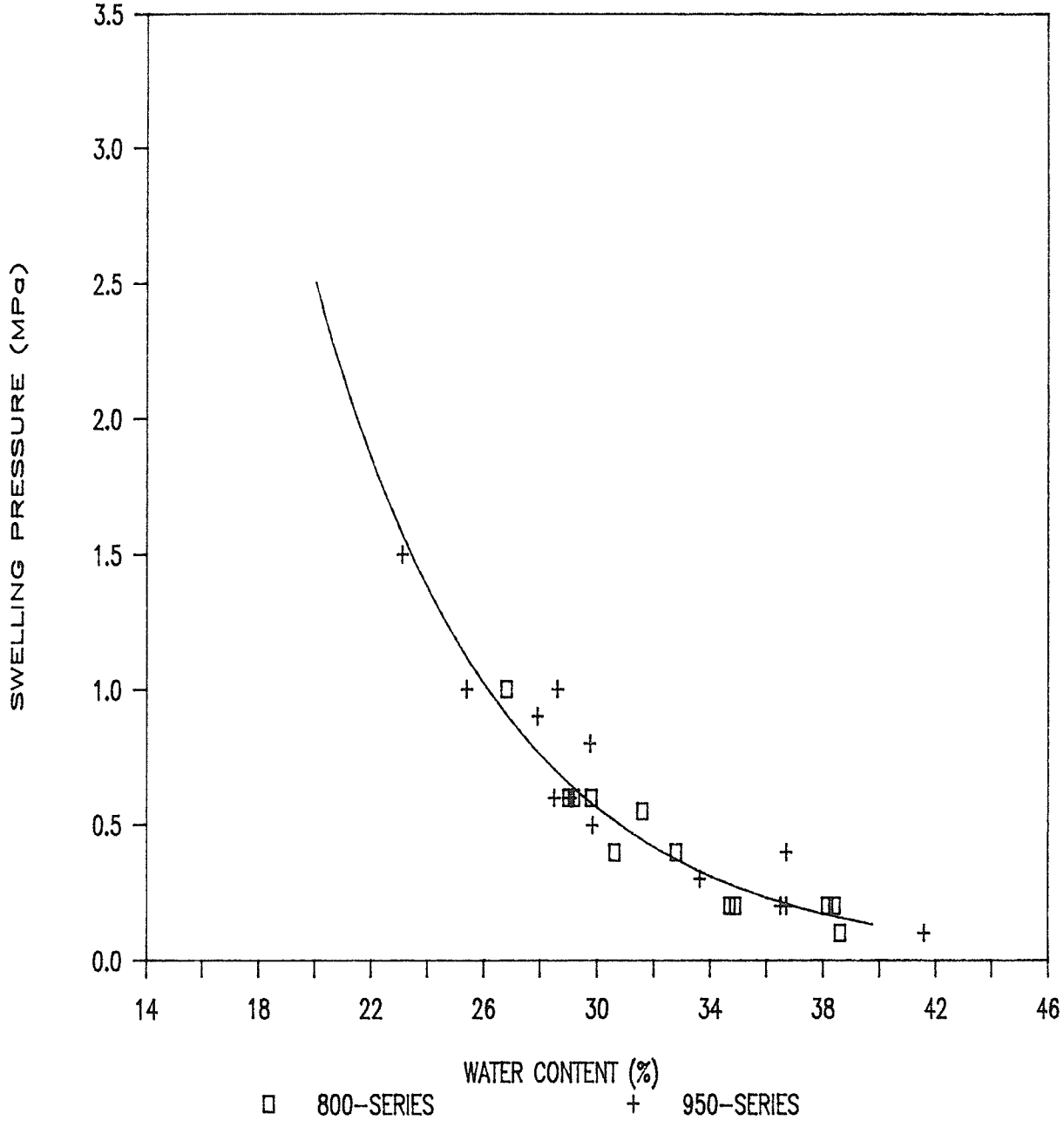

FIG. 4.5 - RELATIONSHIP BETWEEN SWELLING PRESSURE AND WATER CONTENT AT END OF TRIAXIAL CONSOLIDATION (800-SERIES AND 950-SERIES)

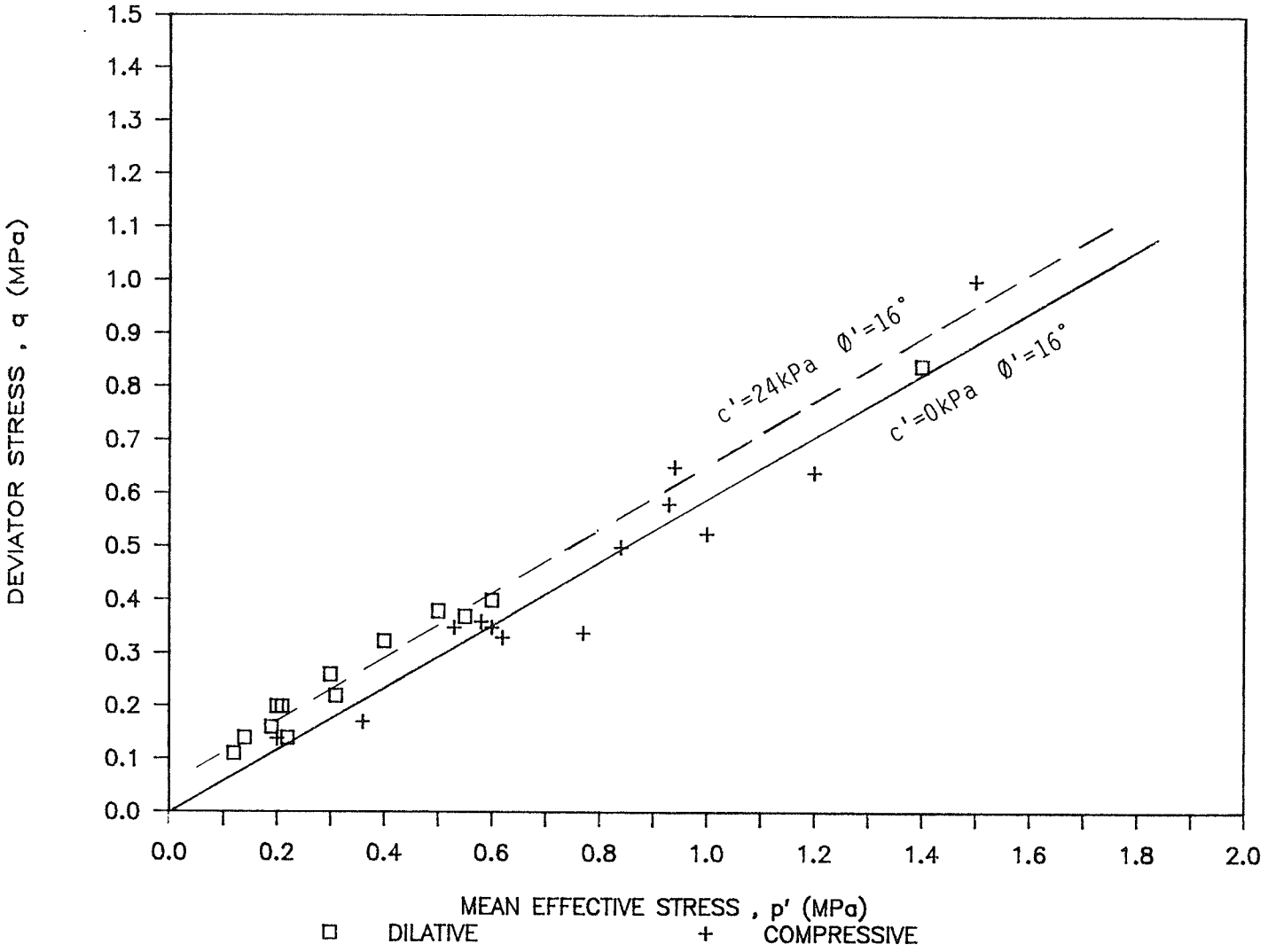

FIG. 5.1 - COMPOSITE SHEAR STRENGTH ENVELOPE FROM 800-, 900- AND 950-SERIES (AFTER GRAHAM ET AL., 1986b)

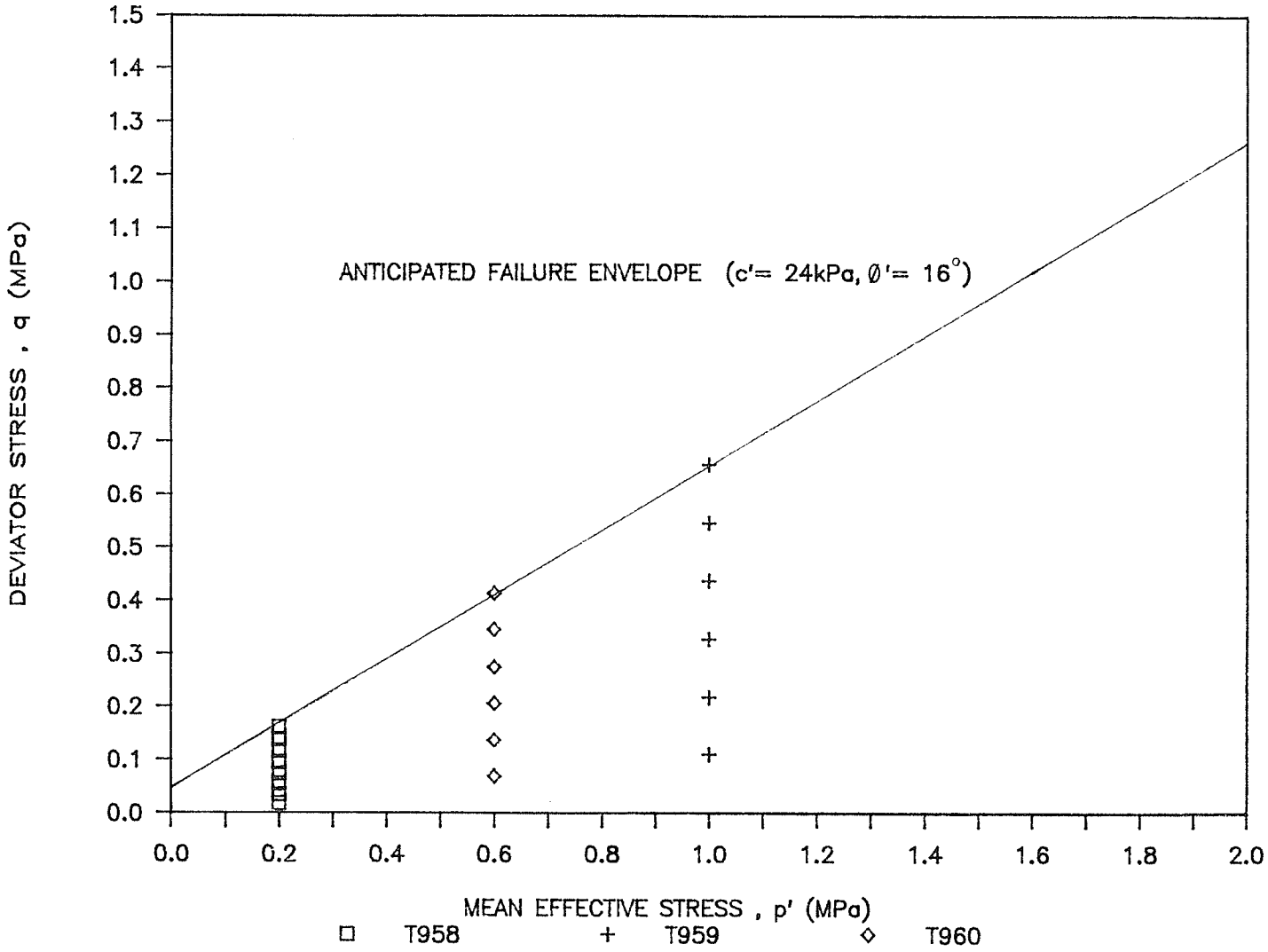

FIG. 5.2 - PROPOSED STRESS PATHS FOR LOAD-CONTROLLED CONSTANT-p' DRAINED SHEAR TESTS

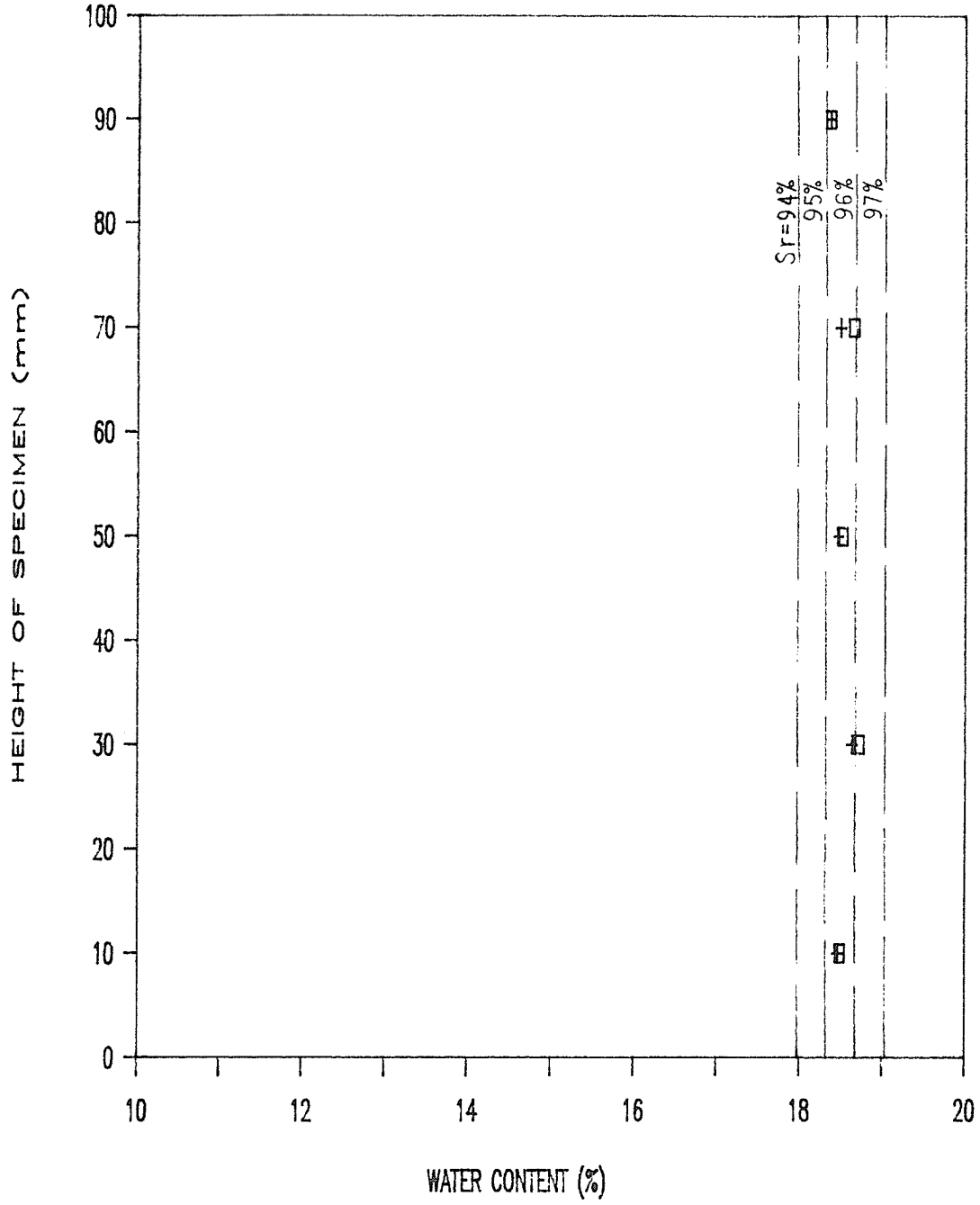

FIG. 6.1 - VARIATION OF WATER CONTENT ALONG THE HEIGHT OF THE SPECIMEN - QC955-2

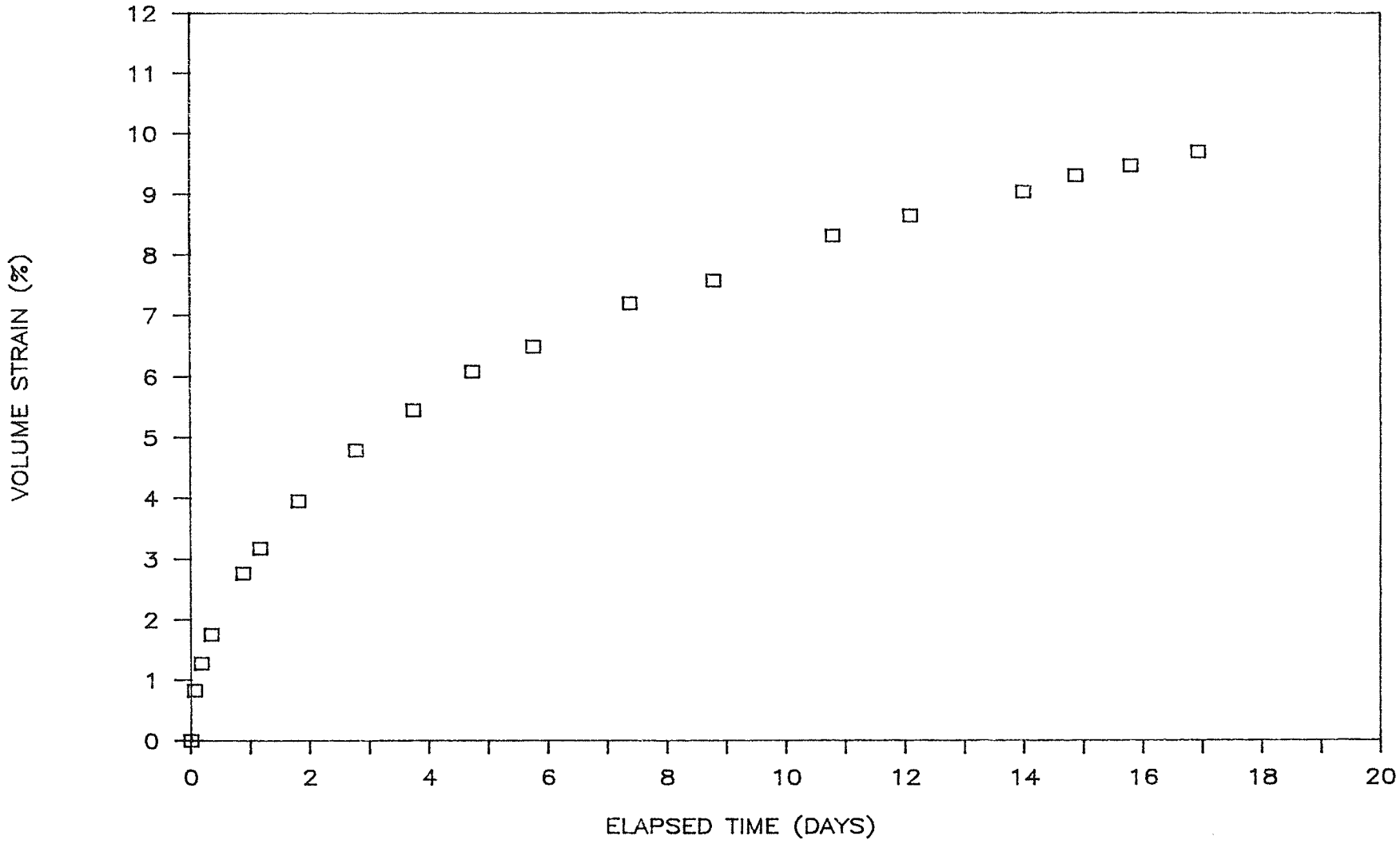

FIG. 6.2 - VOLUMETRIC STRAIN VS. CONSOLIDATION DURATION - T951

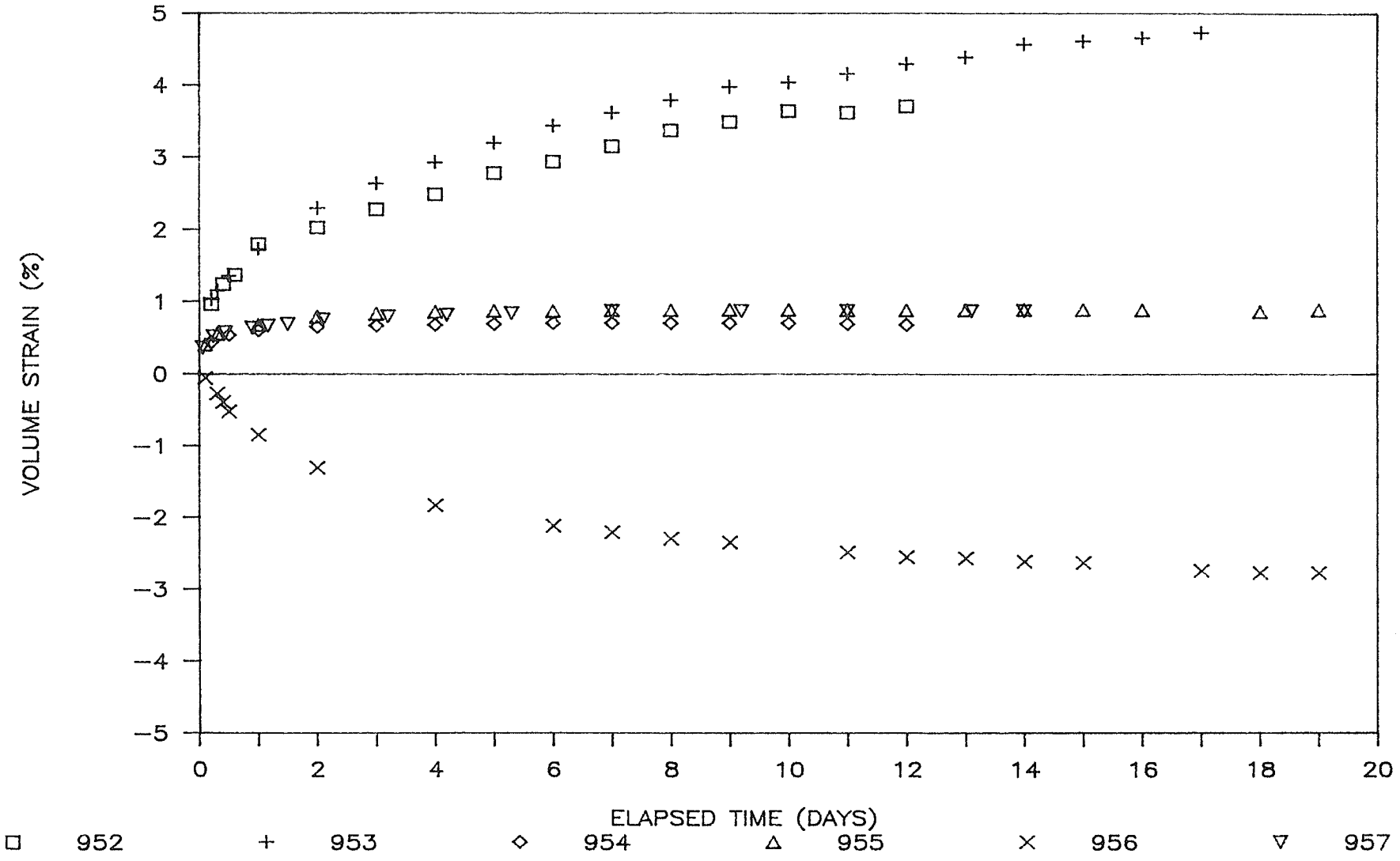

FIG. 6.3 - VOLUMETRIC STRAIN VS. CONSOLIDATION DURATION - T952 TO T957

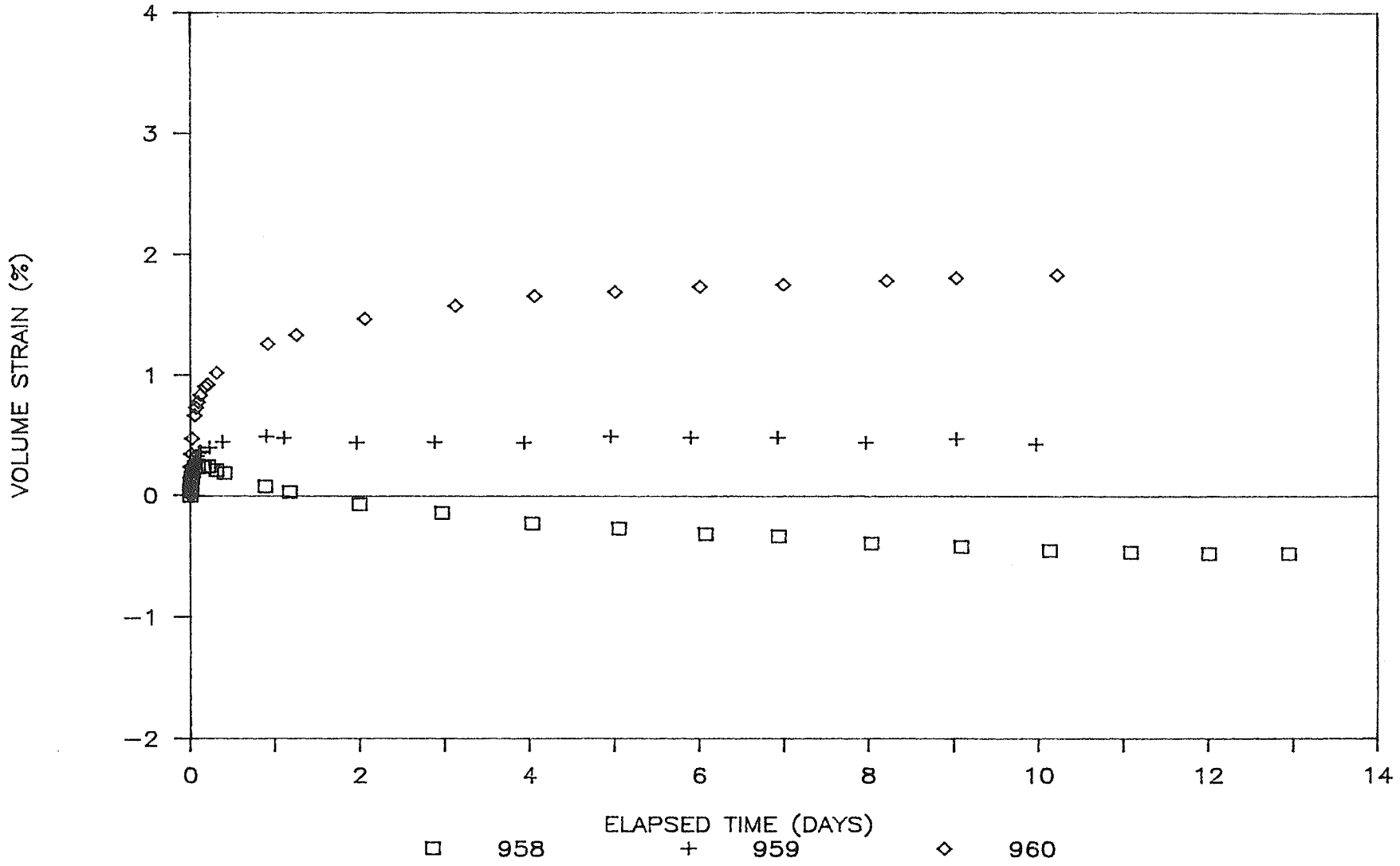

FIG. 6.4 - VOLUMETRIC STRAIN VS. CONSOLIDATION DURATION - T958 TO T960

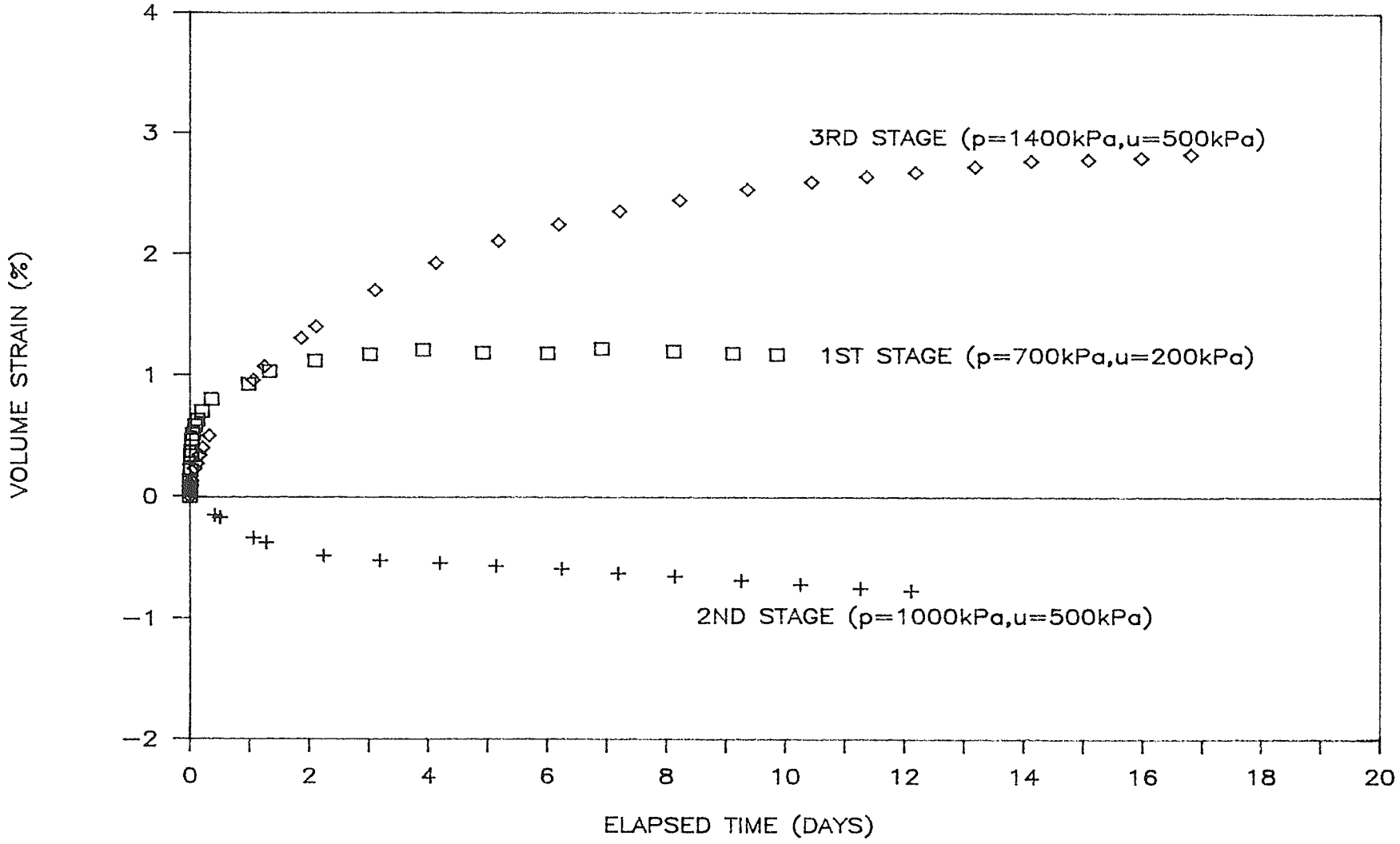

FIG. 6.5 - VOLUMETRIC STRAIN VS. CONSOLIDATION DURATION - T961

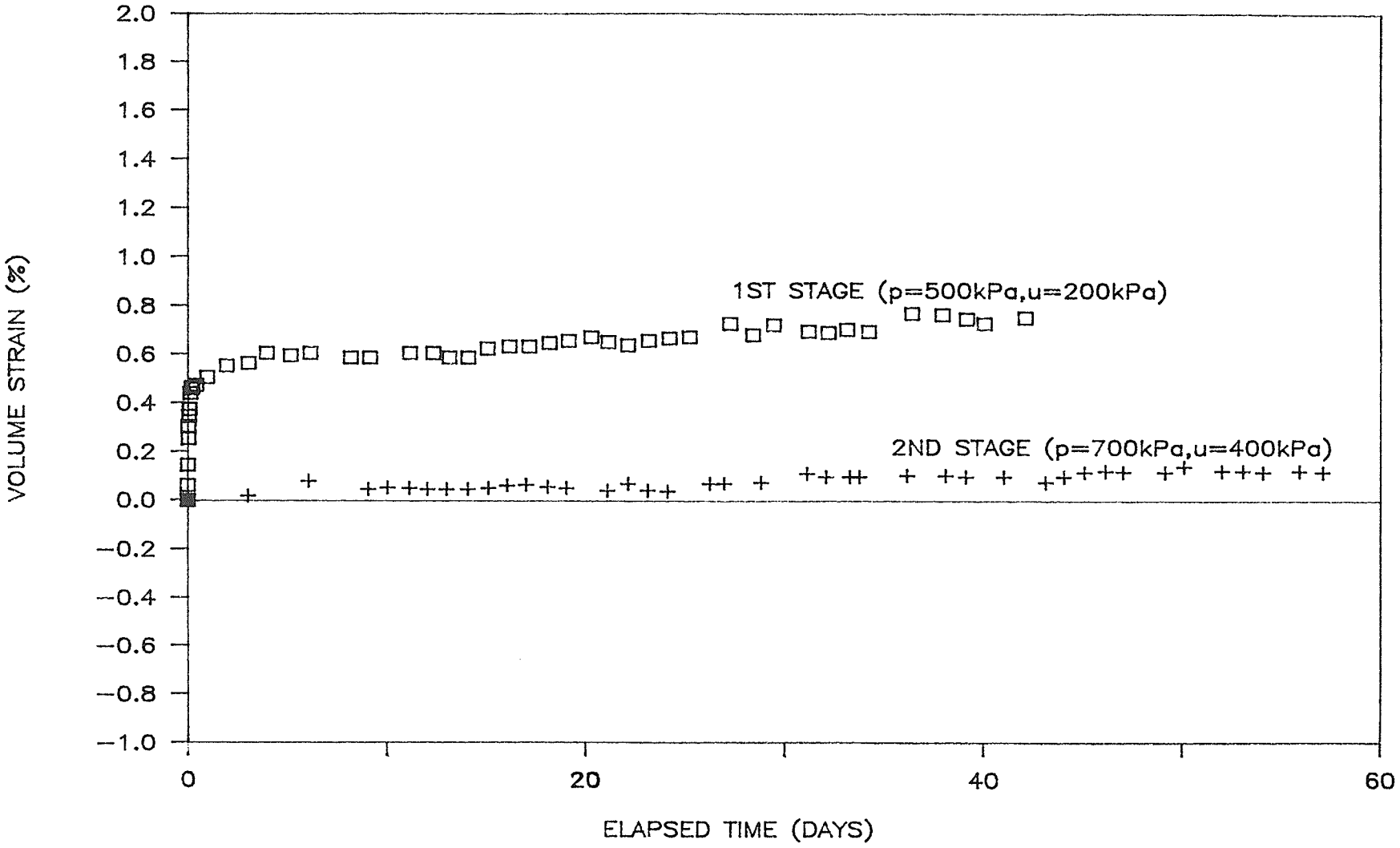

FIG. 6.6 - VOLUMETRIC STRAIN VS. CONSOLIDATION DURATION - T962

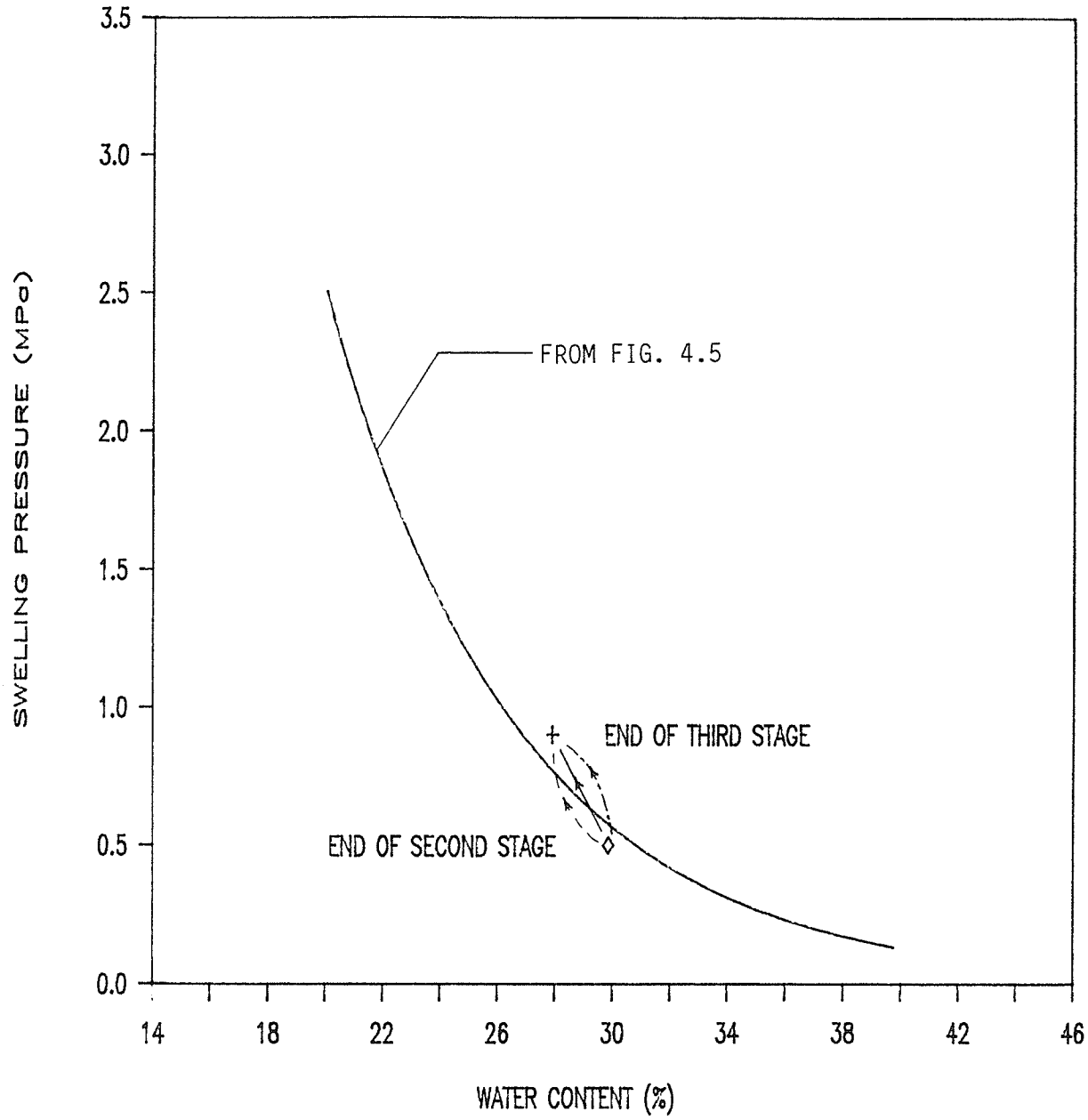

FIG. 6.7 - COMPARISON OF MEASURED AND PREDICTED WATER CONTENTS OF SPECIMEN T961 AT END OF CONSOLIDATION

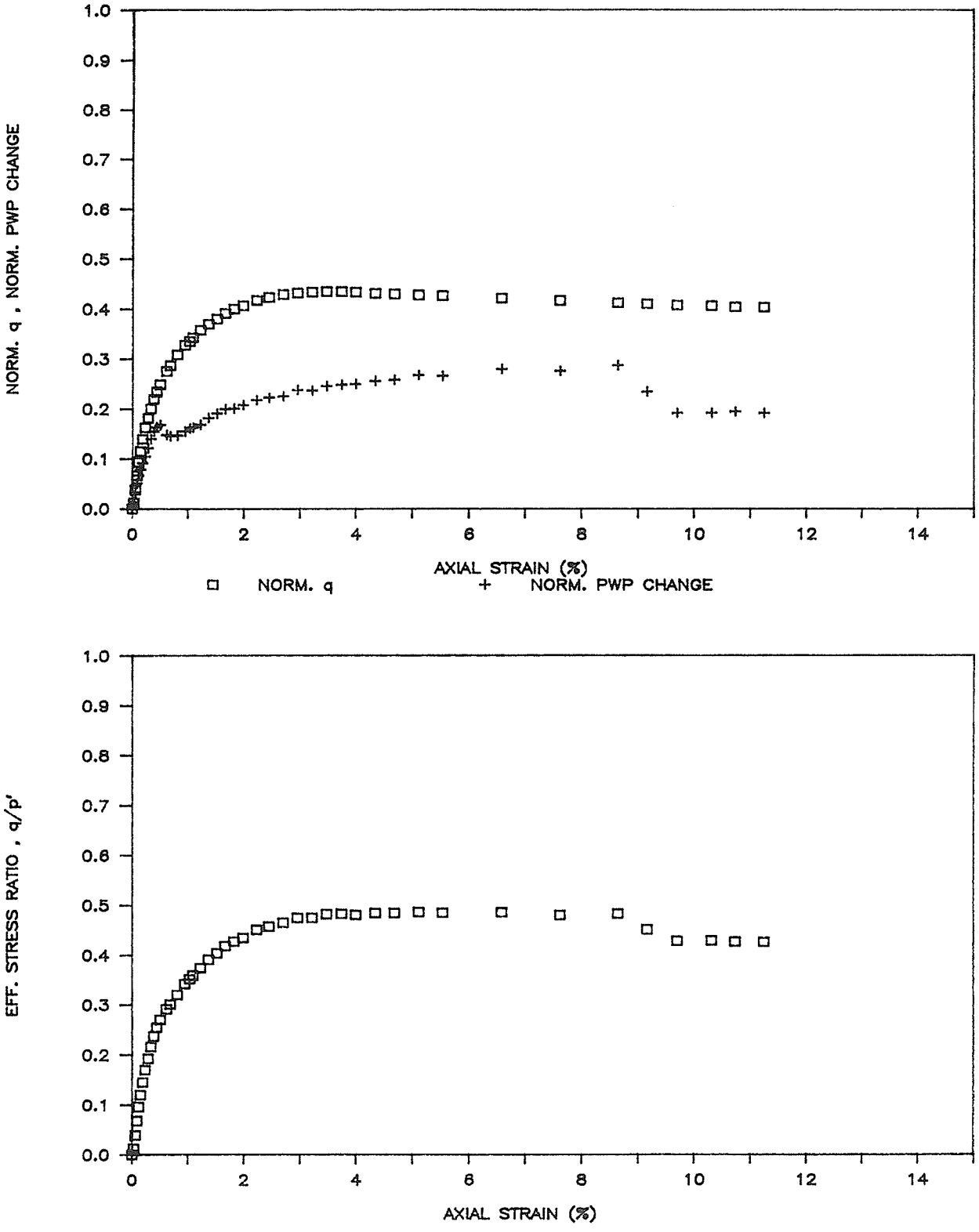

FIG. 6.8 - STRESS-STRAIN/POREWATER PRESSURE/STRESS RATIO CURVES IN UNDRAINED TRIAXIAL COMPRESSION - T951

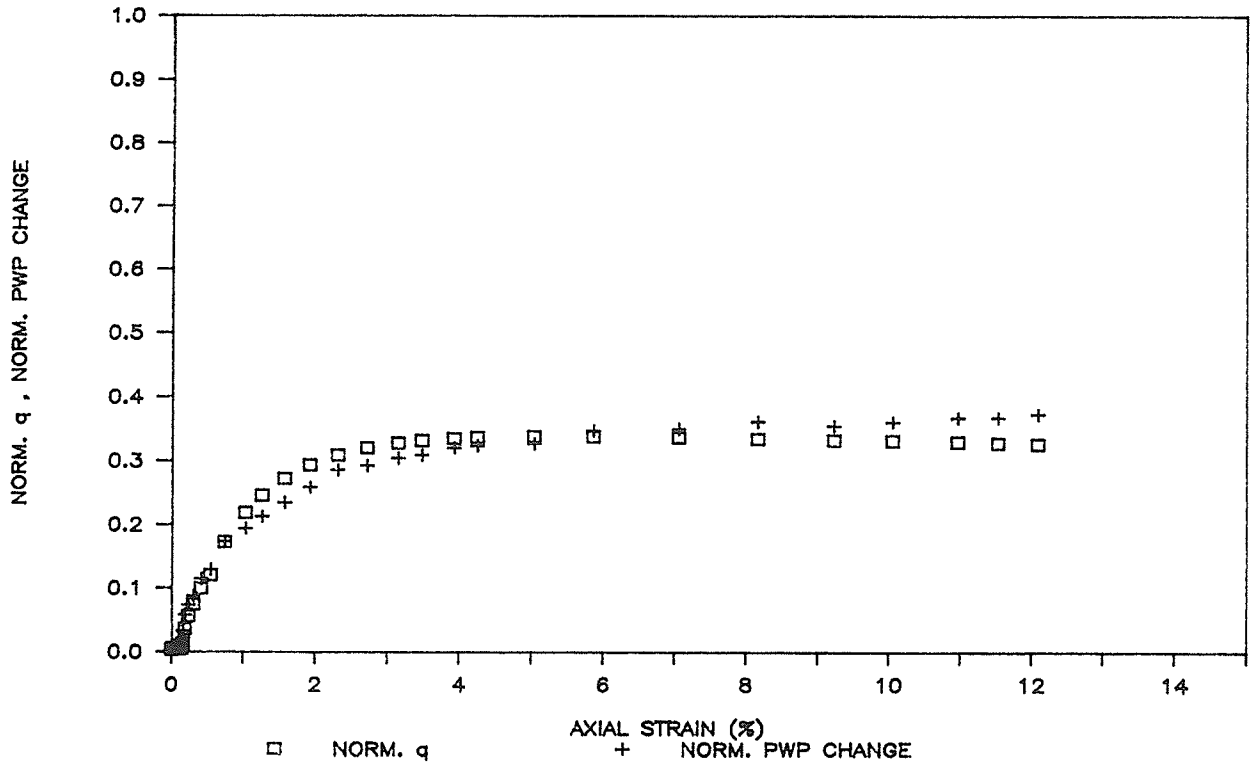

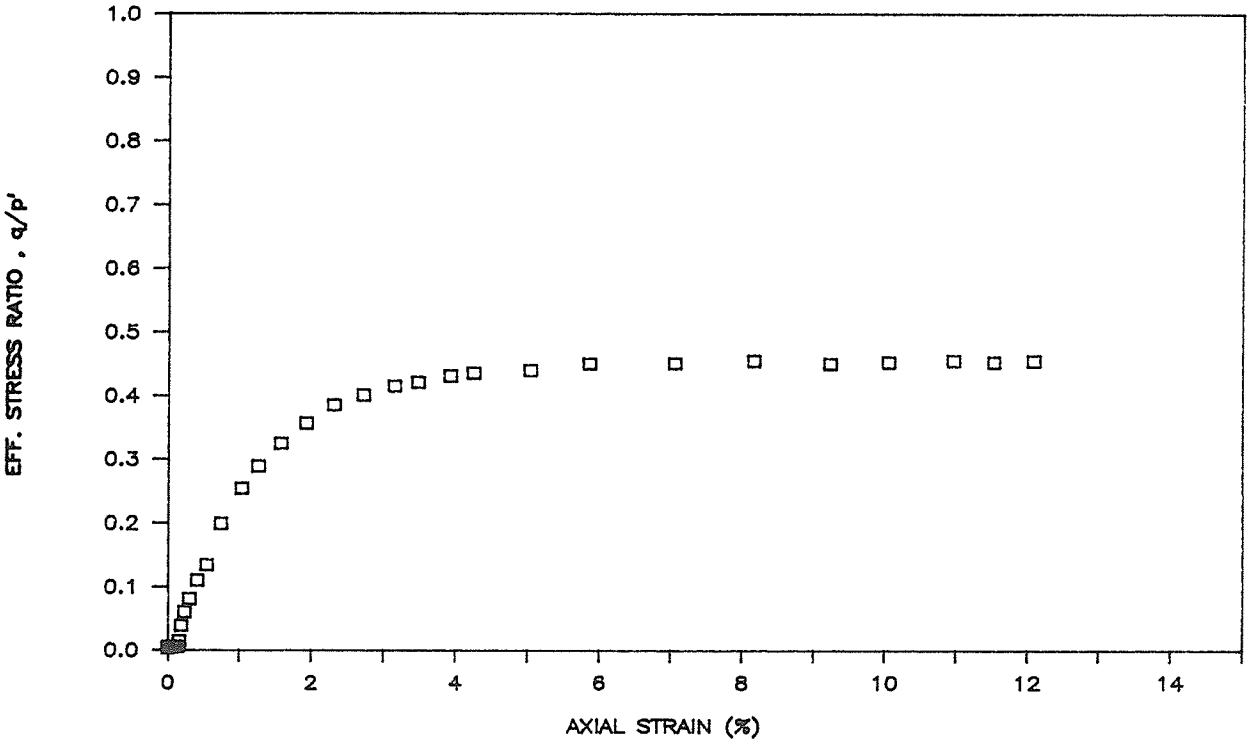

FIG. 6.9 - STRESS-STRAIN/POREWATER PRESSURE/STRESS RATIO CURVES IN UNDRAINED TRIAXIAL COMPRESSION - T952

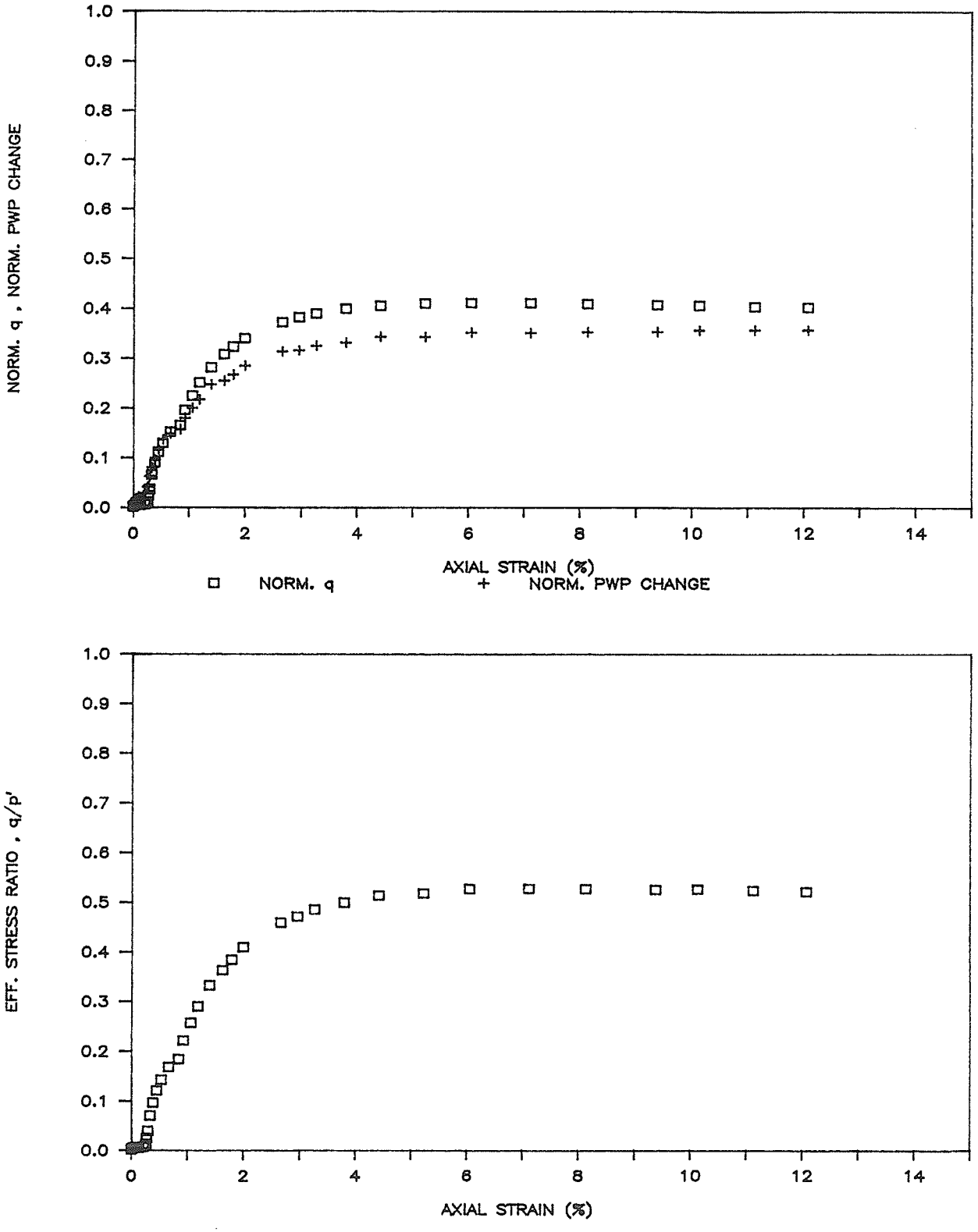

FIG. 6.10 - STRESS-STRAIN/POREWATER PRESSURE/STRESS RATIO CURVES IN UNDRAINED TRIAXIAL COMPRESSION - T953

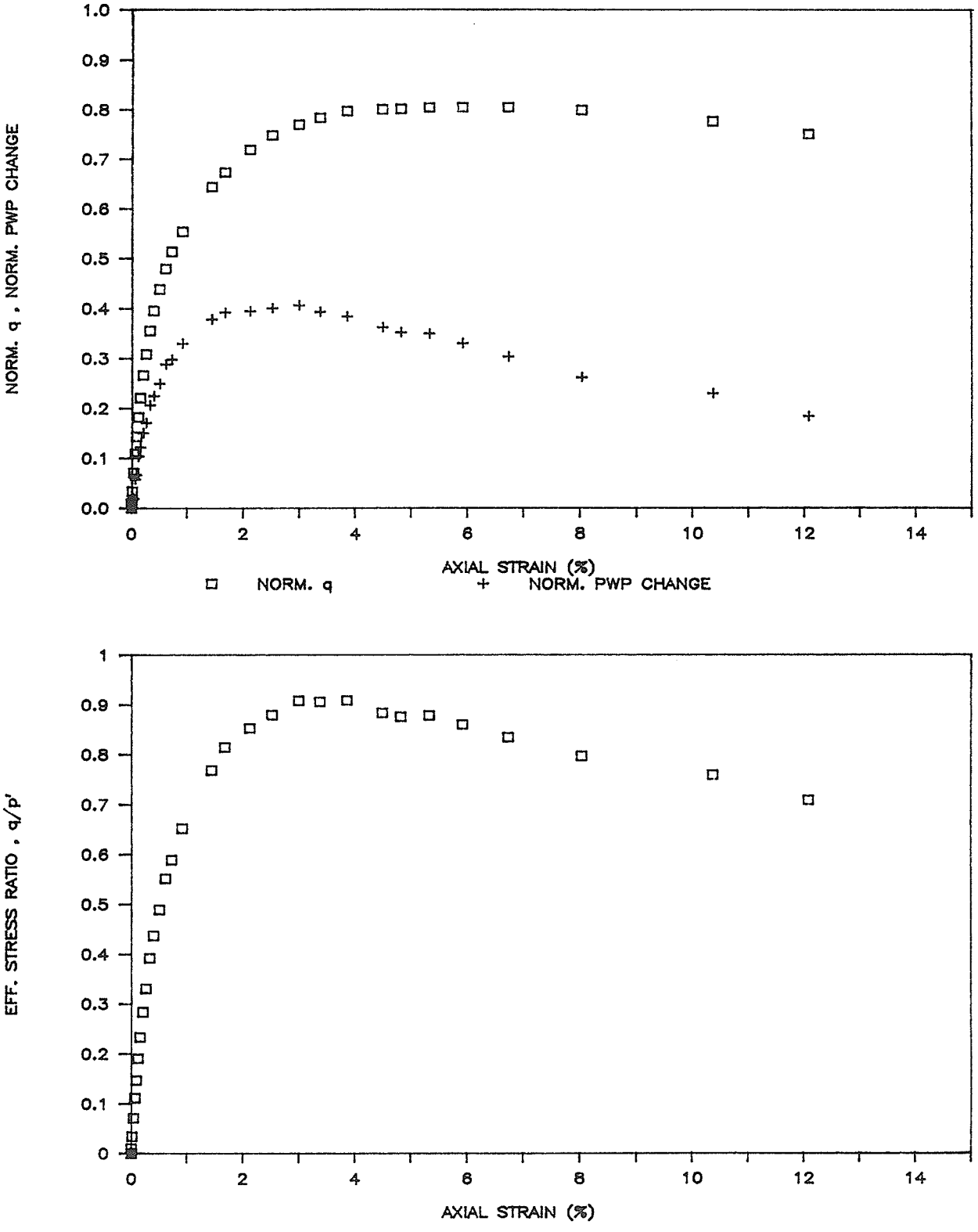

FIG. 6.11 - STRESS-STRAIN/POREWATER PRESSURE/STRESS RATIO CURVES IN UNDRAINED TRIAXIAL COMPRESSION - T954

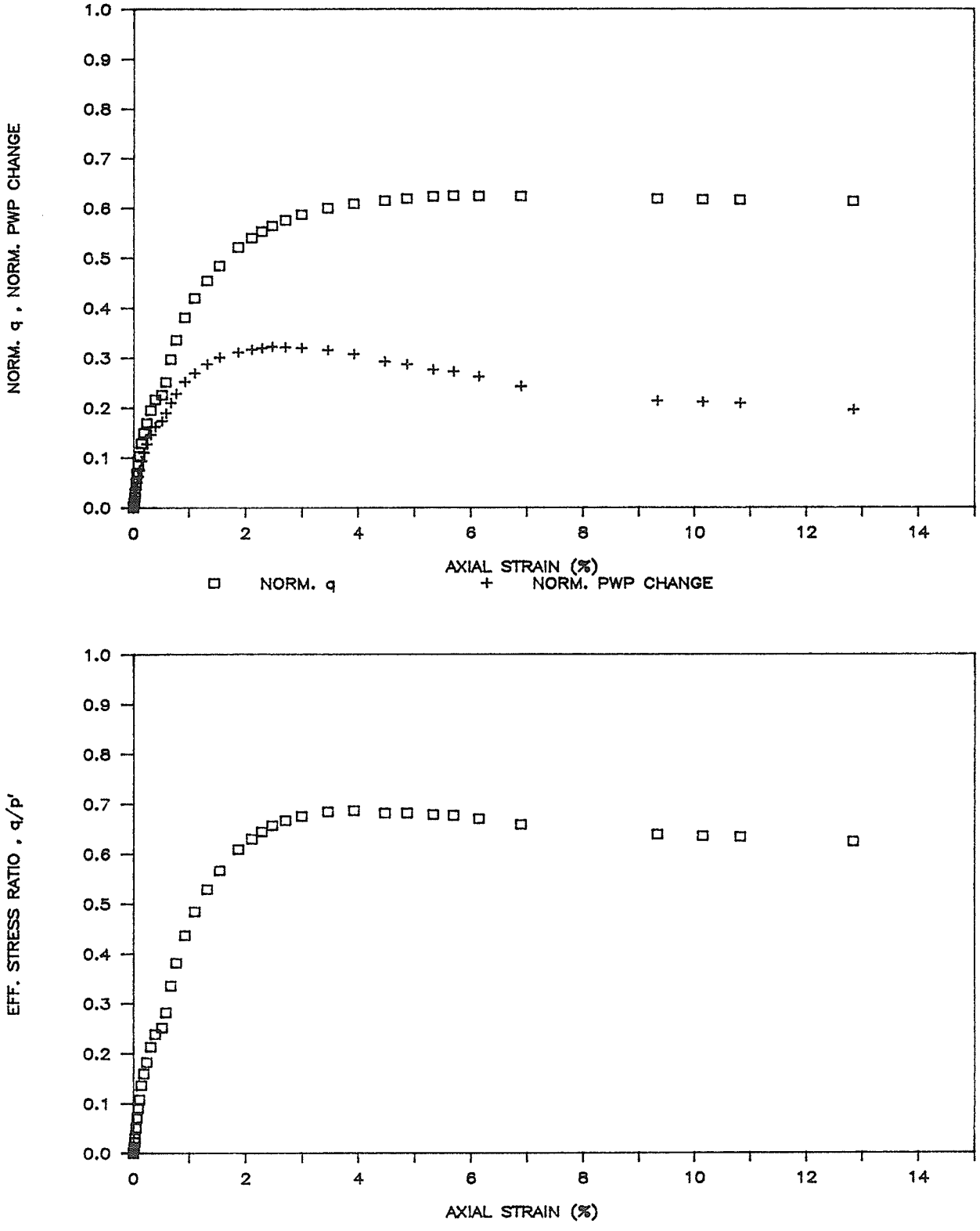

FIG. 6.12 - STRESS-STRAIN/POREWATER PRESSURE/STRESS RATIO CURVES IN UNDRAINED TRIAXIAL COMPRESSION - T955

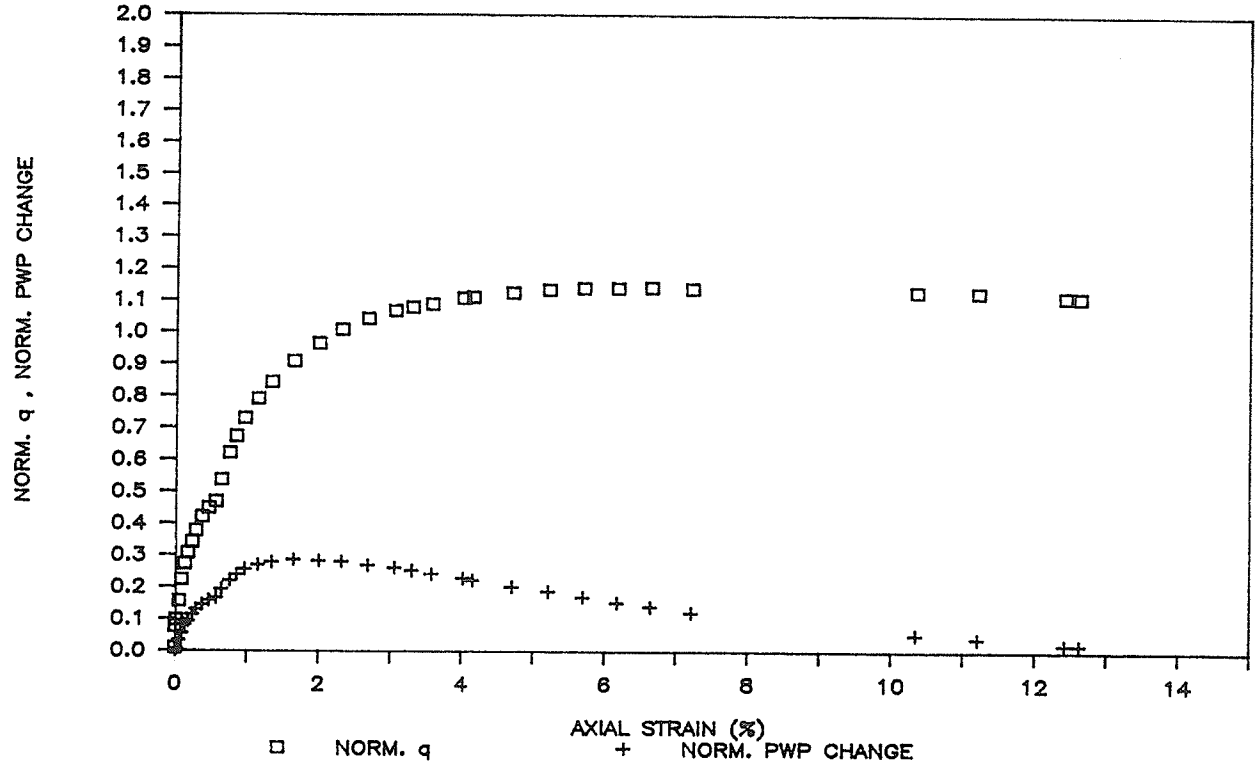

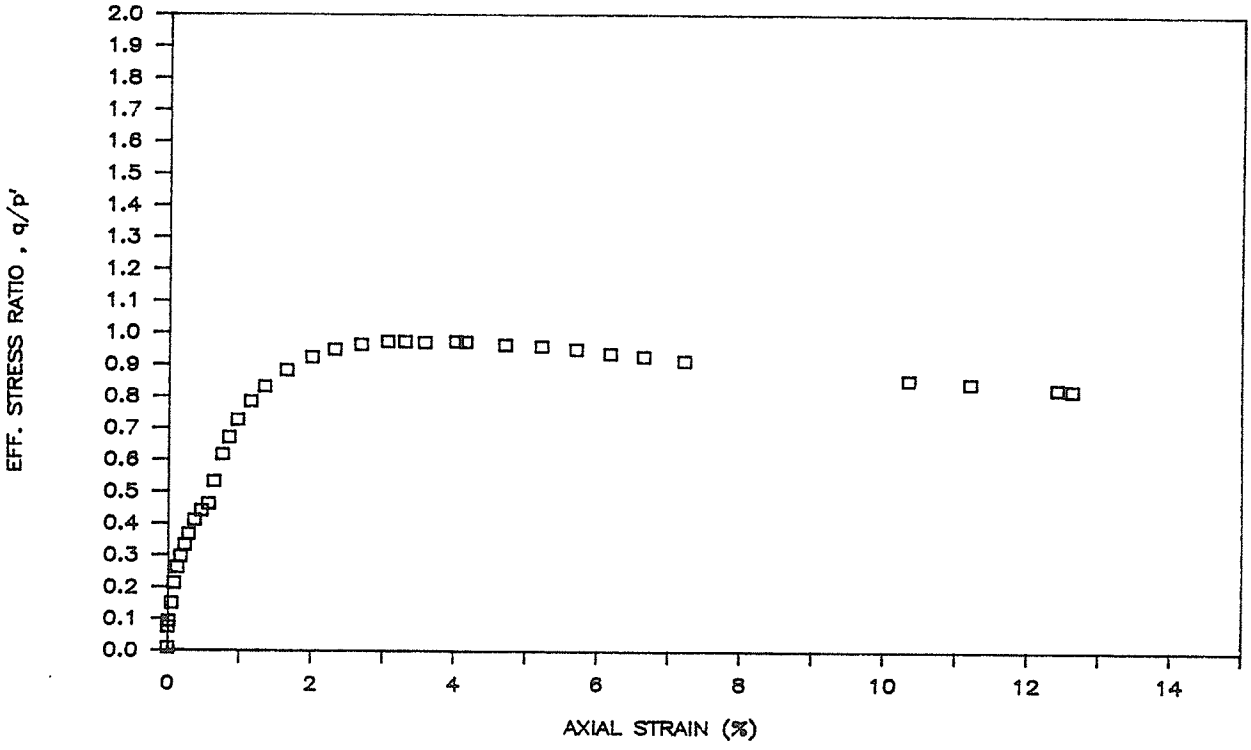

FIG. 6.13 - STRESS-STRAIN/POREWATER PRESSURE/STRESS RATIO CURVES IN UNDRAINED TRIAXIAL COMPRESSION - T956

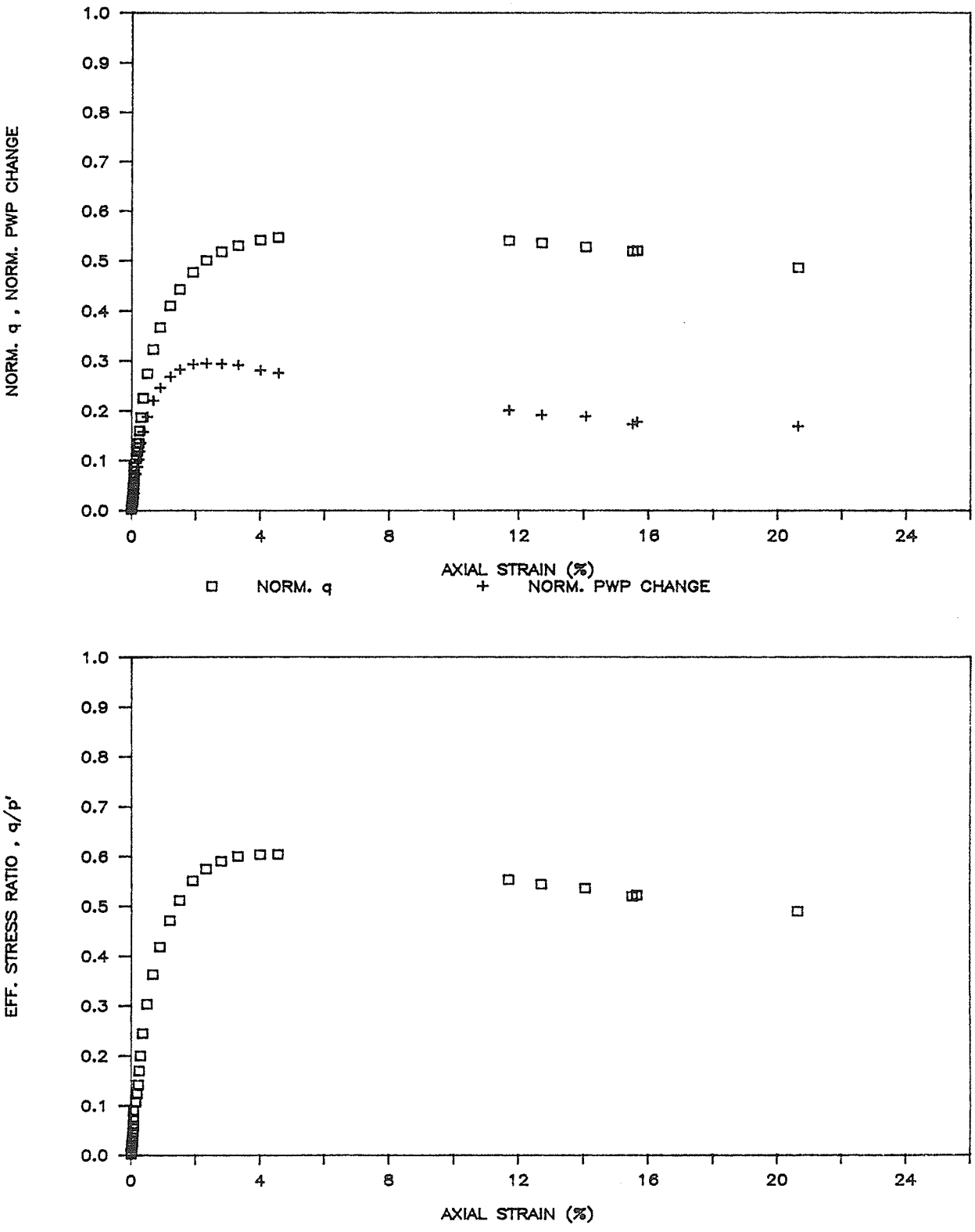

FIG. 6.14 - STRESS-STRAIN/POREWATER PRESSURE/STRESS RATIO CURVES IN UNDRAINED TRIAXIAL COMPRESSION - T957

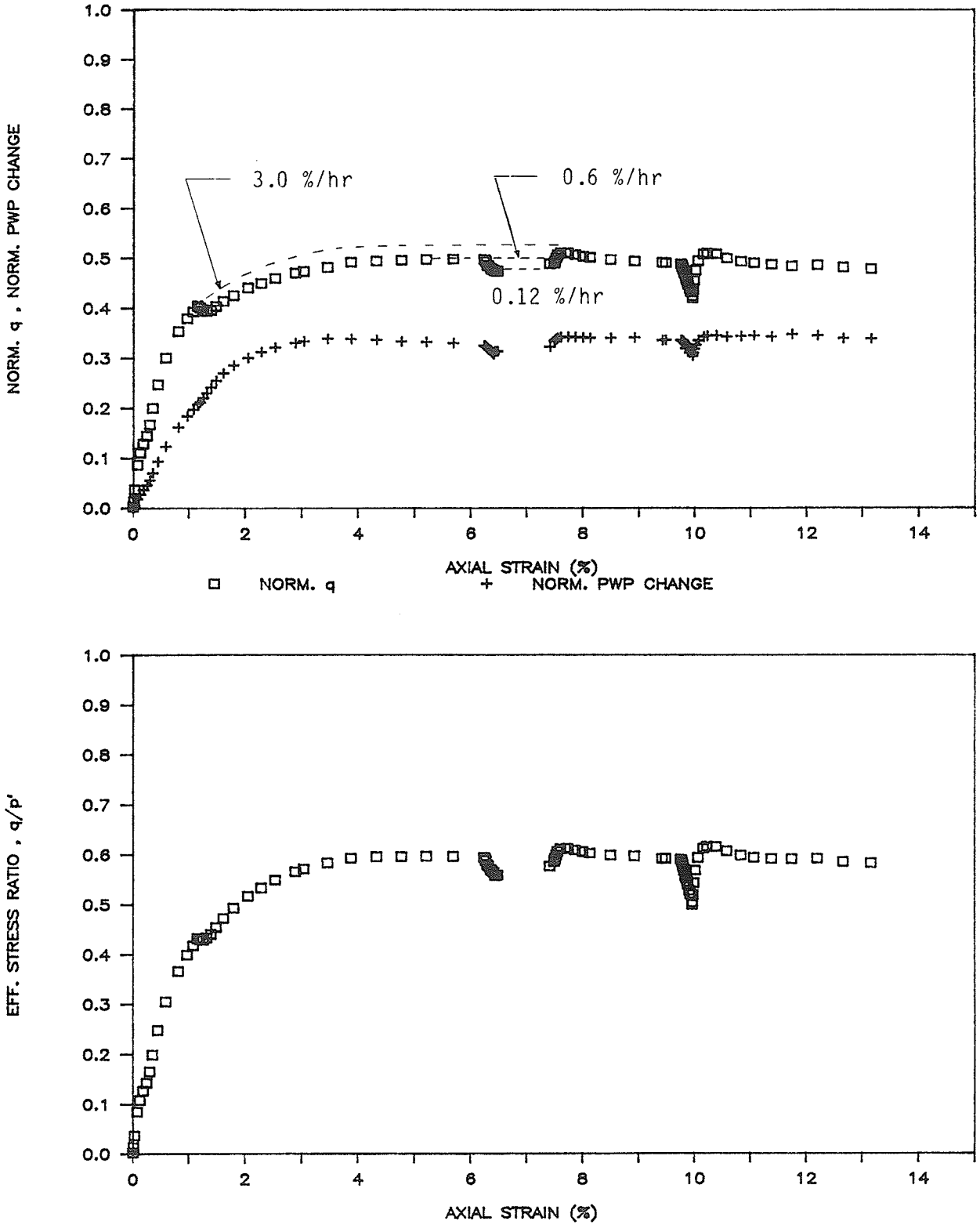

FIG. 6.15 - STRESS-STRAIN/POREWATER PRESSURE/STRESS RATIO CURVES IN UNDRAINED TRIAXIAL COMPRESSION - T961

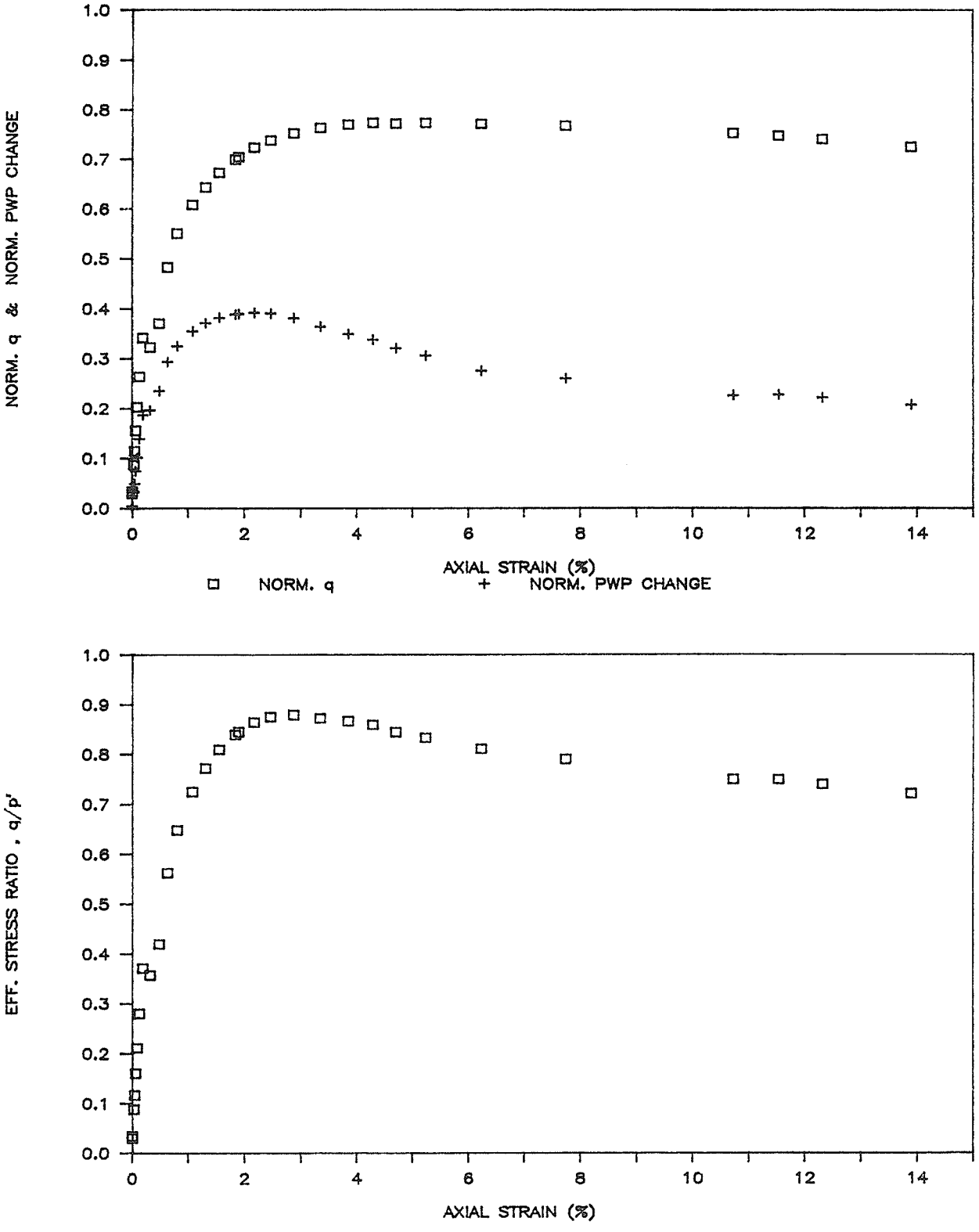

FIG. 6.16 - STRESS-STRAIN/POREWATER PRESSURE/STRESS RATIO CURVES IN UNDRAINED TRIAXIAL COMPRESSION - T962

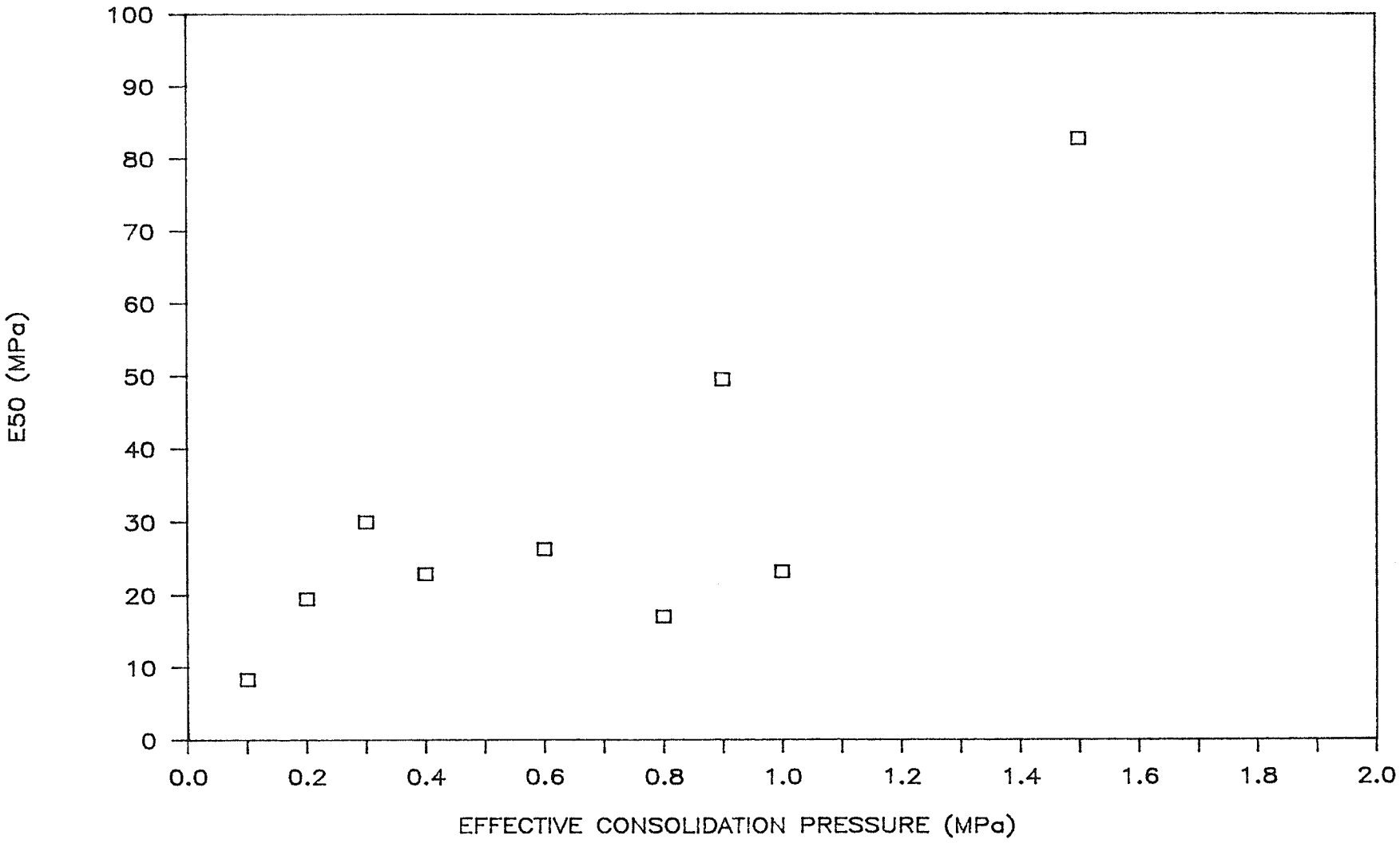

FIG. 6.17 - RELATIONSHIP BETWEEN UNDRAINED SHEAR MODULUS AND CONSOLIDATION PRESSURE

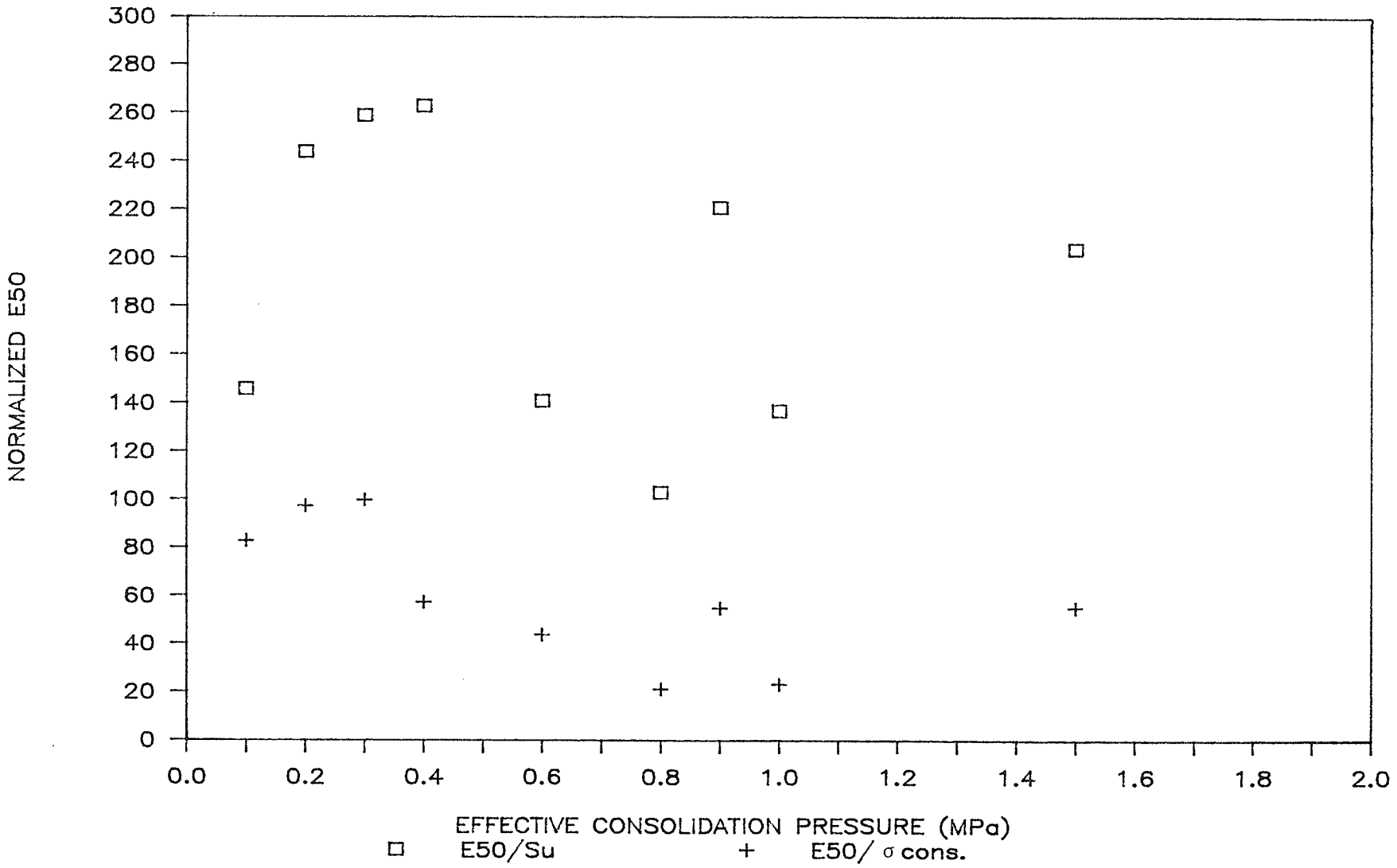

FIG. 6.18 - RELATIONSHIP BETWEEN NORMALIZED UNDRAINED SHEAR MODULUS AND CONSOLIDATION PRESSURE

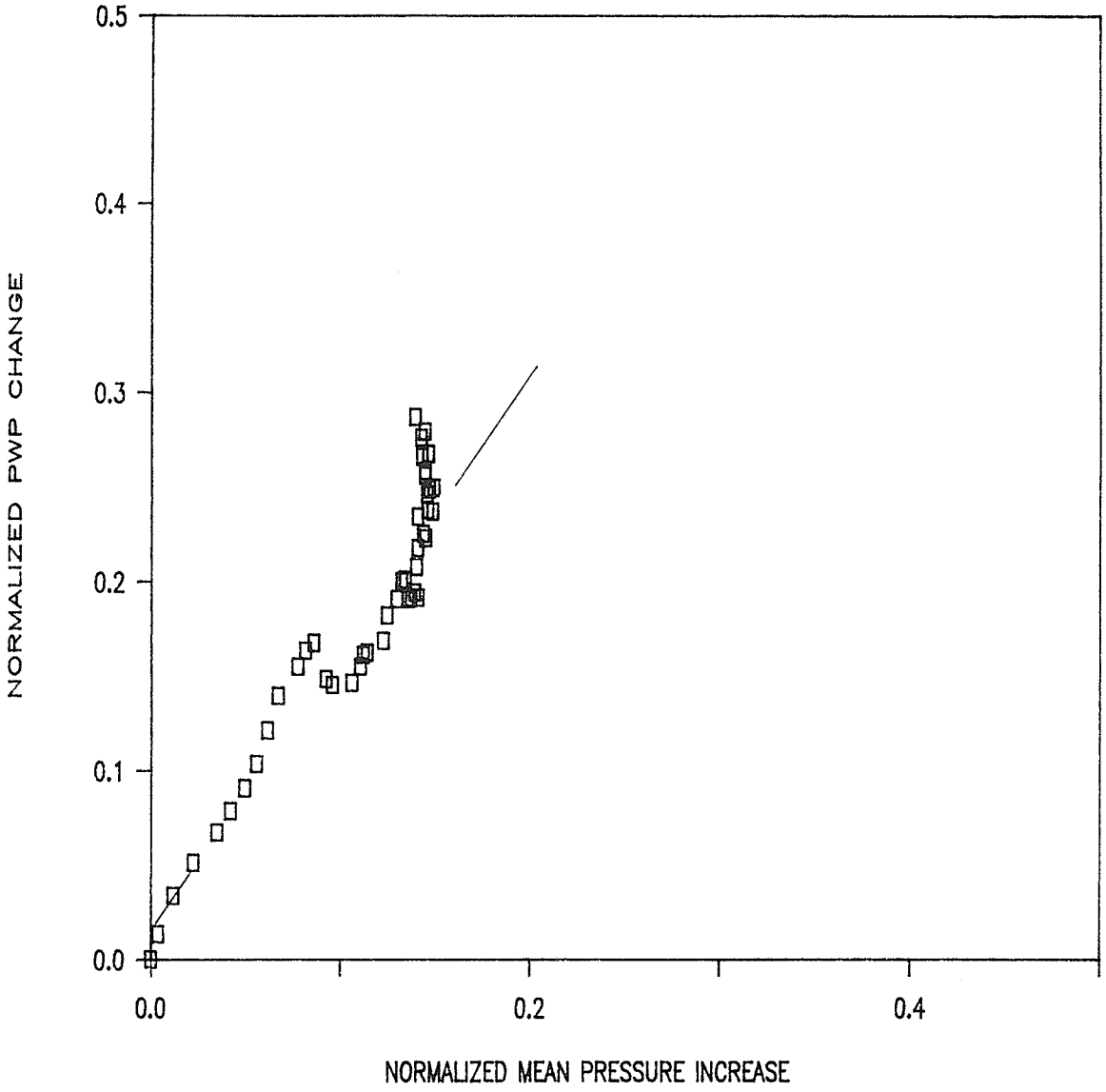

FIG. 6.19 - NORMALIZED POREWATER PRESSURE CHANGES VS. NORMALIZED MEAN TOTAL PRESSURE CHANGES - T951

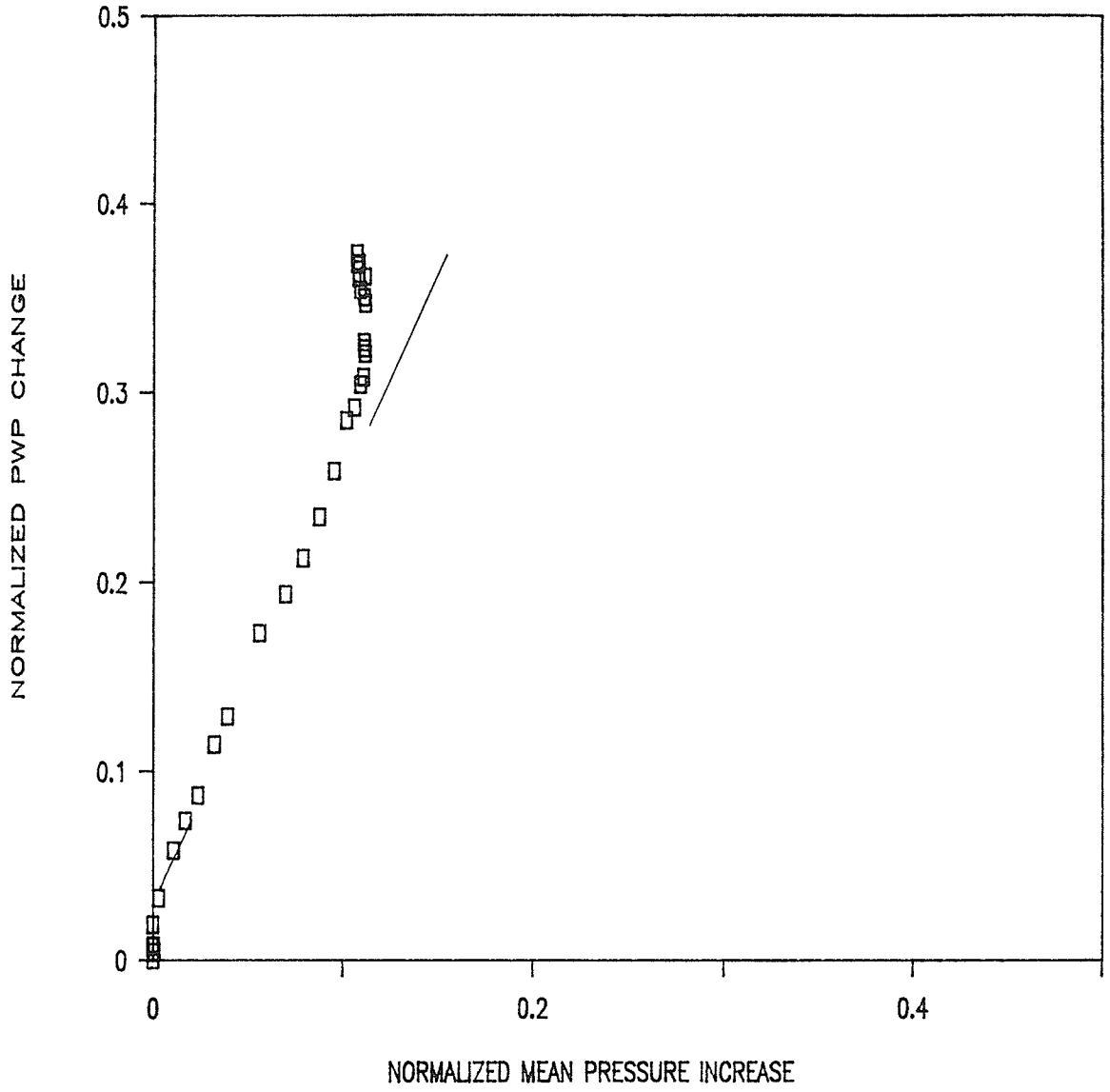

FIG. 6.20 - NORMALIZED POREWATER PRESSURE CHANGES VS. NORMALIZED MEAN TOTAL PRESSURE CHANGES - T952

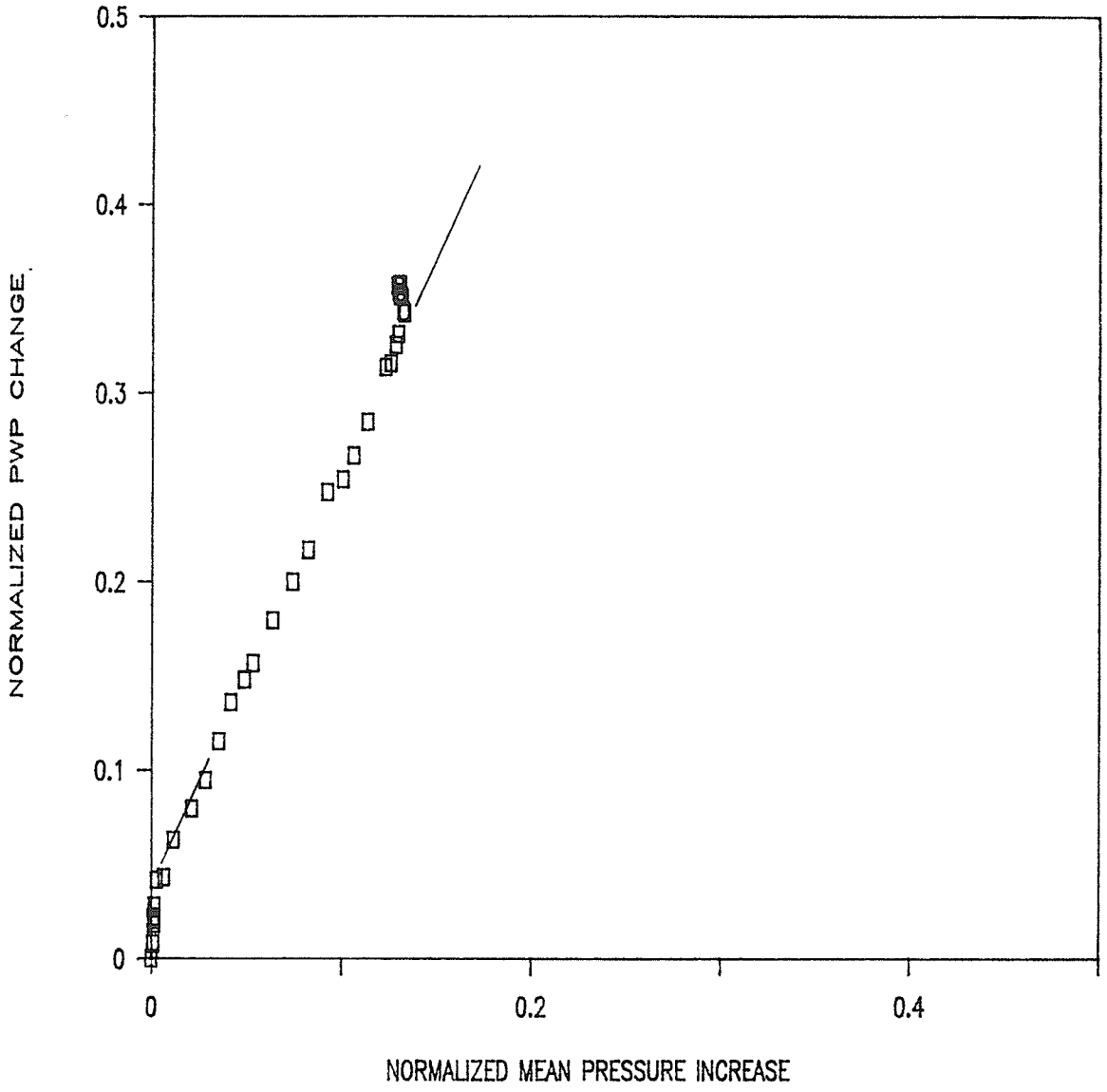

FIG. 6.21 - NORMALIZED POREWATER PRESSURE CHANGES VS. NORMALIZED MEAN TOTAL PRESSURE CHANGES - T953

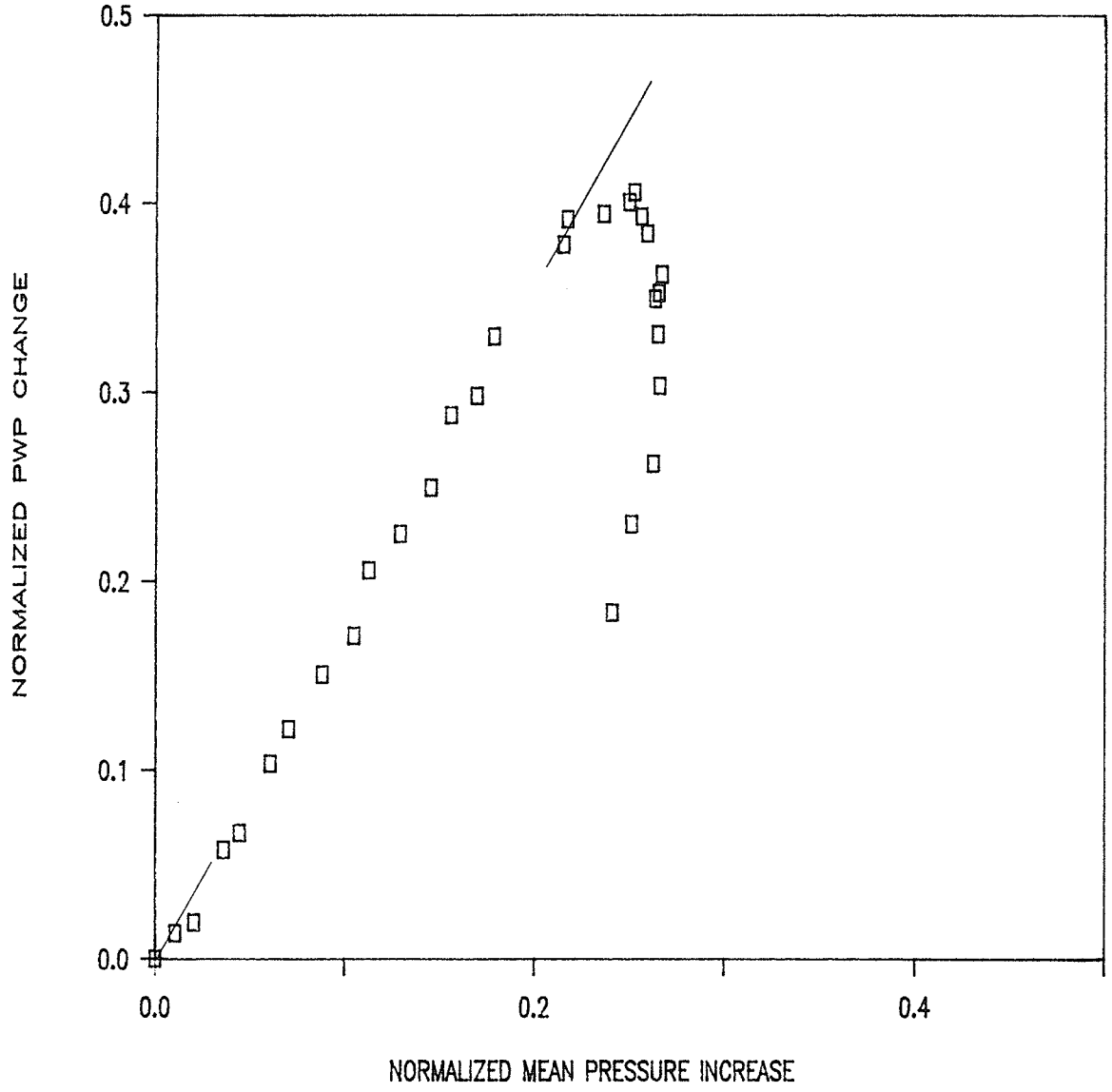

FIG. 6.22 - NORMALIZED POREWATER PRESSURE CHANGES VS. NORMALIZED MEAN TOTAL PRESSURE CHANGES - T954

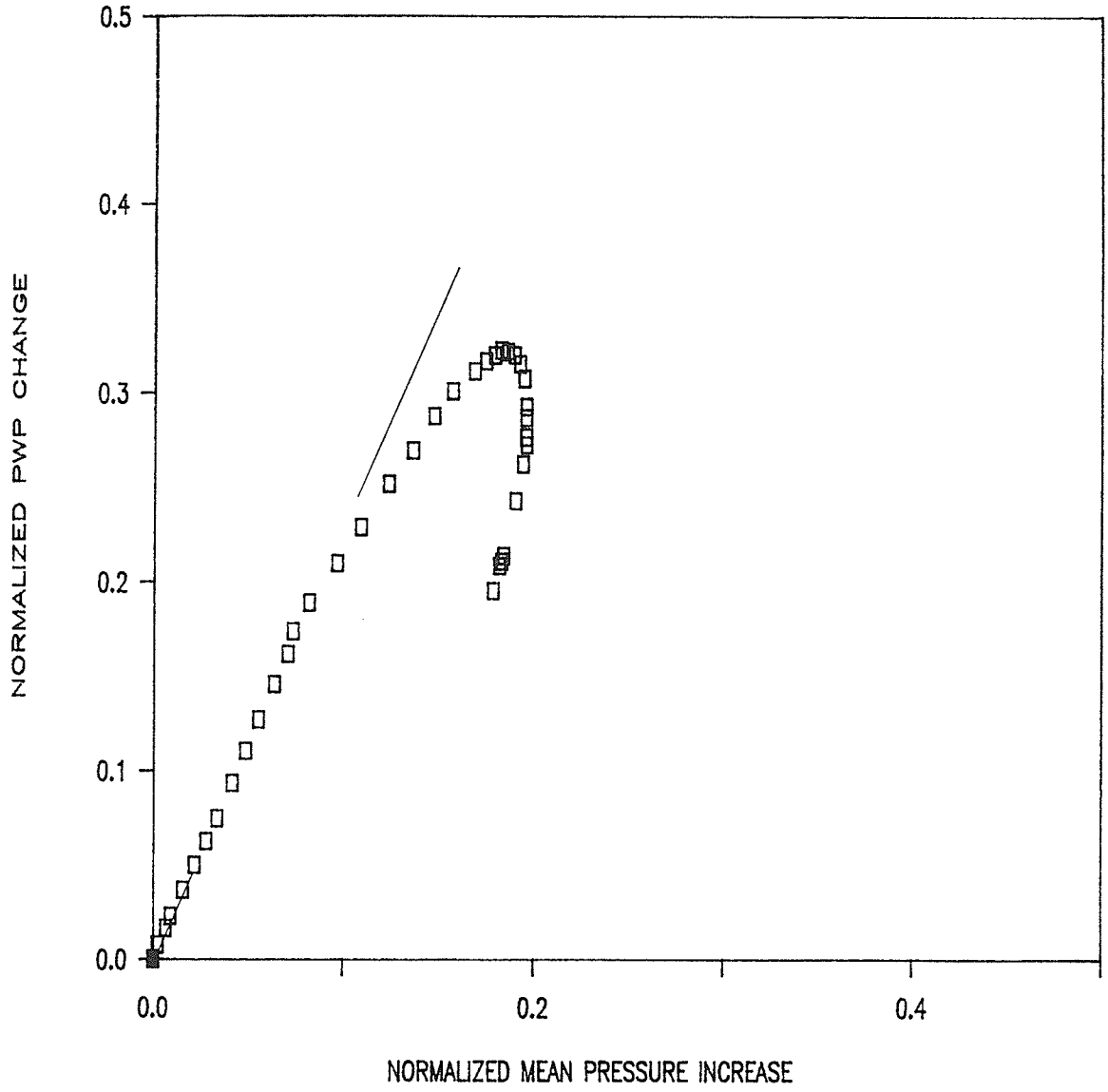

FIG. 6.23 - NORMALIZED POREWATER PRESSURE CHANGES VS. NORMALIZED MEAN TOTAL PRESSURE CHANGES - T955

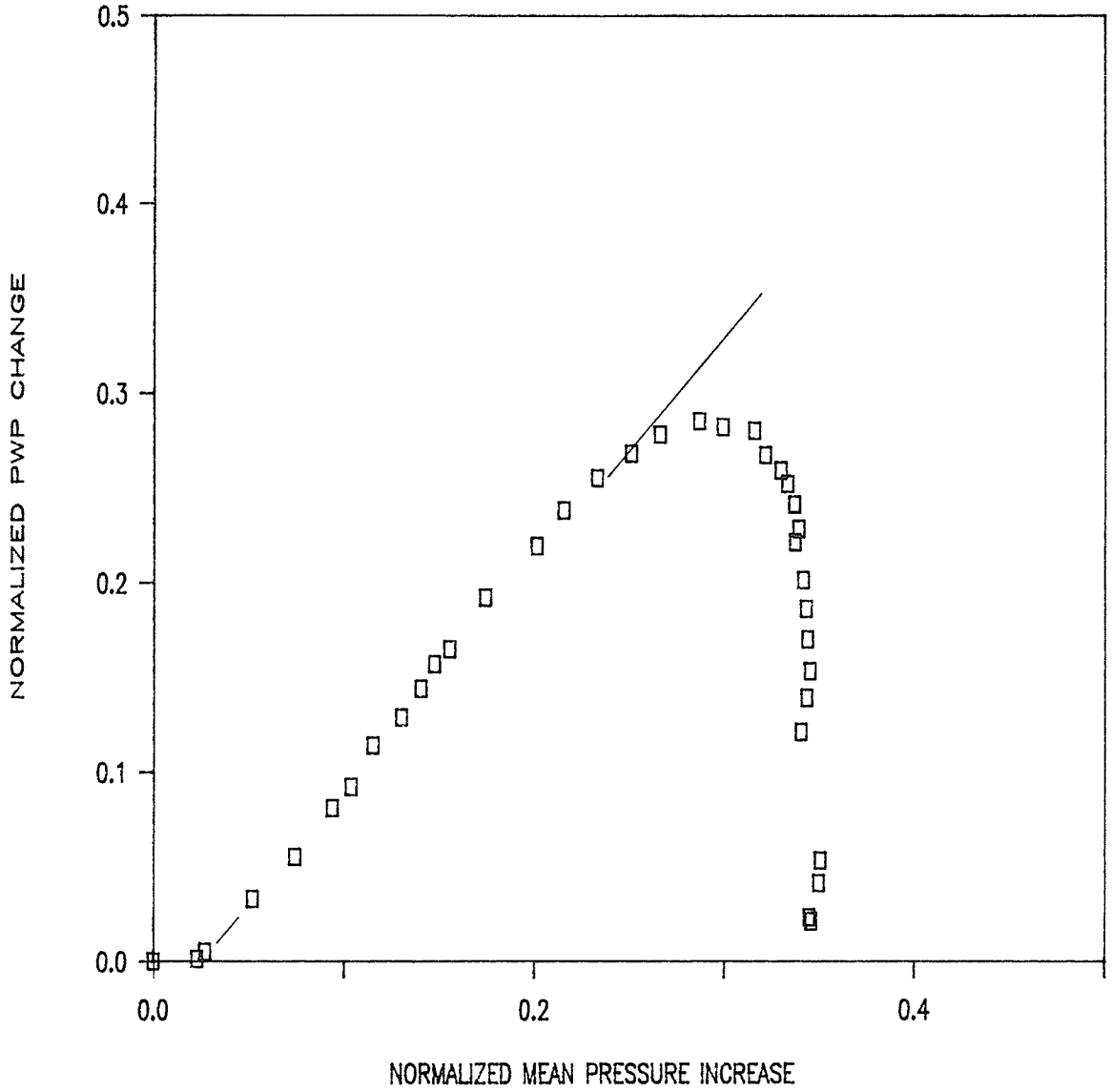

FIG. 6.24 - NORMALIZED POREWATER PRESSURE CHANGES VS. NORMALIZED MEAN TOTAL PRESSURE CHANGES - T956

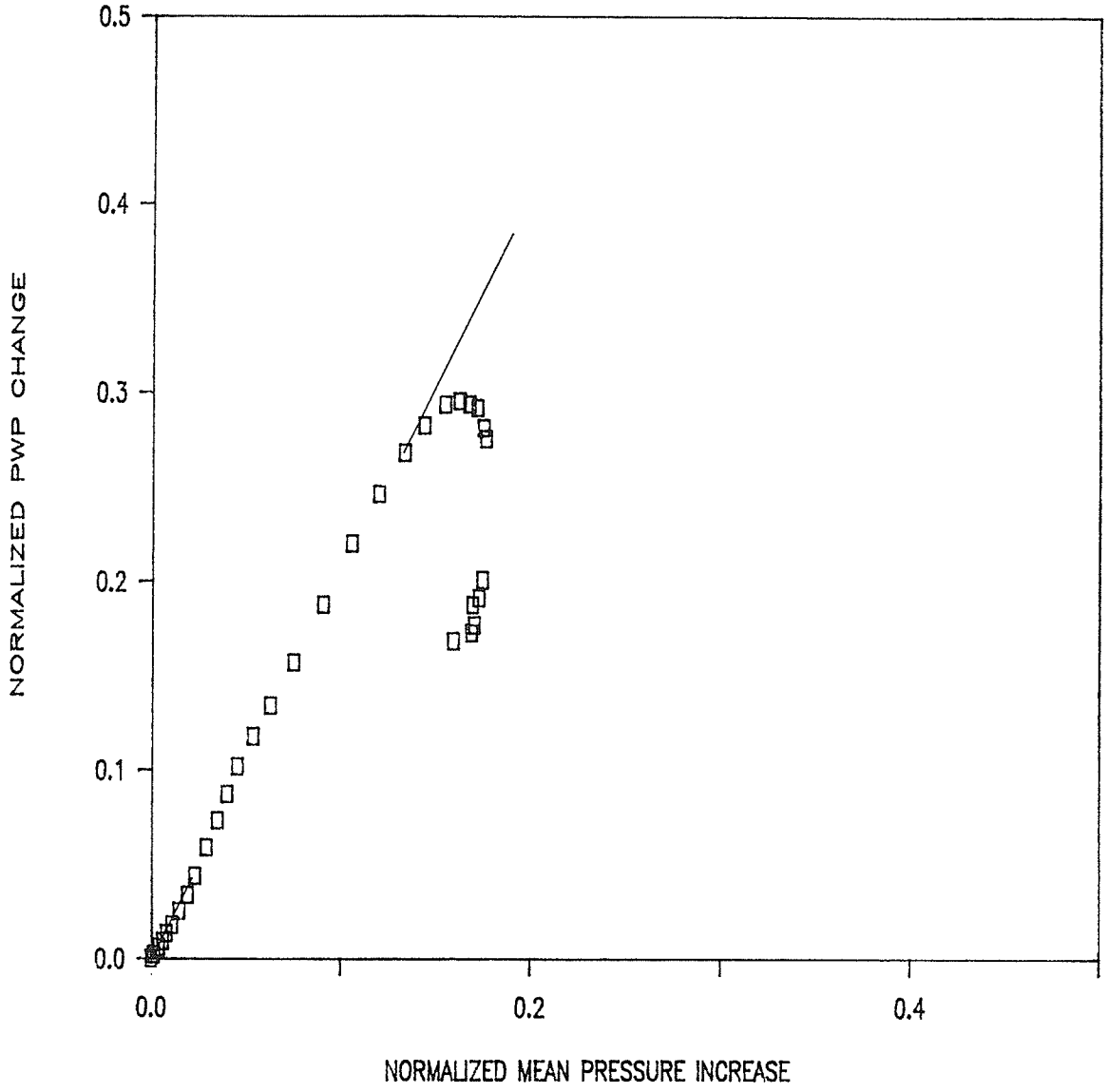

FIG. 6.25 - NORMALIZED POREWATER PRESSURE CHANGES VS. NORMALIZED MEAN TOTAL PRESSURE CHANGES - T957

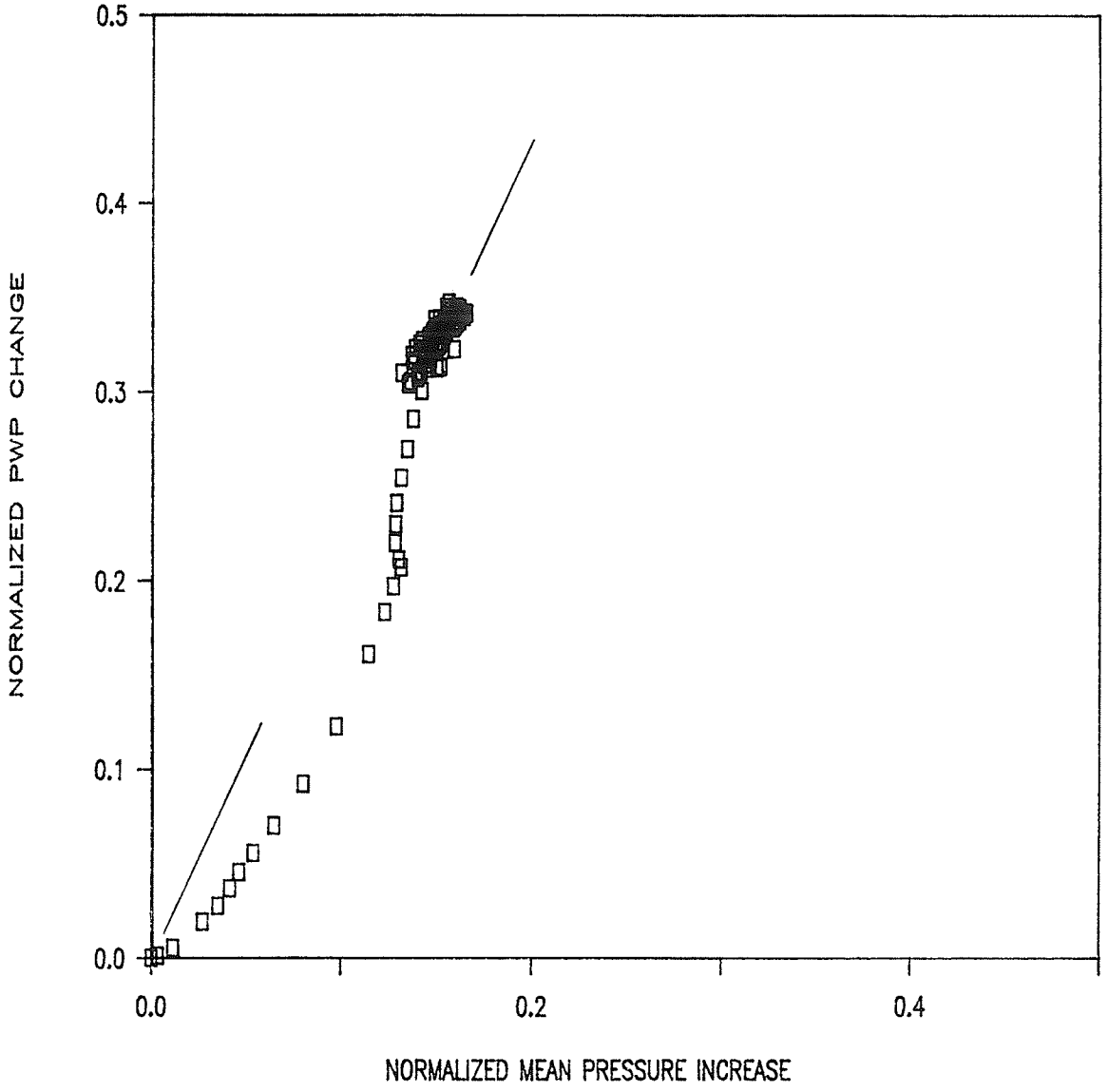

FIG. 6.26 - NORMALIZED POREWATER PRESSURE CHANGES VS. NORMALIZED MEAN TOTAL PRESSURE CHANGES - T961

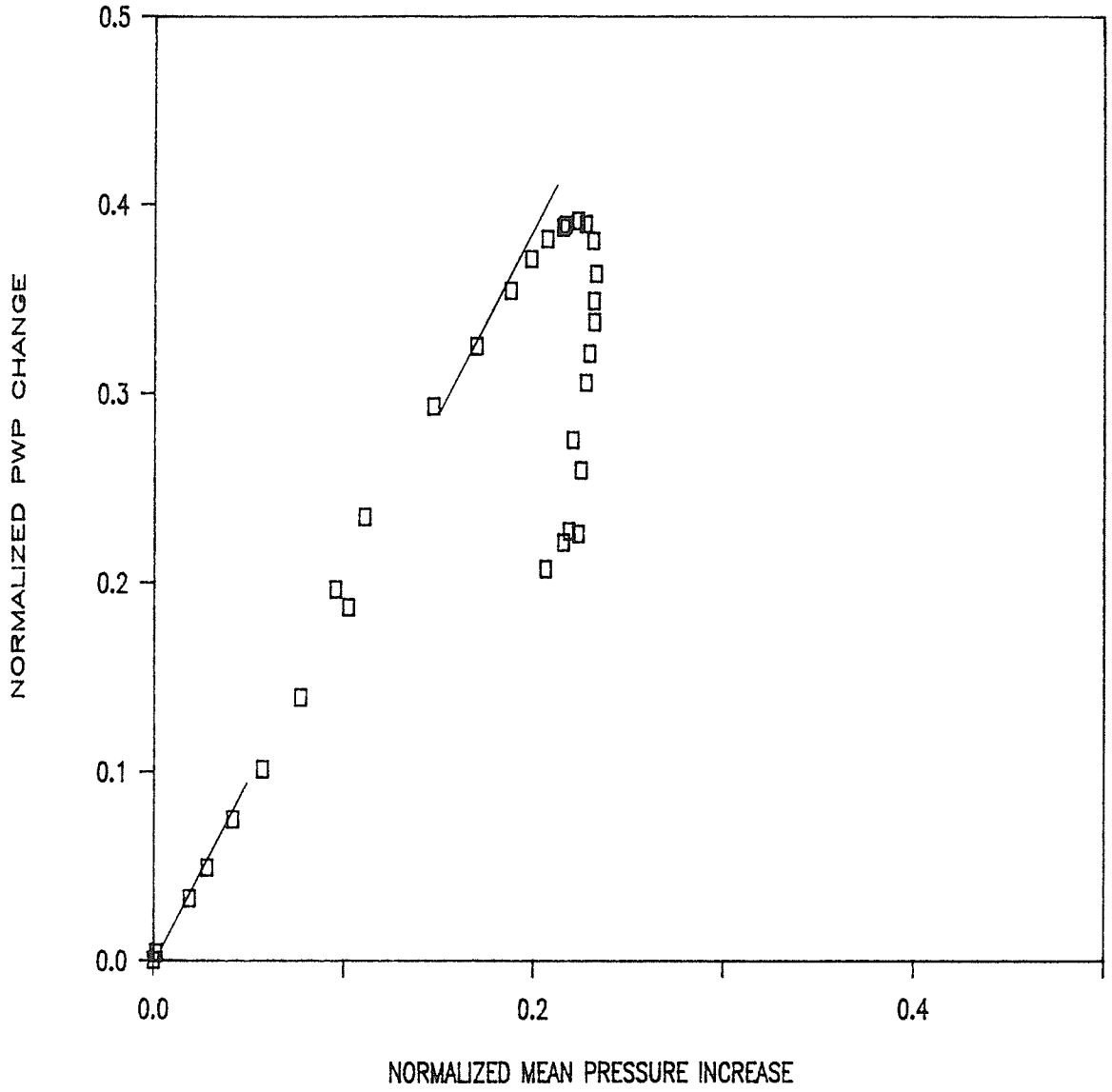

FIG. 6.27 - NORMALIZED POREWATER PRESSURE CHANGES VS. NORMALIZED MEAN TOTAL PRESSURE CHANGES - T962

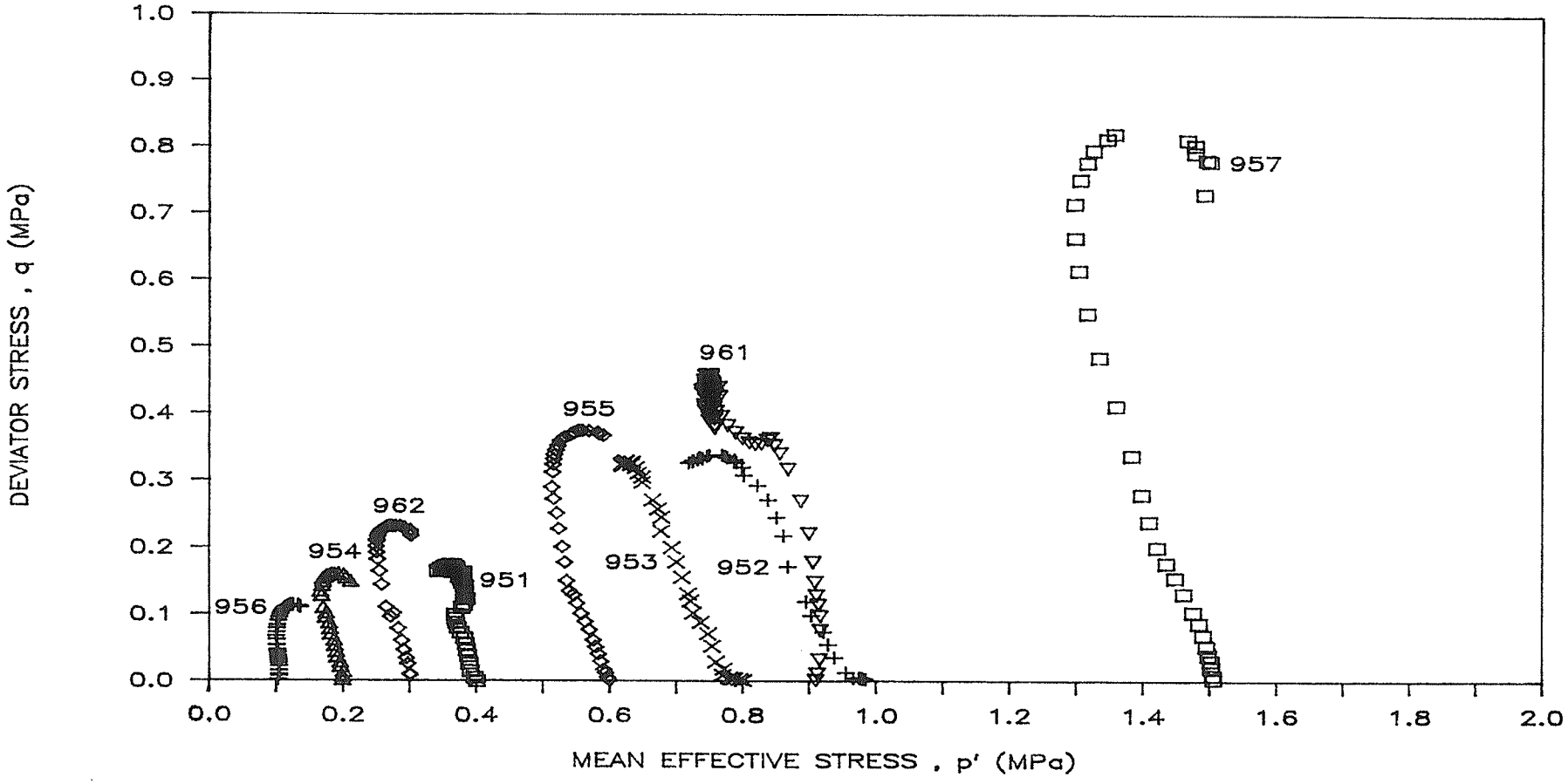

FIG. 6.28 - EFFECTIVE STRESS PATHS FROM UNDRAINED SHEAR TESTS

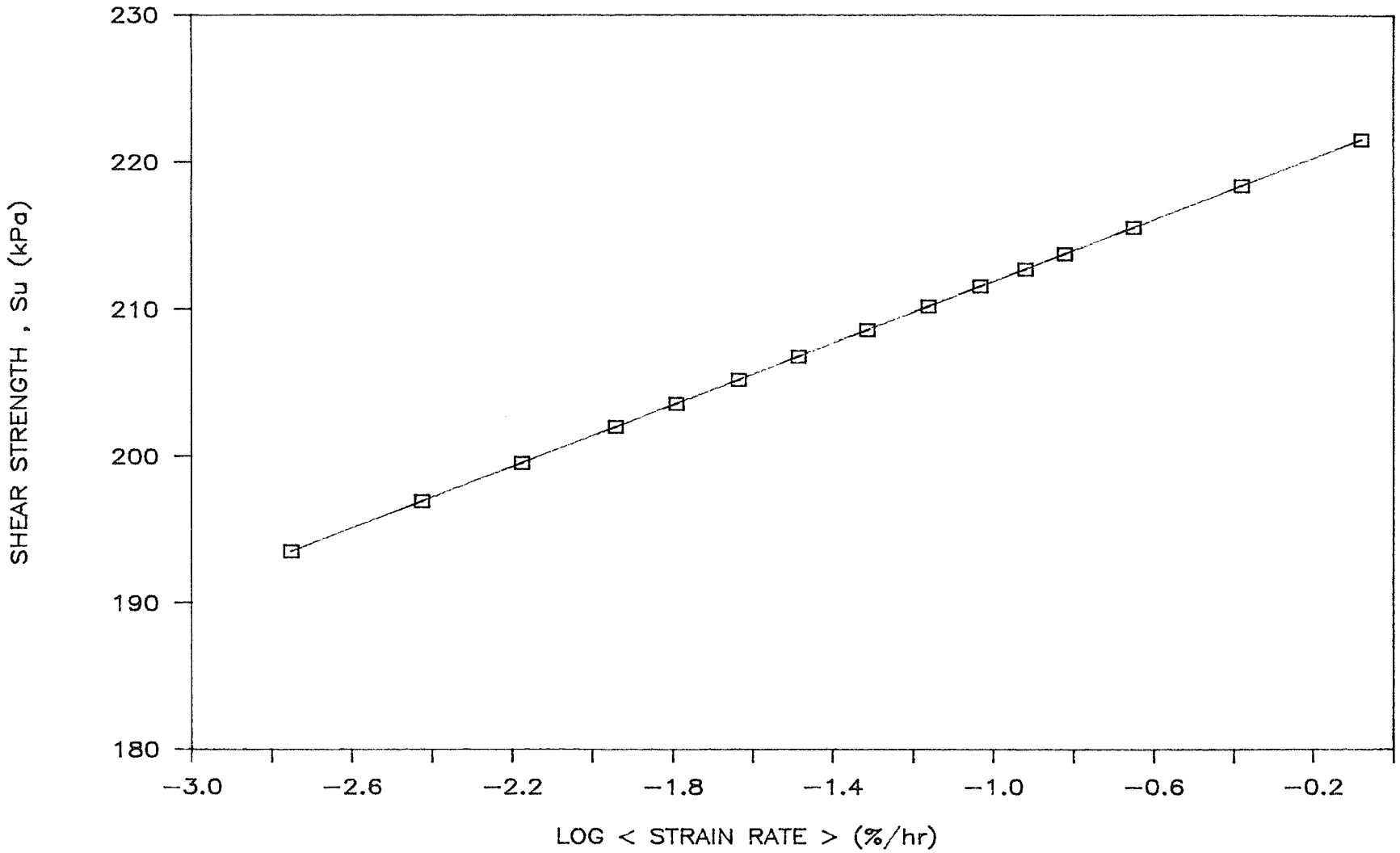

FIG. 6.29 - CHANGE IN UNDRAINED SHEARING RESISTANCE WITH LOG<STRAIN RATE>

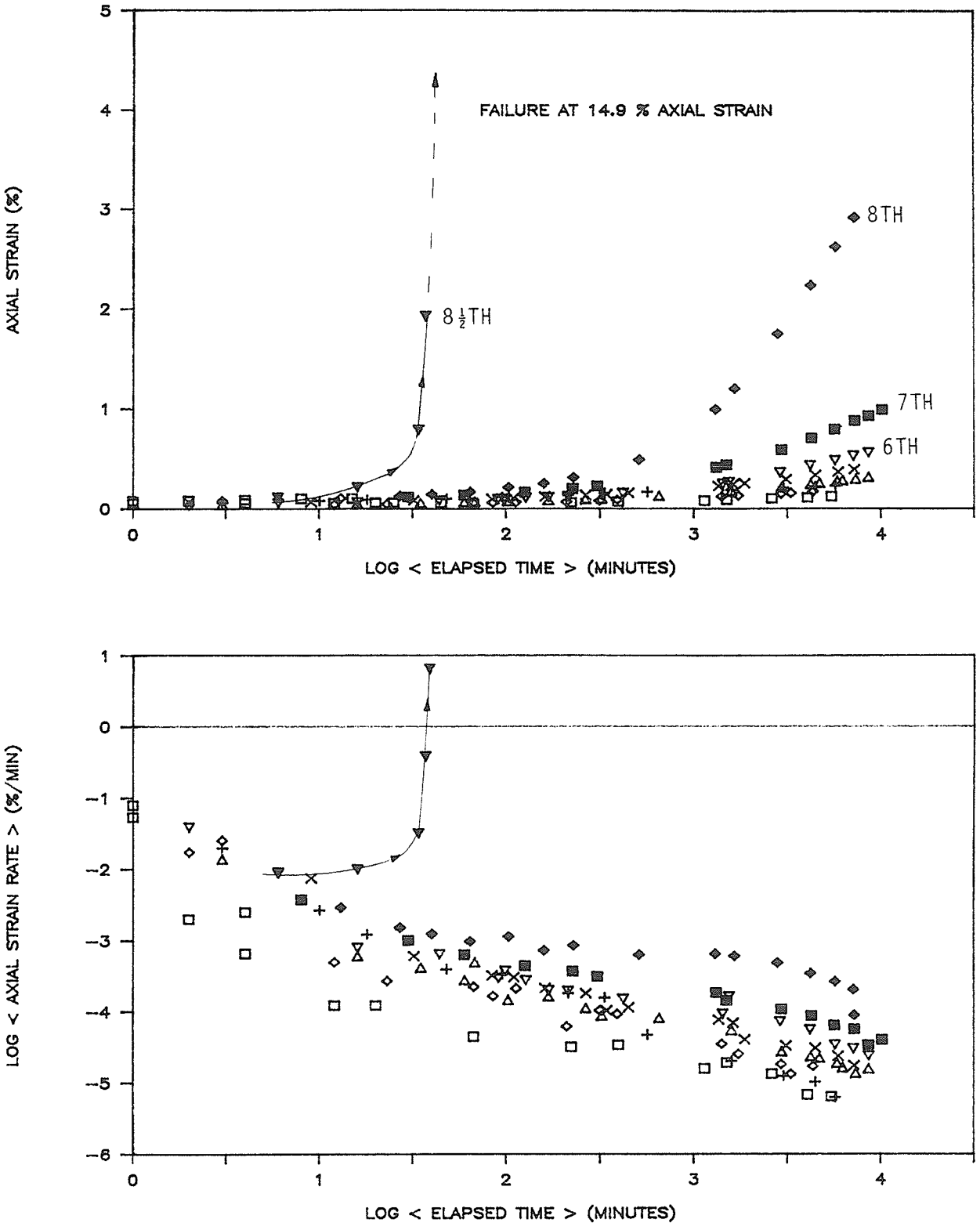

FIG. 6.30 - INCREMENTAL DRAINED SHEAR CONSTANT-p' TEST - T958
(A) AXIAL STRAIN VS. LOG<ELAPSED TIME>
(B) LOG<AXIAL STRAIN RATE> VS. LOG<ELAPSED TIME>

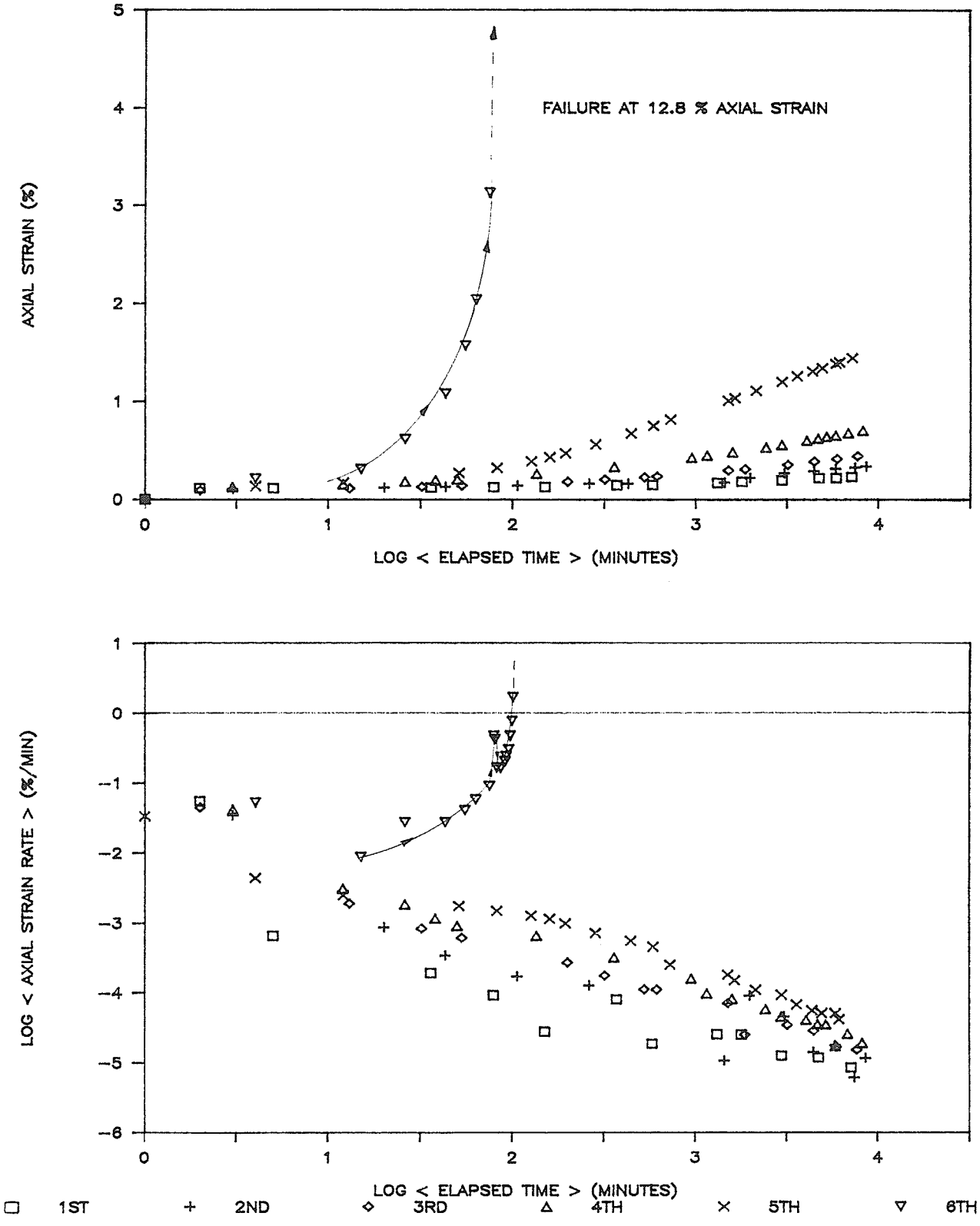

FIG. 6.31 - INCREMENTAL DRAINED SHEAR CONSTANT-p' TEST - T959
(A) AXIAL STRAIN VS. LOG<ELAPSED TIME>
(B) LOG<AXIAL STRAIN RATE> VS. LOG<ELAPSED TIME>

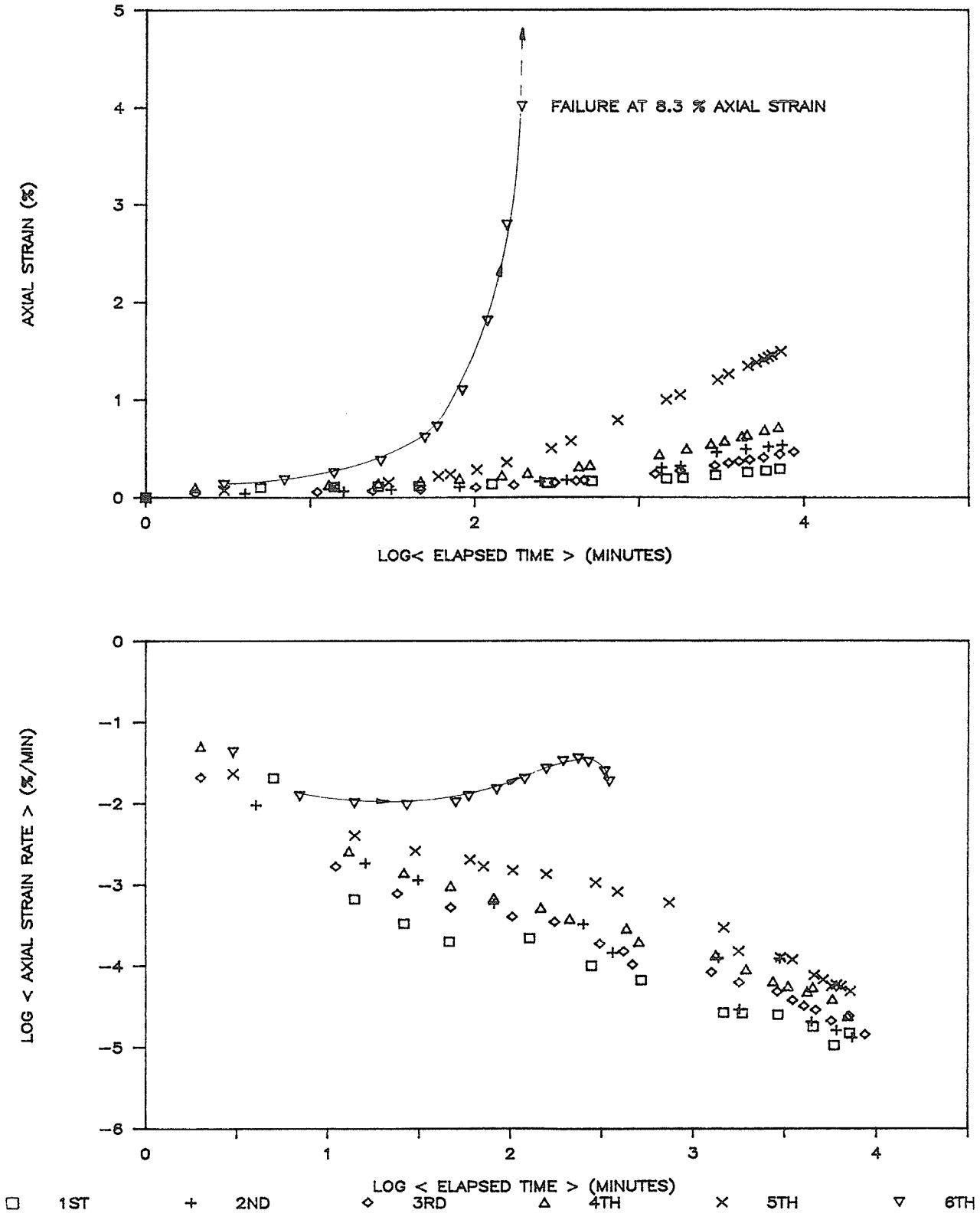

FIG. 6.32 - INCREMENTAL DRAINED SHEAR CONSTANT-p' TEST - T960
(A) AXIAL STRAIN VS. LOG<ELAPSED TIME>
(B) LOG<AXIAL STRAIN RATE> VS. LOG<ELAPSED TIME>

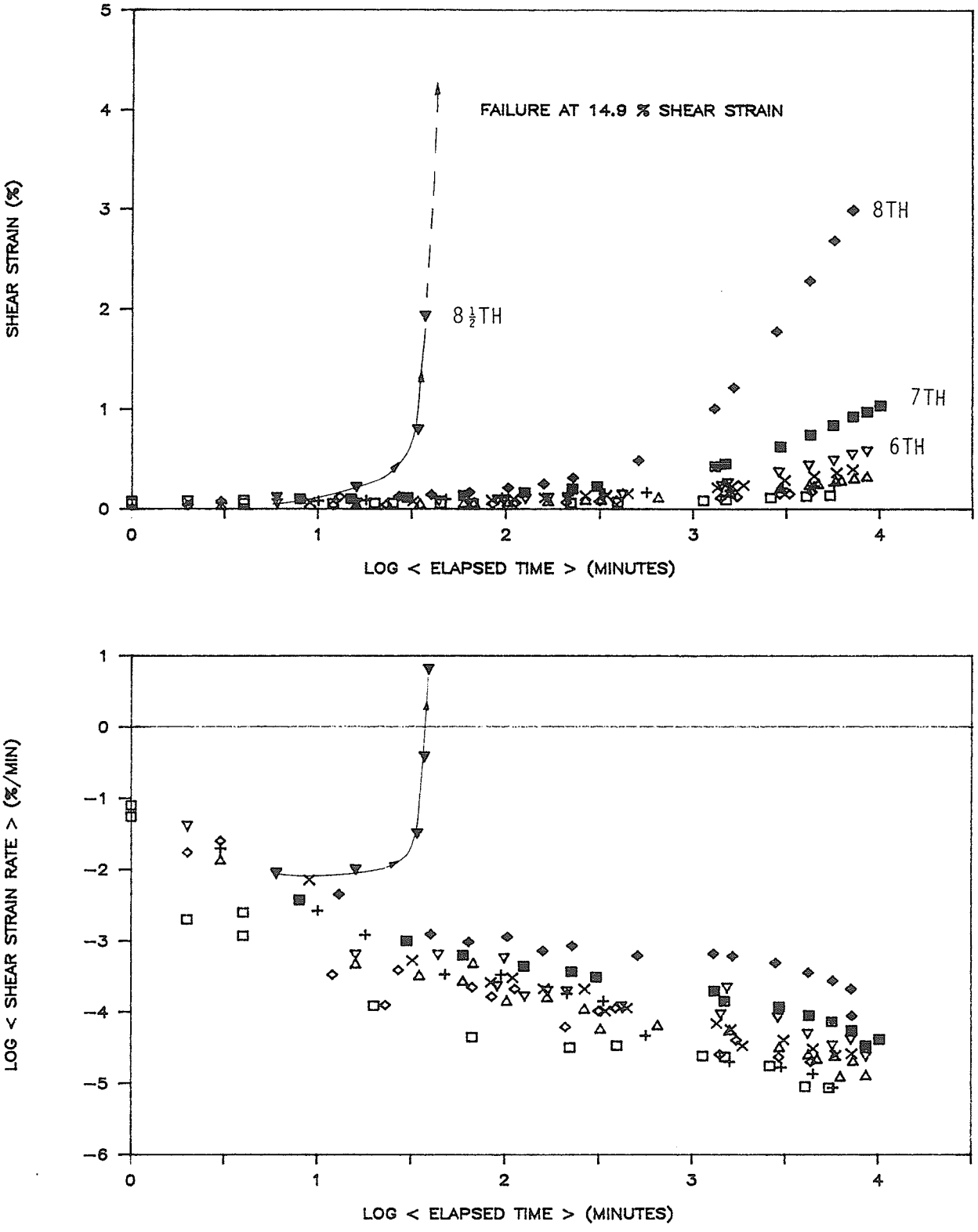

FIG. 6.33 - INCREMENTAL DRAINED SHEAR CONSTANT-p' TEST - T958
(A) SHEAR STRAIN VS. LOG<ELAPSED TIME>
(B) LOG<SHEAR STRAIN RATE> VS. LOG<ELAPSED TIME>

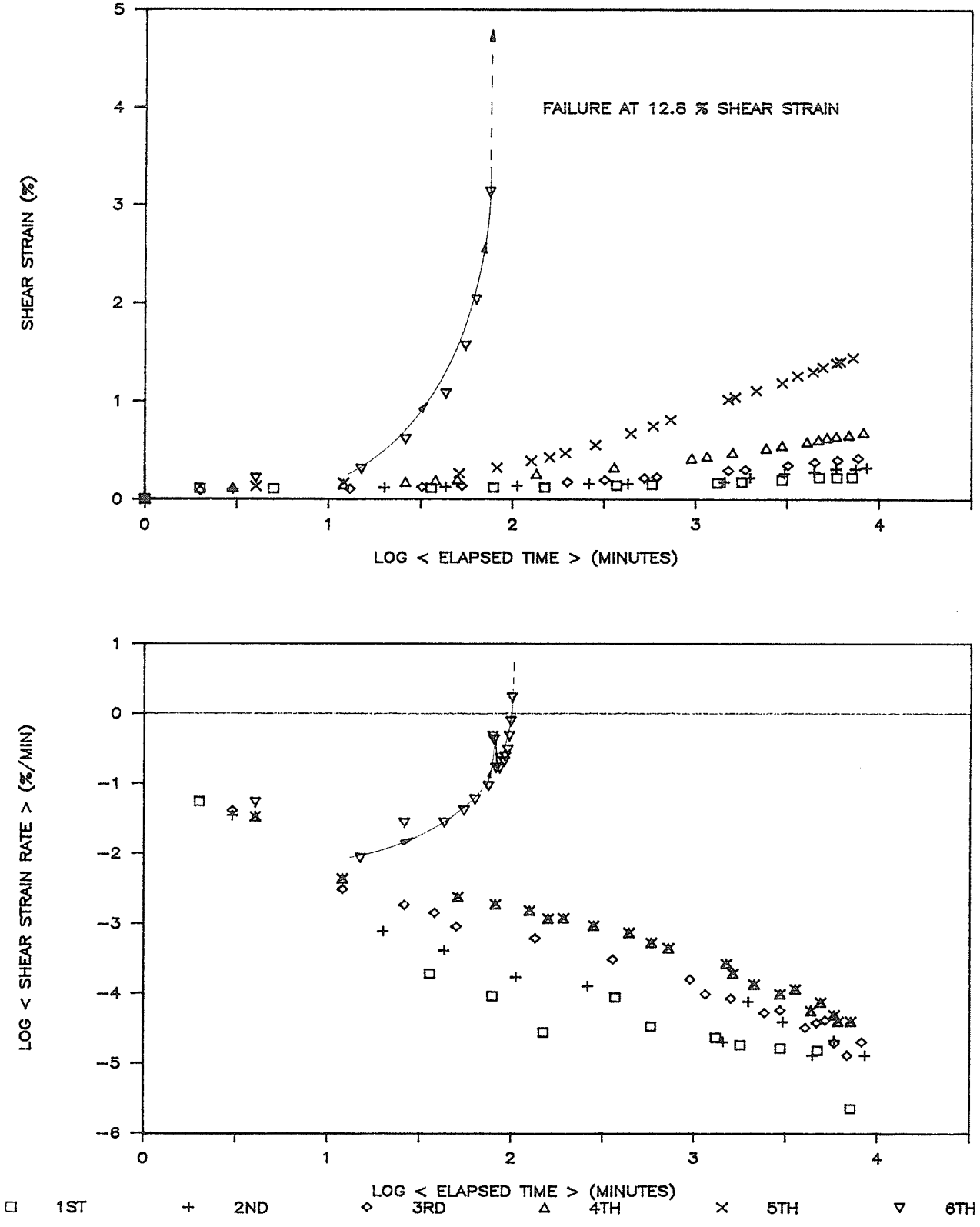

FIG. 6.34 - INCREMENTAL DRAINED SHEAR CONSTANT-p' TEST - T959
(A) SHEAR STRAIN VS. LOG<ELAPSED TIME>
(B) LOG<SHEAR STRAIN RATE> VS. LOG<ELAPSED TIME>

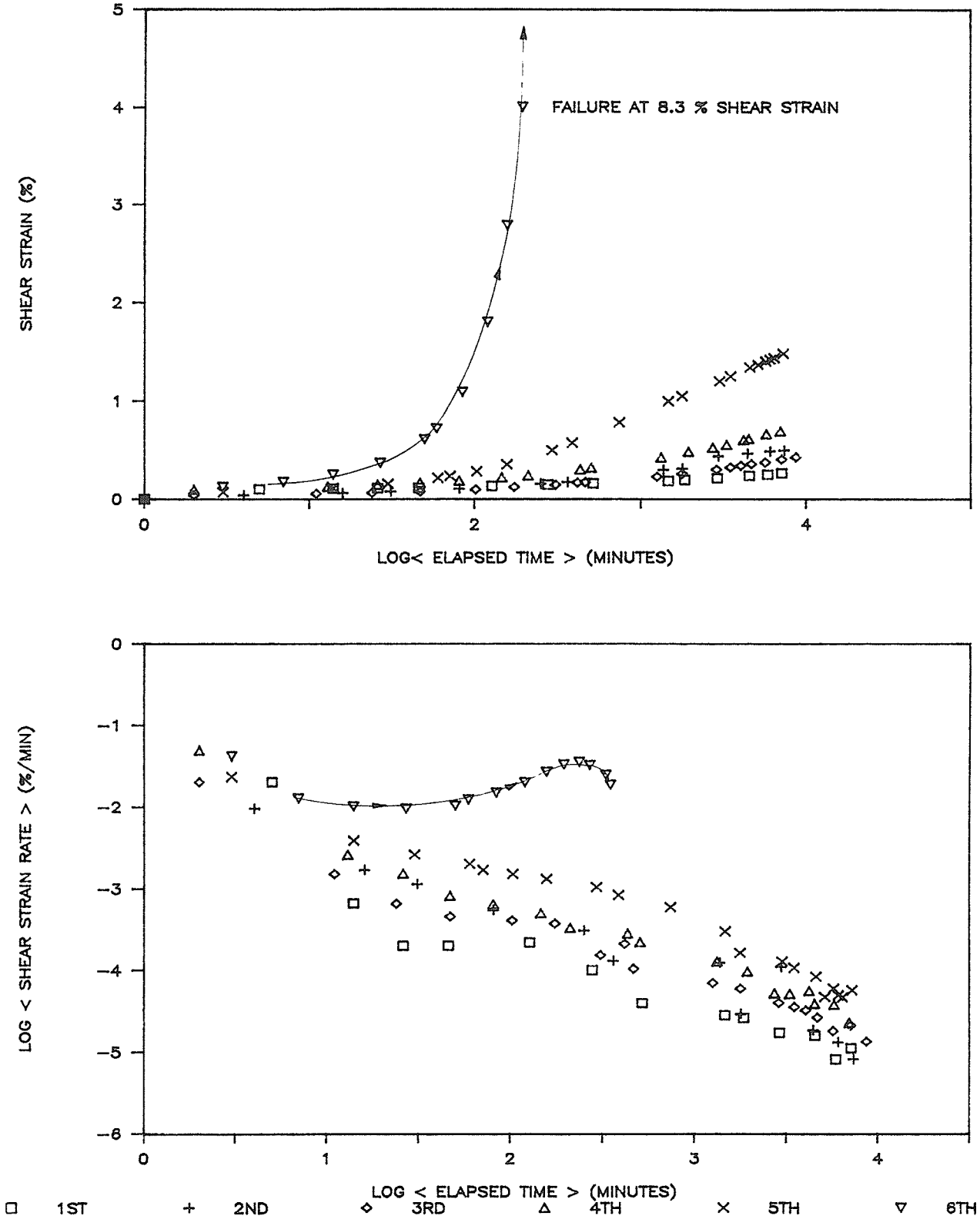

FIG. 6.35 - INCREMENTAL DRAINED SHEAR CONSTANT-p' TEST - T960
(A) SHEAR STRAIN VS. LOG<ELAPSED TIME>
(B) LOG<SHEAR STRAIN RATE> VS. LOG<ELAPSED TIME>

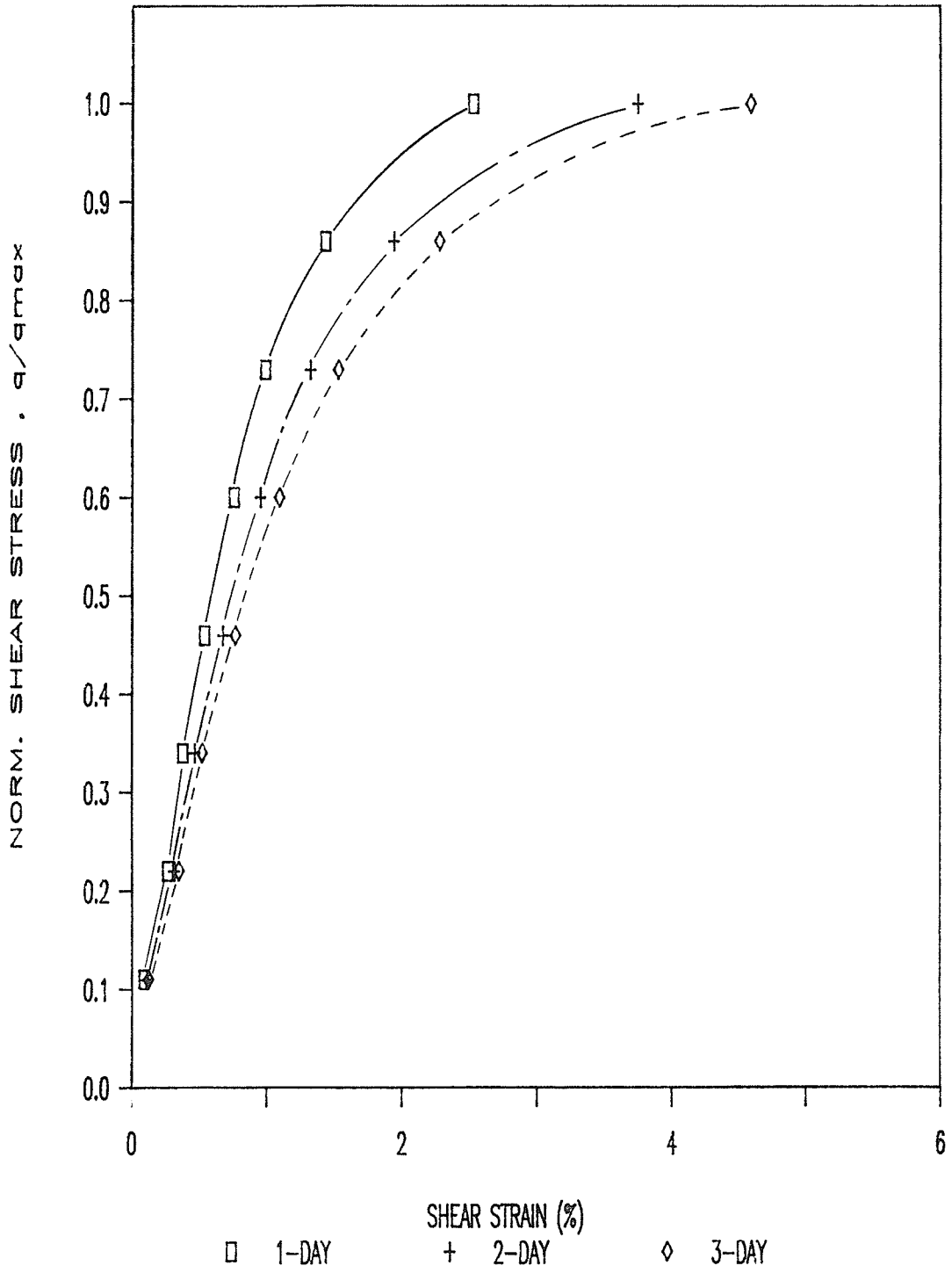

FIG. 6.36 - NORMALIZED SHEAR STRESS VS. ACCUMULATED SHEAR STRAIN - T958

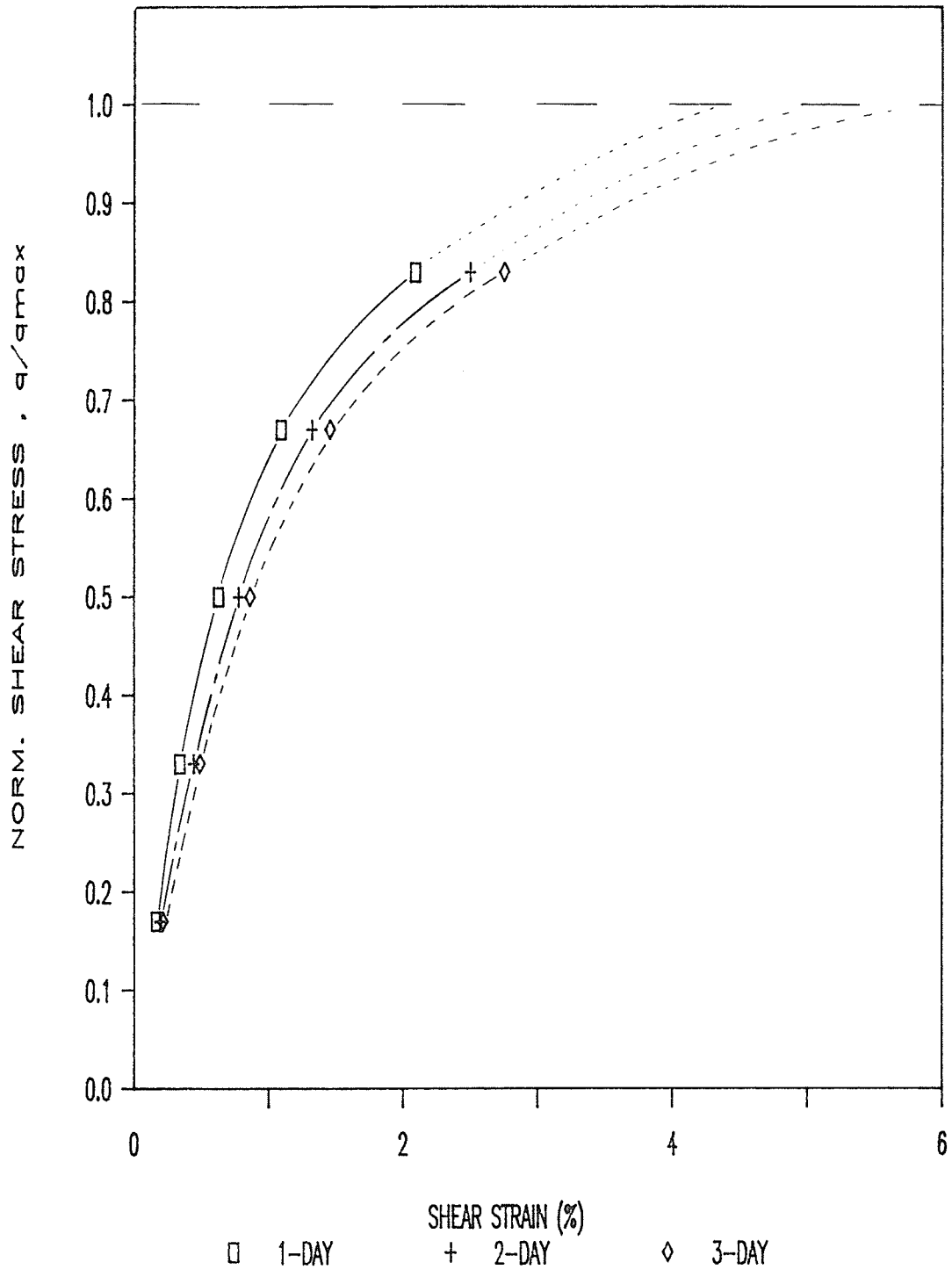

FIG. 6.37 - NORMALIZED SHEAR STRESS VS. ACCUMULATED SHEAR STRAIN - T959

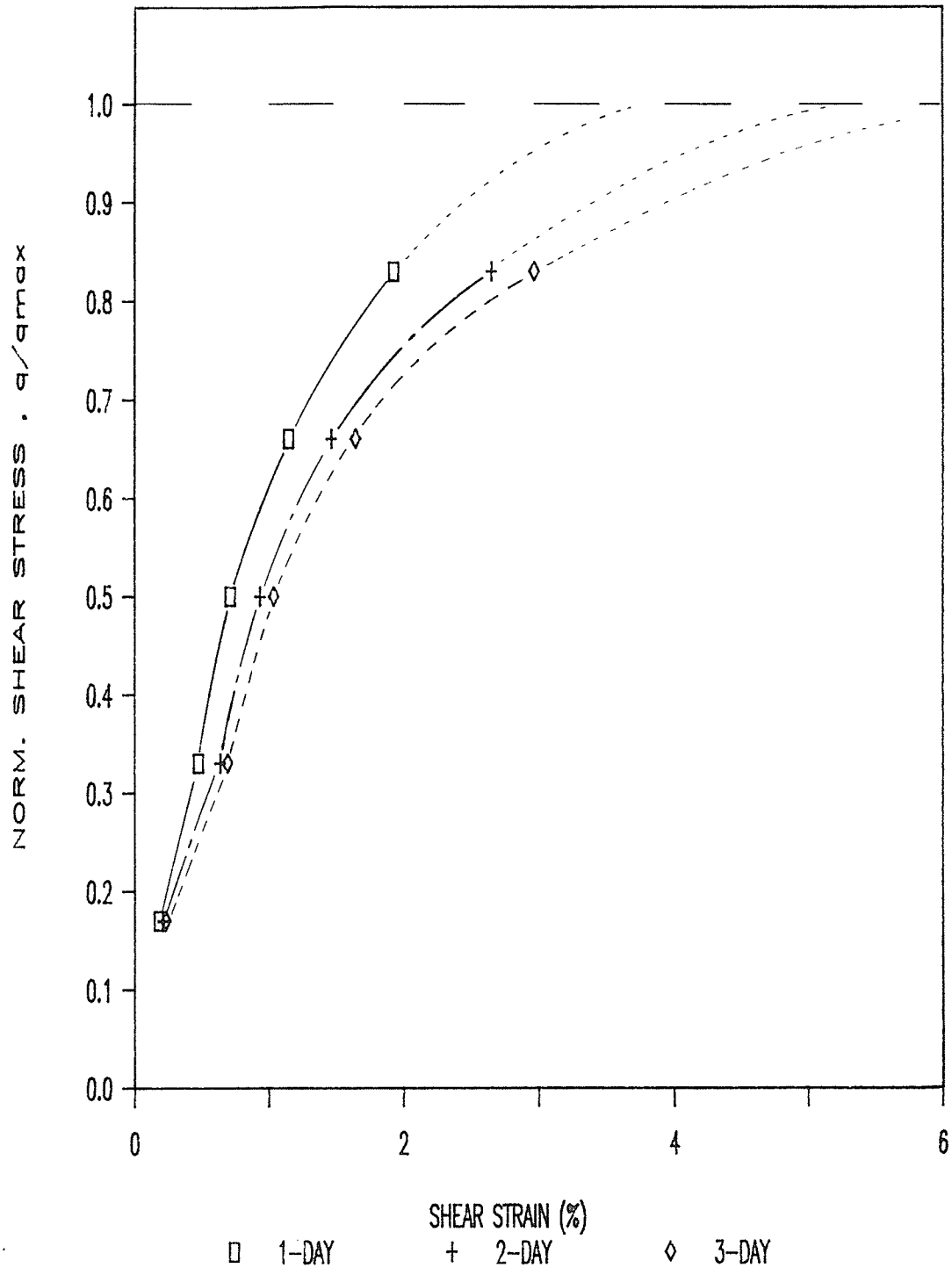

FIG. 6.38 - NORMALIZED SHEAR STRESS VS. ACCUMULATED SHEAR STRAIN - T960

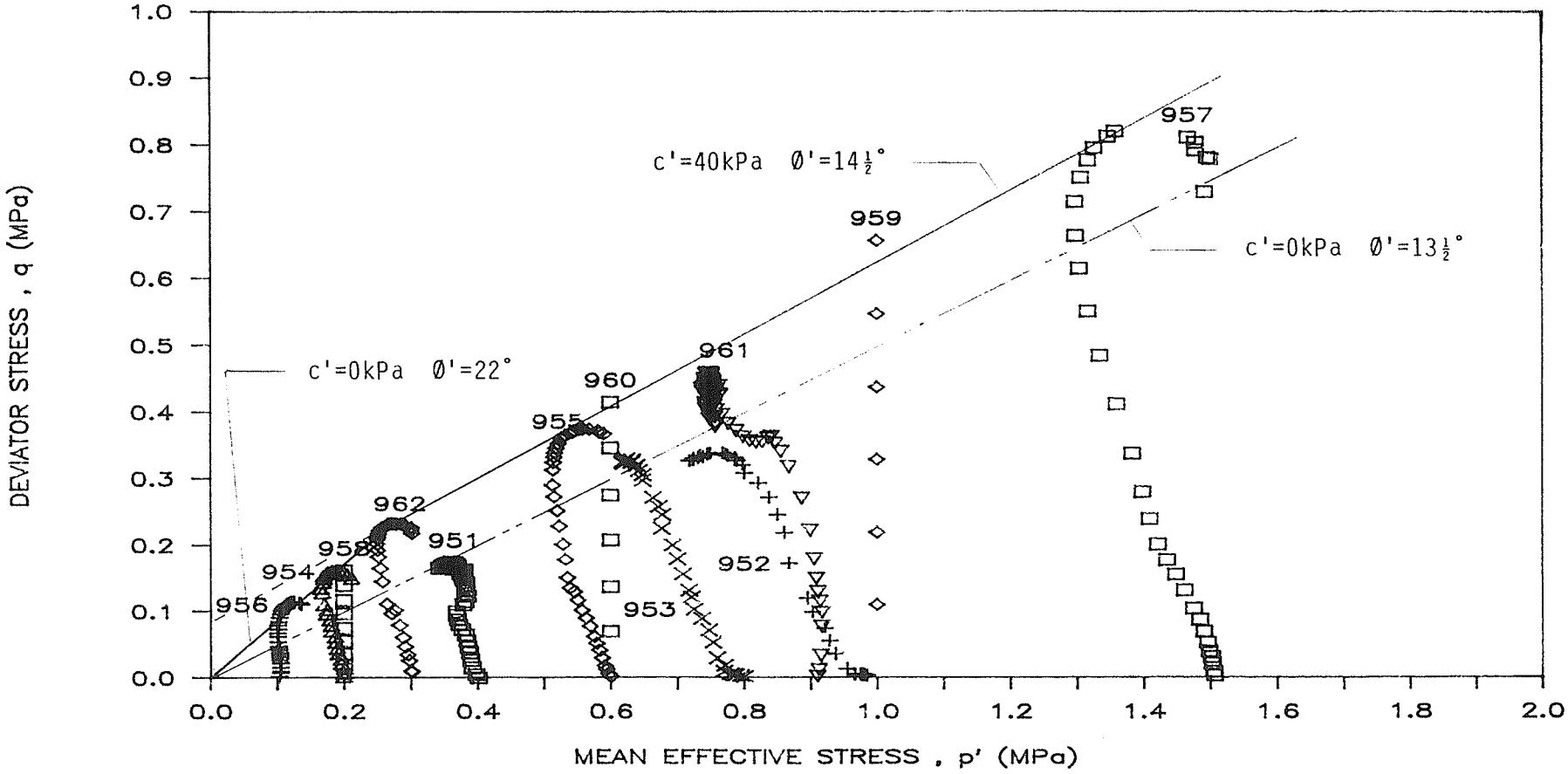

FIG. 6.39 - EFFECTIVE STRESS PATHS AND COULOMB-MOHR ENVELOPES

FABRIC UNIT	STRUCTURE	LEVEL OF RECOGNITION	ORDER OF MAGNITUDE (mm)
AGGREGATE	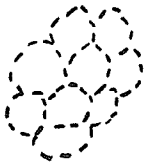	MACROSCOPIC	10
PED		MACROSCOPIC	1
CLUSTER		MICROSCOPIC	0.1
DOMAIN		SUB-MICROSCOPIC	0.01
PARTICLE		SUB-MICROSCOPIC	0.001

FIG. 7.1 - DIAGRAMMETIC REPRESENTATION OF STRUCTURE OF CLAY FABRIC UNITS

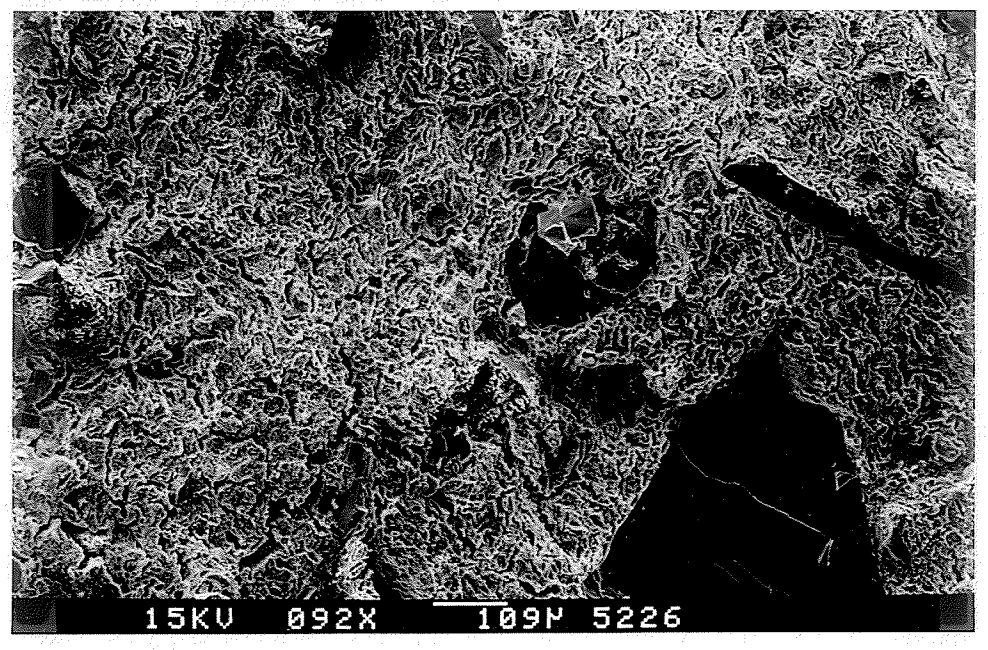

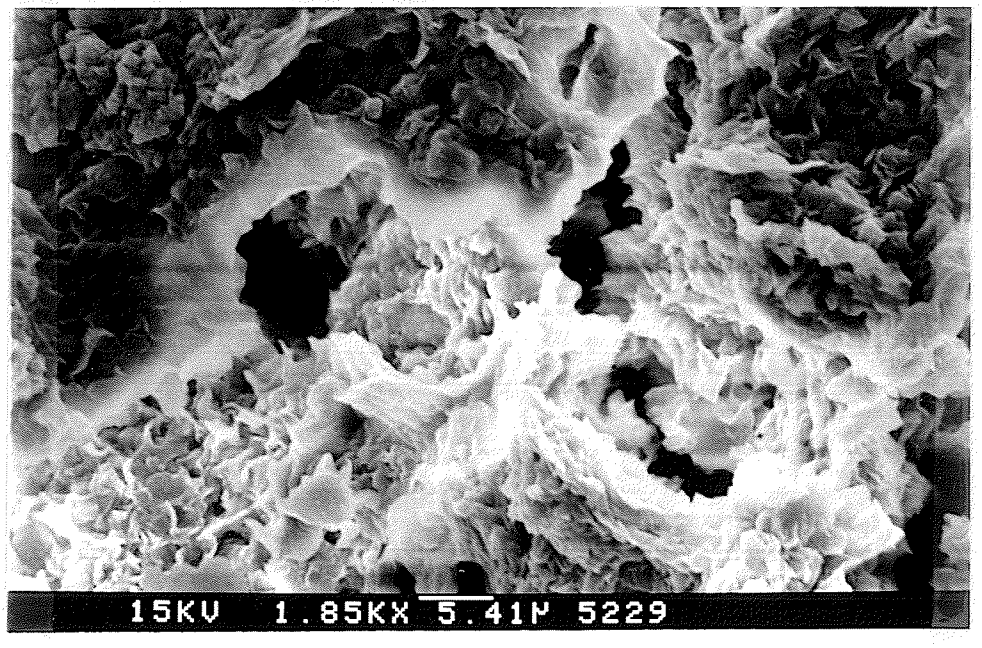

FIG. 7.2 - ELECTRON MICROGRAPHS OF BUFFER (w = 40%)

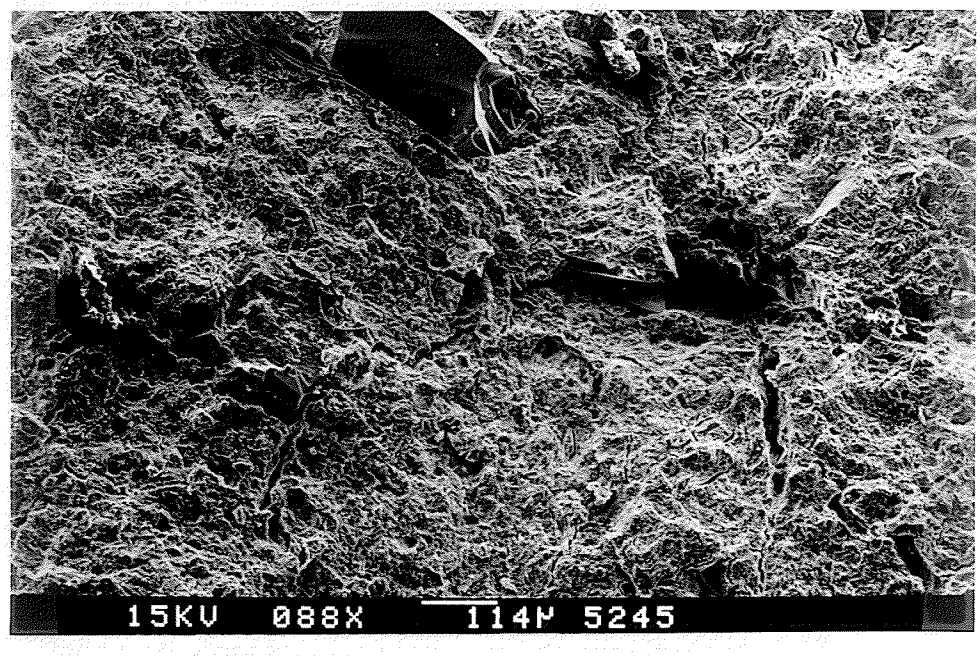

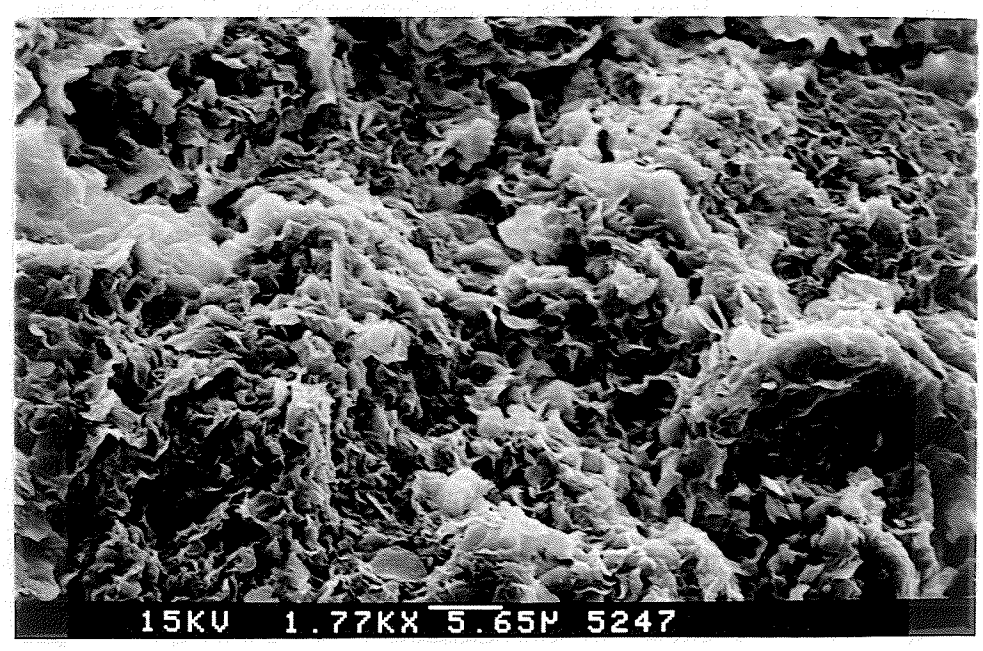

FIG. 7.3 - ELECTRON MICROGRAPHS OF BUFFER (w = 20%)

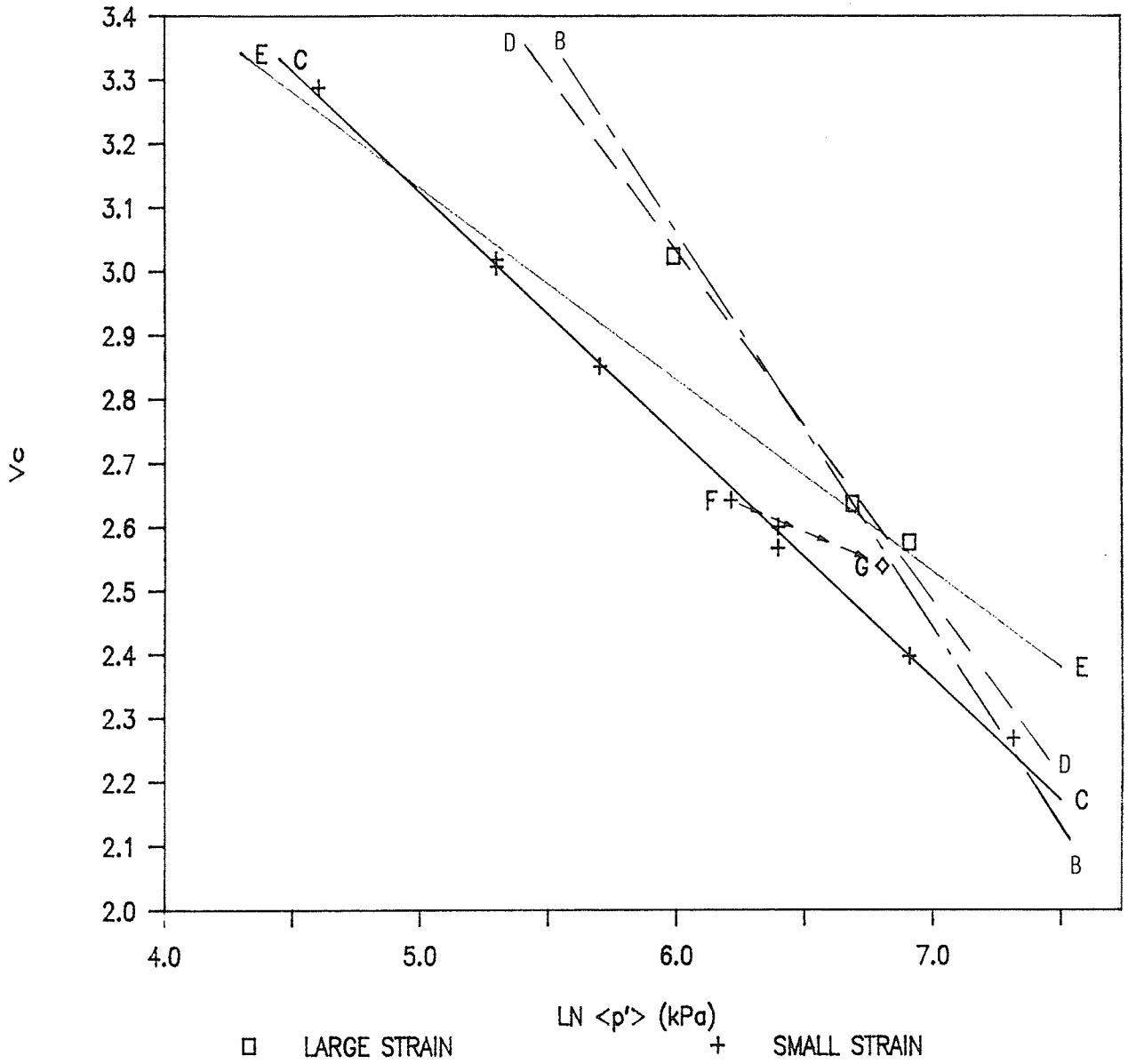

FIG. 7.4 - END OF CONSOLIDATION DATA IN V_c:LN(p') SPACE

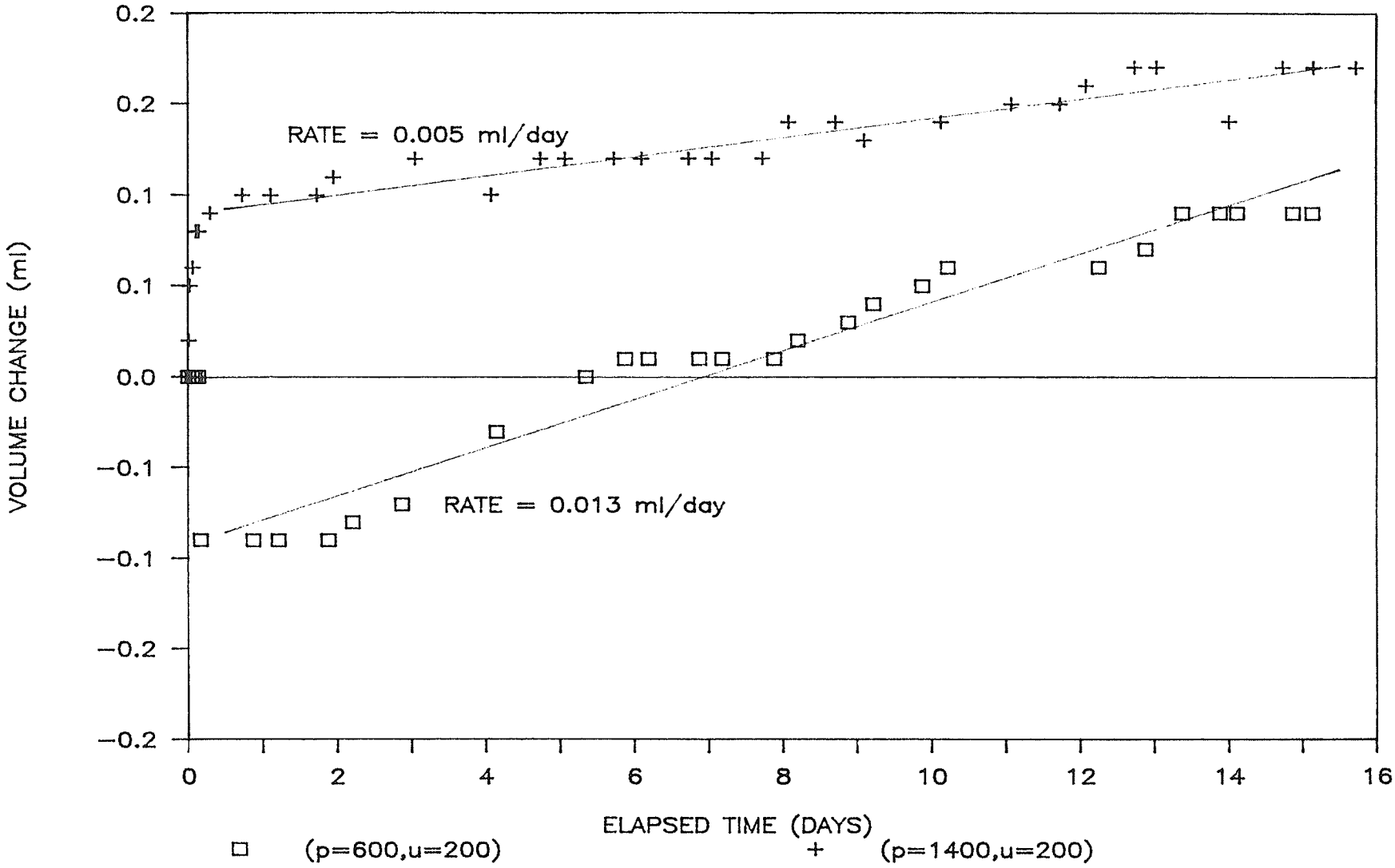

FIG. 7.5 - LATEX MEMBRANE LEAKAGE TEST RESULTS

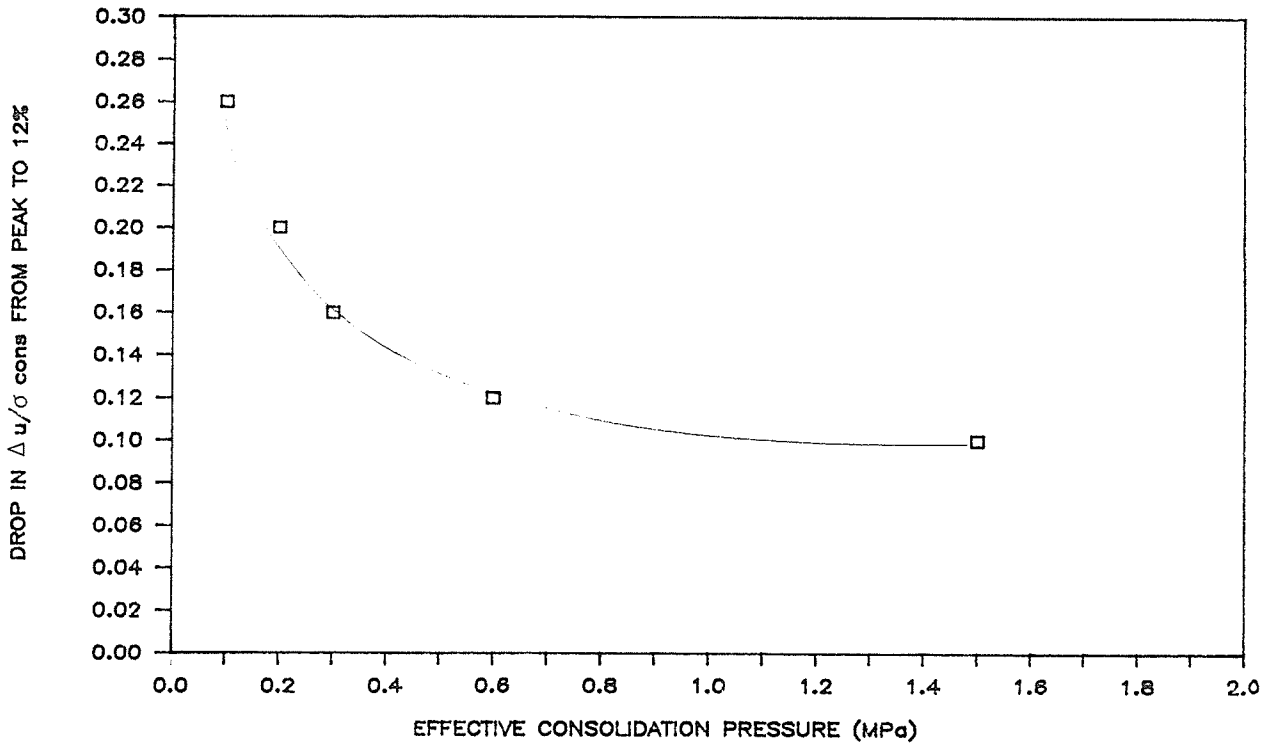

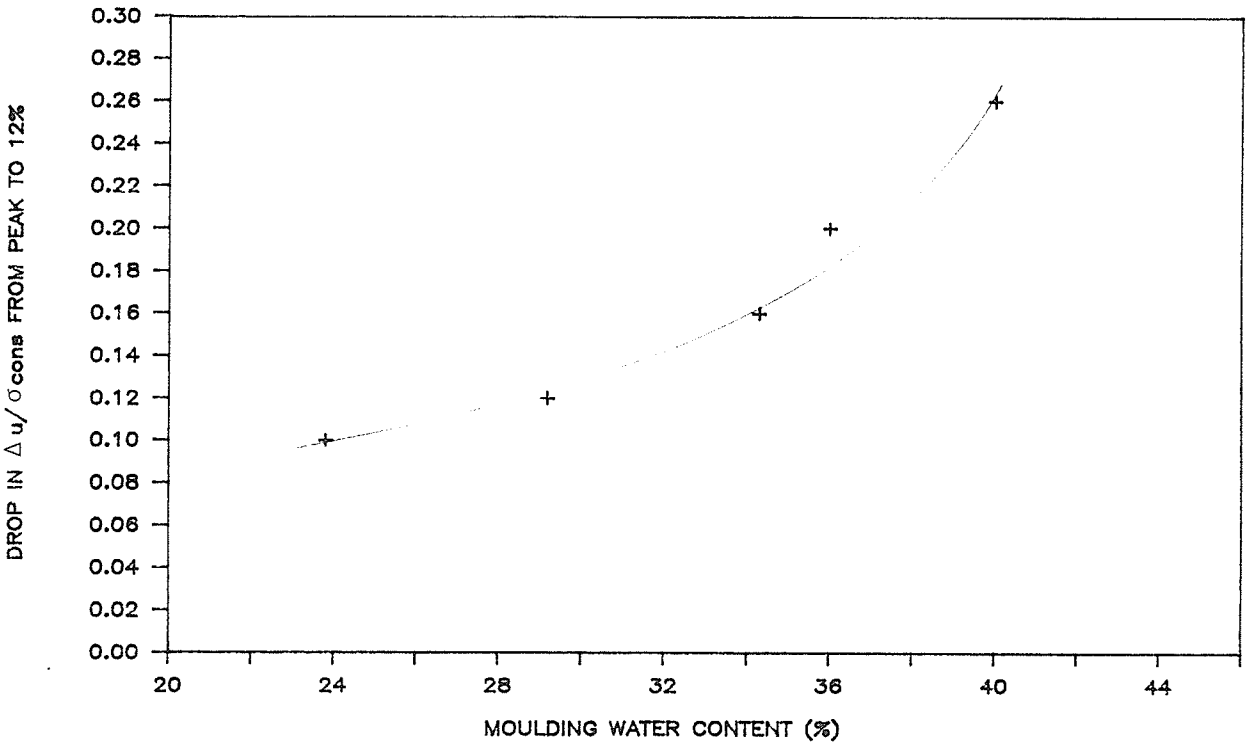

FIG. 7.6 - RELATIONSHIP OF DILATANCY WITH CONSOLIDATION PRESSURE AND MOULDING WATER CONTENT

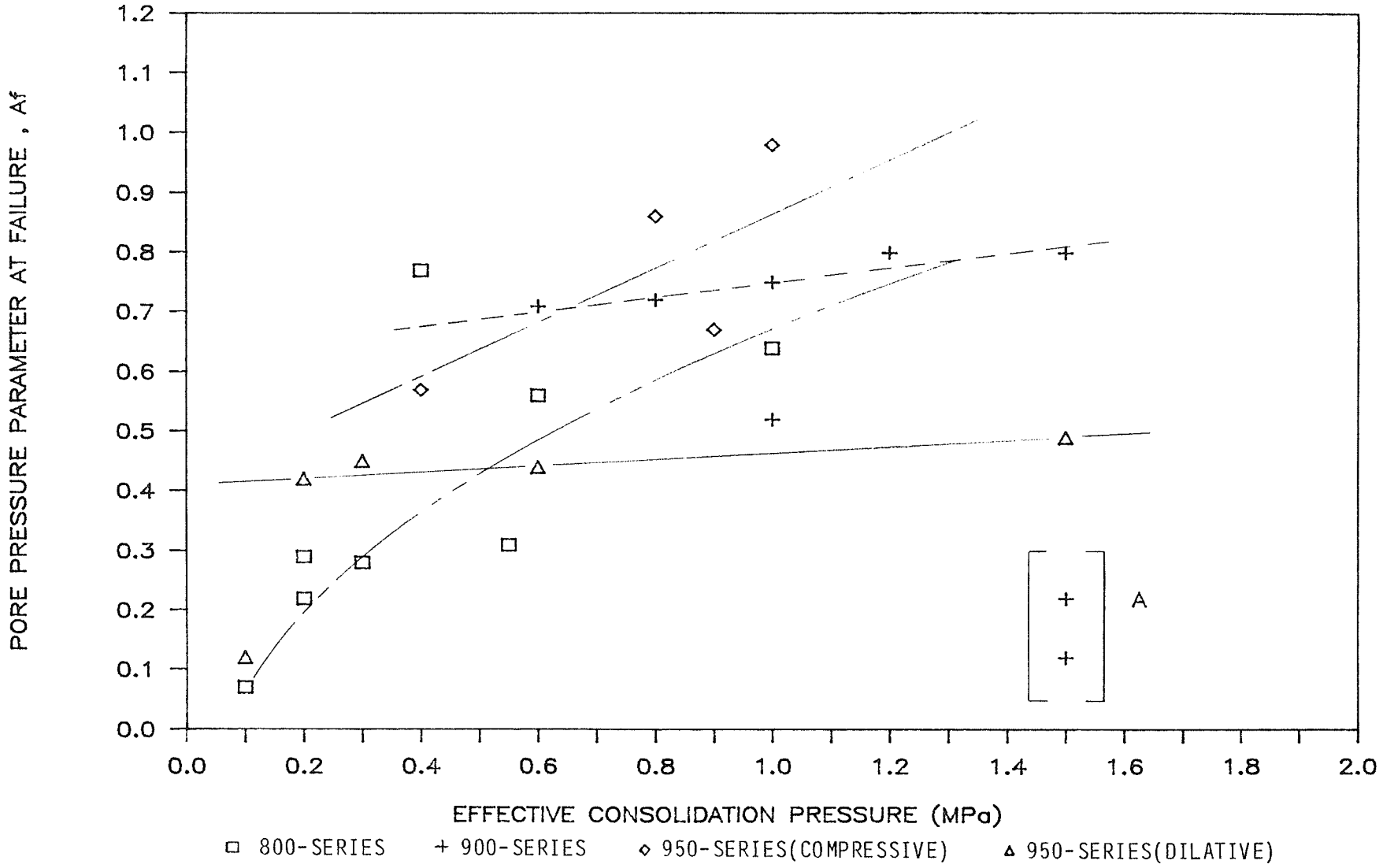

FIG. 7.7 - RELATIONSHIP OF POREWATER PRESSURE PARAMETER AT FAILURE WITH CONSOLIDATION PRESSURE

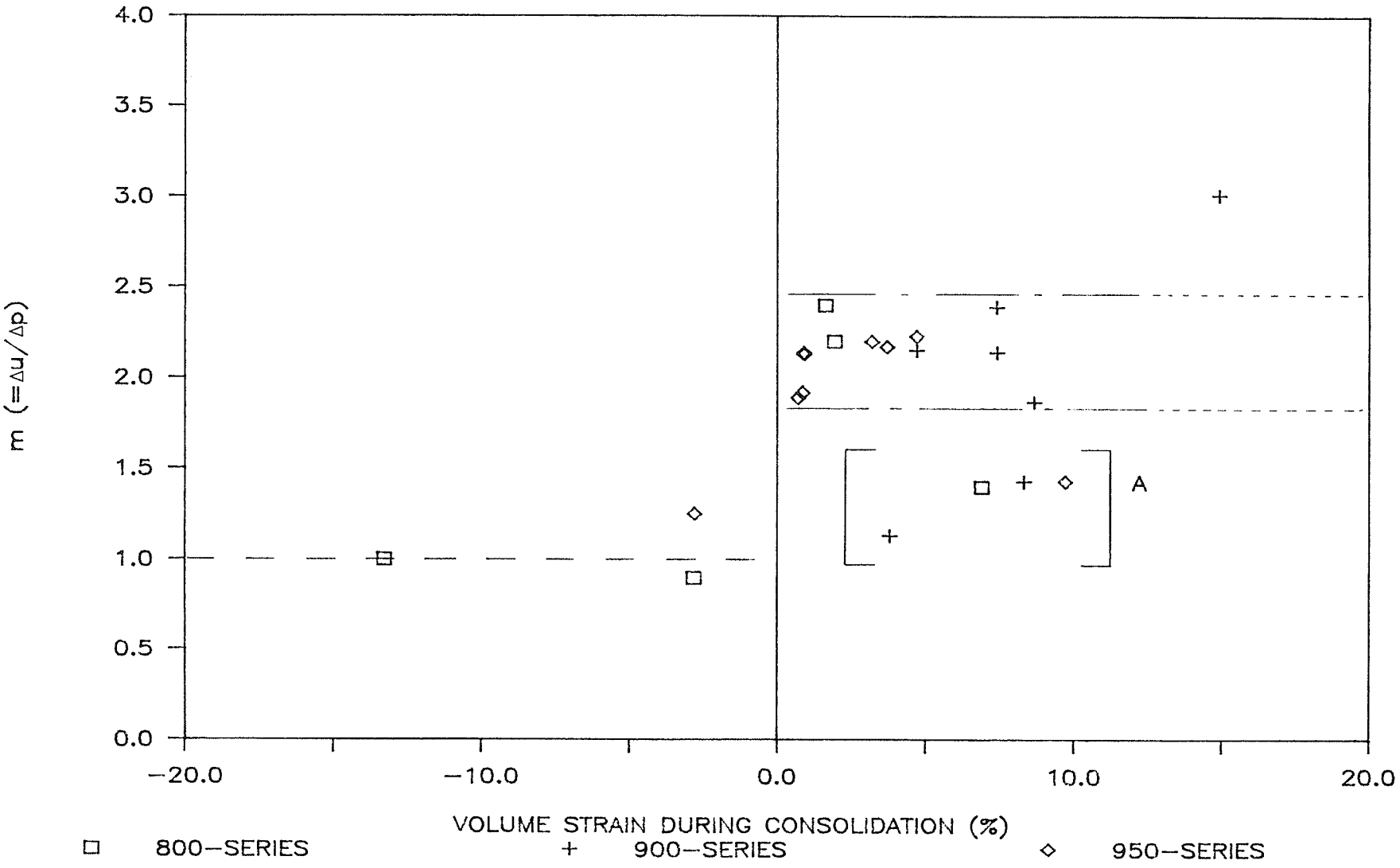

FIG. 7.8 - RELATIONSHIP OF m (= Δu/ Δp) WITH CONSOLIDATION VOLUME STRAIN

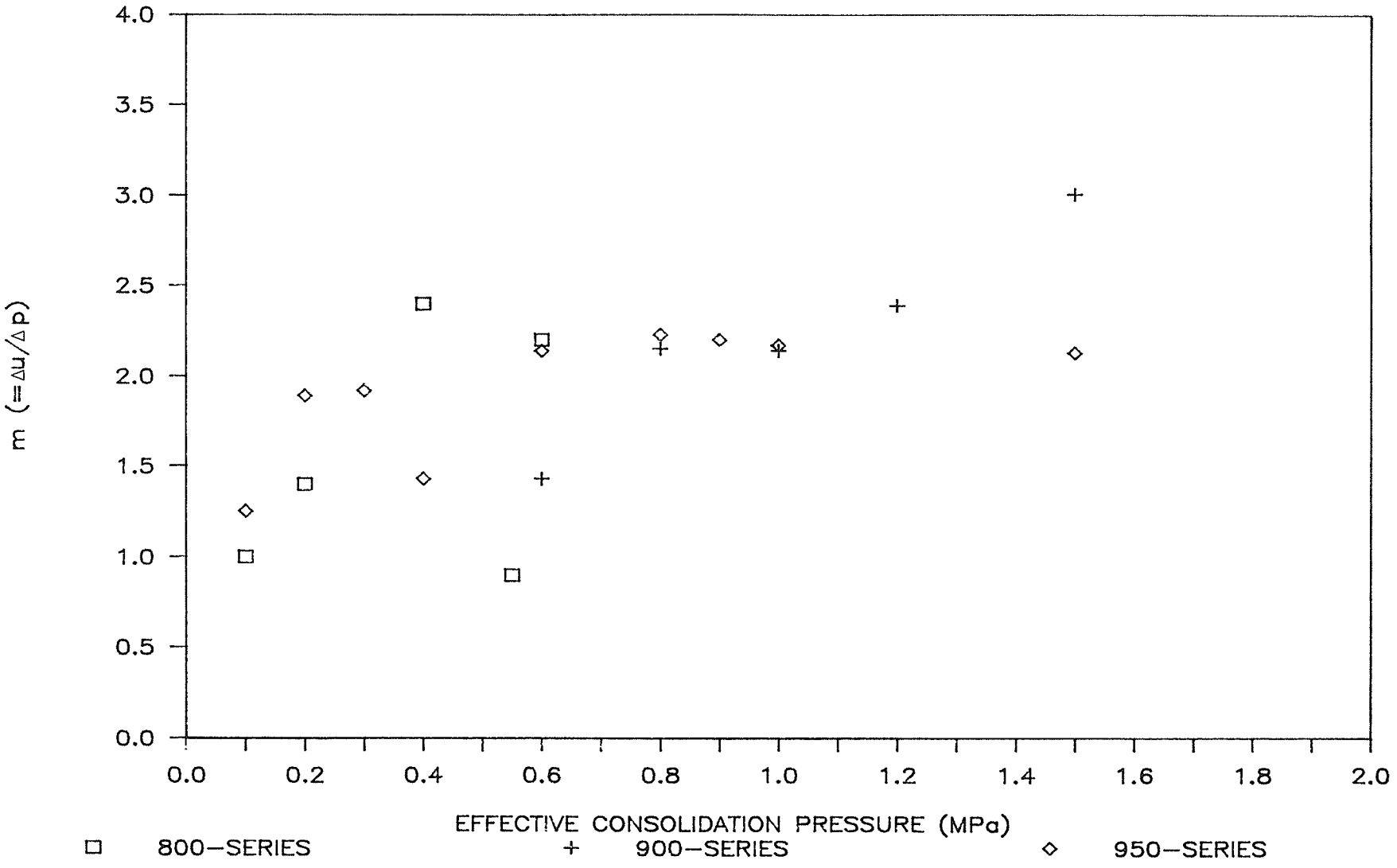

FIG. 7.9 - RELATIONSHIP OF m (= Δu/ Δp) WITH CONSOLIDATION PRESSURE

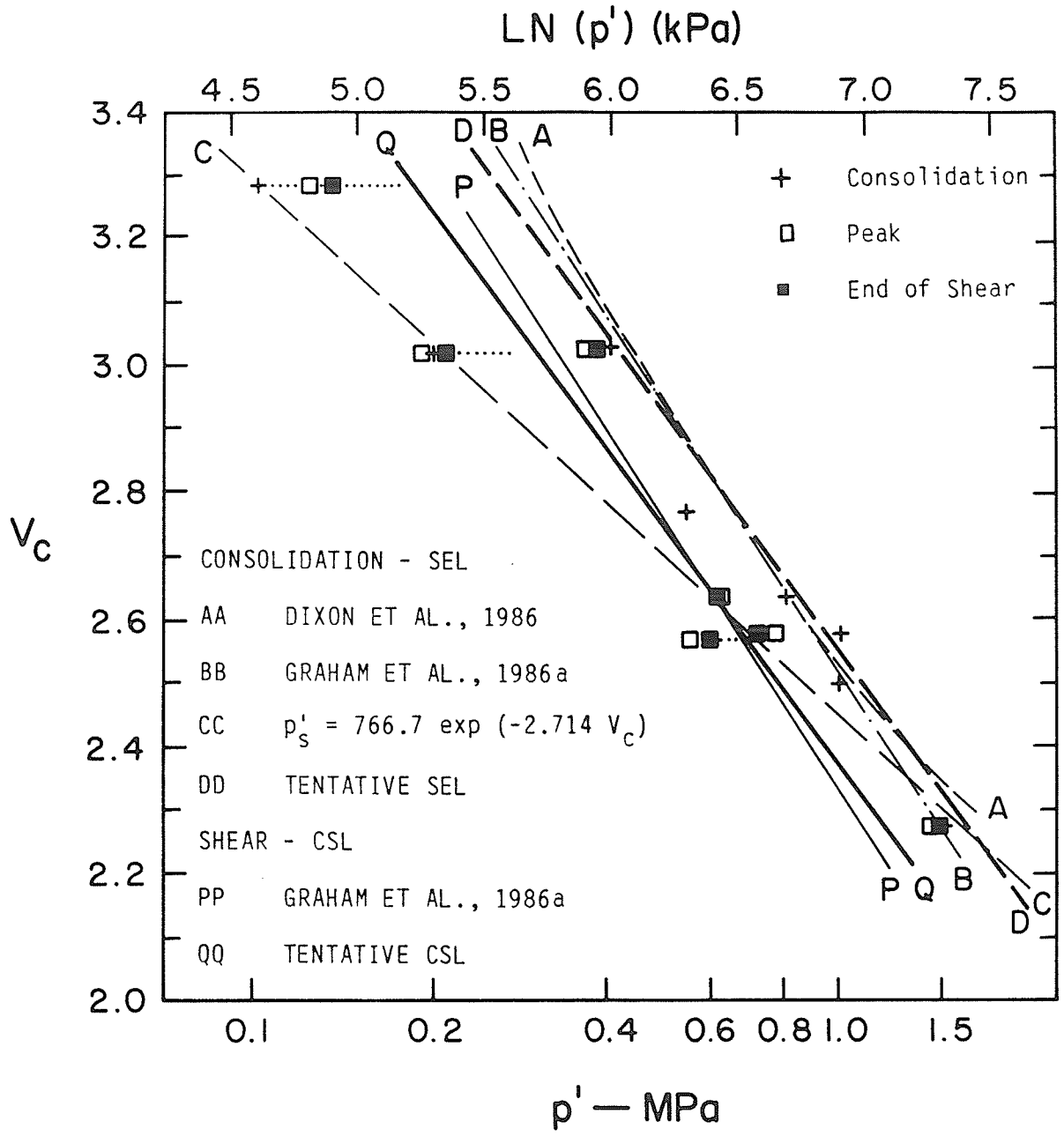

FIG. 7.10 - TENTATIVE CONCEPTUAL MODEL (NOVEMBER, 1986)
(AFTER GRAHAM ET AL., 1986b)

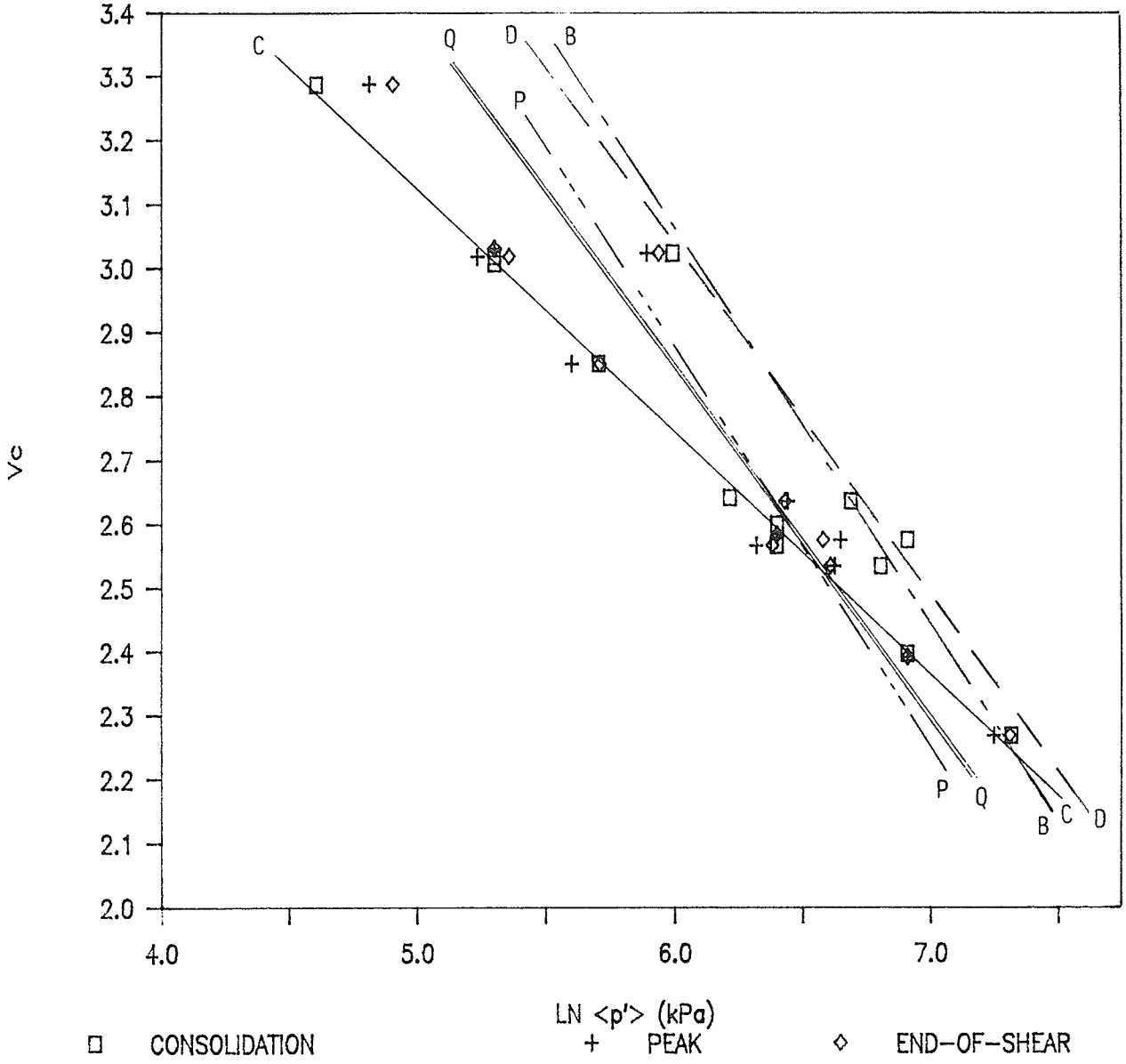

FIG. 7.11 - MODIFIED CONCEPTUAL MODEL